Geophysical exploration

for offshore evidence of relict shorelines on the northern coast of Ireland

Benjamin **Thébaudeau**

A thesis for the degree of Doctor of Philosophy submitted to the University of Dublin, Trinity College

May **2014**

Declaration

This thesis presents my own work unless stated otherwise.

All references are duly acknowledged.

It has not been previously submitted as an exercise for a degree at this or any other University.

I agree that the Library may lend or copy the thesis upon request. This permission covers only single copies made for study purposes, subject to normal conditions of acknowledgement.

Benjamin Thébaudeau

Summary

The current generation of postglacial Relative Sea Level (RSL) change simulations in formerly glaciated margins display significant deviations from field evidence. This is particularly true in Ireland where the RSL history is strongly controlled by the combined effects of local ice loading and the influence of adjacent ice masses over Britain and Fennoscandinavia. On the northern coast of Ireland, the resulting complex interplay between glacioisostatic rebound and eustatic sea-level rise is expressed as an oscillating postglacial RSL curve that comprises intervals with sea levels both above and below present. Whilst the details of the timing, magnitude and rates of these changes are subject to debate, the non-monotonic nature of postglacial RSL change in the region is a common feature across sea-level curves, irrespective of whether they are derived from glacial rebound modelling or the interpretation of field data.

Both types of reconstruction rely on sea-level data which have so far been almost entirely collected on land and dated mainly to the Holocene. The period of time when the RSL was locally below the modern sea-level is critical to our understanding of the region coastal evolution and formation. Evidence on the amount of RSL fall, or the level of the RSL lowstand, can be found in painstaking and costly diving surveys but also prominently in desk-based study using high-resolution bathymetric survey as well as sub bottom exploration using seismic reflection. Indeed, published studies using local seismic data and associated ground truthing coring survey have identified sub bottom features (palaeochannels) and depositional evidence (erosional surfaces) that suggest that current Glacial Rebound Models (GRMs) underestimate the magnitude of postglacial RSL fall for the northern coast of Ireland.

This study explores the recently collected Joint Irish Bathymetric Survey (JIBS), a multibeam high-resolution bathymetric survey, and the large corpus of seismic data collected over the last 15 years by staff of the School of Environmental Sciences from the University of Ulster for the northern coast of Ireland for any evidence of submerged relict shorelines to constrain the magnitude of the local postglacial RSL fall.

The recent high resolution survey of the bathymetry of the north coast of Ireland (JIBS) is used here as an opportunity to explore the geomorphological evidence of past RSL offshore. A marine terrace database is developed for the study area in order to study the morphological parameters of these features and the influence of the lithology of the rocks these features were formed in with their morphology.

Summary

A wave erosion model is run using four of the recently published GRMs to test the origin of some of the recognised marine terraces where modelled output are compared to the measured profiles to select the parameters for the best fit. These simulations permit a first order assessment of the extent and distribution of potentially inherited features.

Local seismic stratigraphic data is explored for any depositional evidence of recent RSL change. The whole corpus of seismic data both already used in publication and more recently collected is consistently examined for ground truthing targets. 14 cores are presented from the selected areas of Church Bay, Runkerry Bay and the Bann estuary/Portstewart area where local depth and the thickness of the various seismic units described were considered optimal for vibrocoring. Acoustic-lithological correlations are used to decipher the depositional history of the cored areas which are then extrapolated to the whole northern Irish coast. 7 main phases of sediment deposition are recognised for the study area spanning the period from the Last Glacial Maximum (LGM) to the present and this scenario carries strong implications for the postglacial RSL change.

This study highlights the difficulties in relating hard rock erosional coastal features to their contemporary RSL which reflects the relative lack of interest of modern literature to their use in postglacial RSL study. The information from the soft sediment stratigraphy is limited but its higher precision provides some definite evidence for the timing and depth of the most recent lowstand. The comparison of both lines of investigation points to only a slight underestimation (2 to 5m in North Antrim and 2m in Derry) of the current GRMs' simulation of the magnitude of the last RSL lowstand of. Furthermore, the westward differential glacial uplift consistently found in GRMs is somewhat visible in these new lines of evidence but not to the same extent as modelled. Hence it appears the current generation of GRM is appropriate at simulating postglacial RSL change in the study area. However, some recommendations can be made for the future improvement of GRMs.

Hence by using a comprehensive and multi-technique study, this thesis makes a valuable contribution to the study of palaeoclimatology in terms of ice sheet distribution and development, RSL change and coastal geomorphology for formerly glaciated margins.

Acknowledgements

Funding for this project, coring survey and lab analysis were gratefully received from Science Foundation Ireland.

I wish to thank Robin Edwards for obtaining this research grant and taking a chance on a geophysical mature student with very little background in natural sciences. His supervision and advice, especially concerning the writing up process were invaluable and all his comments made for a much better thesis. His help on the micropalaeontological analysis and dating samples were crucial at the time when other events in my life were taking precedence.

My co-supervisor Rory Quinn and his team-mates Ruth Plets and Kieran Westley had a tremendous input in this project in terms of initial data processing, advice and workshops. Both studies on the bathymetry and seismic stemmed directly from their work. All the visits I made there always boosted my work and they made me feel truly like their colleague.

Alan Trenhaile, who I have not yet met in person, has given me an amazing example of an established professor taking the time to answer the email of a PhD student and accepting to collaborate on a research article. His work on the erosional models were an inspiration first and thanks to him became an important part of this project.

I wish to thank Xavier Monteys for his regular advice in the planning of the coring survey and his participation on the cruise. Xavier and Seán Cullen were crucial in the success of this cruise by pulling the institutional weight of the GSI behind the chartering of the vessel (thanks to Koen Verbruggen as well for signing up on it) and by loaning us their vibrocoring equipment.

Thanks as well to Harry McClenahan of the CIL who was able to organise the logistics of the chartering of the vessel. Additionally, I wish to thank the crew of the ILV Granuaile for their patience, their good humour and professionalism during the coring survey.

I wish to acknowledge the kind help of the members of the Marine Institute, Bernadette Ní Chonghaile for her help in the administrative preparation and Aodhán Fitzgerald for the gift of consumables and the transport of the equipment for the cruise.
Similarly, this cruise could not have run without the volunteered help of Niall Finn of the GSI and Will Evans of the University of Ulster. Their presence and involvement were greatly appreciated.

Acknowledgements

Stephen McCarron of the National University of Ireland in Maynooth has been a great guide in the analysis and treatment of the recovered cores and I wish to thank him for the storage of these in his facility as well.

The fast tracking of the radiocarbon dates by the members of the dating facility at Queen's University Belfast were greatly appreciated in light of this thesis' submission deadline.

I wish to thank John McKenna for his advice on the study of hard rock shore-platforms. Some of the simulated RSL curves were supplied directly by Sarah Bradley, Joseph Kuchar and Alun Hubbard and I wish to thank them for their very helpful involvements.

The contribution of the two examiners for this thesis, Pete Coxon and Andrew Cooper, is gratefully acknowledged as their detailed review and their comments during the Viva Voce allowed for the work undertaken for this project to be presented in a much better light.

Finally, I want to acknowledge the patient help of Elaine Treacy, Brida Walsh and Frank Hendron when I was working in the geomorphology and palynology laboratories.

I want to finally thank the technical staff of the Geology department, Frank Hendron, Maura Morgan, Noel McGinley and Neil Kearney for their help in facilitating my research in the department. Additionally, the whole staff from the department were very welcoming and integrated me despite my lack of geological background and the fact that my project was so different to their research interests. They have allowed me to develop in interest in geology and practice my teaching skills in tutorials and on field trips.

I would like to thank my best mates from the URL, Kieran and Niamh, whose company was sorely missed when they finished their PhDs before me but their experience was then entirely exploited for the benefit of this thesis. Similarly, those crazy young kids that are Kyle and Mike and their habit of working late and/or on the weekends during their early years of PhD allowed me to have some fun during my hours of need.

Je voudrais remercier mes parents, Chantal Faucou et Denis Thébaudeau, qui m'ont toujours soutenu dans mes études et dans mes choix de vie en général. Leurs attentions et leur intérêt pour ma recherche sont inégalés. Leur amour et l'éducation qu'ils m'ont prodigué m'ont poussé vers ce but d'obtenir un doctorat dont je suis très fier et je le leur dédicace. De même, mes frères et sœur, Alexis, Mathieu, Philippe et Fanny, ainsi que mes

neveux et nièces, Lucas, Tom, Nino, Mycéa, Moira et Lily, ont tous formé un soutien sans faille qui fut très important pour moi. Mon grand-père, Alfred Faucou, a toujours été intéressé par mes recherches et je tiens à lui être redevable de son intérêt et de sa confiance en moi.

Mes bons vieux potes de Cachan, John, Richard et Olli, m'ont montré le chemin de la recherche et m'ont bien averti de certaines déconvenues possibles. Grâce à eux, je commençais ma recherche en bien meilleur connaissance de cause.

And finally, the most important person in the world, my wife Keira Kennelly whose constant support and tremendous love were a sine qua non condition for this research's completion and my happiness in life in general. I love you and you need to know that it would not have been possible without you. I hope this makes you proud. Le grá go deo.

Contents

Appendices (CD)

List of Figures

1. Introduction

2. Study area and origin of its coastline

List of Figures

3. Datasets and methodologies

4. Geomorphological indicators of sea-level change

List of Figures

5. Modelling the development of the coastal profiles of the study area

6. Sub bottom investigation of RSL change evidence

List of Figures

List of Figures

7. Synthesis

List of Figures

2. Study area and origin of its coastline

3. Datasets and methodologies

4. Geomorphological indicators of sea-level change

5. Modelling the development of the coastal profiles of the study area

6. Sub bottom investigation of RSL change evidence

List of Tables

7. Synthesis

Statement of Contributions

This document has been drawn to recognise the contributions of various people in the work presented in this thesis.

The erosional model presented in chapter 4 was developed and run by Professor Alan S. Trenhaile at the University of Windsor, Ontario, Canada. However these were guided by my original input and further collaboration resulted in the publication of an article (Thébaudeau et al., 2013) presented in appendix 4.1 from which the findings of chapter 4 are extracted.

The JIBS datasets is being actively used by staff at the University of Ulster. Backscatter data from the JIBS, used in Chapter 3, was processed and interpolated by Doctor Ruth Plets there. Similarly, the corpus of seismic data, presented in Chapter 5, for the study area were integrated and processed, for the major part, by her. The processing of the remaining seismic lines and the consistent interpretation of the results was carried out by me in Trinity College.

Finally, the radiocarbon dating, presented in Chapter 5, were obtained from the facility in Queen's university Belfast. However, I carried out initial sample preparation in the Geomorphology laboratory in Trinity College.

Chapter 1

Introduction

1.1 Scientific context for the project

1.1.1 Quaternary climate and associated sea-level changes

The Cenozoic era, starting 65.5 Myrs ago, is divided into the Tertiary and Quaternary period. The Quaternary period, which beginning is set at 2.6 Myrs ago just after the Gauss-Matuyama palaeomagnetic reversal (Bowen and Gibbard, 2007), has seen a worlwide cooling of the climate; a trend that started in the late Tertiary. These climatic records were extracted from ice cores of Greenland and Antarctica and marine sediment cores (Lisiecky and Raymo, 2005). They show a wide variety of climate evolution during the Quaternary both in terms of amplitude and wavelengths (figure 1.1). The cyclicity of these climate changes is due in part to variations of the insolation that are orbitally induced and has evolved from a predominant 41 kyrs cycle from 2,600 to 700 kyrs ago (linked with the periodicity of the Earth's tilt) to a predominant 100kyrs cycle from 700 kyrs ago to the present (linked with the periodicity of the Earth's eccentricity). In addition to this shift in period, the amplitude of the climate forcing has increased in the last 700 kyrs compared to the earlier part of the Quaternary with more extreme period of cold stages in particular associated with more extensive ice sheets in the higher latitudes. Figure 1.1 introduces this climatic record for the past 3.6 Myrs based on a composite oxygen isotope curve (Walker and Lowe, 2007). Each spike on the curve was given a Marine Isotope Stage (MIS) number starting at the present working back in time with odd numbers corresponding to interglacial or warm stages (we live currently in the MIS 1) and even numbers corresponding to glacial or cold stages (the last glaciation took place during MIS 2). We can recognise on this figure the onset of the Quaternary and the shift in climate forcing between the two different periods of cyclicity.

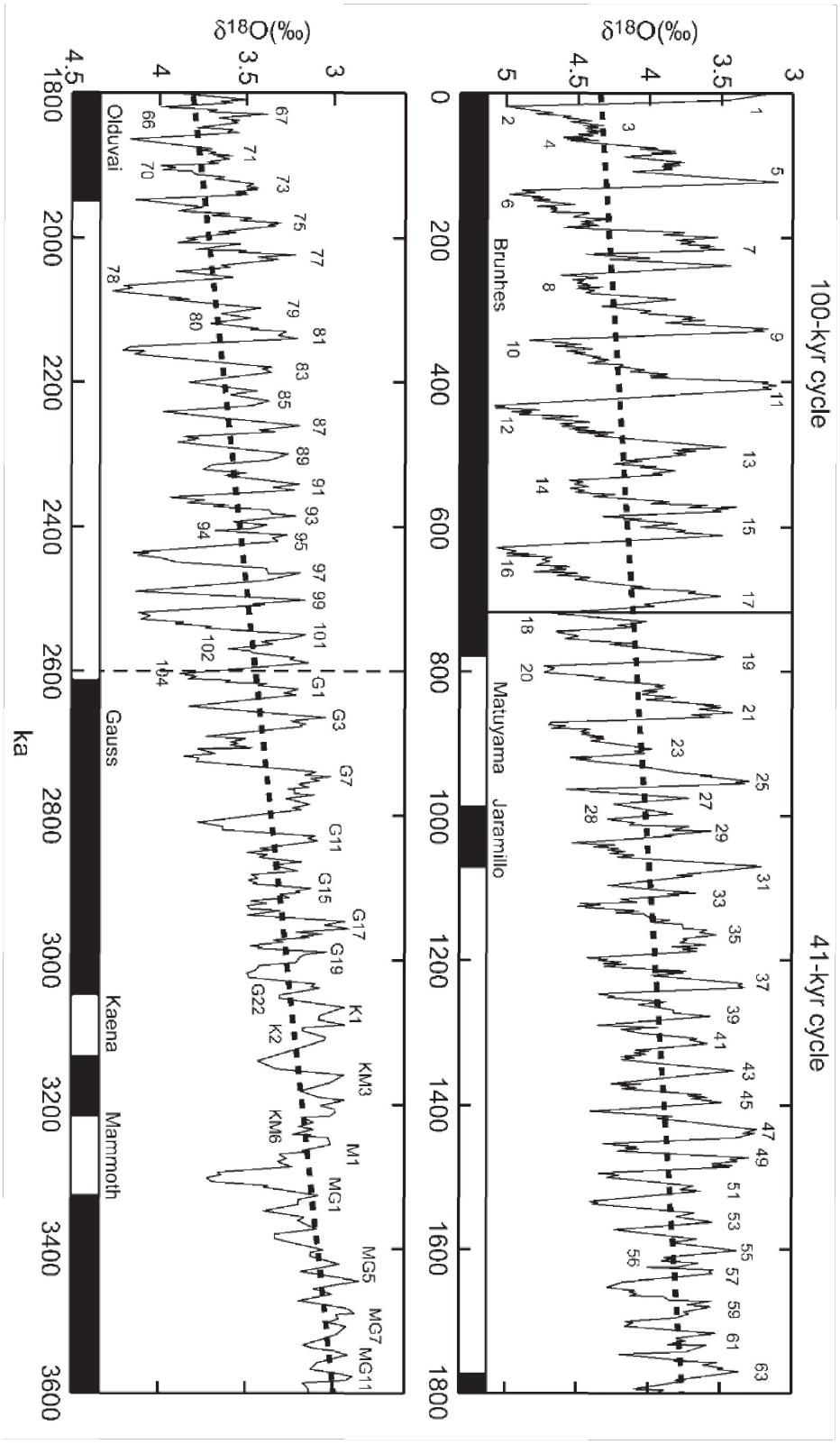

Figure 1.1: A composite oxygen isotope curve for the last 3.5 Myrs, constructed by stacking 57 globally distributed marine sediment record and displayed against the palaeomagnetic time scale (after Lisiecki and Raymo, 2005). The vertical dash line at 2.6Myrs represents the onset of the Quaternary and the continuous vertical line at 700kyrs represents the shift from a 41kyr cyclicity to a 100kyr cyclicity in climate forcing (from Walker and Lowe, 2007).

The Quaternary has been divided into two series, the Pleistocene and the Holocene. Most of the Quaternary is concomitant with the Pleistocene with the Holocene only starting 11,700 years ago at the end of the last glacial stage (MIS2) and the onset of our current interglacial stage (MIS 1). A glacial stage is made up of several parts divided in two categories: stadials and interstadials. Stadials are periods of extensive glaciation and only form a small part of the 100kyrs length of glacial stages. Interstadials are short periods (1 to 2kyrs) during which the climate ameliorates to some degree, possibly reaching temperatures similar to those of the present day (or warmer). Figure 1-2 displays the stable isotopic record of the GRIP ice core compared to a record of abundance of a planktonic foraminifera (*N. Pachyderma* whose presence indicates cold sea temperatures) from ocean sediments (Coxon and McCarron, 2009). High concentration of Ice Rafted Debris (IRD) found in the Troll 8903 marine core (Haflidason et al., 1995) are also added on this figure to compare with the major climatic transitions. This allows the recognition of the latest stadial phase, called the Younger Dryas in Europe or the Nahanagan stadial in Ireland (Coxon and McCarron, 2009) lasting from 12,700 to 11,500 calibrated years BP, and the latest interstadial phase, called in Ireland the Woodgrange interstadial, lasting from 14,500 to 12,700 calibrated years BP. This figure also highlights the rapidity of the transition in climate forcing from one phase to the next.

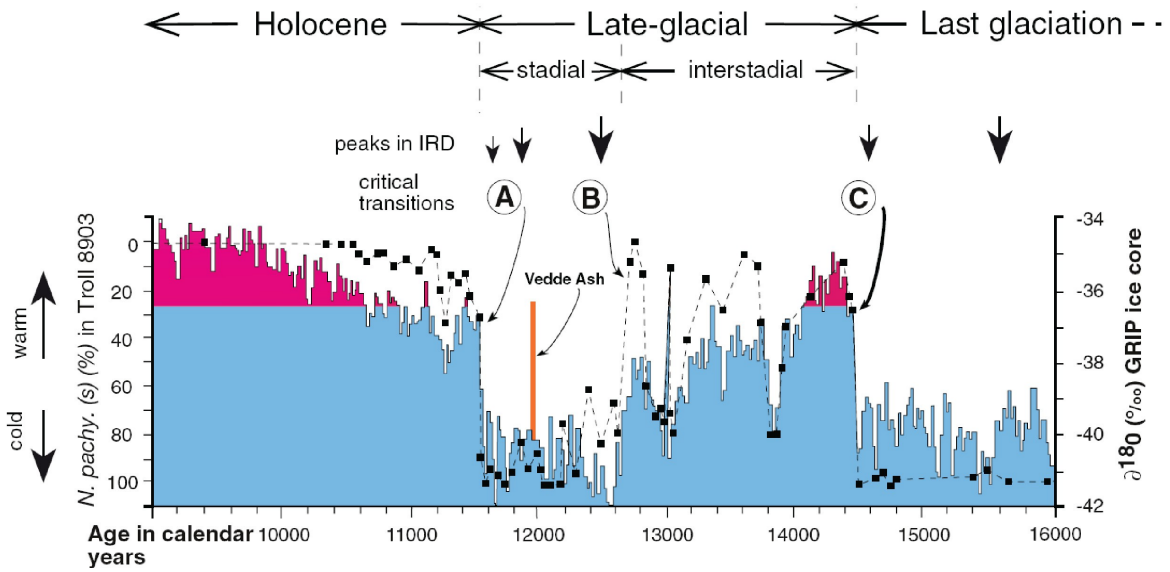

Figure 1.2: Stable isotope record from the GRIP ice core (histogram) compared to the record of N. pachyderma from ocean sediments (dotted line) (from Coxon and McCarron, 2009). High concentration of IRD from the Troll 8903 core are marked with arrows (after Haflidason et al., 1995).

In Ireland, there is definite evidence for only two distinct cold phases (Coxon and McCarron, 2009) both experiencing the presence of an extensive ice sheet with several sequences of build up and decay interspersed by cold, periglacial conditions and cool (or perhaps warm) interstadial periods. This apparent paucity of record is due to the probable erosion and reworking of previous evidence by each stadial. Extensive mapping of the glacial features on land (i.e. moraines, eskers, corries, drumlins, striae, meltwater channels, etc...) as well as the recording of the extensive consolidated subglacial diamicts (tills) lying under the soil has been undertaken for the last 150 years and has been aided by the development of satellite topographical mapping technology and the recent mapping of the offshore bathymetry (see section 2.2). This corpus of data has allowed the recognition of ice flow patterns and ice sheet extents (Clark et al., 2012). The ice dispersal centres in Ireland formed in upland regions such as Donegal or Connemara and lowland areas as domes such as in the Omagh Basin, in the Lough Neagh Basin or in the north Central Midlands (McCabe, 2008b). Whilst generated from a different source, the ice flow patterns indicate that, at least during the last cold stage, the Irish and British ice sectors were coincident along the axis of the Irish Sea forming what was termed the British Irish Ice Sheet (BIIS) (Coxon and McCarron, 2009). The last ice sheet to have covered Ireland decayed rapidly leaving behind the extensive corpus of glacial features mentioned above.

Associated with the Quaternary's climate fluctuations and cycles of ice growth and decay, a corresponding evolution of the global eustatic sea-level has been reconstructed from records of fossil coral terraces and plant fragments and calcareous marine organisms contained within marine sediment cores in far-field zones (such as Tahiti, Barbados or Indonesia) away from the cold stages ice sheets of the high latitudes (Stanford et al., 2011). These reconstructions show a direct relationship between the earth's climate forcing and the evolution of global eustatic sea-level due to thermal expansion and the evolution of land-based ice (Edwards, 2008). In particular, they infer a global eustatic sea-level at -150m at height of the last glaciation. Additionally, pulses of ice-sheet meltwater into the world ocean into these records have been recognised in these records. The largest of such event known as meltwater pulse 1a has seen an estimated 20m sea-level rise in about 500 years globally and was dated to between 14.6 to 12.8 kyrs BP (Stanford et al., 2011).

Relative Sea-Level (RSL) is the sea-level relative to the level of the continental crust. This definition takes into account changes in both levels as changes in RSL can be

caused by either changes in sea-level or changes in land-level or both. In glacial margins, the influence of ice load on the land level is a major, if not the preponderant, factor in the RSL change with isostatic rebound following ice melting resulting in local RSL fall. In particular, during late glacial period, RSL was higher than present in formerly glaciated zones and was falling due to the loss of ice load which counterbalanced the rise in global eustatic sea-level.

1.1.2 RSL change in Ireland during the last deglaciation

The Intergovernmental Panel on Climate Change (IPCC) last published assessment report (Parry et al., 2007; Solomon et al., 2007) points to the inherent significant uncertainties in future sea-level change projections due to a fundamental lack of understanding. In particular, the evolution of Quaternary ice sheets in terms of thickness, distribution and dynamism and their associated influence on sea-level change are still not comprehensively understood (Edwards, 2007a).

Complex interactions on the local RSL are observed in both Greenland and Antarctica today as warming temperatures translate into global eustatic sea-level rise and local glacial rebound of the land. Projections of the future evolution are based on glacial rebound modelling which are calibrated with past RSL change data. Unfortunately, the recently published generation of Glacial Rebound Models (GRMs) fail to simulate the magnitude of change seen in field evidence (Bassett et al., 2007; Long et al., 2008) which bears great consequences for global preparation to future RSL change.

Similarly, discrepancies between field evidence (McCabe et al., 2008a) and modelled evolution of the postglacial RSL exist in formerly glaciated regions such as Ireland (Brooks et al., 2008). As our understanding of the former British and Irish Ice Sheet (BIIS) improves thanks to extensive high resolution topographical data and further field based evidence (Clark et al., 2012), future generations of GRMs might reconcile some of these misfits. However, other differences are much more substantial and appear irreconcilable (Edwards et al., 2008).

Some of these discrepancies appear in the north of Ireland where the RSL history since the Last Glacial Maximum (LGM) remains poorly resolved and the subject of ongoing debate (Carter, 1982; Lambeck, 1995; Lambeck and Purcell, 2001; Peltier et al.,

2002; Shennan et al., 2006; McCabe et al., 2007; Brooks et al., 2008; McCabe, 2008a; Edwards et al., 2008; Bradley et al., 2011; Kuchar et al., 2012). The postglacial RSL history of the region is strongly controlled by the combined effects of local ice loading and the influence of adjacent ice masses over Britain and Fennoscandinavia. The resulting complex interplay between glacioisostatic rebound and eustatic sea-level rise is expressed as an oscillating postglacial RSL curve that comprises intervals with sea levels both above and below present. Whilst the details of the timing, magnitude and rates of these changes are subject to debate, the non-monotonic nature of postglacial RSL change in the region is a common feature across sea-level curves, irrespective of whether they are derived from glacial rebound modelling or the interpretation of field data (e.g. McCabe et al., 2007; Brooks et al., 2008; Bradley et al., 2011; Kuchar et al., 2012).

Both types of reconstruction rely on sea-level data which have so far been almost entirely collected on land and dated mainly to the Holocene (Brooks and Edwards, 2006 and figure 1.3). The period of time when the RSL was locally below the modern sea-level is critical to our understanding of the region coastal evolution and formation. Constraining the amount of postglacial RSL fall for the region is of major interest to the archaeological community as Ireland was first colonised by humans coming from Scotland around this period. Indeed the oldest site excavated in Ireland in Mount Sandel is located in the Derry region (Woodman, 1985) and it is understood that these people lived beside the coastline of the sea and large rivers and relied heavily on seafood and fish for their survival. Hence there is a strong potential for submerged prehistoric coastal landscape of national importance preserved in the region (Quinn et al., 2008)

Evidence for these can be found in painstaking and costly diving surveys but also prominently using high-resolution bathymetric survey as well as sub bottom exploration using seismic reflection. Indeed, published studies using local seismic data (Cooper et al., 2002; Quinn et al., 2009; 2010) and associated ground truthing coring survey (Kelley et al., 2006) have identified sub bottom features (palaeochannels) and depositional evidence (erosional surfaces) that suggest that current GRMs underestimate the magnitude of postglacial RSL fall for the northern coast of Ireland (the RSL curve for Derry in figure 1.3).

This study wishes to explore the recently collected Joint Irish Bathymetric Survey (JIBS), a multibeam high-resolution bathymetric survey, and the large corpus of seismic

data collected over the last 15 years by the School of Environmental Sciences from the University of Ulster for the northern coast of Ireland for any evidence of submerged relict shorelines to constrain the magnitude of the local postglacial RSL fall.

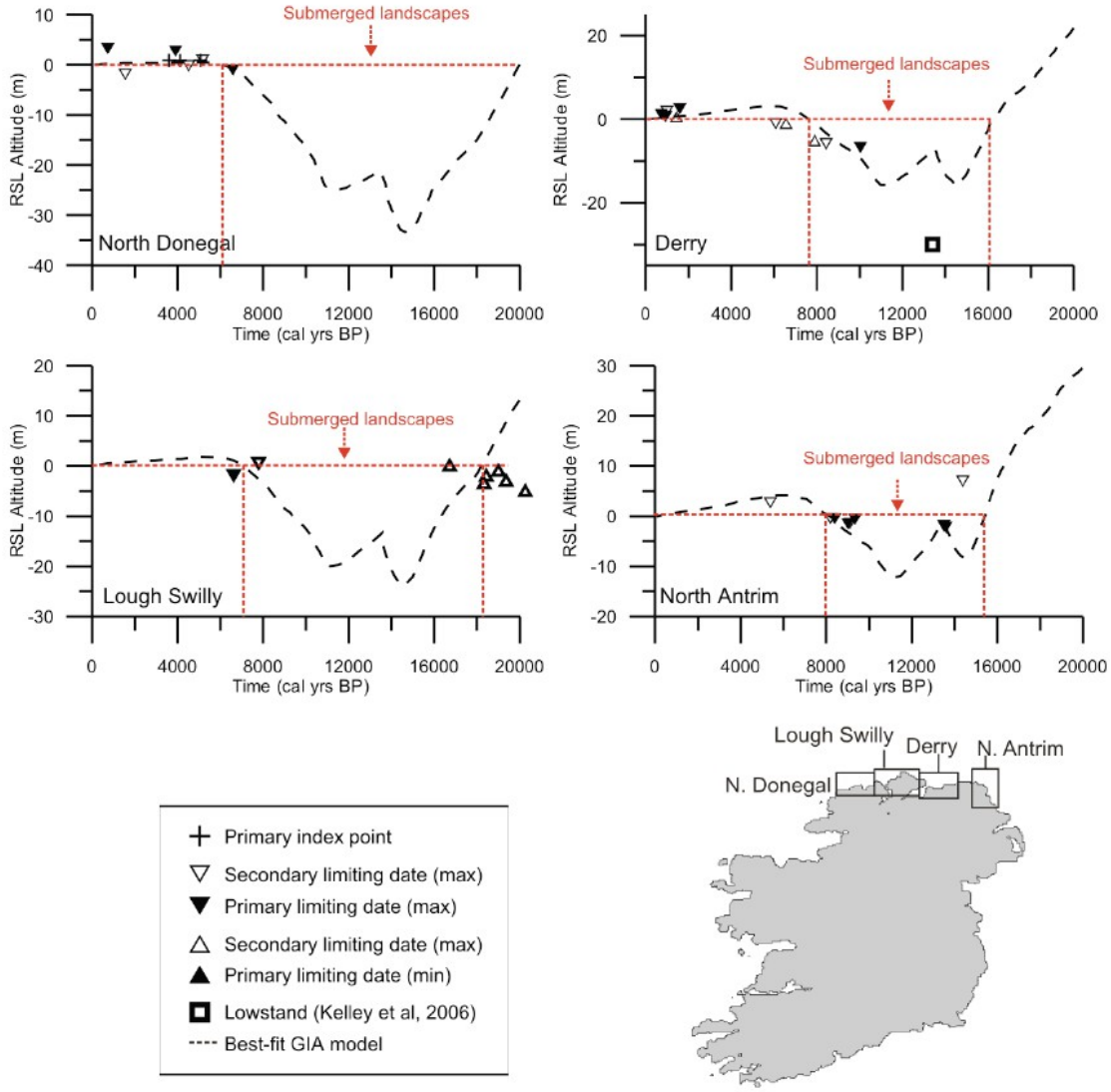

Figure 1.3: RSL data and modelled RSL curves for the northern coast of Ireland from Brooks et al. (2008) highlighting the periods of time with potential for submerged landscapes (from Quinn et al., 2008).

1.2 Research question and testable hypothesis

This thesis aims to address the question whether the current generation of GRM can correctly simulate the rate and magnitude of RSL change in formerly glaciated margins such as the northern coast of Ireland. This will be addressed by examining new and existing offshore datasets in the study area to identify evidence of relict shorelines in the form of erosional features, such as marine terraces and cliff notches, and depositional features, such as submerged beach barrier and stratigraphical evidence. The presence of suitable data will first be tested in both the bathymetric and sub-bottom datasets. The morphology, local context, depth and age of the features identified will then be used to understand their formation and association with former RSL. New sea-level indicators identified will then be compared with recently published modelled RSL curves.

One of the consistent results of all GRMs for the study area is the significant differential isostatic rebound across Ireland following the ice retreat on land after the LGM. This results in pronounced differences in the evolution of postglacial RSL between the northeast and the southwest of Ireland (Brooks et al., 2008; Bradley et al., 2011; Kuchar et al., 2012). In the study area, this contrast is visible with a variation in contemporaneous level of up to 27m between the eastern side of North Antrim and the western side of Lough Swilly (figure 1.3). This should result in observable dipping of contemporary shorelines toward the west along the study area with comparable features and lithofacies found at contrasting depths. Hence this constitutes a testable hypothesis which if rejected would imply key shortcomings in the models' ability to describe glacio-isostatic adjustment process.

1.3 Thesis outline

Chapter 2 presents the study area of the northern coast of Ireland in terms of its geological and glaciological history (sections 2.1 and 2.2 respectively). This is used to define the context of its modern coastal landscape and the type of features that are actively forming (section 2.3). This is a necessary first step in the exploration of relict shorelines. The state of RSL knowledge for Ireland as a whole and the study area in particular is presented in details identifying the existing discrepancies between the field based reconstructions and the GRMs' results (section 2.4).

Chapter 3 introduces the various methodologies used in this research project. The recent high resolution survey of the bathymetry of the north coast of Ireland (JIBS) is presented first representing an opportunity to explore the geomorphological evidence of past RSL offshore (section 3.1). The use of bathymetric histograms and the development of a marine terraces database are then presented (section 3.2). Section 3.3 details a wave erosion model used for the reconstruction of shore profile evolution. Finally, sections 3.4 and 3.5 explore respectively the corpus of seismic data used and interpreted and the details of the ground-truthing coring survey and the core analysis undertaken for this study.

Chapter 4 investigates the physical evidence for coastal features linked with former RSL both on topographical and bathymetric data. After a brief description of the features forming on rocky coasts (section 4.1), the extensive previous work on the terrestrial raised shorelines will be presented and analysed (section 4.2). The potential for suitable data whether erosional or depositional is explored in the histogram of the bathymetric data (section 4.3.1) and the extensive corpus of newly identified submerged marine terraces is presented. These are analysed in terms of their local geological and environmental context and its influence on their morphological parameters to understand their relationship with former RSL (sections 4.3.2 and 4.5).

Chapter 5 pushes the analysis further by modelling the formation of the rock coast profiles of the study area. The wave erosion model, presented in section 3.3, is run using four of the recently published GRMs (Brooks et al., 2008; Bradley et al., 2011; Kuchar et al., 2012) to test the origin of some of the previously recognised marine terraces. The modelled output are then compared to the measured profiles to select the parameters for the best fit (section 5.3). This analysis aims at identifying the actual influence of the postglacial RSL change on hard rock erosional features in terms of their formation and preservation.

Chapter 6 presents the exploration of the stratigraphical sequence of local seismic data for any depositional evidence of recent RSL change. Published seismostratigraphic knowledge from the area are first analysed. The whole corpus of seismic data both already used in publication and more recently collected is consistently examined for ground truthing targets (section 6.1). Such ground-truthing survey was undertaken in order to core at target locations to geologically correlate their seismic stratigraphy (section 6.2). After the correlation of the local evidence to build a regional stratigraphy described in sections

6.3 and 6.4, the significance of the depositional scenario for the local RSL change is presented in section 6.5.

Finally in chapter 7, the various lines of evidence from the study area will be compared and tested in light of their RSL meaning. Evidence from the erosional model presented in chapter 5 are used first to understand the age and formation of the marine terraces described in chapter 4 (section 7.1). And secondly, the newly identified RSL indicators are analysed and compared in light of the GRMs' RSL simulations (section 7.2.1). In particular, the evidence for a differential glacial rebound is presented (section 7.2.2).

In conclusion, Chapter 8 suggests general recommendations for future generations of Glacial Rebound Models.

Chapter 2

Study area and origin of its coastline

This chapter will present the modern coastal landscape for the northern coast of Ireland. First the geological context is presented chronologically and a brief description of the subglacial evidence of Quaternary glaciations is analysed. Modern coastal features are described then highlighting the potential for preserved submerged relict shorelines. Finally the state of the RSL research for Ireland is presented displaying the discrepancies between field data and modelled curves.

2.1 Overview of the local geology and origin of the coastline

The study area extends along the north coast of Ireland from Torr Head in County Antrim through the northern coast of County Derry/Londonderry to Fanad Head in County Donegal (figure 2.1). The Geology of the area is dominated by the extensive Palaeocene basalt plateau and the coast outline is dominated by late Tertiary faulting that allowed the complex older metamorphic lithologies of the Dal Riada complex from the late Precambrian to appear in places. The main line of faulting is from the south west to the north east and has its origins in the Caledonian Orogeny from the Ordovician to the Silurian. As such all lithologies visible at the coastline extend north east from it. Two of the main three bays of the area are defined by such major faults: Lough Foyle has its origins in the Foyle fault and the town of Ballycastle, at the centre of Ballycastle Bay, lies over the Tow Valley fault. The third major bay of Lough Swilly is a fjord but also shows evidence of overdeepening linked with the Leenan fault (Evans, 1973). The bays along this coastline are marked by the softer sedimentary lithologies of Carboniferous sandstones and coal measures at Ballycastle Bay and Mulroy Bay, Triassic New Red Sandstone at Red Bay to the east of the study area and Jurassic Lias Clays at White Park Bay.

Beside the extensive volcanic activity at the origin of the Basalt plateau, further intrusive igneous lithologies appear clearly on the coastline. Two Tertiary Dolerite sill complexes form the headland of Fair Head in County Antrim and the skerries islands and portrush headland in County Derry/Londonderry.

The following short description of the local lithologies per geological eras is based on Holland & Sanders (2009).

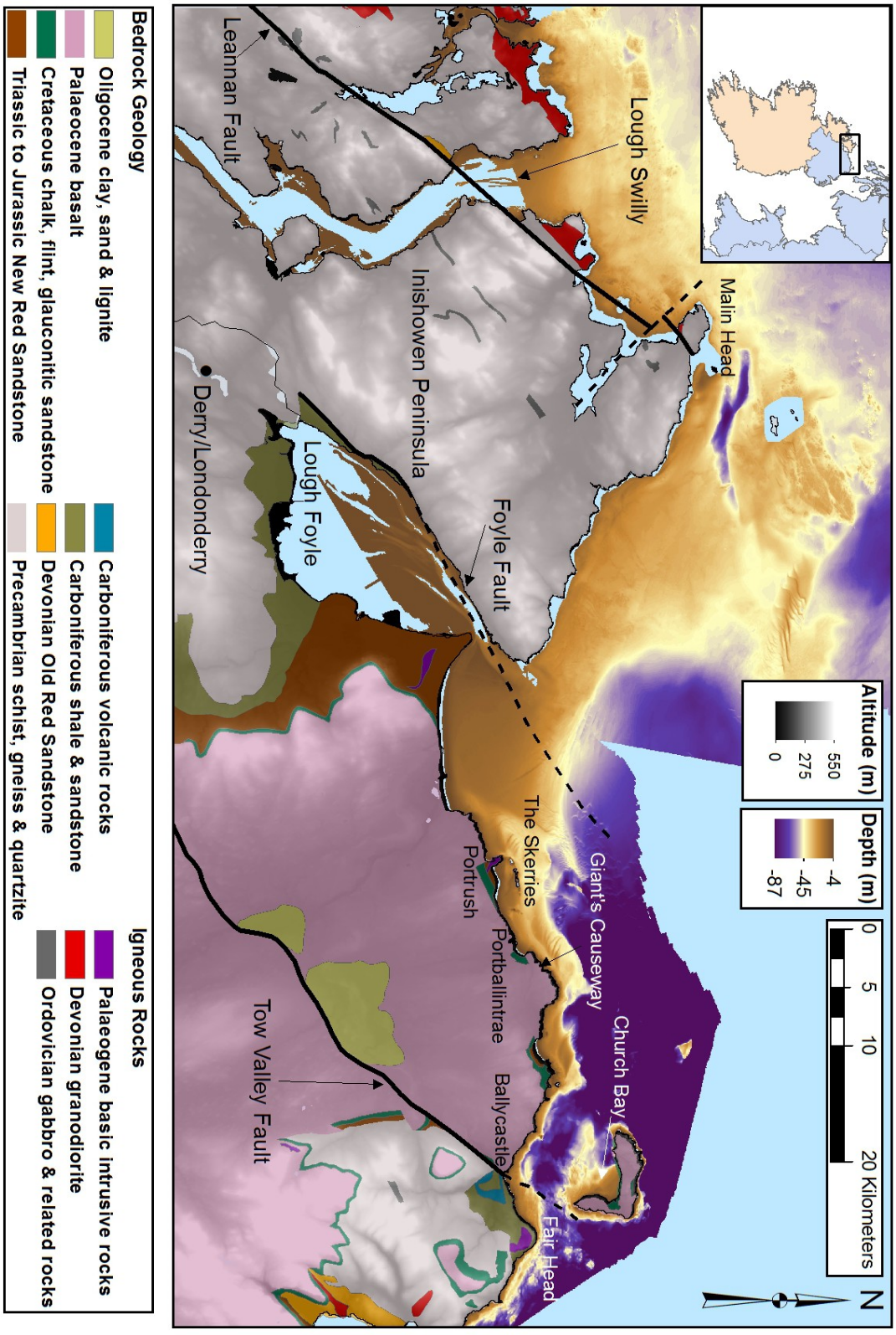

Figure 2.1: Local Geology of the study area draped over the topographic and bathymetric data. (data sources: Geological Survey of Ireland (GSI) for geology, Ordnance Survey Ireland (OSI) and Ordnance Survey Northern Ireland (OSNI) for the topography and Marine Institute (MI) for the bathymetry).

2.1.1 Precambrian metamorphic rocks

The late Precambrian metasediment basement for the area is named after the ancient gaelic kingdom of the north east of Ireland (Dal Riada) and has been found from Galway to Scotland. However, the oldest known rocks from the island of Ireland are syenitic orthogneisses of the Rhinns Complex exposed on Inishtrathull off Malin Head, at the top of the Inishowen peninsula. The Dalradian Group of lithologies mainly outcrops over most of county Donegal to the west of the Foyle fault but also appear between Ballycastle, east of the Tow Valley fault, and Cushendall. They are visible as rock cliffs over most of north Donegal, (apart from a granodiorite pluton outcrop toward the two opposing shores at the north end of Lough swilly) and from Murlough bay to Cushendun.

The eastern inlier is composed mainly of schist and schistose grit (figure 2.2) whereas the Inishowen rocks of Donegal are mainly Quartzite, Schist, Marble and Amphibolite (figure 2.3).

Figure 2.2: View of exposed Dalradian complex rocky coastline to the south east of Murlough bay showing gently sloping rock cliff with a modern shore platform and no beach.

Figure 2.3: View of Dalradian complex cliffs and raised terrace (3 to 4m above modern sea-level) on the north coast of Inishowen.

2.1.2 Late Caledonian orogeny and related magmatism

Gabbro intrusions of Ordovician age are present in the Dalradian complex alongside the north-east south-west main lines of deformations linked with the closure of the Iapetus ocean and the late Caledonian orogeny.

The Fanad pluton, a granodiorite pluton dated to the Devonian outcrops to the north of the Lough Swilly estuary. It is linked with the main Donegal pluton of further south-west.

2.1.3 Devonian to Cretaceous sedimentary rocks

Resting unconformably above the Precambrian Dalradian complex, the Devonian Old Red Sandstone is only present on the northern coast to the south east of the study area at Cushendall. The formation is 1.38km in thickness and is stratified by 620m of conglomerates, followed by 160m of sandtsones and topped by 600m of conglomerates. A raised marine terrace is visible in this top layer just north of the town of Cushendall at 3 to 4m above the modern shore platform (Prior, 1965 and figure 2.4)

Carboniferous (Visean) sandstones, where the famous coal measures were formed, and shales form the eastern part of Ballycastle Bay between Fair Head and Ballycastle town (figure 2.5). These extend offshore towards the Tow Valley fault (Westley, pers. comm.).

Triassic sandstone and mudstone outcrop at the coast south of Cushendall although dating of this formation is still uncertain and it could actually come from the Devonian.

Figure 2.4: Former seacave at the north of Cushendall (Prior, 1965) formed in the Old Red Sandstone conglomerate.

One of the most famous features of the landscape in the study area are the cliffs and modern platform system of the Ulster White Chalk Formation. This lithology is linked to the Chalk Group of southern England but has a much greater hardness and lower porosity (see Hancock 1963 for an explanation of this phenomenon). It has a maximum thickness of over 120m and lies unconformably over the local basal greensand and Lower Jurassic (Lias) marine clays which are only a few tens of metres thick. It is particularly visible at the White rocks east of Portrush, on the south coast of Rathlin Island (figure 2.6) and from Dunseverick to Ballycastle where raised terraces from the Holocene can be seen overlying the modern shore platform by 2 to 6m in places (figures 2.7 and 2.8). Nodules in the chalk are the main source of flints in Ireland.

Figure 2.5: Modern shore platform formed in the eastern side of Ballycastle Bay in the Visean sandstone with Fair Head in the background

Figure 2.6: Close up view of the chalk cliffs of Rathlin Island

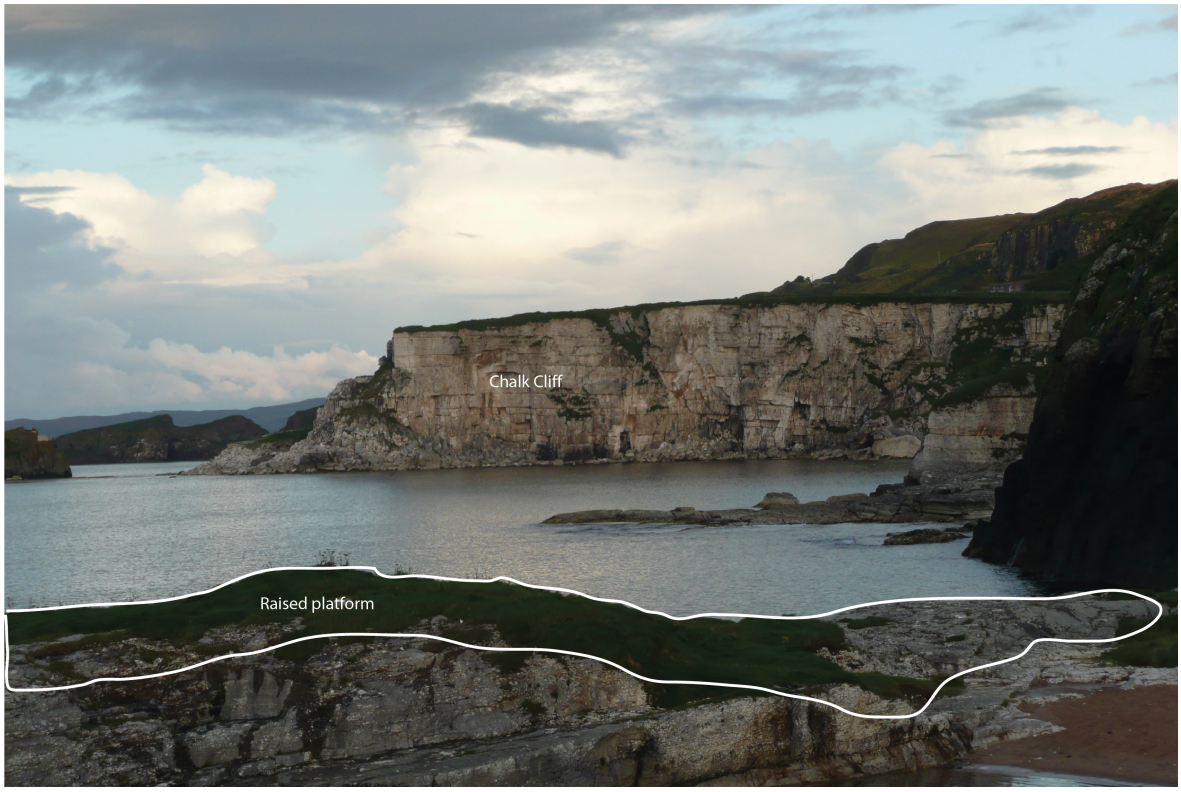

Figure 2.7: View east of Ballintoy harbour of chalk cliff and raised platform

Figure 2.8: Raised platform to the west of Ballycastle town

2.1.4 Palaeocene-Tertiary basalt

The landscape of the north-east corner of Ireland is dominated by the tertiary basalts of the Antrim Plateau, covering an area of some 4000km^2. These rocks occur as a series of horizontally layered lava flows with a total thickness of over 750m. The lava pile has been built up of very many individual flows ranging in thickness from less than 1m up to 30-40m. They form spectacular cliffs along the north and east coasts, including the Giant's Causeway which has been designated as a World Heritage Site for its cliff scenery and for its historical importance in the development of the science of geology (figure 2.9).

There are three main phases to the Antrim Lava group; the Lower Basalt, a widespread formation forming the escarpment overlooking Belfast and the cliffs of the north and east Antrim coast, an interbasaltic bed of lateritised basalts, residual bauxites and iron ores and the Upper Basalt, which occurs mainly as outliers on the higher ground in the north and east. To the north and west of the Tow Valley fault, a more localised series of basalt flows, the Causeway Basalts, interrupted the interbasaltic hiatus: these basalts are unusually fine grained and exhibit excellent columnar jointing (figure 2.10). Almost all the flows were interrupted and cooled subaerially (a few flowed into lakes).

Intrusive features such as plugs, dykes and sills, were formed alongside the extrusive acitivity. Most famous of all are the sill of the Skerries archipelago off Portrush and the great dolerite sill of Fair Head, well known for its glacially striated rock pavement (figure 2.5). This sill forms a promontory so distinctive it was recognised and charted on Ptolemy's map as Rhobodgium (Darcy & Flynn, 2008).

Figure 2.9: Modern and raised platform from the Giant's Causeway (picture by Kieran Westley)

Figure 2.10: Basaltic columns from the Giant's Causeway, under wikimedia commons licence

2.1.5 Offshore basins

The main sedimentary basin for the area is called the Rathlin Basin from the Tow Valley fault in the east to the Foyle fault. North west of it lies the Middle Bank which continues into the Islay-Donegal Platform further west. South east of the Tow Valley fault lie the Arran and North Channel Basins (figure 2.11 from Holland and Sanders, 2009). As detailed in the inset of figure 2.11, these basins are filled mainly by Mesozoic and Permian sedimentary rocks occasionally underlaid by Carboniferous sedimentary rocks as in the Rathlin Trough.

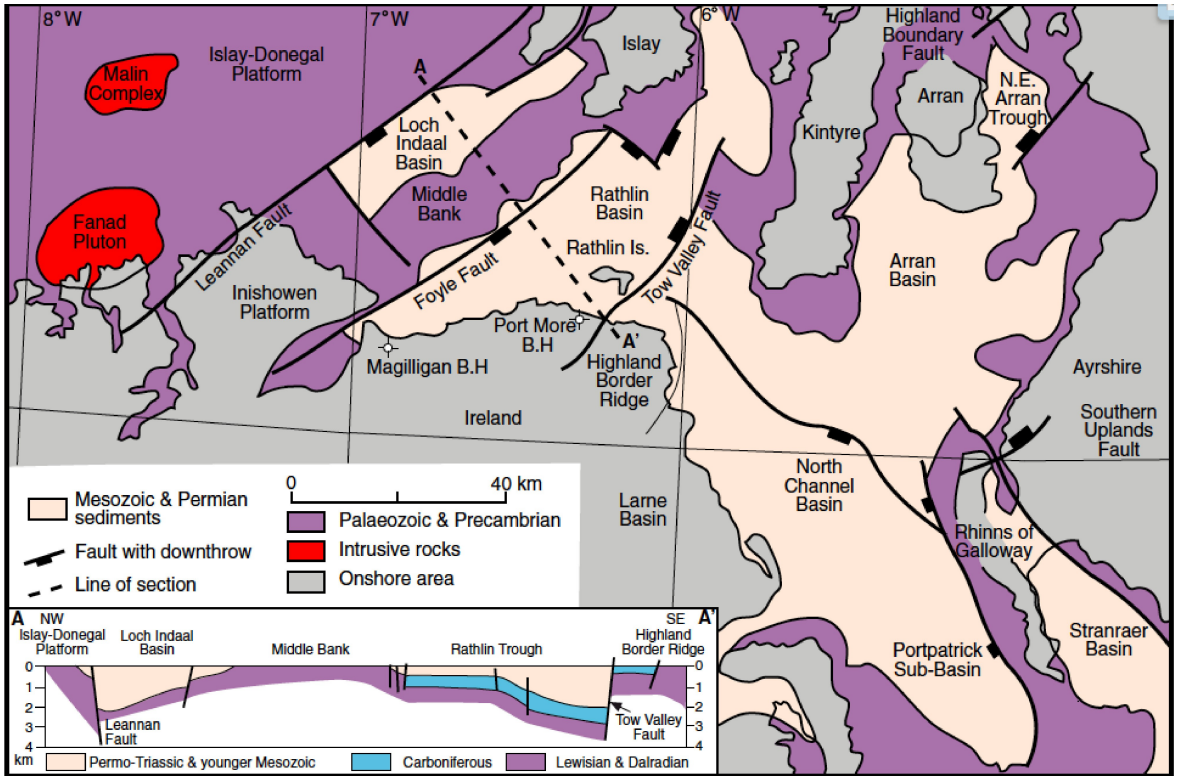

Figure 2.11: Offshore depositional basins for the larger region of the North-East of Ireland (from Holland and Sanders, 2009).

2.2 Quaternary evolution of the landscape

In an effort for consistency and to fit the majority of the current literature, the ages reported in the sections below are in calendar ages BP (1950) unless stated otherwise.

2.2.1 Evidence on land

There is clear evidence for two glaciations in the study area (Knight et al., 2004). The earlier glaciation is inferred to be of Scottish origin from shelly till lithofacies distribution and microgranite erratics of Ailsa craig origin (Kilroe et al., 1888). It has been suggested that it corresponds to the Marine Isotope Stage (MIS) 6 (175,000 to 120,000 years BP) although dating and extent is uncertain (Stephens et al., 1975; Coxon and McCarron, 2009).

The second and latest glaciation corresponds to the MIS 2 to 4 that started around 80,000 years BP and reached its climax in terms of ice extent at the Last Glacial Maximum 20,000 years BP (McCabe and Dunlop, 2006; Dunlop et al., 2010). Irish and Scottish ice are believed to have been confluent in the North East of Ireland then with Irish ice thick enough to prevent extensive penetration by the Scottish ice. Ice flow was mainly from the centre of ice in Lough Neagh to the north as evidenced by the drumlin field of the Bann valley and the carriage of local indicative erratics. As far as the western part of the study area is concerned, the recently published maps of Greenwood and Clarke (2008) indicate the main ice flow to be following a south west to north east trajectory that aligns with the main faults and modern river flow of the area (figure 2.12).

As the Irish ice decayed from 20,000 till 15,000 years BP, the ice front retreated south but was followed by a readvance of Scottish ice that ended in the Armoy moraine forming an arc from Ballycastle to Coleraine through Armoy and Ballymoney (figure 2.13). A glaciolacustrine stratigraphy south of Armoy has its origins in a meltwater lake sitting in between the Scottish ice front and the retreating Irish ice front (Creighton, 1974). Drumlinisation, indicating rapid ice flow, is thought to have occurred in the north of Ireland at c. 17,000 years BP (McCabe et al., 1986) . The age of the Antrim coast advance/Armoy stage is conjectural and has been nominally placed at c. 14,000 years BP (Stephens et al., 1975) but more recent work (Clark et al., 2012) suggests it is likely to be much earlier (c. 17,000 years BP). Hence it has been suggested that north-eastern Ireland's coastline becomes ice free 16,000 years BP and that ice had retreated to the south of the study area by then (see Clark et al., 2012 for a recent review).

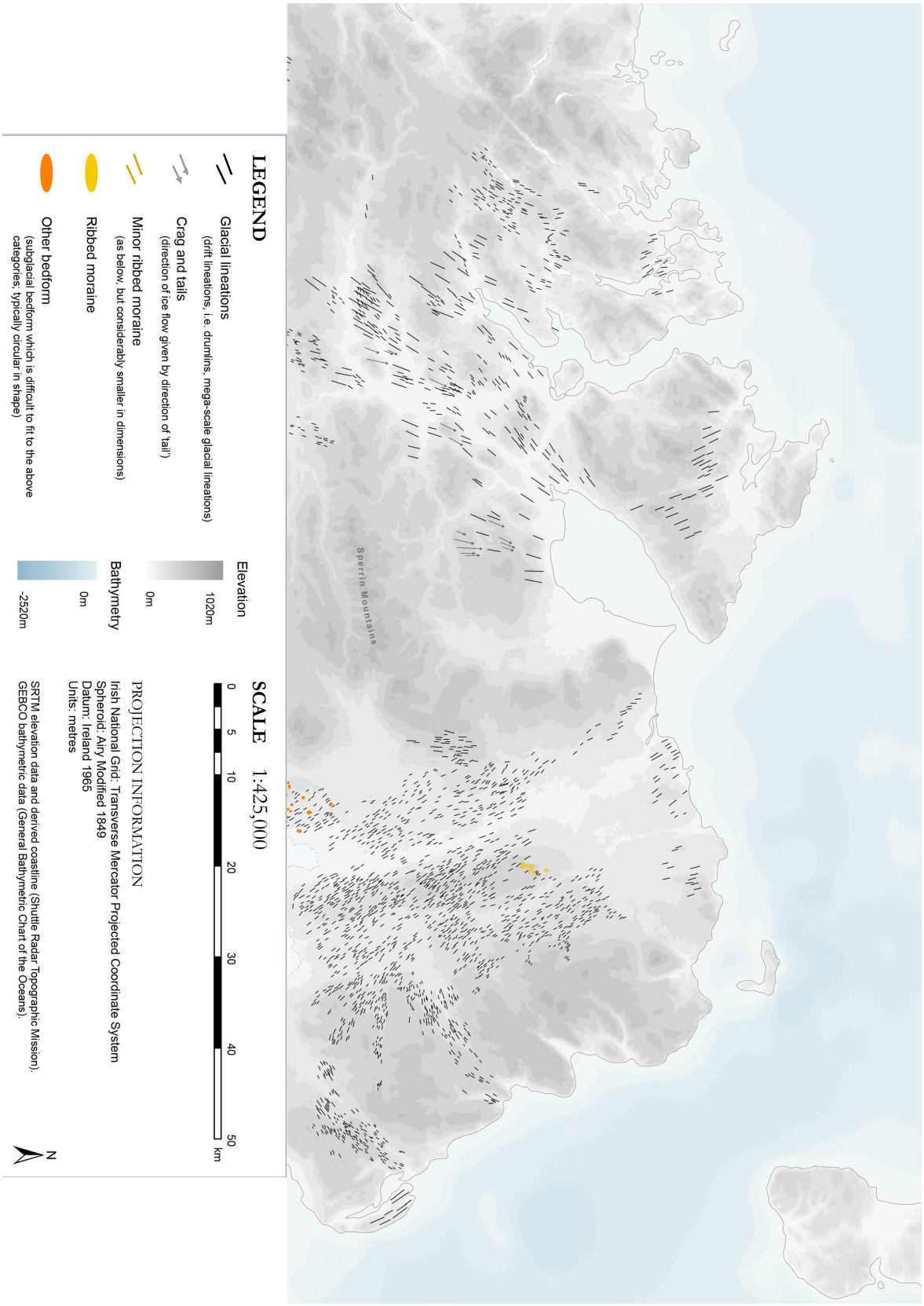

Figure 2.12: Close up of the study area for maps from Greenwood and Clark (2008) displaying subglacial bedforms.

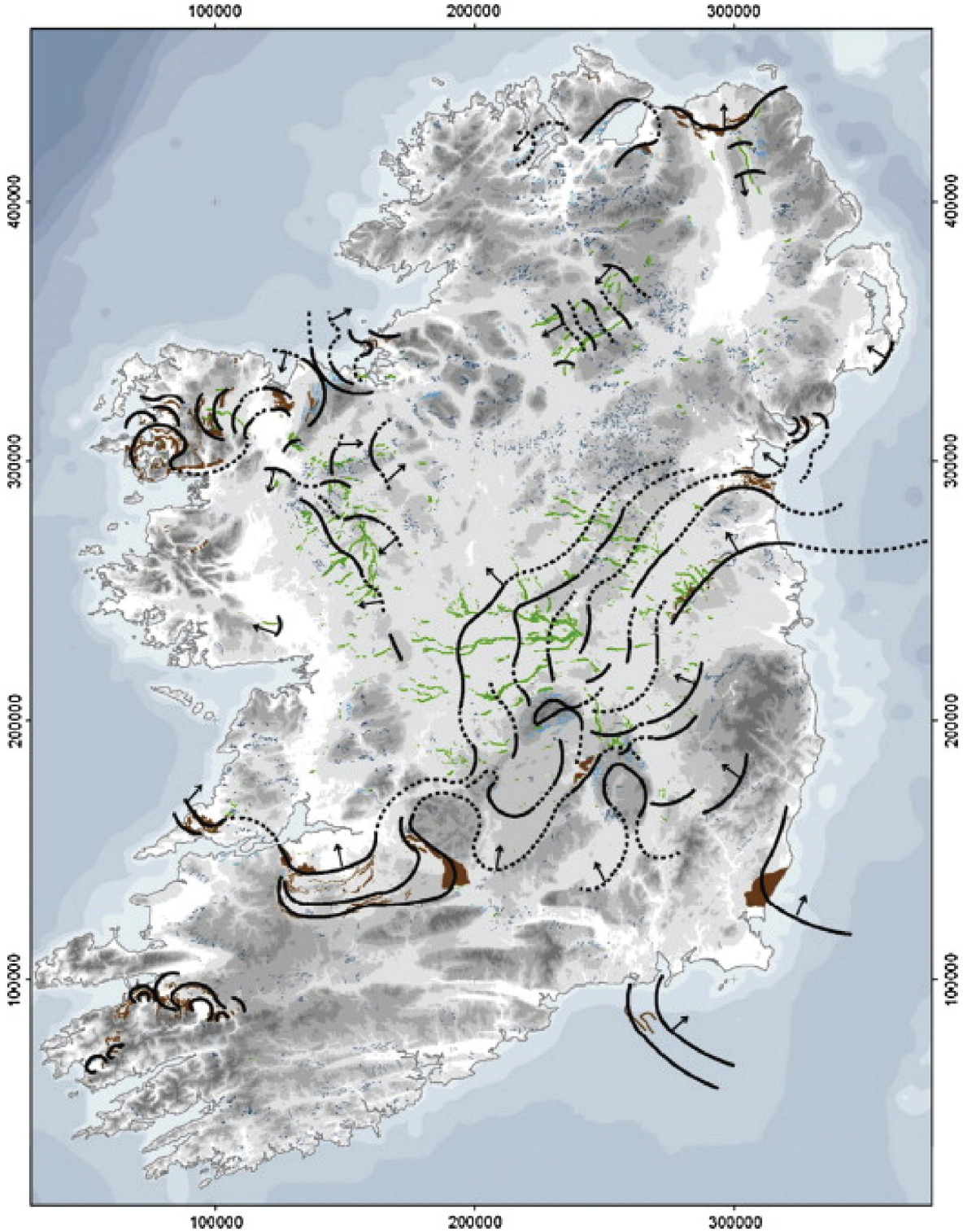

Figure 2.13: Map from Clark et al. (2012) of the moraines (brown) and meltwater landforms (eskers in green and channels in blue) of Ireland with reconstructed ice sheet margin positions (solid black lines, dotted are only conjectural). The Armoy moraine appears clearly as the semi circle to the north of Antrim with the arrow pointing north.

Similarly, the Irish ice was not monotonically retreating after the LGM. Ice sheet readvances have left some clear evidence in their terminal moraines, sometimes associated with raised coastlines features such as swash gullies, washing limits, gravel ridges and erosional notches and terraces (McCabe, 2008b). Several segmented lines of moraines are still visible following the northern coast of Donegal from the Lough Foyle mouth to Bloody Foreland situated to the west of the study area and although not continuous, it has been suggested that they are all contemporaneous (McCabe, 2008b). A push moraine at the mouth of Lough Foyle (Stephen and Synge, 1965), associated with a raised shoreline continuing along the modern lough to the south, and a truncated moraine at Trawbreaga bay (McCabe and Clark, 2003) to the north west of the Inishowen peninsula allowed a tentative date to be given to this readvance of between 15,000 and 14,000 ^{14}C years BP (thanks to radiocarbon dated foraminifera in reworked marine sediments at Corvish (McCabe and Clark, 2003)).

Contemporaneous with the Scottish ice readvance towards the north-east coast c.17,000 years BP, another ice sheet readvance (the Killard Point readvance) has been recorded in county Down, south of the study area. This was preceded by a more extensive readvance (the Clogher Head readvance) that was dated to c. 18,000 years BP on the basis of radiocarbon dated foraminifera from marine muds overlain by till, boulder pavement and glacial outwash (figure 2.14). These are closely associated with raised beaches and erosional shoreline features and were used to date some of them in the region and reconstruct the local sea-level curve (McCabe et al., 2007).

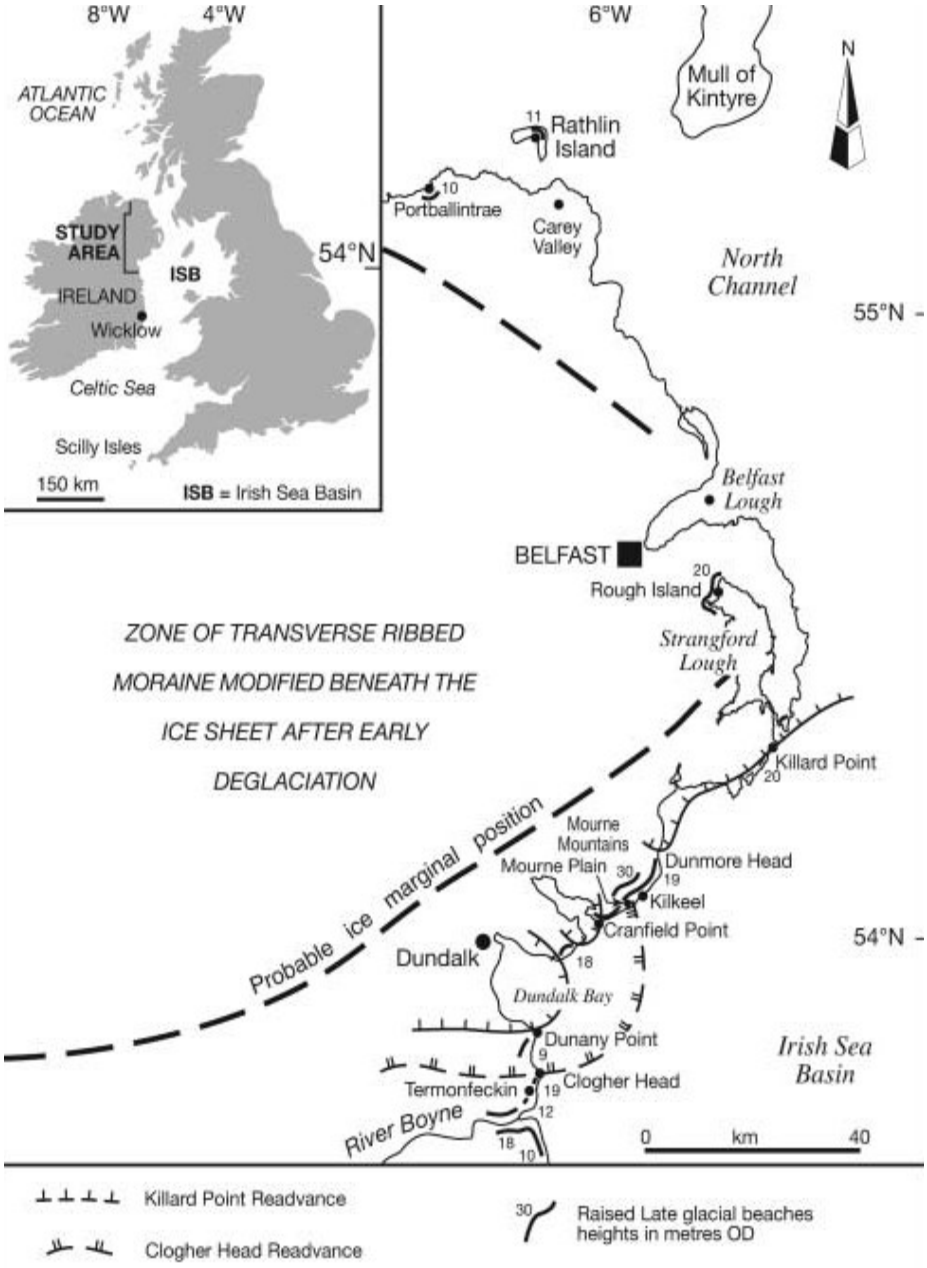

Figure 2.14: Location of North eastern Ireland post-LGM ice-sheet readvances terminal moraines (from McCabe et al., 2007)

2.2.2 Offshore evidence

No subglacial or periglacial landforms have yet been identified on the seabed of the study area. It is likely that some may exist buried under reworked sediments or that some existed but were destroyed/overridden by the Armoy advance stage. Submarine moraines were identified further to the north west, on the Malin shelf, and all along the west coast of Ireland (Benetti et al., 2011 and figure 2.15).

2.3 Coastal landscape

2.3.1 Contemporary coastal geomorphology

Wave action is a key factor in the formation of any shoreline and this is commonly described in terms of wave frequency, height, direction and variability. The north of Ireland, due to the preponderance of westerly driven weather system from the north Atlantic, is subjected to regular swells with a general north west to south east orientation throughout the year. The waves crashing on the rocky cliffs and platforms and shaping the softer beaches and sand bars are then refracted differentially by the headlands along the coastline. The tides are semidiurnal with a spring tidal range of around 3.5m in the west of the region, decreasing to around 0.9m in the east. The environmental conditions of exposure to modern wave action and local tidal range are presented in tables 2.1 and 2.2 based on data from the weather buoys of the Irish Department of Transport and the British Admiralty tide tables (2011) respectively. In addition to these usual conditions, regular cyclonic passages form sea waves with significant deep-water wave height (in the range of 15-20m, Devoy, 2000) with 50 year extreme wave heights of about 25m inshore (Carter & Draper, 1988).

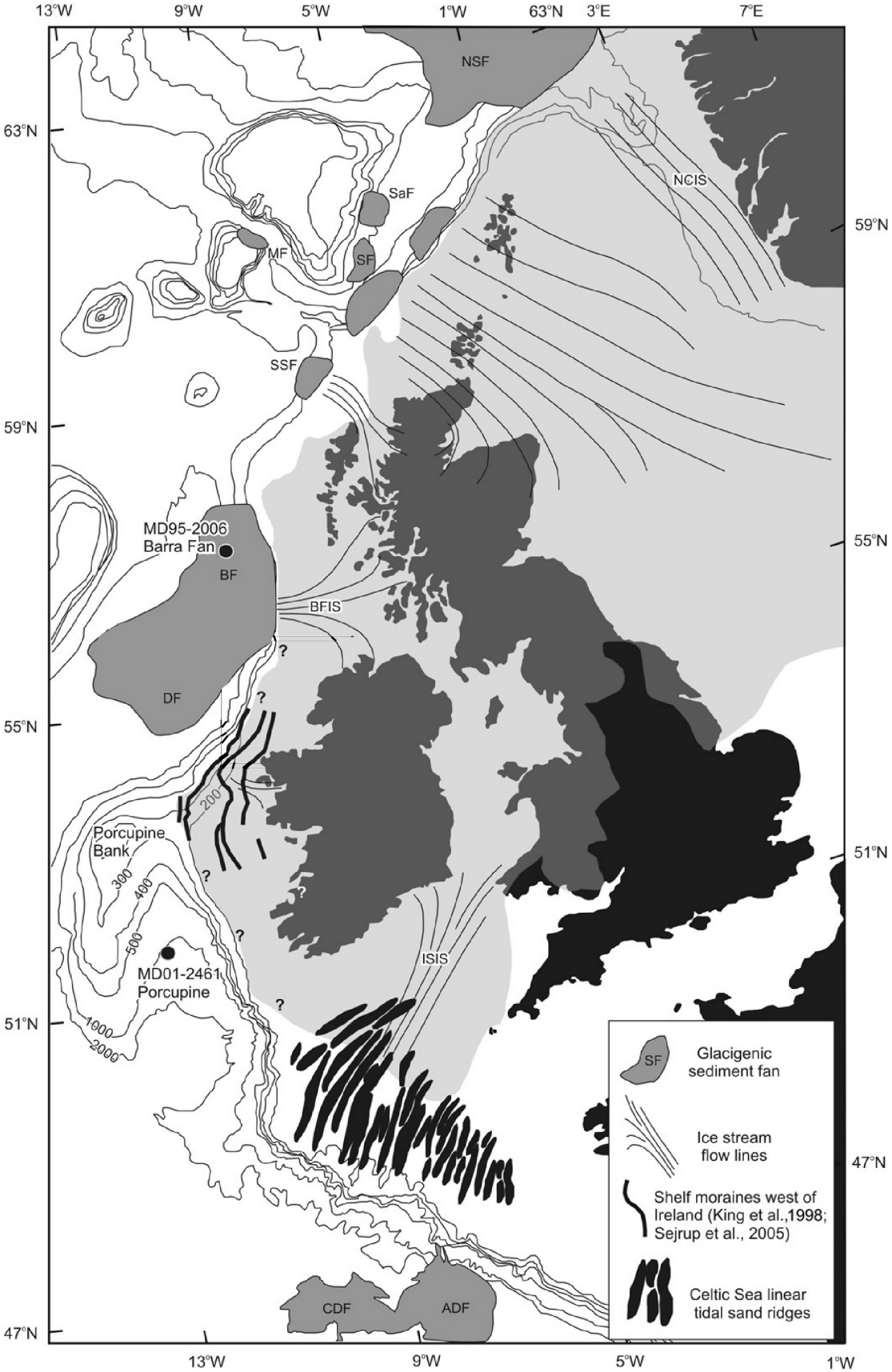

Figure 2.15: Map from O'Cofaigh et al. (2012) highlighting the end moraines, ice streams and sediment fans visible on the shelf around Britain and Ireland.

H_0 (m)	F (%)	T (s)
<1	5.6	5.1
1–2	31.0	5.7
2–3	28.2	6.7
3–5	26.0	7.8
5–7	7.1	9.2
7–9	2.1	10.3

Table 2.1: Summary wave data derived from the Irish Department of Transport buoy M4 (Station 62093), Donegal Bay (water depth = 72m). H0 = binned significant wave height (metres); F = proportion of the total record in each bin; T = average wave period within each bin (seconds) (from Thébaudeau et al., 2013).

The high energy, wave dominated coastline of the north of Ireland comprises rocky cliffs and shore platforms (figures 2.3 to 2.9 and section 4.1), commonly associated with gravel ridges, beach sand and aeolian dune deposits (Carter, 1982; Jackson et al., 2005). The sediment supply for these deposits comes from reworking of shelf sands of glacial origin (Cooper et al., 2002) or local erosion of bluffs of glacial sediments (Carter, 1991). In places, this rugged coastline is punctuated by more sheltered sea loughs (estuaries of glacial inheritance such as Lough Swilly and Lough Foyle) and embayments (such as Church Bay in Rathlin Island) which permit the accumulation of lower-energy, finer grained estuarine sediment (Carter, 1982). Whilst rocky coasts are traditionally regarded as being less vulnerable to the effects of climate and sea-level change than their lower-energy sedimentary counterparts (Nicholls et al., 2007; Cooper, 2007), their actual resilience is poorly quantified and a better understanding of long-term rocky coast evolution is required (Naylor et al., 2010). This issue has particular significance along the rocky coast of the north of Ireland, not least because of the presence of the Giant's Causeway World Heritage Site and associated concerns regarding climate-related increases in erosion and inundation (Orford et al., 2007).

Tidal Station	Tidal Data (m OD Malin Head)			
	MHWST	MHWNT	MLWNT	MLWST
Ballycastle (Area 1)	+0.5	+0.2	−0.1	−0.4
Portrush (Area 2)	+0.7	+0.6	−0.3	−0.8
Fanad Head (Area 3)	+1.3	+0.3	−1.2	−2.2

Table 2.2: Summary tidal data for the three locations (m OD Malin Head). MHWST = Mean high water of spring tides; MHWNT = mean high water of neap tides; MLWNT = mean low water of neap tides; MLWST = mean low water of spring tides (from Thébaudeau et al., 2013).

2.3.2 Relict coastal features

In addition to its actively forming features, relict coastal landforms and facies are exposed along the northern coast of Ireland at a range of elevations above their contemporary counterparts (Praeger, 1896; Coffey and Praeger, 1904; Movius, 1953; Stephens, 1963; Prior, 1965; Orme, 1966; Synge and Stephens, 1966; Carter, 1982). This varied association of 'raised shorelines', which consists of erosional features such as rock platforms, notches, terraces and 'washing limits', and depositional features such as gravel ridges, or marine deltas, has been cited as evidence of higher than present relative sea-level resulting from glacioisostatic rebound of this formerly glaciated region (Devoy, 1983; 1995; McCabe et al., 2007). Similarly, investigation of the inner shelf has identified potential beach deposits and erosional notches now submerged by several tens of metres of water, suggestive of periods during which RSL was below present (Cooper et al., 2002; Kelley et al., 2006). These lines of evidence will be presented in more details in sections 4.2 and 6.1.

2.4 Relative sea-level

The RSL history of the region is strongly controlled by the combined effects of local ice loading and the influence of adjacent ice masses over Britain and Fennoscandinavia. The resulting complex interplay between glacioisostatic rebound and eustatic sea-level rise is expressed as an oscillating postglacial RSL curve that comprises intervals with sea levels both above and below present (McCabe et al., 2007; Brooks et al., 2008).

2.4.1 Sea-level data and RSL reconstruction

Figure 2.16 shows the available sea-level data points for the study area, representing the evidence available in the literature and were classified for the whole of Ireland into a sea-level database (Brooks and Edwards, 2006). There is a comprehensive lack of reliable precise data as no Sea-Level Index Points (SLIP) were published for the study area. SLIPs are a central development of recent RSL studies (Edwards, 2005) as they aim to fix precisely the past elevation of RSL in both time and space. In brief, such a data point must contain information regarding its location, its elevation, its age and its indicative meaning defined as its vertical relationship to contemporaneous tide level (Brooks and Edwards, 2006). Limiting dates are dated samples which were deposited outside of the tidal frame and so constrain the contemporaneous RSL by providing either a maximum or a minimum limit (Brooks and Edwards, 2006). Limiting dates were further categorised into primary (1) and secondary (2) based on the level of understanding of their source environment. A number of limiting dates were recognised in the study area but most of these give information for the Holocene and, due to their origin on land, correspond to periods when the relative sea-level was higher or similar to today's level. These limiting dates vary in origin from basal peat, organic soil and sediment deposition, corresponding to either a terrestrial or marine context, to shells and wood fragments, whose natural habitat is defined by a particular relation to sea-level (Brooks and Edwards, 2006).

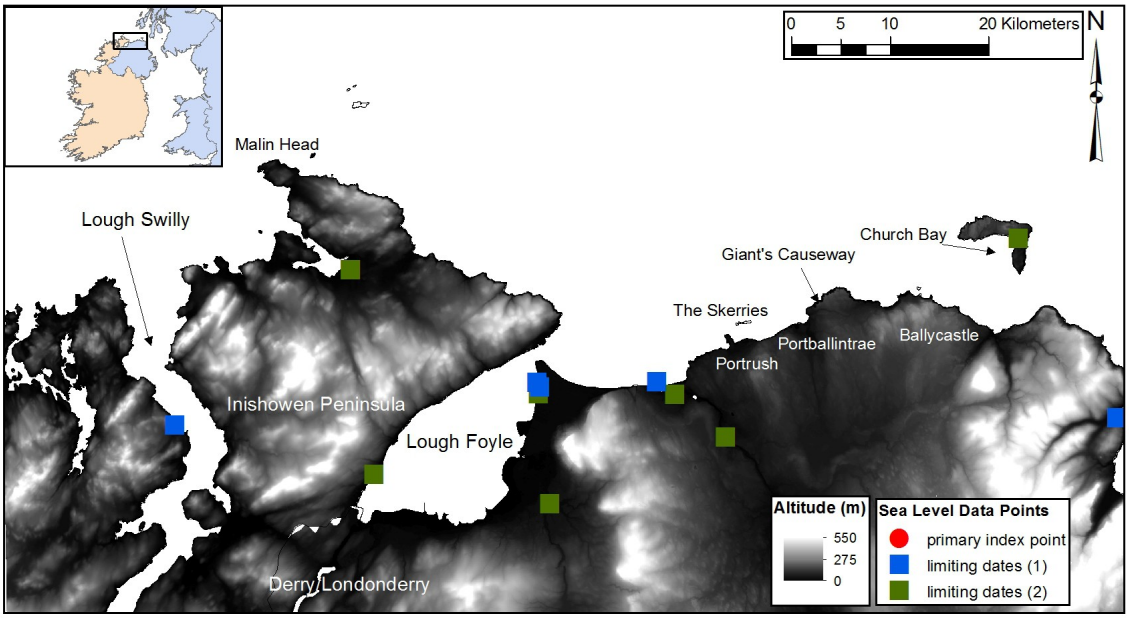

Figure 2.16: Map displaying the published sea-level data and their classification for the study area (after on Brooks and Edwards, 2006).

2.4.2 Glacial rebound models

In the absence of precise local RSL data for this period (Carter, 1982; Brooks and Edwards, 2006 and figure 2.16), a range of glacial rebound modelling studies have been undertaken and RSL scenarios were derived from them (Lambeck, 1991; 1993a; 1993b; 1995; 1996, Shennan et al., 2000a; 2000b; Lambeck & Purcell, 2001; Peltier et al., 2002; Shennan et al., 2002; 2006; Brooks et al., 2008; Bradley et al. 2011; Kuchar et al., 2012). Glacial Rebound Models (GRM) are geophysical models that simulate the local amount of depression and rebound of the continental crust due to ice and water loading. They are also called Glacial Isostatic Adjustments (GIA) models. The models are composed of three elements: an earth model where the thickness and elasticity of the lithosphere are defined; an ice model to define the thickness of the local and global ice geographically and chronologically based on our current understanding of ice centres and ice flows; an algorithm to compute changes in relative sea-level based on the most recent form of the sea-level equation (Mitrovica and Milne, 2003). The model is run over the length of time of the defined ice model starting (for instance, with ice loading at the last interglacial (MIS 5e)) and computing its effect on RSL at predefined time steps. The outputs are then compared with RSL data from the various localities and adjustments in the ice model and

earth model parameters can be made to try and fit the observable data.

Glacial rebound in the British Isles is a complex issue due to the various interactions of the major ice centres in Fenno-scandia and Laurentia and the local British and Irish Ice Sheet (BIIS). After the early applications of GRM for the British Isles (work of Lambeck since 1993) several new iterations were built following advances in the sea-level equation and improvements in the speed of computation and the size of database of new computers. These new iterations allowed the addition of processes overlooked in earlier simpler models such as hydro- and glacio-isostasy, earth rotational effects on the local and global sea-level and terrain correction significantly altering the ice thickness in mountainous areas. In Brooks et al. (2008), a new ice model is defined for Ireland based on more recent geological evidence for a more laterally extensive Irish Ice Sheet than had been previously postulated (see McCabe and Dunlop, 2006; Ballantyne et al., 2007; 2008) and the latest sea-level equations are used (Mitrovica and Milne, 2003). The model is compared with the range of RSL data that were classified in their previously published database (Brooks and Edwards, 2006). Significant improvements in the fit of the data compared to the earlier, more general, models helped build a new understanding of the environment evolution of Ireland since deglaciation, in particular on the presence or absence of a land bridge between Ireland and Britain (Edwards and Brooks, 2008).

However, discrepancies between some of the data and modelled RSL curves, notably in North Mayo (figure 2.17) and the north east (figure 2.18), were still present and provided reasons for some of the research community to disbelieve the modelling approach altogether (McCabe, 2008a; Edwards et al., 2008). This conflicting evidence is based on dated marine muds (using radiocarbon dates of associated monospecific assemblages of either foraminifera or bivalves) and show discrepancies from the modelled curve of up to 60m in North Mayo (figure 2.17). Furthermore, a reconstruction of the RSL change was built for the whole North East of Ireland based on various field evidence (shingle ridge, raised marine muds and palaeochannels filled with marine muds plotted on figure 2.19) from various areas (McCabe et al., 2007). This curve (figure 2.18) shows dramatic variation in a very short period of time indicating a very dynamic interaction between isostatic rebound and eustatic variation; so dynamic in fact that the RSL rises and falls with rates of several 10s of mm/year in close succession where the modern maximum measured uplift rate is close to 10mm/year near Hudson Bay in northern Canada where the ice was

thickest during the LGM (Sella et al., 2007). The lines of evidence used for this reconstruction came from various locations that models described as separate with varying local RSL change that therefore cannot be combined in one area. Even in individual localities, critical evaluation of each of the datapoints points to uncertainties in the associated indicative meaning of the order of several meters (Edwards et al., 2008). Nevertheless, they pointed to real issues in the modelling of RSL change in Ireland linked with either the ice model or the earth model used.

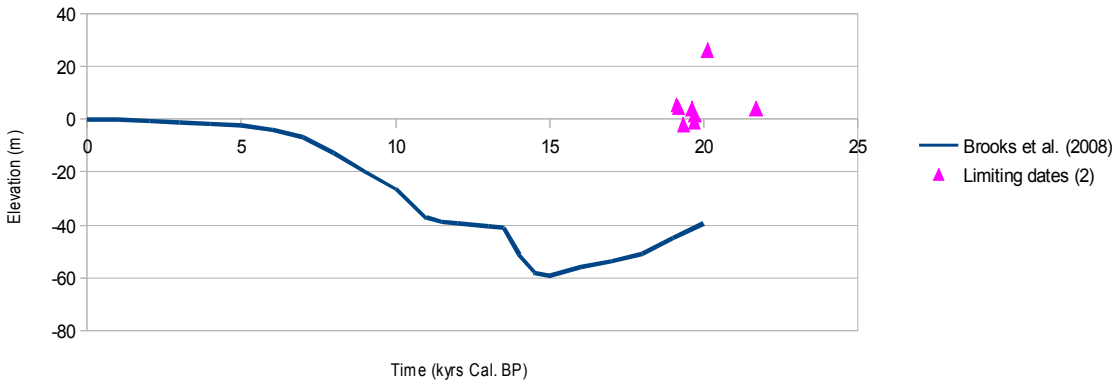

Figure 2.17: Computed sea-level curve (Brooks et al., 2008) and associated sea-level data for North Mayo.

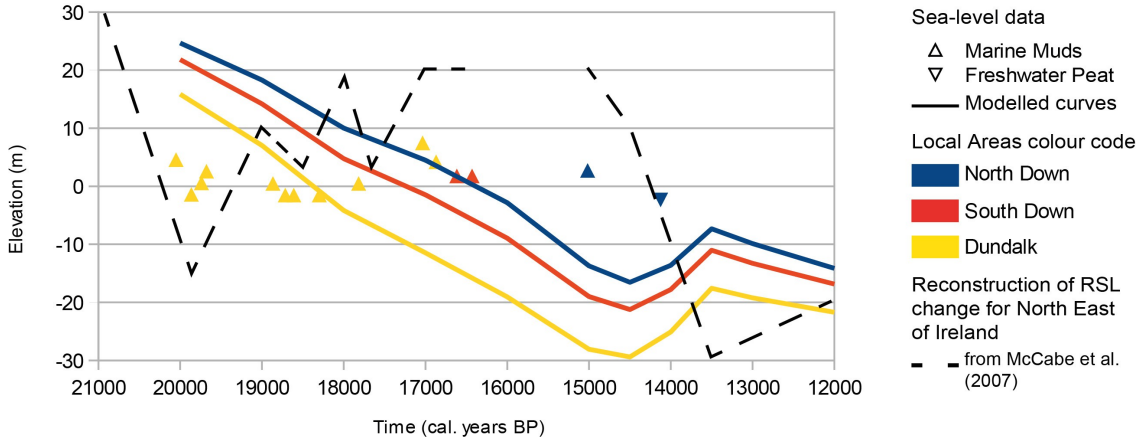

Figure 2.18: Computed sea-level curve (Brooks et al., 2008) with associated sea-level data for the three areas of North Down, South Down and Dundalk. The published RSL reconstruction (McCabe et al., 2007) based on the sea-level data alone for the whole North East of Ireland has been added.

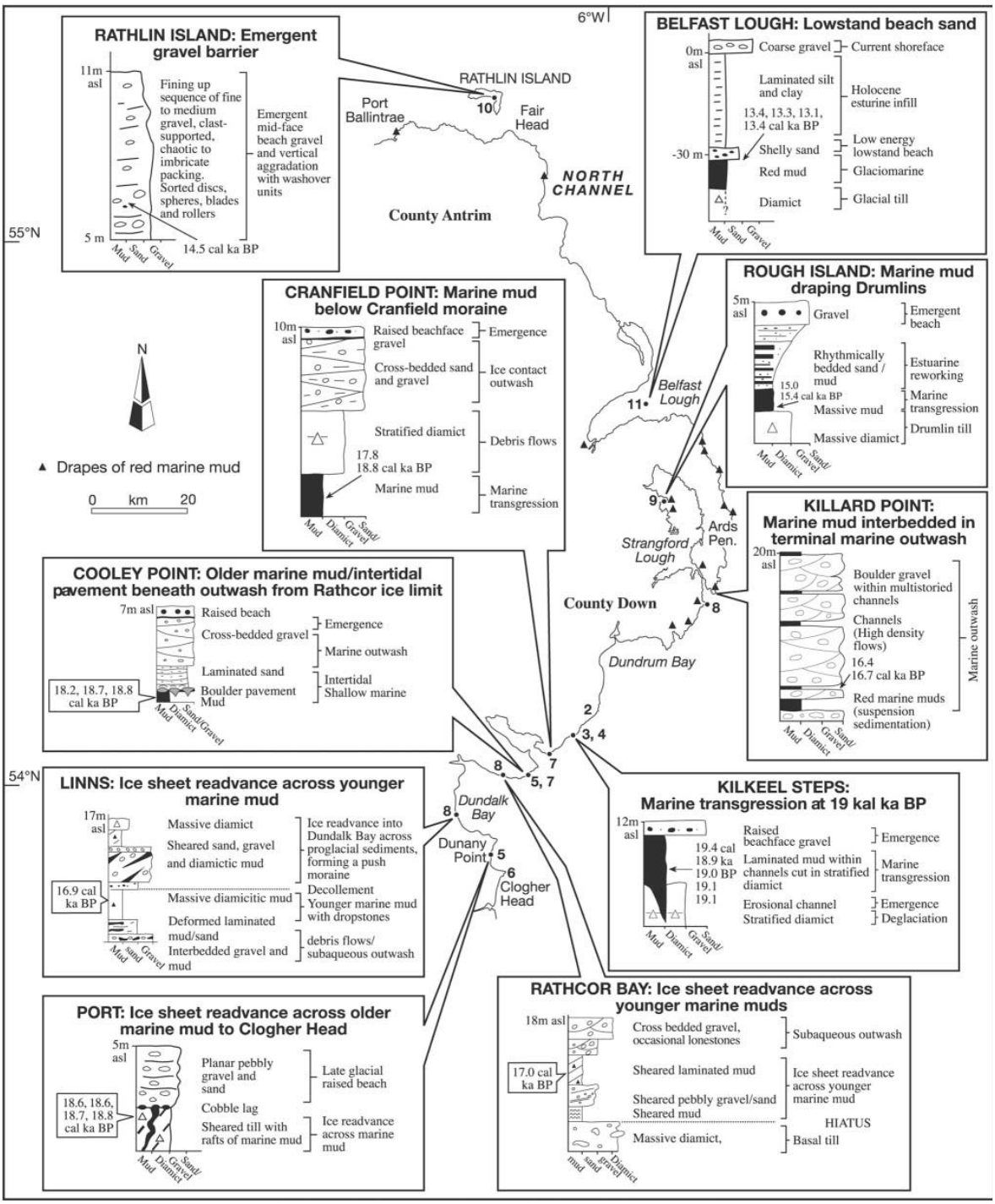

Figure 2.19: Schematic log of critical sedimentary successions at sites exposed in the north east of Ireland (from McCabe et al., 2007).

In Bradley et al. (2011), a new eustatic modelling of the melting history of the non-local ice sheets is used to build a more accurate prediction of the global and local eustatic sea-level change. New GPS data on crustal movements are used to constrain further the earth model. But the ice model is the same created for the Brooks et al. (2008) model. The RSL curves modelled show a much more constrained range of change for the RSL with lower highstands and shallower lowstands than previously modelled. But the major discrepancies described above were still not resolved.

Further work using the earth model and sea-level equation of the Bradley et al. (2011) was published by Kuchar et al. (2012). In this novel study, three numerical ice models built from palaeo-climate and environmental data (Hubbard et al., 2009) rather than observations of ice extent (moraines) and thickness (trimlines) are input as the ice model driving the Glacial Rebound Model. These three models of minimal, median and maximum ice volume produced ice sheets much thicker than reconstructions based on trimlines suggested. Although similar methodologies were used for the larger, thicker and more extensive ice sheets such as Fenno-Scandia, no attempt had previously been made to use it with the more complex case of the British Isles. The fact that this process produced misfits between the RSL curves and the observed data of similar order (but larger) than the previous two models suggest that trimlines should be reinterpreted as boundaries between warm- and cold-based ice (Ballantyne, 2010). Earlier discrepancies were still not resolved.

The main differences between the reconstructed and modelled RSL curves for Ireland are due to the rates and magnitude of glacial uplift that are constrained for the modellers by the mantle viscosity of their earth model and tend to build a much less “abrupt” curve. Most recent studies (Shennan et al., 2006; Brooks et al., 2008; Bradley et al., 2011) tend to attempt to fit RSL data to modelled curves through the adjustments of the viscosity of the lithosphere and of the upper mantle in a range defined in Dziewonski and Anderson (1981). Whereas reconstructions such as the one published by McCabe et al. (2007) use the RSL data as extremities for their curves without consistent considerations of their indicative meaning or the physical constraints associated with such rapid transition of movements (figure 2.18). Although crustal movement due to active faulting might bring potential abrupt differences in the evolution of RSL from one locality to another locality separated by a fault, such considerations have proven out of reach for the current generation of GRMs as consistency in RSL change from one locality to its neighbouring

ones is an integrate part of the modelling process. The difficulty in reconciling the two methodologies is clear in places where there is a lack of precise RSL data such as Ireland (McCabe, 2008a; Edwards et al., 2008) and, in particular, the study area.

2.4.3 RSL change for the study area

The latest modelled RSL curves for the study area from Brooks et al. (2008), Bradley et al. (2011) and Kuchar et al. (2012) "minimal" and "maximal" ice volumes curves were used for this study for comparison. Whilst all the RSL curves show similar overall patterns, including differential east-west isostatic rebound, and an inflection at 14,000 years BP related to Meltwater pulse 1a, they differ in the rate of RSL change as well as the duration and magnitude of RSL high or lowstands.

Figures 2.20, 2.21 and 2.22 display the sea-level curves computed for the study area from the four afore mentioned more recently published GRMs plotted against the sea-level data published for the last 20,000 years. Assumptions from marine geophysical data on the local RSL lowstands made previous to this study were added to the plots for reference. These potential RSL constraints are a general break of slope at -30m depth for the eastern side of the study area (Quinn et al., 2008; 2009; 2010) as well as palaeochannels bottom depth and a particular seismic reflector thought to correspond to freshwater peat (Cooper et al., 2002; Kelley et al., 2006; Quinn et al., 2008; 2009; 2010). They were observed in bathymetric and seismic datasets and are presented in detail in chapter 6. The study area has been subdivided into three smaller region based on the distribution of RSL data points published; Antrim to the east, Derry to the centre and Lough Swilly to the West.

These curves share a similar evolution through the various GRMs and regions. They all show RSL higher than present at the time of early deglaciation and falling due to the isostatic rebound of the shelf until a first lowstand around 14,500 years BP. This is followed by a rapid rise due to the Meltwater pulse 1a at 14,500 years BP that makes way for continued sea-level falling as the isostatic rebound becomes prevalent again until a second lowstand at 11,000 years Cal. BP. As the rate of uplift decreases, the sea-level rises more steadily then until a Holocene highstand between 6,000 and 7,000 years BP (the date depends on the GRM) particularly in Antrim. As the rate of eustatic sea-level rise decreases and the slower uplift continues, the local RSL falls slowly to its modern level.

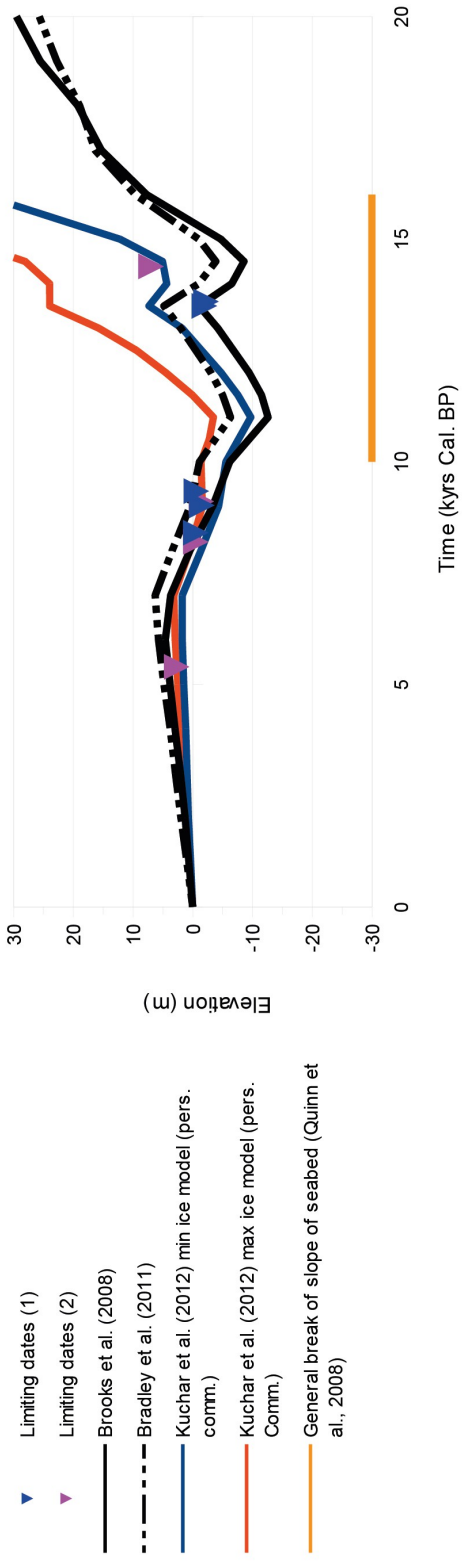

Figure 2.20: Computed sea-level curves and associated sea-level data for North Antrim (eastern part of study area)

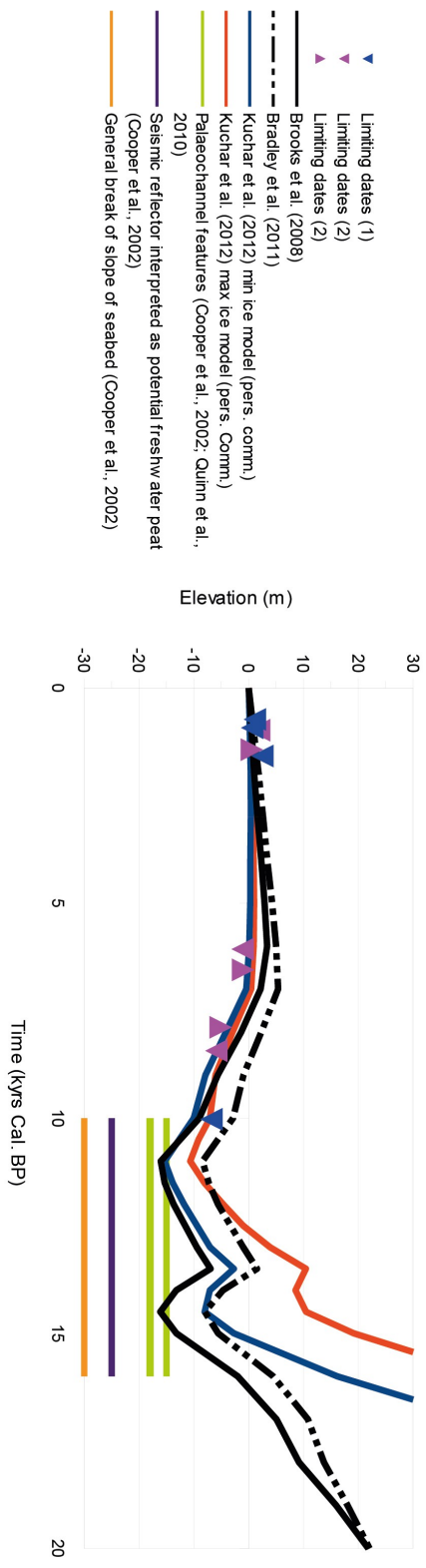

Figure 2.21: Computed sea-level curves and associated sea-level data for Derry (central part of study area)

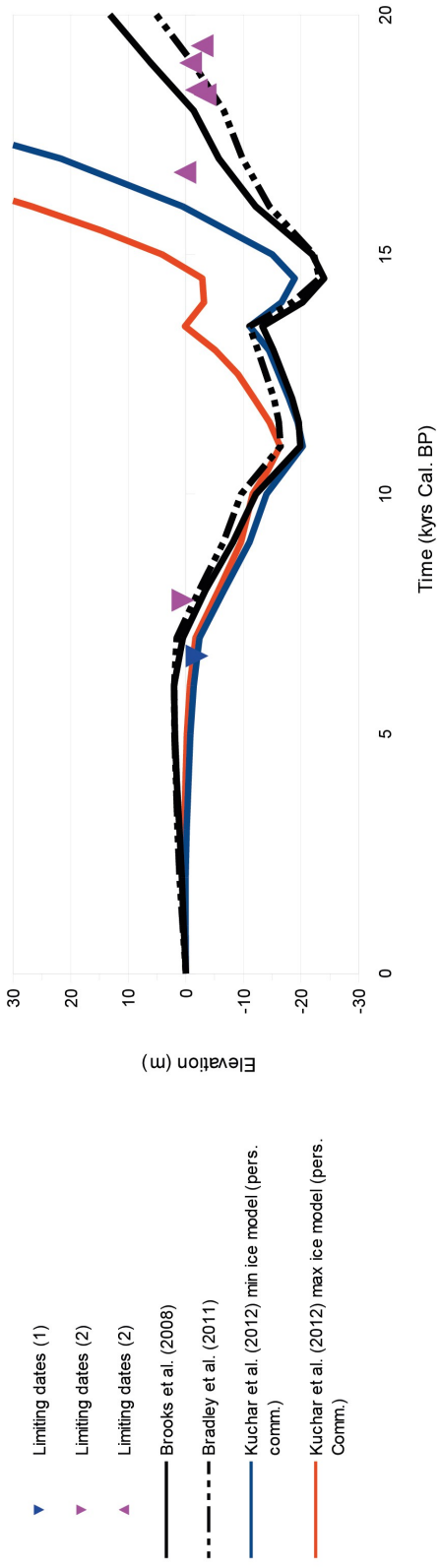

Figure 2.22: Computed sea-level curves and associated sea-level data for Lough Swilly (western part of study area)

Ice models developed for Ireland have located the thickest ice in the North East of the island just south of the study area. The local GRMs also need the information from adjacent ice sheets, in this case the ones in Britain, Fennoscandinavia, Iceland, Greenland and North America. The first two of these ice masses being of a much greater thickness than the Irish one and due to their proximity have a much greater influence on the computed isostatic rebound of Ireland. Hence every GRM computed for Ireland shows a similar contrast between the north east and the south west of the island due to their relative position to the ice centres in Britain and Fennoscandinavia. For example in the study area of this thesis, the three curves for the three regions of Antrim, Derry and Lough Swilly show a clear distinction from the east to the west. The Antrim curve displays a higher RSL overall the early deglaciation and the lowstands and the Holocene highstand compared to the Lough Swilly curve. The curve for Derry sits somewhat in between those two.

The sea level data points plotted on top of the RSL curves of figures 2.20, 2.21 and 2.22 are all limiting dates and their representation as an upward or downward triangle serves the purpose of understanding the ideal sea-level curve to pass above or below the arrow. Although most of the computed sea-level curves do not sit exactly in the right place to these arrows, it is reasonable to accept them as they all sit in the range of the vertical uncertainties associated with the plotted limiting dates with the noted exceptions of the Bradley et al. (2011) and Kuchar et al. (2012) curves for Antrim for the lowstands around 15,000 years BP and for the Brooks et al. (2008) and Bradley et al. (2011) curves for Lough swilly for the early deglaciation period before 15,000 years BP. Therefore the computed curves for the area resolve the more recent changes in RSL but struggle to compare with the field collected data for the earlier deglaciation period.

No definite sea-level data exist for any elevation below 9m depth for the study area and the elevation of the lowstands for the study area are only assumptions based on the GRM. The potential coastal features observed either on the seabed with bathymetric data or beneath with seismic data are far below the modelled lowstands (Cooper et al., 2002; Quinn et al., 2010) with the exception of two palaeochannel features observed on seismic lines in the Derry region (see sections 6.1.2 and 6.1.4) that are in the range of the lowstands computed for Brooks et al. (2008) and Kuchar et al. (2012) min ice model.

2.5 Conclusion

This chapter has sought to establish the geological and glaciological background as well as the modern energy conditions of the northern coast of Ireland. This was presented in order to understand the formation of the main features of the coastline associated with modern and ancient sea-level. The general lack of precise RSL data for the area have pushed toward the modelling approach which produced good fit with the available data. However the absence of offshore sea-level data points prevents making any assumption as to the accuracy of the GRMs' simulations of the magnitude and rate of RSL change. This study will explore the offshore evidence using both the geomorphological data, controlled by the local lithologies (Chapter 4 and 5), and the sediment stratigraphical data, controlled by the local environment conditions (chapter 6). The next chapter (chapter 3) will develop the methodologies used in this study.

Chapter 3

Datasets and methodologies

This chapter will present the various methodologies used for this study. First, the dataset used for the geomorphological part of the study will be presented followed by a description of bathymetric histograms and their use in submerged landscape recognition. This chapter continues by describing the manner in which the marine terraces database was created and analysed. A wave erosion model was consequently used and its functioning mechanisms are presented here. The methods of seismic data analysis and seismostratigraphy are introduced in conjunction with a presentation of the seismic data available from the study area. Finally, sediment core collection and analysis methodologies used in this project are described in conjunction the results of the coring survey undertaken for this project.

3.1 The Joint Irish Bathymetric Survey (JIBS)

3.1.1 Description of the project

In recent years, several European funded projects have aimed to update the hydrographic chart around Ireland in order to create backdrops for new records of marine resources, hydrocarbon exploration, biodiversity mapping and earth science research. The study area, being located at the border of the Republic of Ireland and the United Kingdom, necessited a collaboration of these two states for undertaking the survey of its inner shelf. The Joint Irish Bathymetric Survey (JIBS) is the name of this collaboration for the multibeam survey of the seabed from the coastline out to 3 nautical miles (5.55km) offshore and from Torr Head in Co. Antrim to Fanad Head in Co. Donegal (see figure 3.1 and http://www.marine.ie/home/services/surveys/seabed/JIBS.htm).

Echosounding is the process of emitting a high frequency sound pulse and recording the arrival time of its reflection at the seafloor (Quinn et al., 2008). The higher frequency allows for most of the energy to be reflected rather than penetrating the substrate. Given knowledge of the velocity of sound in seawater (calculated from its salinity and temperature) the travel time of the acoustic pulse can be converted into a measure of water depth. The strength of the reflected signal, which is known as backscatter, is dependent on the type of substrate on the sea floor. Typically, bedrock will produce a high amplitude reflection whereas soft sediments such as mud will absorb more energy through refraction of the pulse and so have a lower amplitude reflection. Mulitbeam surveys use several emitters and receptors at the same time hence allowing faster coverage and greater resolution through overlapping of the data. The raw data has to be checked and spikes linked with weather conditions or the composition of the water column are filtered out (Quinn et al., 2008). Tidal corrections are also applied using tidal gauges deployed both offshore and onshore. All depths are then levelled to their shallowest possible occurrence which happens at “lowest astronomical tides”. This bathymetric survey offers the highest available resolutions with a vertical resolution of the order of centimetres and enough datapoints to create Digital Elevation Model (DEM) of up to 1m lateral resolution in the shallower sections (lateral resolution being partially a function of water depth).

The JIBS Project (funded by the EU through its INTERREG IIIA Programme) was co-ordinated by the Department of the Environment for Northern Ireland (UK) and led by

the Maritime and Coastguard Agency (UK) in partnership with the Marine Institute of Ireland (Republic of Ireland). It was surveyed using the R/V Celtic Voyager from the Marine Institute and 3 contract vessels (the Jetstream, the Meridian and the Victor Hensen) from the Maritime and Coastguard Agency from November 2007 to May 2008 (see table 3.1 for the type of instruments used). The data was processed and made freely available and downloadable on the Marine Institute portal by the end of 2008.
It may be viewed at http://gsigis1.dcmnronline.ie/imf/imf.jsp?site=JIBS. The data may be downloaded at https://jetstream.gsi.ie/jibs/index.html.

Vessel	Part of survey covered	Instrument used	Frequency
R/V Celtic Voyager	Republic of Ireland	Kongsberg Simrad 1002	95 kHz
R/V Celtic Voyager	Republic of Ireland	Kongsberg Simrad 3002	293 kHz
Jetstream	Northern Ireland (UK)	Kongsberg Simrad 3002	293 kHz
Meridian	Northern Ireland (UK)	Reson 7125	200/400 kHz
Victor Hensen	Northern Ireland (UK)	Kongsberg Simrad 710	71 to 97 kHz

Table 3.1: List of multibeam echosounder instruments used by the various vessels for the JIBS.

Such a high resolution survey compares most favourably with the topographic Lidar data on land provided by the Ordnance Survey Ireland (OSI) for the Republic of Ireland and the Ordnance Survey Northern Ireland (OSNI) for the United Kingdom part of the study area. The DEMs from these 2 agencies, although with a very high vertical resolution comparable to the multi-beam data, has a lateral resolution of only 10m which is insufficient for recognition of raised coastal features. The JIBS datasets on the other hand allows for the investigation of the northern Irish coastline in search for relict buried shorelines associated with RSL lowstands. The composite figure 2.1 (chapter 2) is made of the DEMs from the JIBS multi-beam survey, recent Lidar and shallow multibeam data from the INFOMAR project in Mulroy Bay, Lough Swilly and Lough Foyle and the OSI and OSNI topographic Lidar data put together using the ArcGIS 9 software.

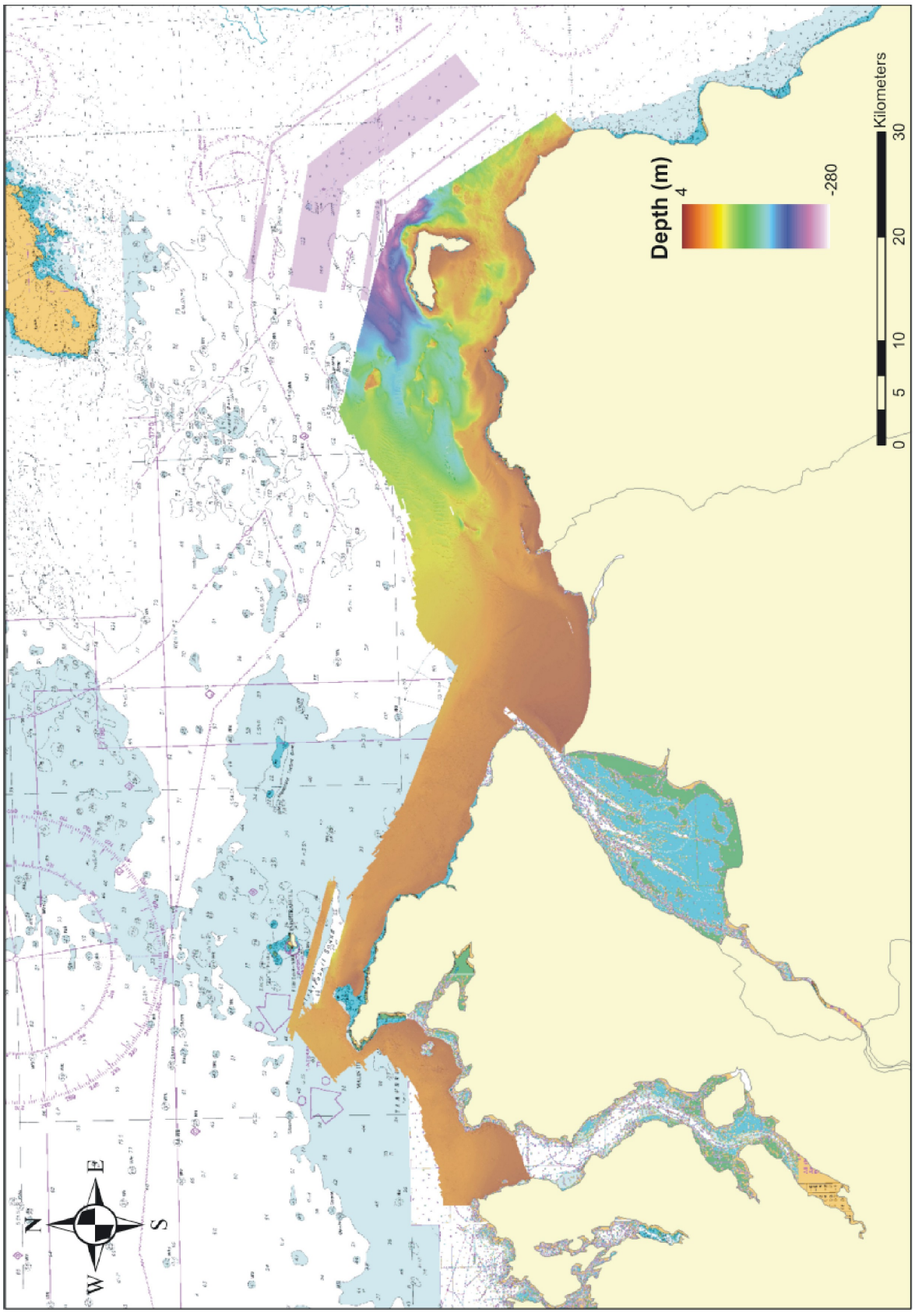

Figure 3.1: Coverage of the JIBS datasets plotted over the bathymetric chart (from Quinn et al., 2008)

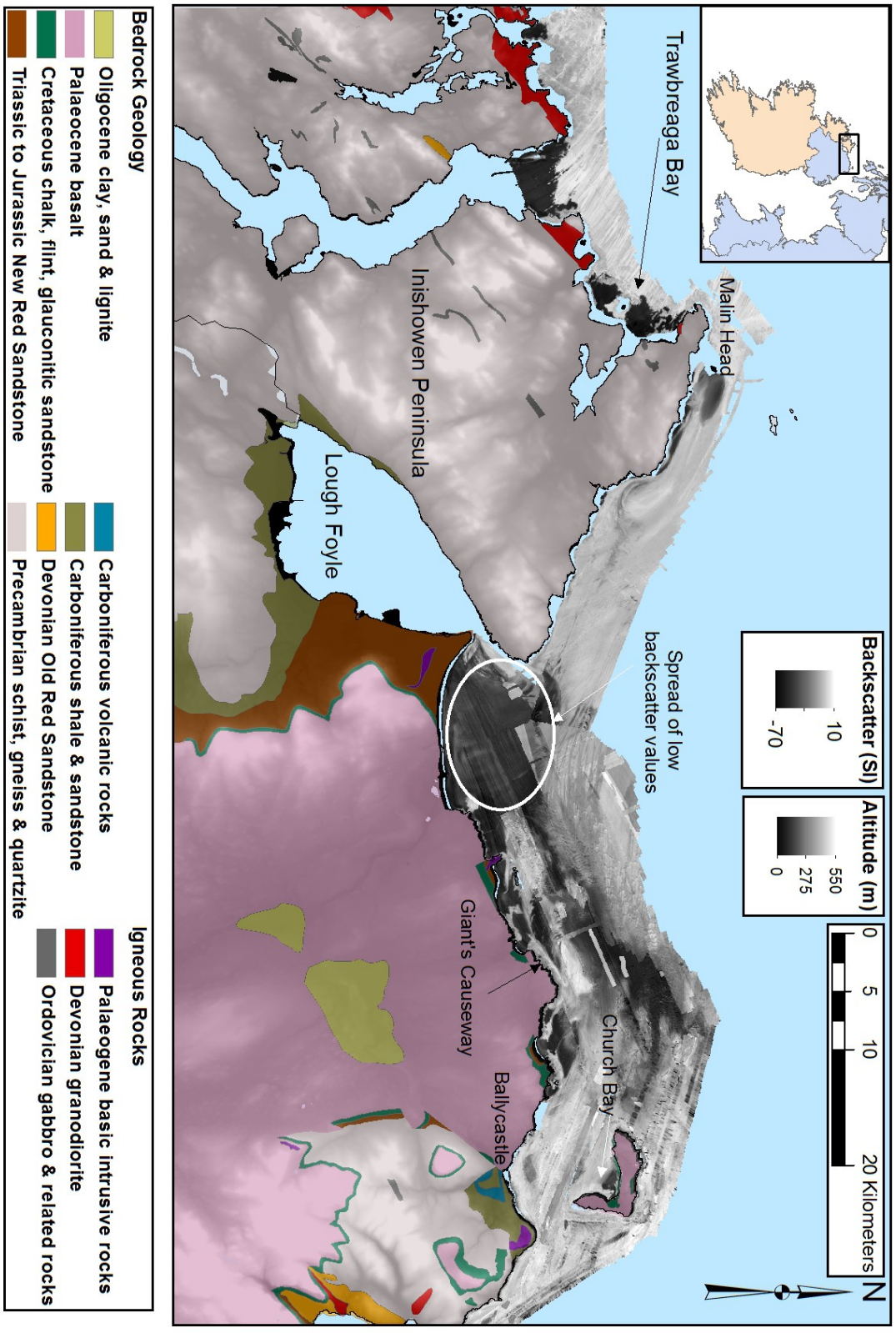

Figure 3.2: Mosaic of the backscatter data from the JIBS.

All depths and altitudes refer to the Malin Ordnance Datum (OD) and the coordinate system used and represented on location maps is the projected UTM (Universal Transverse Mercator) zone 29N using the WGS(World Geodetic System) 1984 geoid. A geoid is an ideal representation of the globe of our planet with a particular radius and elliptical parameters. This allows the projection from an angular set of coordinates on a geoid to a planar coordinate system divided in rectangles or zones on the globe for better accuracy. The Malin Ordnance Datum is a vertical reference point used to measure elevation on land; here the reference is the mean sea level at Malin Head between January 1960 and December 1969.

3.1.2 Processing of geophysical data

The cleaning process of the raw data mentioned above was conducted by the Marine Institute. There, interpolation of the data was undertaken using the IVS Dmagic 7 software and a range of DEMs were created with a vertical resolution of about 0.5m and with various horizontal resolutions:

- 4m and 6m for the dataset of Northern Ireland
- 2m and 5m for the dataset of the Republic of Ireland.

Due to the interpolation process, DEMs are rectangular in shape and need to be clipped along a given coastline. The created DEMs are directly available to download following the previous link.

The JIBS cleaned datasets were reprocessed by Ruth Plets and Rory Quinn of the University of Ulster to develop a DEM of 1m horizontal resolution for more detailed analysis of seabed features and archaeological wrecks (Quinn et al., 2009, 2010, 2011). Similar treatment was undertaken there on the backscatter data using the IVS FM Geocoder software in order to create a seamless mosaic of the data collected by various vessels under various conditions. Issues related to the change of frequency parameters used for the recording of the bathymetric data by some of the vessels prevented the final backscatter mosaic being seamless everywhere (figure 3.2). These issues originated from a lack of acquisition notes for these changes in parameters and limitations in the Geocoder software. This study uses the 4m and 6m DEMs and backscatter mosaic. Sections of the dataset were re-interpolated to create a 1m DEM of the bathymetry as a test to determine its usefulness for this projects particular requirements. Whilst clear improvements in the

DEM resolution allowed a better recognition of the nature of the seabed, the time involved with the new interpolation was deemed too long for the limited improvements it brought. The 4m and 6m DEMs were plotted and analysed using the IVS Fledermaus 7 software and the backscatter data was georeferenced and analysed using the ArcGIS 9 software.

3.2 Methodologies used for the exploration of the multibeam data

3.2.1 Bathymetric histograms

The analysis of the histograms for the bathymetric datasets was initially undertaken. This rapid process allows for the recognition of potential relict shoreline in the concentration of flatter areas appearing as spikes on the curves (Passaro et al., 2010). As RSL evolves, it might sit at particular elevation for periods of time called still-stands long enough for the wave action to form a ledge or a marine terrace in the substrate. Such a feature, if large enough and consistent over a wide enough stretch of coast can appear in the histogram as a spike.

Bathymetric histograms are visualisation of the concentration of bathymetric points at particular depths. The number of points in the bathymetric data grid that have depths inside an interval of depths or a bin size are grouped and added together. The histograms were calculated after exporting the bathymetric data into the ArcGIS 9 software. The ArcGIS 9 software uses 256 bins based on the range of depth of the dataset, meaning that a dataset with a range of data between 0 and 256m will have a bin size of 1m for its computed histogram. Issues linked with bin effects have been recognised to lower the depth of large spikes and prevent the recognition of discrete spikes (Passaro et al., 2010). Figure 3.3 displays the histogram for the Northern Irish bathymetry with bin sizes of 1m or more computed by averaging the data from the 1m bin size histogram. This plot shows the expected smoothing of the curve overlooking the more localised spikes but also the change in depth of a spike on the data due to the change in bin size. Since the total depth range of the data presented in figure 3.3 is the largest encountered in the JIBS datasets (0 to 256m), all histograms presented in this study have bin sizes of the order of 1m or less which allows their direct comparisons.

Histograms were computed for the 2 datasets of Northern Ireland and the Republic of Ireland, as well as for subdivision of these datasets (section 4.3.1). These subdivisions

were extracted on the ArcGIS 9 software. The various histograms have been normalised by dividing the values for each bins by the maximum encountered in each histogram, obtaining values between 0 and 1. This was done in order to compare them accurately.

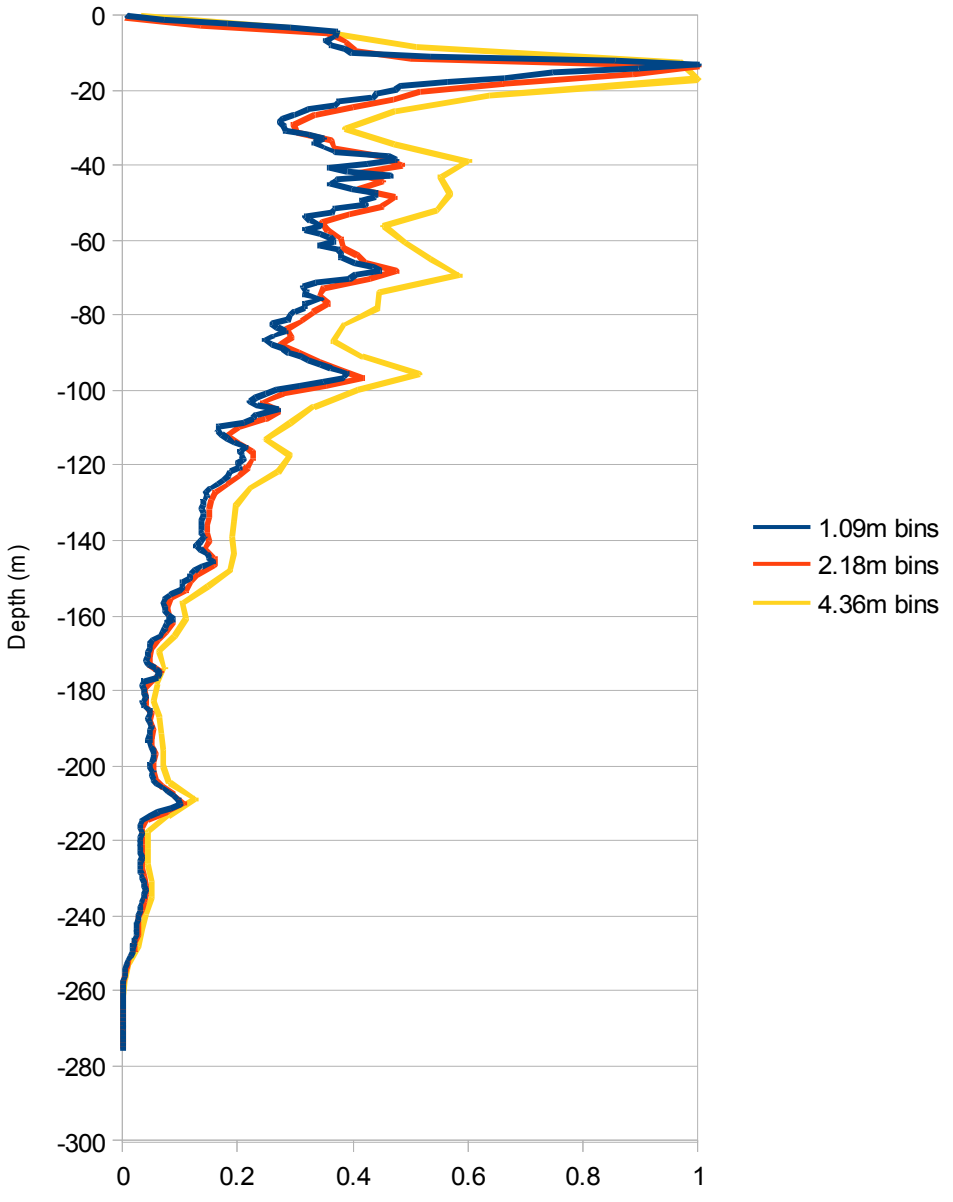

Figure 3.3: Bathymetric histogram for the Northern Irish dataset with different bin sizes.

The lack of multi-beam data for the zone from the coast to the 20m depth contour is made obvious for Lough Swilly and prevents any direct comparison at these depths. This lack of data is due to the local wave exposure that prevented the surveying boat (R/V Celtic Voyager) from approaching the coast much further. Histograms for the topographic datasets (not shown) were also produced but showed no spikes in the coastal area as their lateral resolution precluded the identification of such features.

3.2.2 Building a marine terrace database

3.2.2.1 Identification

The extensive multi-beam survey provides a powerful means to detect offshore relict shorelines; in particular, marine terraces which are defined here following Trenhaile (2002) as "gently sloping [terrain] bounded on the landward side by a steeper ascending slope, and on the seaward side by a steeper descending slope". Such features detected by visual inspection on the bathymetric data of the study area were classified and their parameters recorded in order to build a database. These parameters were selected following recent studies on the morphology of shore-platforms controlled by their lithology and local environmental processes (Sunamura, 1992; Trenhaile, 1978; 1999; Thornton and Stephenson, 2006; Dasgupta, 2010). The DEMs with higher resolutions (4m for Northern Ireland part and 2m for the Republic of Ireland part) were systematically analysed using the IVS Fledermaus 7 software. As a 3D visualisation software, it allows the change in the lighting orientation in order to reveal relief with particular orientation. Similarly, the vertical exageration can be modified to highlight the finer features.

The first step was the recognition of breaks of slope using the elevation profile tool of the software where the slope gradient of the profile was above 10° (or below -10°). The regions of seafloor then delimited in-between these were cross-referenced with backscatter data on the ArcGIS 9 software to establish the nature of the substrate (figure 3.4). In general, the terraces selected appeared as bare rock on the backscatter data but some were covered, entirely or partially, with sheets of modern sandy sediments (areas with lower backscatter). Where a rock terrace feature was identified, its dimensions, depth, and gradient were recorded, along with the morphology of the delimiting breaks of slope above

and below it, the lithology of the rock and the thickness of any modern sediments associated with it.

Features, marine terraces and shore platforms will be mentioned intermittently from now on and their meaning in this section is interchangeable.

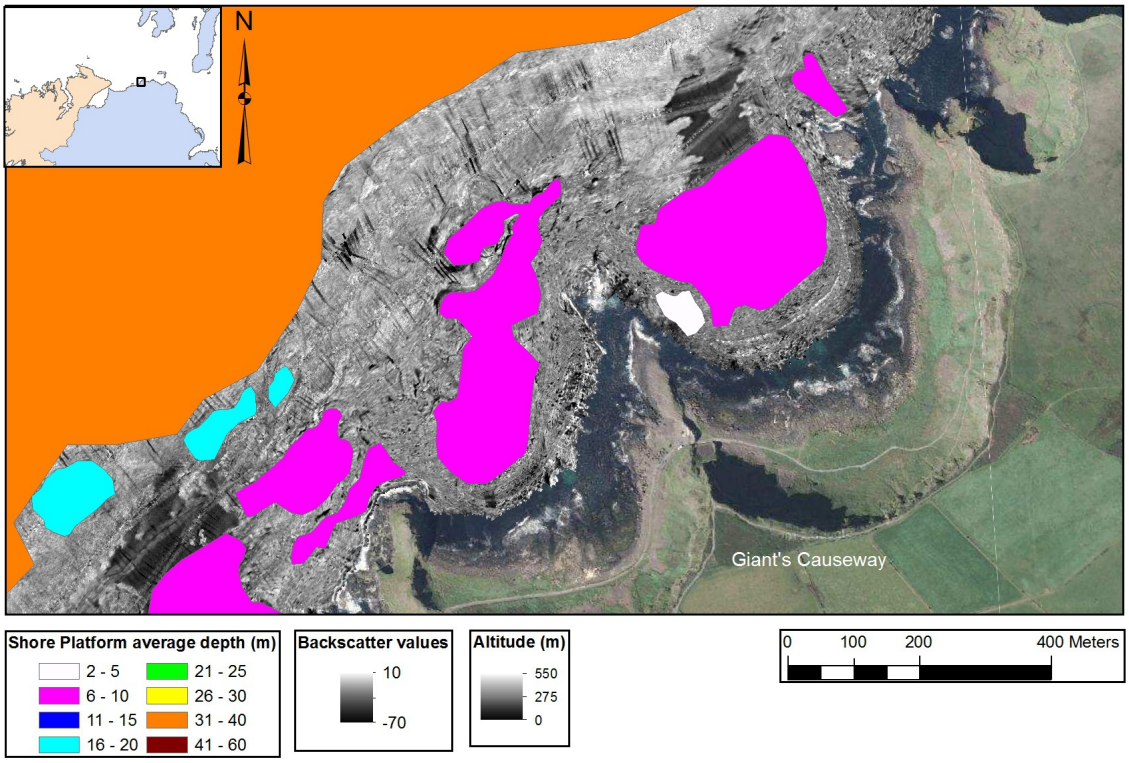

Figure 3.4: Marine terraces features plotted according to their median depth for the Causeway coast.

The morphological parameters, displayed on figure 3.5 and table 3.2, recorded for the terraces were:

- the median depth measured to the nearest meter halfway across the width of the feature,
- the minimum depth measured to the nearest meter at the shallowest point (cliff-platform junction) by the break of slope,
- the average width (perpendicular to the shoreline) measured to the nearest meter,
- the maximum length (parallel the shoreline) measured to the nearest meter,
- the angle of slope perpendicular to the shoreline was measured in order to classify the terrace feature according to Sunamura (1992) in ramp like platforms of type A (angle above 0.9°, figure 3.6) or sub-horizontal platform of type B (angle below 0.9°, figure 3.7),
- the abruptness of the break of slope seaward of the terrace as appreciated visually ranging from very smooth (several meters depth change over 100m distance) to very sharp (several meters depth change over 10m distance),
- the rugosity of the surface of the terrace as appreciated visually ranging from low to high (figures 3.6 and 3.8),
- the computed surface of the area delimited by the polygon created of the feature on the ArcGIS 9 software.

Parameters	Minimum	Maximum	Comments
Median depth (m)	2	80	
Minimum depth (m)	0	55	
Average width (m)	5	4380	
Maximum length (m)	15	17120	
Angle of slope	B (less than 0.9°)	A (more than 0.9°)	(Sunamura, 1992). See figures
Abruptness of break of slope	very smooth (5/100)	very sharp (5/10)	
Rugosity	1	6	Visually appreciated categorisation. See figures
Computed surface area (m^2)	59	44426981	
Recognition confidence index	1	5	Linked with definition of features in local geomorphology context
Coastal profile of backing shore			Headland or bay and presence of active shore platform, cliff and/or beach
Lithology			Basalt, Sedimentary or Metamorphic
Nature of substratum			Bare rock or loose sediment (grain size)

Table 3.2: List of parameters recorded for each of the features with their associated range.

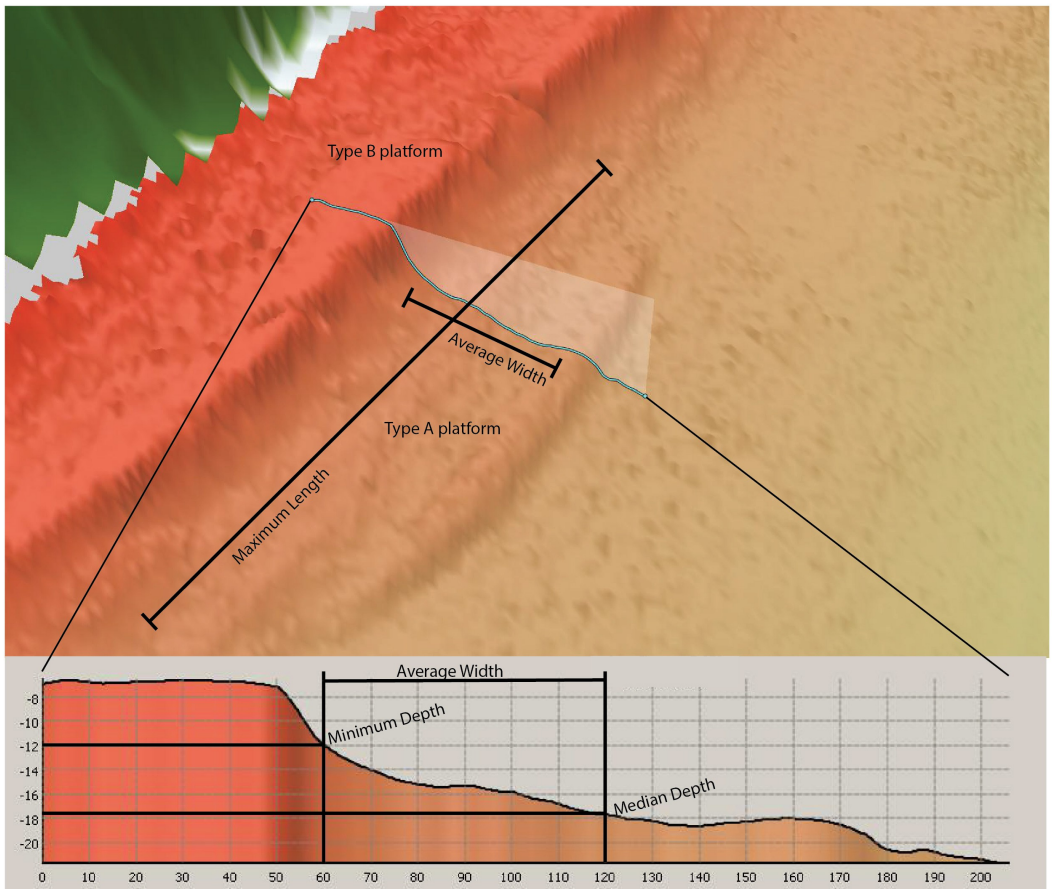

Figure 3.5: Description of the main morphological parameters recorded in the database with a presentation of the difference between terraces of type A and type B.

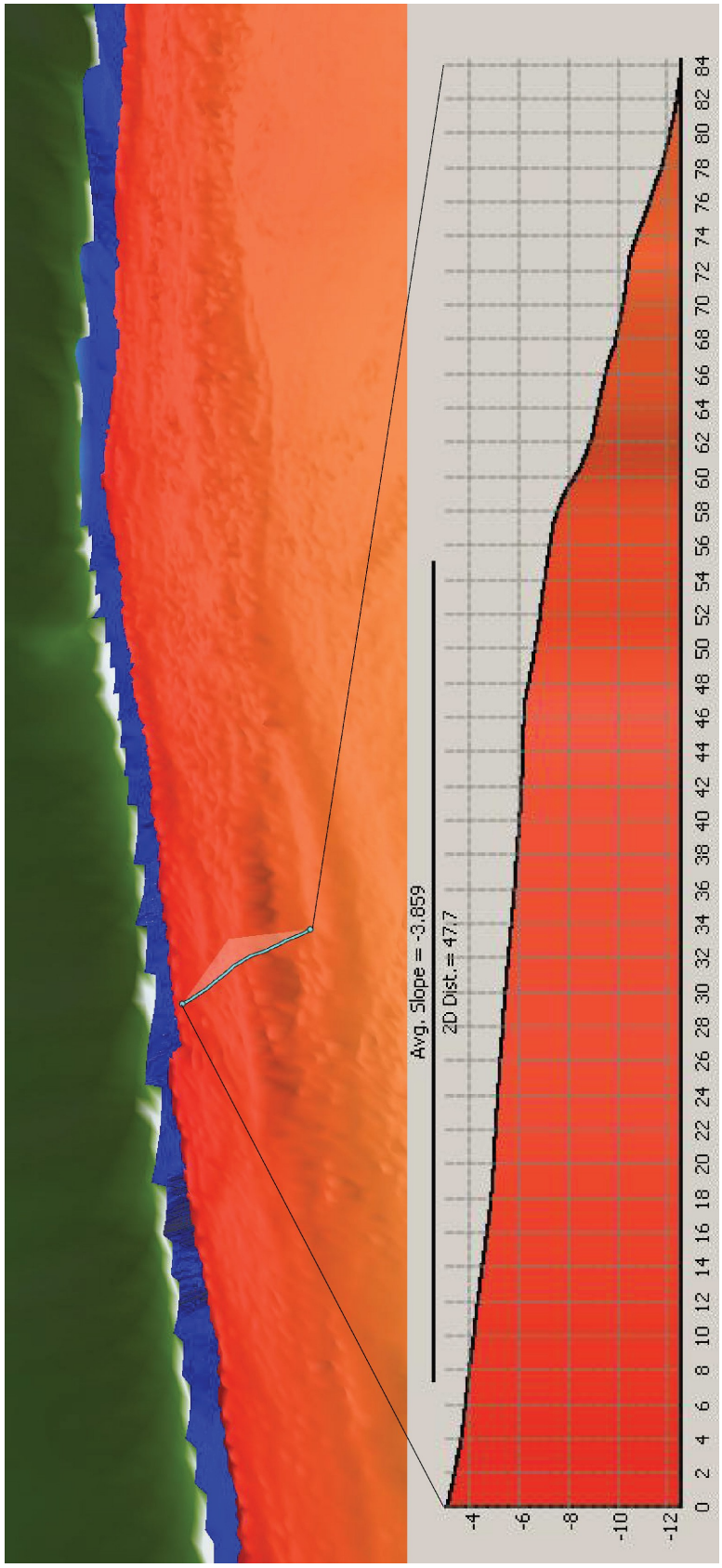

Figure 3.6: Example of type A marine terrace with low rugosity (2) and smooth break of slope

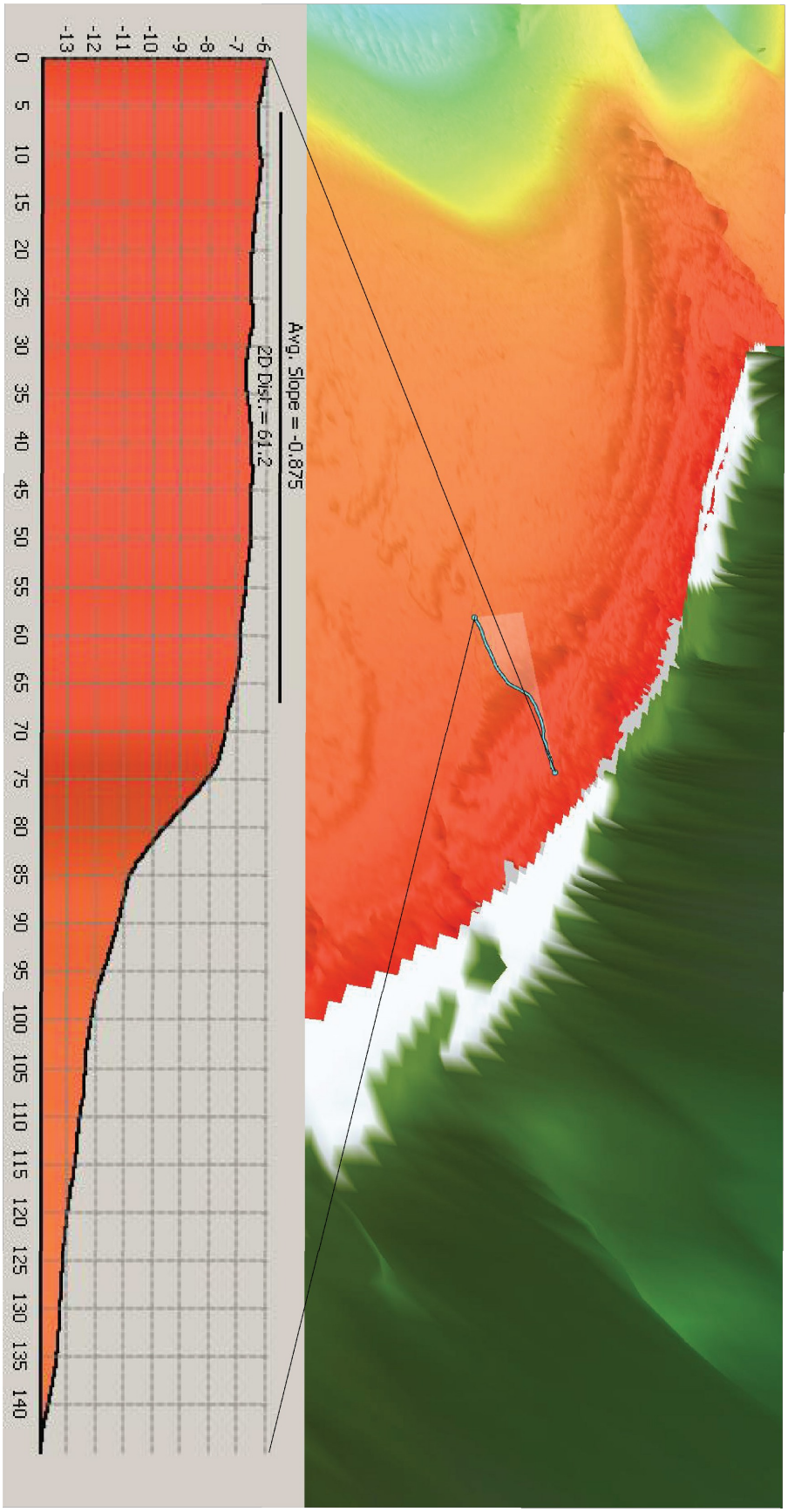

Figure 3.7: Example of type B marine terrace with medium rugosity (3) and sharp break of slope.

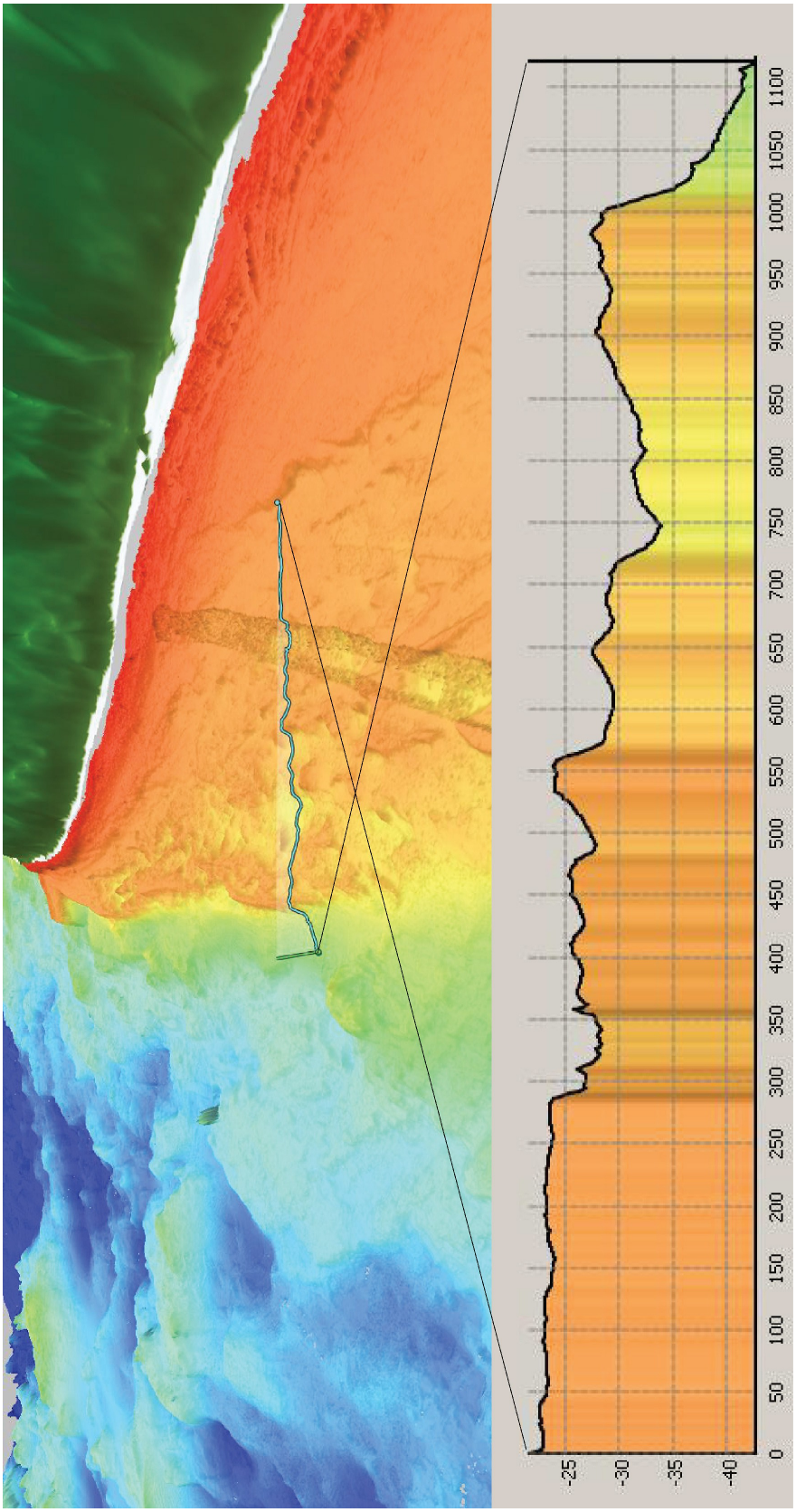

Figure 3.8: Example of marine terrace with very high rugosity (6) and very sharp break of slope. The linear feature running toward the shore is a glitch from the raw data cleaning.

A recognition confidence index (RCI) ranging from 1 to 5 was added for each recognised feature to describe the confidence in the recognition process of a wave-cut platform with 1 being of low confidence and 5 being of very high confidence. A small comment was added when needed to explain the reasons of the lack of confidence which was generally due to the local lithological and structural context. Indeed many basalt flows have been identified visually due to their general morphologies and continuation from land and these sometimes form platform features unrelated to wave action. Similarly, isolated bedrock outcrops can have a flat top and have then been recorded here but with a RCI depending on the local structural context.

The coastal profiles backing the recognised features were also recorded describing whether these were located in a bay or off a headland, whether an active cliff with a modern shore platform was present or whether beach deposits are present in the intertidal zone.

Identification of the general lithology was only problematic where Palaeocene basalt overlies Cretaceous chalk at varying elevations along the coast. In these instances, lithology was identified with reference to borehole data (McCann, 1988) and offshore geology map (Fyfe et al., 1993; Holland and Sanders, 2009). Lithology is one of the major controls on the morphology of erosional features such as rock platforms due to their varied resistance to weathering (Sunamura, 1992; Dasgupta, 2010). This study has consistently divided the lithologies of the local area into three categories:

- Basalt of Tertiary origin present as the Northern Irish Basalt plateau,
- Sedimentary rocks of Carboniferous or Mesozoic age present in Northern Ireland (that include the Ulster White Chalk formation),
- Metamorphic rocks of Precambrian age present in Donegal and to the east of the Tow Valley Fault in Northern Ireland. In this category the igneous granodiorite of Devonian age present in the Lough Swilly area was included.

Using the backscatter data, the nature of the substratum was recorded for each of the features, in particular whether modern sediment was covering the feature as most features were actually bare. The nature of this modern sediment coverage and its thickness were added according to the maps created for the offshore BGS report for the area (Fyfe et al., 1993).

The entire dataset was compiled in a spatial database shapefile using the ArcGIS 9 software containing more than 500 features for the study area. This database could then be used to create maps displaying the variation of one or many of these factors and the database itself was exported to produce graphs on the evolution of these factors. The local lithology was added to the ArcGIS file as a shapefile downloaded from the Geological Survey of Ireland online repository. Due to projection issues, the coastline used to clip the lithological shapefile differs to the one used to clip the topographic, bathymetric and backscatter data. On the maps exported from ArcGIS, a black area is visible where the topographic data below the lithological data appears.

3.2.2.2 Ground truthing dives

Limited diving ground truth of the recognised features was carried out in 2010 and 2011 by the CMA in collaboration with the National Facility for Scientific Diving (NFSD) with funding from the National Environmental Research Council (NERC) (Quinn et al., 2010, Westley, pers. comm.). These were located in Ballycastle Bay and Church Bay and are used as a test of the recognition process described above and completed prior to the dives. Figure 3.9 plots the location of the dives over the recognised marine terraces with a colour code based on their recognition confidence index. The results are presented in table 3.3.

This ground truthing survey showed a precise agreement with the recording process in terms of the location, depth, lithology and the morphology of the identified features. It has even added the location of cliff notches in between the recognised terraces (figure 4.5). However, it also highlighted one of the shortcomings of the use of a 4m resolution DEM for the identification of marine terraces. In places, a boulder field can be averaged into a relatively smooth surface with virtual breaks of slope that could be interpreted as marine terraces. Most of these more problematic areas had been pointed out using the recognition confidence index but further testing using the 1m resolution DEM is clearly needed.

Transect No	Location	RCI	Underwater Observations	Onshore Geology
BC_1	Western Ballycastle Bay	5	Submerged cliff between -11.7 to -8m which is fronted by boulder slope which itself leads to sand at c. -15.5m. Small notch/ledge on the cliff face at -10.7m. Observation of geology/geomorphological features hindered by dense kelp	Site directly opposite modern chalk shore platforms and cliff. Immediately to the west, the chalk dips and modern shoreline consists of a basalt headland
BC_2	Western Ballycastle Bay	5	Submerged cliff between -11.5 to -9m which is backed by a gradual slope up to 6m and fronted by a boulder slope at -13m. Observation of geology/wave-cut features hindered by dense kelp.	Site directly opposite modern chalk shore platforms and cliff. Immediately to the west of the site is a fault in the chalk (Giant's Cut) that is visible onshore and also offshore on the JIBS data.
BC_4	Western Ballycastle Bay	5	Submerged cliff face at c. 13-11m depth. Cliff appears to be chalk. Sample taken from the cliff face with hammer: flint. Undercuts visible along the cliff face, up to 0.5m high and appeared to be continuous to semi-continuous. Precise determination of their extent was hindered by kelp growth.	Site situated directly opposite modern chalk shore platforms. The cliff face backing these is covered by a talus deposit, and hence geology cannot be determined.
BC_7	Western Ballycastle Bay	4.5	Submerged cliff is not obvious here, instead there is a series of small ridges which appear to be composed of chalk with flint outcrops. Samples of chalk and flint taken with hammer	Site situated directly opposite modern chalk shore platforms backed by talus slope.
BC_3	Western Ballycastle Bay	5	Submerged cliff at 22-20m depth fronted by sand with some boulders. Sand thickness is variable, in some areas appearing to be a veneer over bedrock. Samples from cliff indicate chalk with flint. Kelp cover less dense, and it was possible to observe that the cliff was undercut extensively.	Site directly opposite modern chalk shore platforms and cliff. To the west of the site is a fault in the chalk (Giant's Cut) that is visible onshore and also offshore on the JIBS data.
BC_5	Western Ballycastle Bay	5	Low submerged cliff at 22-20m depth fronted by boulders. Samples from the cliff indicate chalk with flint. Kelp cover less dense, and it was possible to observe that the cliff was undercut.	Site situated directly opposite modern chalk shore platforms. The cliff face backing these is covered by a talus, and hence geology cannot be determined.
BC_1	Western Ballycastle Bay	5	Submerged cliff between 13-11m depth. Kelp was cleared in order to facilitate observations of the cliffs. Some minor undercutting but observation and photos hindered by poor visibility.	Site directly opposite modern chalk shore platforms and cliff. Immediately to the west, the chalk dips and modern shoreline consists of a basalt headland.
BC_6	Western Ballycastle Bay	4.5	Gully cut into the platform. The cliff was not obvious in this area, however, the platform surface was reported to have obvious undercuts and potentially wave-cut/water-eroded channels/gullies.	Site directly opposite basalt cliff with modern chalk platforms at the water's surface.
BC_9	Western Ballycastle Bay	4	Submerged cliff with base at -13 to -14m, sand comes directly up to cliff base. Cliff is chalk (with flints) and has undercuts, esp. at the top of the cliff.	Site situated directly opposite a gravel beach and talus. There is a dipping chalk cliff topped by basalt to the east and a modern chalk platform to the west.
BC_10	Eastern Ballycastle Bay	3 and 4	Bathymetry suggests 2 steps. Dive indicates seabed is made of boulders (larger than on shore) with no obvious breaks in slope.	Boulder field
CB_1	Southern Church Bay	4.5	Clear bedrock cliff/slope with a number of steps and notches. Samples taken = flint and chalk. Cliff was not sheer but rather a steepish incline. Base of cliff was covered in sand. Occasional boulder noted on slope.	Onshore Geology seems to be basalt.
CB_2	Western Church Bay	5	Notches observable from 16 to 10m depth on gently undulating sloping platform. Boulder slope from 18 to 16m depth. Sample at 16m depth was flint.	Junction of chalk and basalt.
CB_3	Western Church Bay	4.5	Boulder slope which prevents oberva-tion of bedrock. No break of slope.	Chalk cliff with quite a few notches running horizontally and a small platform. To the east the chalk is fronted by a boulder beach.

Table 3.3: List of ground truthing dives showing their location , the RCI of the terrace targeted and their results (after Quinn et al., 2010).

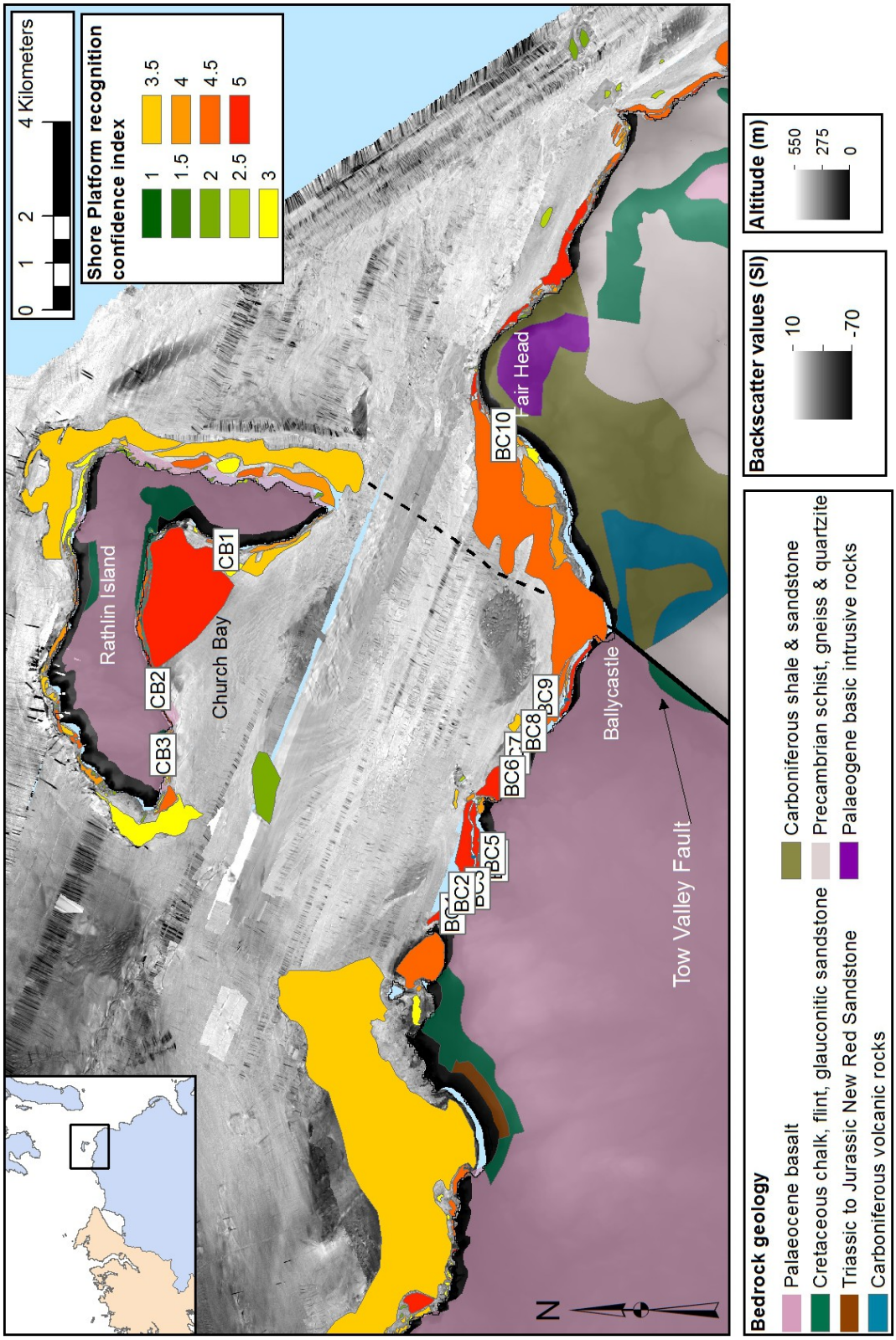

Figure 3.9: Location of ground truthing dives for Ballycastle Bay and Church Bay over their recorded platforms colour coded by their Recognition Confidence Index (RCI).

3.2.2.3 Correlation between parameters

Dasgupta (2010) reviews the various studies on the geological control on the morphology of shore platform. As mentioned above, it is the main factor in the width of a platform as its resistance to erosion or rock strength varies according to its components, structure and process of formation. In particular, Sunamura's (1992) laboratory work demonstrated that one of the main control on the angle of slope of a shore platform is its lithology as sub-horizontal type B features are more likely to form in more resistant rocks. Similarly Thornton and Stephenson (2006) concluded from their field study in Australia that the mean platform elevation was significantly related to rock strength, measured by a Schmidt hammer, but not significantly to width, angle of slope or the platform's location in a bay or at a headland. Structural control on the morphology of shore platforms is also clear from recent surveys in Wales and Sweden (Cruslock et al., 2010) but limited to the meso-scale (cm-m) which is below the best resolution of the datasets. The meso-scale structural control of the lithology, too difficult to recognise even at the dataset's maximum resolution, was not recorded and the general lithology was used as a proxy for the rock strength or the resistance of the rock to erosion. As the main objective of this study is to relate platforms to a potential RSL signal, correlations between the general lithology of the bedrock where the recorded features formed and its morphology were investigated. Similarly, any correlation between the morphological and local parameters and the median depth of the recorded terraces was investigated in light of recently established vertical uncertainty for the level RSL corresponding to the formation of hard rock shore-platforms (McKenna , 1990; McKenna et al., 1992).

3.2.3 Accretional features

The potential for accretional coastal features such as beach barriers preserved on the bathymetry was investigated following the morphological parameters described in Woodroffe (2002). Elongated, shore parallel, elevated features located in areas of low backscatter values are interpreted as beach barriers. Larger zones of low backscatter values with a lenticular shape and located further away from the coast were recorded as sand bars. The length, width, minimum and maximum depths of these features were also recorded.

3.3 Wave erosion modelling

Recent studies using a mathematical wave-erosion model have simulated the development of rock shore platforms and examined their morphology in relation to contrasting patterns of RSL change during the Holocene (Trenhaile, 2008; 2010). This modelling approach was applied to simulate rocky shoreline development along the northern coast of Ireland. The model was driven using the range of recent postglacial RSL change scenarios presented in Chapter 2 and simulated the erosional effects on rocks of varying resistance. Simulated and measured profiles were then compared for 6 selected representative profiles of 6 more specific area with varying RSL curves to elucidate the formation of observed coastal features.

Wave erosion on hard rock coasts is accomplished mainly by the dislodgement and removal of joint blocks and other rock fragments, usually by broken waves (Trenhaile, 1987; Swantesson et al., 2006; Trenhaile and Kanyaya, 2007; Stephenson and Naylor, 2011). The processes responsible for wave quarrying, such as water hammer (impact) and the wave-induced compression of pockets of air in rock crevices, operate at or close to the water surface, which migrates up and down the foreshore with the tides and with changes in RSL. The evolution and profile development of a rock coast through mechanical wave erosion therefore reflects the amount of erosion accomplished at each elevation according to the resistance of the rock, the wave regime, the effect of submarine topography on rates of wave attenuation, and the amount of time that the waves have operated at each level (Trenhaile, 2000).

These processes were simulated using a wave erosion model that was developed for

rocky coasts and has been used to elucidate their morphological evolution at various locations around the world (see Trenhaile, 2000; 2010). The model, which employs basic wave equations to determine rates of profile backwearing (erosion in the horizontal plane) at the water surface, has been described in detail in Trenhaile (2000 and 2001).

In brief, the mechanical wave erosion by direct wave impact is represented by an excess surf stress expression (1):

$$E_{bf}=N_oK_{bf}(SF-SF_{cr}) \quad (1)$$

where: E_{bf} is the recession ($m.yr^{-1}$) accomplished by a single wave type at a single intertidal elevation each year; N_o is the number of waves of that type at that intertidal level each year (based on wave period, frequency and tidal duration, the latter being the annual total number of hours the tide occupies a given elevation); K_{bf} is a wave erosion calibration coefficient that converts excess surf stress to the rate of cliff or platform recession; SF is the stress (Pa) exerted by the surf at the bluff foot, and SF_{cr} is the threshold (critical) surf stress (Pa), required to initiate erosion by wave impact.

The surf stress (SF) was calculated in the model using (2):

$$SF=[0.5\gamma(H_b/0.78)e^{-\chi.Sw}] \quad (2)$$

where: γ is the specific weight of water (about 1025 $kg.m^{-3}$ for seawater); H_b is the mean breaker wave height (m), χ is a dimensionless surf attenuation constant representing the roughness of the bottom; and Sw is the width of the surf zone. As in previous studies, a value of χ = 0.01 was used to represent surf attenuation over fairly even bottoms (see Trenhaile, 2000; 2001).

A decay function (3) is used to represent slow rates of submarine erosion (E_u):

$$E_u=E_y.e^{s.h} \quad (3)$$

where: E_y is the erosion at the waterline; s (m^{-1}) is a depth decay constant (set to 1 in the runs performed here); and h is the water depth (m).

The model is driven using modern average wave climate and tidal regime (tables 2.1 and 2.2 respectively using data from the Marine Institute: www.marine.ie; and the British Oceanographic Data Centre: www.bodc.ac.uk), with the tidal duration distribution for a given height calculated as outlined in Smart and Hale (1987). Model runs commence at 16,000 BP broadly equating to the time when the coast was first generally free of ice (section 2.2). In the absence of precise local RSL data for this period (Carter, 1982; Brooks and Edwards, 2006), a range of RSL scenarios derived from glacial rebound modelling

were used (section 2.4.3 and figure 3.10). Whilst all the RSL curves show similar overall patterns, including differential east–west isostatic rebound, and an inflection at 14,000 BP related to Meltwater pulse 1a, they differ in the rate of RSL change as well as the duration and magnitude of RSL high or lowstands. Full details of the glacial rebound models and their development are available in Brooks et al. (2008) (hereafter the 'Brooks model'), Bradley et al. (2011) (hereafter the 'Bradley model'), and Kuchar et al. (2012) (hereafter the 'Hub-Min' and 'Hub-Max' models). Threshold rock resistance values (SF_{cr}) are varied between 100 and 1100 to simulate contrasting 'hard' and 'soft' lithologies following Trenhaile, (2000 and 2001). Whilst other wave, tide or RSL scenarios are possible, the values used here are sufficient to provide a first order assessment of shore-profile development in the region.

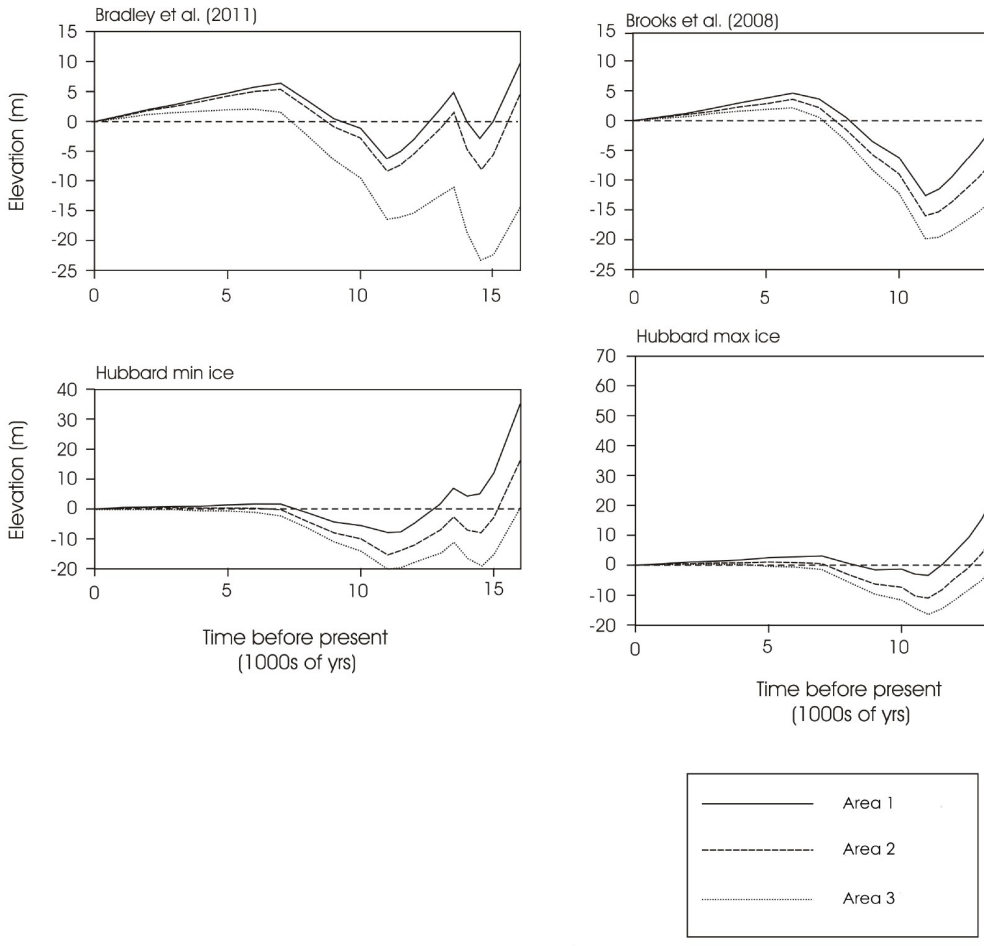

Figure 3.10: Simulated relative sea-level (RSL) curves for the 3 study areas generated by the glacial rebound models of Bradley (Bradley et al., 2011); Brooks (Brooks et al., 2008); Hub-Min and Hub-Max (Kuchar et al., 2012).

The amount of erosion accomplished by wave quarrying in the intertidal zone is calculated from Eq. (1) at the end of each 5-year iteration. Calculations are made at five elevations representing mean high water spring (MHWS), mean high water neap (MHWN), mid-tide (MT), mean low water neap (MLWN), and mean low water spring (MLWS) tidal levels. The amount of submarine erosion is determined using Eq. (3) at 0.5 m vertical intervals extending from the MHWN tidal level to a depth equal to half the wavelength of the waves.

Initial model runs are made on virgin, linear slopes, generally with gradients of 2.5°, 5° or 35°. To examine the effect of inheritance, additional runs are made on profiles that initially comprise two linear slope elements: a gently sloping surface below the modern low tidal level (MLWS) with a gradient of either 2.5° or 5°, and a steep surface with a gradient generally of 35° to represent a degraded former cliff above the low tidal level. The effect of individual factors, such as the slope and shape of the initial surface, the resistance of the rock (SF_{cr}), and the RSL curve is determined by comparing profiles produced by replicate model runs in which all variables bar the one of interest are held constant.

The model was run by professor Alan S. Trenhaile at the University of Windsor, Ontario, Canada. This includes initial model runs for fast and slow erosion (figures 5.3 and 5.4), the selection of the best parameters to fit the measured profiles (figure 5.6) and the creation of the initial figures. Whereas the initial selection of the representative profiles (section 5.1), the analysis of the model runs (section 5.2) and the description of the implications of the comparison between modelled and measured profiles (section 5.3) was carried out by me.

3.4 Methodology of seismic investigation

High-resolution single-channel reflection seismology is the most commonly used exploration geophysics method for the exploration of Quaternary glaciated margins (Davies et al., 1997). It stems from the original seismic reflection methodology developed for oil exploration in the beginning of the 20th century and aims at the understanding of the local stratigraphy by the detection of the shape and nature of the various layers of sediments or rocks

This method is based on the generation and detection of acoustic waves. A sound pulse is emitted by the source, passes through the water and penetrates the seabed. A hydrophone records the arrival time of sound pulses reflected at boundaries between sediment/rock layers with different impedance. These reflections are of various intensities based on the impedance contrast, linked in part with their density, of the two layers. As the signal travels deeper in the sediment/rock column, it encounters layers of increasing density. In these more usual cases, reflections of the incoming signal are positive (meaning will keep the same phase as the incoming signal) and appear as such on the datasets but some features such as gas, peat or wood can produce a negative feedback (opposite phase) due to their lower density. Part of the energy is reflected again at the sea surface, the seabed or any other boundaries. This produces multiples of the original reflections in the data collected, the strongest and most visible of these being the seabed. Although the main seabed multiples are recognisable, they usually prevent the interpretation of the data below them. As such the seismic penetration is water-depth dependent. Seismic investigations are routinely carried out on land or at sea where the emitter/receiver can either be integrated in the hull of the vessel or towed at the surface or on the seabed. The record can then be continuous and the horizontal resolution of the data is dependent on the speed of the vessel.

The resolution of a reflection seismic dataset is dependent on the frequency of the signal; a higher frequency meaning a higher resolution. But a high frequency also entails a high attenuation of the signal and so less penetration of the sediment/rock column. The range of instruments used in shallow seismic exploration (see below for the study area) are generally high frequency allowing penetration of up to 100m, (depth dependent) with a high resolution.

Recent work using shallow seismic reflection to build palaeoenvironmental reconstructions have been carried out in the Quaternary glaciated margins of North East America (Barnhardt et al., 1997; Kelley et al., 2010; Brothers et al., 2011; Harris et al., 2013), the English Channel (Lericolais et al., 2003; Van Landeghem et al., 2009), Britain's east coast (Stoker et al., 2009) and west coast (Roberts et al., 2011) and in lakes (Eyles et al., 2000; Turner et al., 2012). Similarly it is used for palaeoenvironmental studies at lower latitudes such as the Mediterranean (Zecchin et al., 2011; Anastasakis and Piper, 2013) or the Pacific (Leroy et al., 2008). Recently seismic data has been used in conjunction with high resolution bathymetry and backscatter to correlate the ancient depositional environments more coherently with the modern deposits on the sea floor (Leroy et al., 2008; Quinn et al., 2010; Harris et al., 2013).

In Ireland, shallow seismic have been collected in Clew Bay, Mayo (Carolan, 2006), Belfast Lough (Cooper et al., 2002) and the study area (Cooper et al., 2002; Huang, 2004; McDowell et al., 2005; Kelley et al., 2006; Quinn et al., 2009; 2010) and local environmental reconstructions were proposed.

3.4.1 Data collection

The datasets analysed in this chapter have been collected over 13 years from 1997 to 2010 by various research projects mainly by the University of Ulster (see table 3.4 for list). Although some have been already presented in previous articles and reports (Cooper et al., 2002; Huang, 2004; McDowell et al., 2005; Kelley et al., 2006; Quinn et al., 2009; 2010), never has the whole corpus of seismic data for the region been analysed and compared consistently. This analysis presented some challenges as the coverage of the region is sparse (figure 3.11) and the datasets were collected with 2 instruments of differing characteristics; namely Chirp and Pinger. These are described below (based on Stoker et al., 1997).

The Chirp system is a digital, frequency modulated seismic source which is distinct from other systems due to its signature source; a swept frequency pulse (2-16kHz) which is amplitude and phase compensated. The main advantage of this method is an easier adjustment of the signal to noise ratio. The instrument used was an Edge Tech X-Star towfish and the data were originally collected on tapes.

The Pinger system is a low energy, short pulse system that is originally an echo

-sounder of which the frequency of the pulse was lowered (here at 3.5kHz) in order to penetrate further than the seabed. The instrument used for the surveys in this study was a SES Probe 500 attached to the hull of the Marine Institute vessels.

These two systems resulted in different penetration from 3 to 100m depending on the nature of the sediments and have a vertical resolution between 10 and 40cm. Having been selected for different surveys, only one type of instrument was used for various areas or bays which helped the segmentation of the study area in various bays with one type of seismic data used for each of them (figure 3.11). This allowed a direct recognition of seismic units based on their acoustic signatures as these can appear different based due to the type of instrument used and the following processing involved which can differ depending again on the type of instrument used. The Bann Estuary area does contain seismic data collected by the two instruments but only the Chirp datasets were used there as they were the shallowest and closest to shore.

3.4.2 Processing

All the datasets for the study area have been integrated in an SMT Kingdom suite software project at the University of Ulster by Ruth Plets. This process is described at length in Quinn et al. (2009) and will only be summarised here. The Chirp data was recorded originally on analogue tapes and needed to be digitised first before integration. This process revealed discrepancies in the navigational data and prompted extensive work in the relocation of the seismic lines. The GPS used in these older data (pre 2007) would have had a minimum error of the order of 30m which limits the accuracy of these navigational datasets. More recent data were positioned using a DGPS system of the vessel with a much improved accuracy (+/-3m) which when corrected with the layback location of the towfish allows an overall position error of within a few meters.

Issues related to tidal height were tackled using the vertical shift tool of the SMT Kingdom software by comparing the measured seabed depth with the measured depth from the multibeam dataset (JIBS). This is only approximative though as the velocity of sound through the water at the time of surveys is not known and only approximated to 1500 m/s. Post-processing, which allows a clearer visualisation of the seismic data was then undertaken. Resampling of some of the dataset to a sampling rate of 0.05ms was performed in order to allow further processing in the SMT Kingdom software designed to cope only

with data with such a sampling rate. Early spectrum analysis helped with the selection of cut-off frequencies for a trapezoidal bandpass filter (2.5, 3, 7, 7.25kHz for the Chirp for instance) in order to reduce the main source of noise from the data. Automatic Gain Control of 10ms were then applied and the result was enveloped to help visualise the main reflectors in the dataset. A comparison of the output of the various processes is shown in figure 3.12. This process was performed on most of the dataset already at the University of Ulster and the SMT Kingdom project was used for this study at that stage. Some more recent seismic lines were added subsequently and pre-processed (see table 3.5 for list of where each process was undertaken).

Area	Instrument	Year of survey	Publications using the dataset	Source	Comments
Offshore Magilligan to Portstewart	Chirp	1997	McDowell et al., 2005; Quinn et al., 2009, 2010	J. McKenna and A. Cooper, UU	RSL change study
Skerries area	Chirp	1997	Cooper et al., 2002; Kelley et al., 2006; Quinn et al., 2009, 2010	J. McKenna and A. Cooper, UU	RSL change study
Whitepark Bay	Chirp	1997	none	J. McKenna and A. Cooper, UU	RSL change study
Offshore Bann estuary to Portstewart, close to shore	Chirp	2001	McDowell et al., 2005; Quinn et al., 2009, 2010	L. McDowell and R. Quinn, UU	L. McDowell PhD study
Runkerry Bay	Chirp	2001	Cooper et al., 2002; Huang, 2004; Kelley et al., 2006; Quinn et al., 2009, 2010	J. Huang and R. Quinn, UU	J. Huang PhD study
Lough Foyle	Pinger	2005	none	A. Cooper, UU	1 line, very fast survey
Portstewart to Portrush, close to shore	Chirp	2007	Quinn et al., 2009, 2010	R. Quinn, UU	extra coverage for RSL change studies
Lough Swilly	Pinger	2009	none	A. Cooper, UU	1 discontinuous line
Offshore Causeway coast, parallel to coast	Pinger	2009	none	R. Quinn, R. Plets and K. Westley, UU	Student training and JIBS project
Church Bay	Pinger	2009	none	R. Quinn, R. Plets and K. Westley, UU	Student training and JIBS project
Ballycastle Bay	Pinger	2009	none	R. Quinn, R. Plets and K. Westley, UU	Student training and JIBS project
Bann estuary, further offshore	Pinger	2010	none	R. Quinn, R. Plets and K. Westley, UU	Student training and JIBS project

Table 3.4: List of sources and previous publications for each seismic datasets.

Area	Instrument	Year of survey	Georeferencing and importing in SMT Kingdom	Processing	Time to Depth conversion	Interpretation
Offshore Magilligan to Portstewart	Chirp	1997	CMA, SES, University of Ulster	CMA, SES, University of Ulster	Benjamin Thébaudeau	Benjamin Thébaudeau
Skerries area	Chirp	1997	CMA, SES, University of Ulster	CMA, SES, University of Ulster	Benjamin Thébaudeau	Benjamin Thébaudeau
Whitepark Bay	Chirp	1997	CMA, SES, University of Ulster	CMA, SES, University of Ulster	Benjamin Thébaudeau	Benjamin Thébaudeau
Offshore Bann estuary to Portstewart, close to shore	Chirp	2001	CMA, SES, University of Ulster	CMA, SES, University of Ulster	Benjamin Thébaudeau	Benjamin Thébaudeau
Runkerry Bay	Chirp	2001	CMA, SES, University of Ulster	CMA, SES, University of Ulster	Benjamin Thébaudeau	Benjamin Thébaudeau
Lough Foyle	Pinger	2005	CMA, SES, University of Ulster	CMA, SES, University of Ulster and Benjamin Thébaudeau	Benjamin Thébaudeau	Benjamin Thébaudeau
Portstewart to Portrush, close to shore	Chirp	2007	CMA, SES, University of Ulster	CMA, SES, University of Ulster	Benjamin Thébaudeau	Benjamin Thébaudeau
Lough Swilly	Pinger	2009	CMA, SES, University of Ulster	CMA, SES, University of Ulster and Benjamin Thébaudeau	Benjamin Thébaudeau	Benjamin Thébaudeau
Offshore Causeway coast, parallel to coast	Pinger	2009	CMA, SES, University of Ulster	CMA, SES, University of Ulster and Benjamin Thébaudeau	Benjamin Thébaudeau	Benjamin Thébaudeau
Church Bay	Pinger	2009	CMA, SES, University of Ulster	CMA, SES, University of Ulster	Benjamin Thébaudeau	Benjamin Thébaudeau
Ballycastle Bay	Pinger	2009	CMA, SES, University of Ulster	CMA, SES, University of Ulster	Benjamin Thébaudeau	Benjamin Thébaudeau
Bann estuary, further offshore	Pinger	2010	CMA, SES, University of Ulster	Benjamin Thébaudeau	Benjamin Thébaudeau	Benjamin Thébaudeau

Table 3.5: List of operators for each of the processes of each seismic datasets.

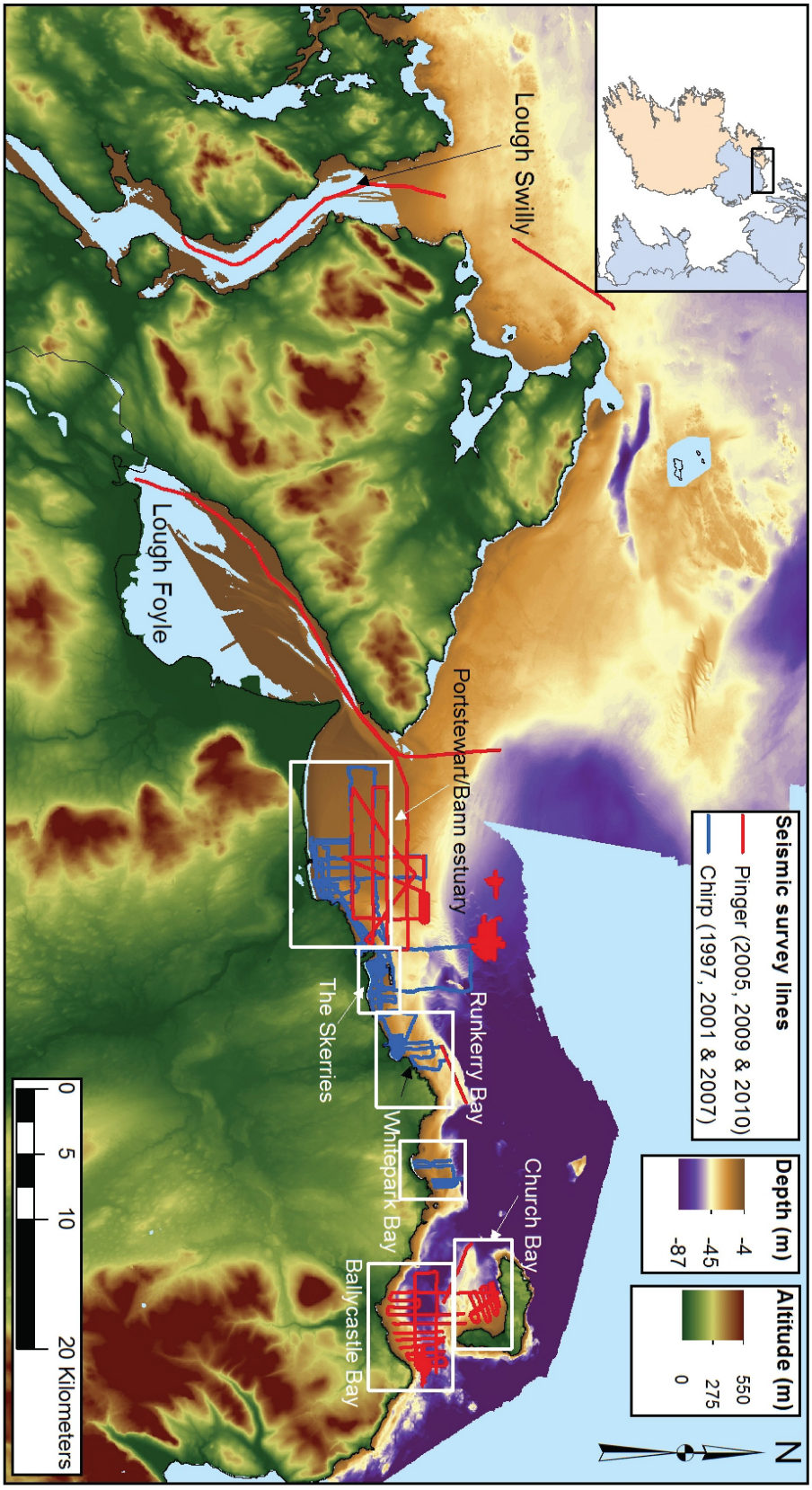

Figure 3.11: Location of the seismic lines of the study area, colour coded by the instrument used to record them, with the location of the bays used to descrine the data below.

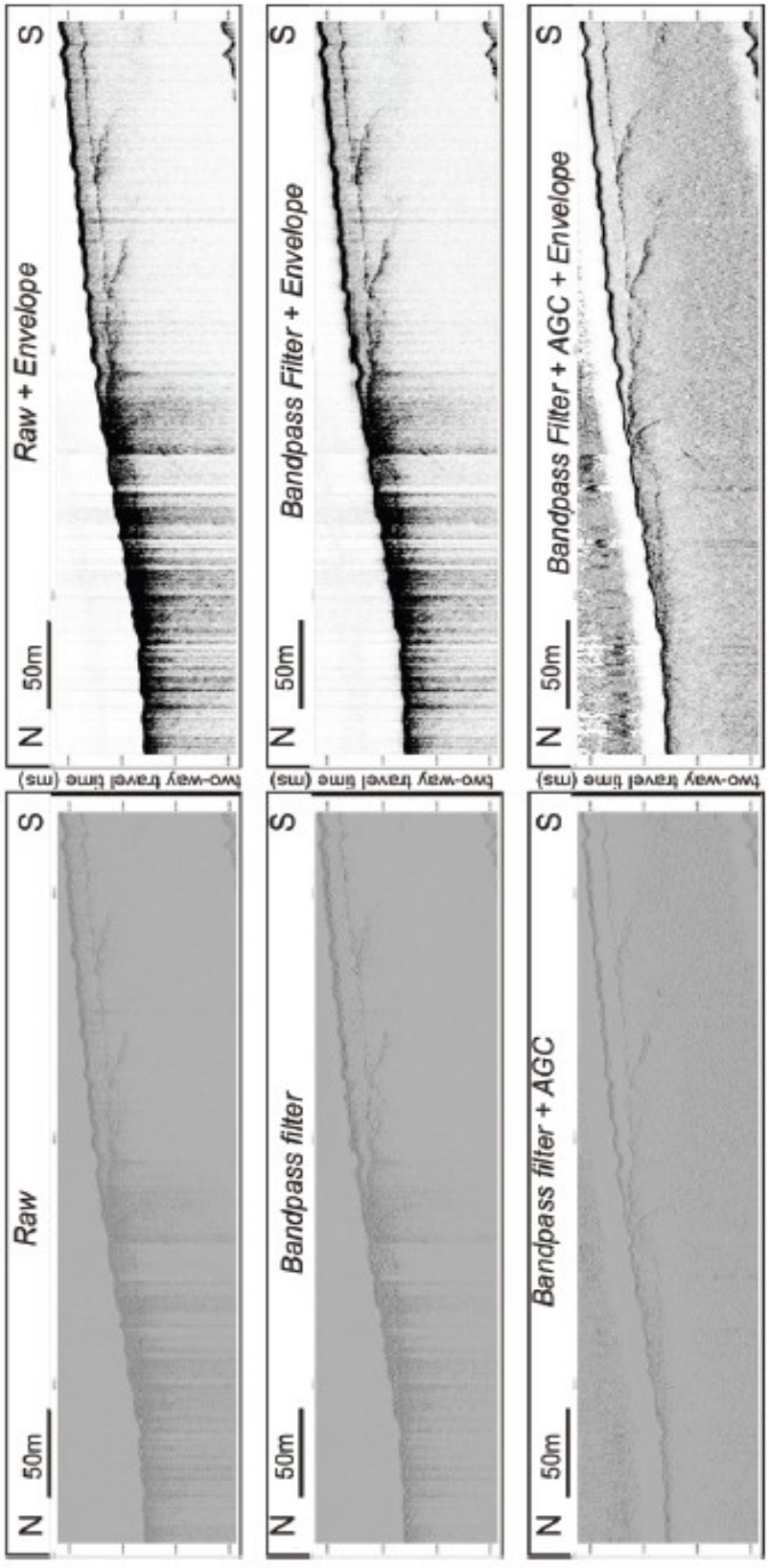

Figure 3.12: Example of outputs for the various stages of the post-process on the SMT Kingdom software (from Quinn et al, 2009).

3.4.3 Interpretation

This step of the study was entirely and consistently carried out by Benjamin Thébaudeau in Trinity College Dublin (table 3.5). All seismic lines were subjected to an approximate time/depth conversion using an average acoustic velocity of 1500m/s (Cooper et al., 2002; Stoker et al., 2009; Quinn et al., 2009; 2010). Then the reflectors visible on the datasets were digitised in order to create what are called horizons for the software. This was done by starting from the lowest reflector reached defined as the acoustic basement and recognising the main reflectors delimiting seismic units towards the surface (Abbot and Carter, 2007; Cooper, 2007; Stoker et al. , 2009; Zecchin and Catuneanu, 2013; Catuneanu and Zecchin, 2013). These horizons were then gridded by the author using the inverse distance to power weighting with a cell size of 10m, a distance weight power of 2 and a search distance of 500m (distance of extension of the grid beyond the last recorded points). In this process, data are weighted so that the influence of one point relative to another declines with distance. The greater the distance weight power, the less effect the points far removed have. Several other types of interpolation methods, such as kriging, were tested but the former one was selected based on its smooth output in either dense or sparsely covered area. These grids were exported as .xyz format and interpolated in the IVS Fledermaus software using the weighted moving average of a 3m diameter to a cell size of 5m in order to create digital elevation models of the surface of a particular units comparable with bathymetric data. For some of the units, a grid of their thickness was computed using the extended math function of SMT Kingdom and similarly exported and interpolated in Fledermaus.

The reflectors previously identified and the units they separated were then described following the methodology of Mitchum et al. (1977) where their following characteristics were mentioned:

- reflector continuity, amplitude and external geometry,
- unit acoustic signature, pattern of internal reflection, external geometry and thickness.

When the recognised seismic units are found outcropping at the surface, the available backscatter data from the JIBS (section 3.1) was used to correlate with their surficial acoustic value (Carolan, 2006). Using this, the seismic acoustic signature and the general geometry of the units and available knowledge on the stratigraphy of the area

based on terrestrial sections, sediment samples and cores, tentative interpretation as to the nature of the units are made and presented in section 6.3.

3.5 Core collection

3.5.1 Method and site selection

Seismic data, like any geophysical data, are great tools for the spatial recognition of stratigraphical units that contrast in their physical properties with each other. The seismic units recognised can only be interpreted based on certain assumptions on their acoustic signature and general morphology and by comparing with known ground-truthed stratigraphies where the seismic units identified where identified through sampling. The sampling of buried marine sediments is harder than on land as coring equipment needs to be activated from a platform or a vessel and the longer the core, the more stable the coring platform must be.

The best proven equipment for such a campaign is a vibrocorer due to its reliable results in terms of sediment retrieval and flexibility of use in various substrate. This tool is a an engine with extra weight sitting on top of a metal tube that is remotely activated (by cable) to vibrate in order to push the tube into the seabed. A plastic liner is located inside the tube and a special sediment catcher ends it in order to retrieve the sediment column. When the vibrating engine indicates that it sits on the seabed or that it has hit a level of resistance too hard to push through, then the whole equipment is lifted back to the coring platform and the liner is extracted, cut in section and sealed.

This research project was able to commission such a survey. It was undertaken in partnership with the Geological Survey of Ireland (GSI) who chartered the vessel ILV Granuaile (figure 3.13) of the Commissioners of Irish Lights (CIL). This large vessel is regularly used for maintaining navigation buoys and lighthouses around the island of Ireland which entails using their Differential Positioning GPS (DP) to maintain a stable location in shallow and violent waters. Despite the absence of an A frame in certain configurations, its large working deck allows its main crane to operate a vibro corer with comfort.

Figure 3.13: The Irish Lights Vessel Granuaile.

The equipment used was a Geo Marine Survey Systems GeoCorer 6000 that was borrowed from the GSI. Further consumables were supplied by the Marine Insitute. This equipment can retrieve cores of up to 6m in length at depth up to 300m (figure 3.14).

Figure 3.14: The Geocorer 6000 set up for coring on the ILV Granuaile.

The number of coring target locations was limited due to financial constraints. The sites were selected based on their depth and location as the vessel was limited in terms of draught and proximity to shore for operation. But most importantly, they were selected based on their potential for a maximum number of the seismic units to be retrieved in a 6m core; for example when seismic units are thinning upwards. Sites where a particular complex relationship between the various units were sought for in order to help decipher the stratigraphy.

Three locations were selected for investigation; Church Bay, Runkerry Bay and the Bann estuary. These three were selected to diversify the potential geological calibrations and so help build a more regional understanding of the Quaternary sediments' stratigraphy. Church Bay was selected as no sub-bottom cores existed in the area and principally because of its sheltered environment which should offer better preservation of the Quaternary stratigraphy. In particular, the unit SCB4 was targeted due to its unusual acoustic signature for the region (see section 6.1.5).

Runkerry Bay was selected to revisit previous findings of Kelley et al. (2006) and Quinn et al. (2009; 2010) for the Skerries area and sites were selected based on their potential for deeper penetration of the corer than the ones retrieved previously.

The Bann estuary area was selected due to its dual sediment influence from rivers (out of Lough Foyle and the river Bann) and the open sea to the north west. In particular, the inferred palaeochannel (see section 6.1.4) was targeted.

3.5.2 Results from the coring survey

The survey took place in late November 2012 over two days and 16 cores were attempted with 14 retrieved. In total, more than 35m of cores were collected with 3 cores over 4.5m in length . Of the 14 cores retrieved, 7 were collected in Church Bay, 4 in Runkerry Bay and 3 in the Bann estuary. Their location is summarised in table 3.6 and plotted on figures 3.15 to 3.17.

Area	Name	Length (m)	Easting	Northing	Depth (m)	Comments
Church Bay	CBT1	5.27	677061.21	6129906.067	10.5	
	CBT2	0	676644.425	6129785.229	15	no penetration
	CBT3	1.02	676355.969	6129723.025	20.4	
	CBT5	3.25	676038.009	6129603.031	30.8	
	CBT7	3.03	675673.072	6129469.868	40.1	
	CB5	2.52	676514.996	6129365.969	27.2	
	CB1	5.24	675479.985	6129827.085	46.5	
	CB2	4.91	674731.037	6129590.023	63	
Runkerry Bay	RK2	2	656375.983	6123047.946	18.4	
	RK5	1	656288.981	6122764.928	16	
	RK6	2	655273.01	6122727.931	26.2	
	RK4	2.4	655211.011	6122844.013	27.7	
Bann estuary	PS1	1.44	641591.006	6117444.937	13.9	
	PS3	1.71	642989.038	6116992.841	12.15	
	PS4	1	644019.09	6117057.858	8.85	
	PS5	0	644038.29	6117058.666	8.5	no penetration

Table 3.6: Location and length of the core retrieved for the three areas investigated.

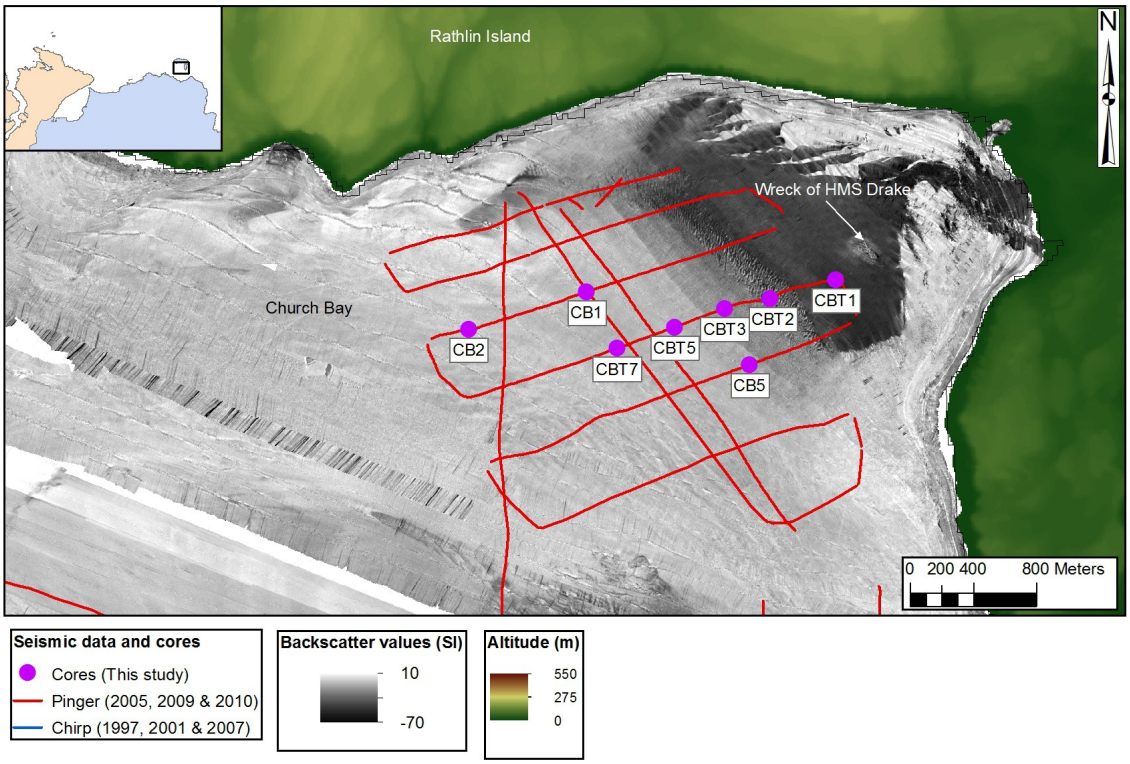

Figure 3.15: Location of the cores retrieved over the seismic data for Church Bay.

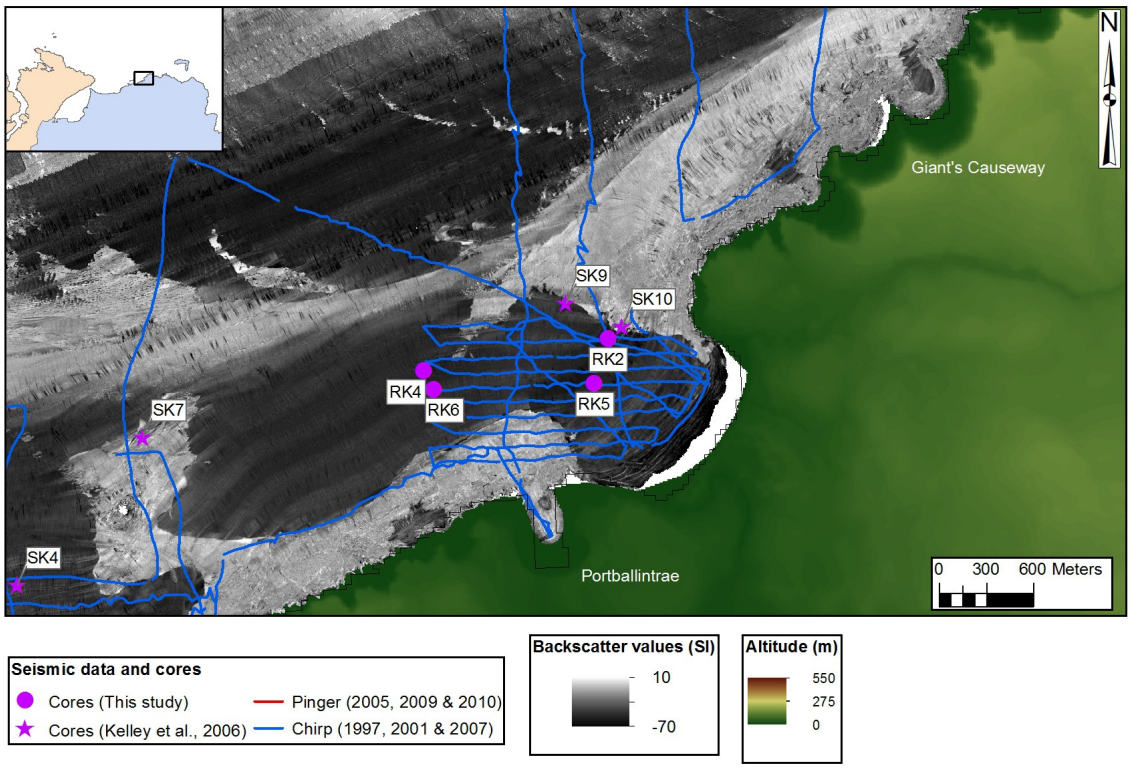

Figure 3.16: Location of the cores retrieved over the seismic data for Runkerry Bay.

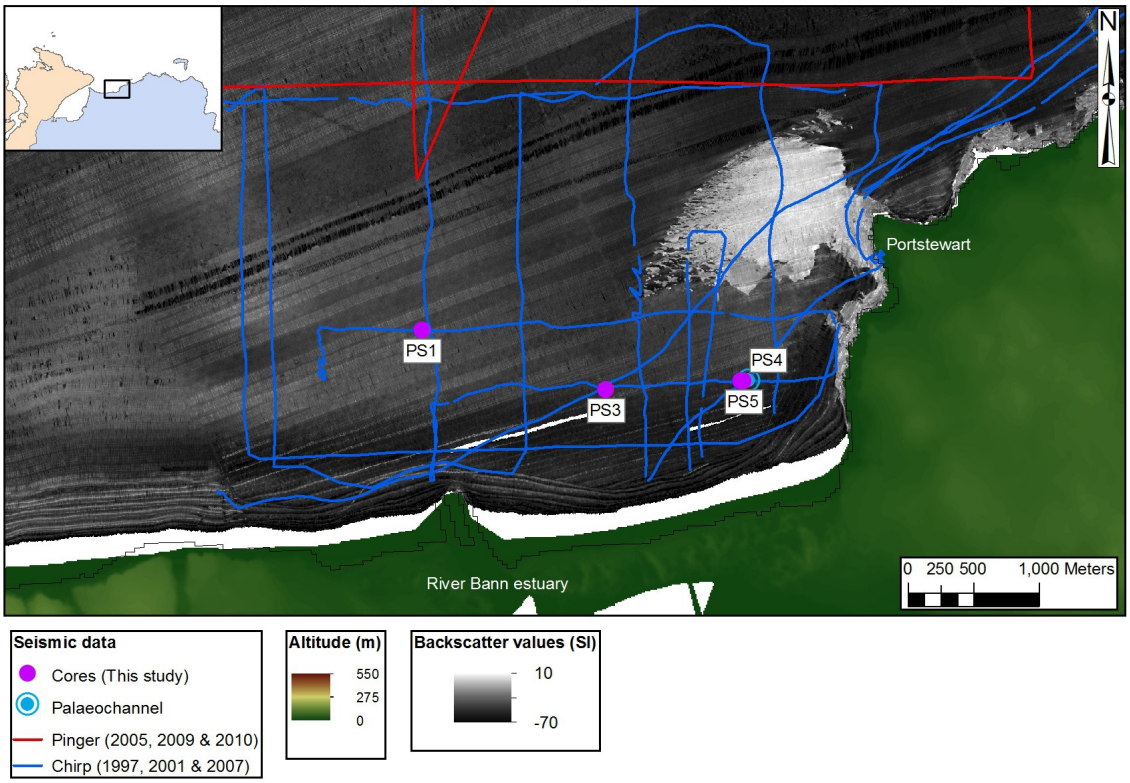

Figure 3.17: Location of the cores retrieved over the seismic data for the Bann estuary area.

3.6 Sediment core analysis

3.6.1 Scanning

The cores retrieved were scanned using a Geotek Multi Sensor Core Logger (MSCL-S) (figure 3.18) at the Irish Sediment Core Research Facilities (ISCORF) at the National University of Ireland Maynooth (NUIM). This practice works like a geophysical scanner of the cores by measuring several physical parameters at once; in this case bulk density through γ ray attenuation, magnetic susceptibility, acoustic P-wave velocity and electrical resistivity. This can be done before or after the splitting of the core. This is of great help to recognise physically contrasting lithofacies and general physical trends in the sediment column as these parameters are correlated with grain size, porosity, nature of the sediment grains and water content (St-Onge et al., 2007). The 14 cores retrieved from this survey were scanned whole before being split in the ISCORF where they were subsequently logged. The scanning data was analysed using the MSCL 7.9 software from

Geotek and visualised using the Corelyser open source software developed for the Corewall suite. The recognised lithofacies' average measured density, magnetic susceptibility, Pwave velocity and resistivity are presented in the result section below and the average Pwave velocity was further used to plot the retrieved cores over the seismic data (appendix 6.2).

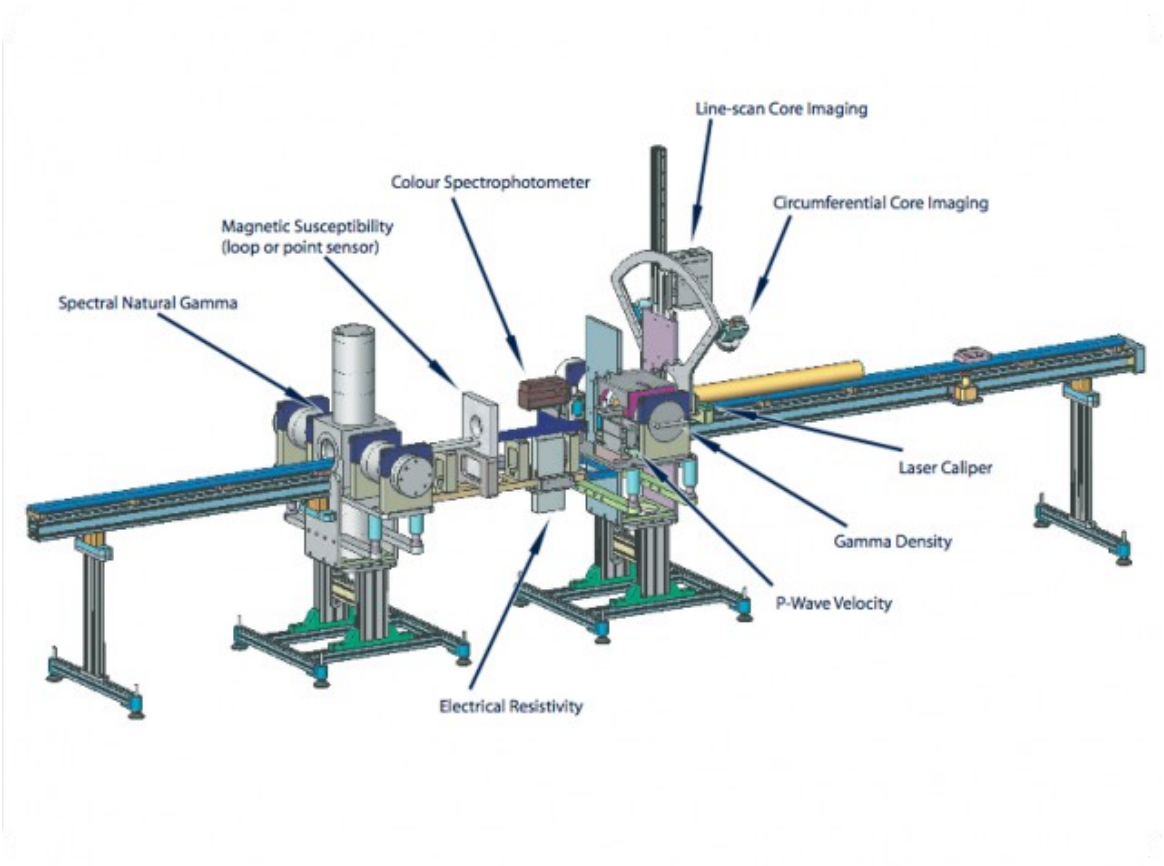

Figure 3.18: 3D diagram of the MSCL-S (taken from www.geotek.co.uk).

3.6.2 Micropalaeontological analysis

Foraminifera are single-cell organisms of which the outer shell or test can be agglutinated, calcareous or porcellaneous. They have evolved to inhabit every marine habitat (both benthic and planktonic) and even some freshwater conditions. The wide range of species, recognisable from their tests, have allowed the development of methodology used to study RSL reconstruction (Scott & Medioli, 1978; Horton et al., 1999; Edwards, 2007b), palaeo sea-temperature (Waelbroeck et al., 2002) and depositional conditions (Sejrup, 1987).10 samples of about 8cm^3 in volume were extracted from three cores from

the Church bay area. These samples were picked from the five different stratigraphic lithofacies identified in the cores (see lithofacies presentation in section 6.2.2.1 and appendix 6.3). These samples were then dried, mixed with sodium hexametaphosphate and wet sieved in order to collect the 500 to 63 µm fraction. As this fraction still contained a significant amount of quartz grains, the samples were separated using Trichloroethylene in order to float the less dense foraminifera. The resulting samples were dried and randomly separated in order to obtain a representative sample of 200 to 300 forams. These were subsequently picked, identified (Murray, 1979) and counted. The results were entered in the C2 software (Juggins, 2007), developed by Stephen Juggins at Newcastle university, for easier visualisation and presentation. This software is available at http://www.staff.ncl.ac.uk/staff/stephen.juggins/software/C2Home.htm.

The resulting assemblages were compared to known assemblages from Europe presented in Murray (2006). This narrowed down the depositional conditions and in particular the sea water temperature for the lithofacies where the assemblages were recognised.

3.6.3 Radiocarbon dating

Four samples were sent for radiocarbon dating at the facility in Queen's university Belfast. These consisted of articulated and unarticulated bivalves found in the fraction of grain size of over 250 µm of sediment samples of about 10 cm^3 in volume from 2 cores from the Church bay area (figure 6.51 and appendix 6.4). The dates returned were then corrected for marine reservoir effect (Hughen, 2007) and calibrated using the IntCAL online tool developed by Queen's university Belfast (http://intcal.qub.ac.uk). A marine reservoir age of 330 +/-40 years was used for the correction. It was obtained by averaging the published reservoir ages of the 10 closest sites from the online database at Queen's university Belfast (Harkness, 1983; Blake, 2005).

3.7 Conclusion

The various methodologies presented in chapter 3 will be used in the next three chapters for the exploration of the marine geophysical datasets available and the analysis of the collected sediment cores. This multidisciplinary approach aims at uncovering the bedforms in the bathymetric data and the elements of the sub bottom stratigraphy in the seismic data whose formation was influenced by relative sea level change and further constraining this RSL change in space in time. The next chapter will describe the results of the analysis of the bathymetric histograms and marine terrace database and give some first interpretation as to the origins of these bedforms.

Chapter 4

Geomorphological indicators of sea-level change

This chapter will investigate the physical evidence for coastal features linked with former RSL both on topographical and bathymetric data. After a brief description of the features forming on rocky coasts, the extensive previous work on the terrestrial raised shorelines will be presented and analysed. The recent high resolution survey of the bathymetry of the north coast of Ireland will be used here as an opportunity to explore the geomorphological evidence of past RSL offshore. Such research has the potential of adding to the corpus of RSL data points for the area, detecting the level of the deglacial lowstands and testing the main results from the various GRMs produced for Ireland. A marine terrace database will be developed for the study area recording the morphological parameters of these features. The analysis of this database will show the extent of the lithological control on the morphology of the terraces recorded. Finally, these findings will be put in context of changing RSL in order to draw some conclusion on their formation.

4.1 Rocky coasts

Rocky coasts occur where the resistant terrestrial lithology abutts the ocean (Sunamura, 1992; Carter & Woodroffe, 1994; Bird, 2000; Woodroffe, 2002; Davidson-Arnott, 2010) and although they make up as much as 80 % of the world's coastline (Emery and Kuhn, 1982) their study is under-represented in textbooks and the literature (see Naylor et al. 2010 for a review). The influence of the underlying rock type on the morphology of such coasts is made obvious by its particular resistance to erosion from the various actions of the waves, tidal currents and weathering both subaerial and submarine. Scientists from the 1980s onwards (Trenhaile, 1987, Sunamura, 1992) have classified the different types of rocky coasts according to the maturity of their coastal profile (Figure 4.1). The first and more immature profiles are called plunging cliffs (or Type C for Sunamura (1992)) where the RSL has only reached its current level recently and has not been able to erode the cliff wall significantly. The early erosion of the cliff wall is called a cliff notch (figures 4.4 and 4.5). The two other types of rocky coast profiles are the results of either a lithology with a weaker resistance to erosion or a longer stable RSL at the modern level creating shore platforms in the intertidal zone. Type B can be described as a cliff with a horizontal shore platform and type A profiles present a ramp or a sloping platform. Although these distinctions can be useful, more recent literature has started to describe these profiles as a spectrum of slope angles for the platforms (Trenhaile, 2010; Thébaudeau et al., 2013).

Rocky coasts evolve generally at slow rates but these rates can vary greatly. A classic example of these processes are the creation of sea caves in faults or weaker areas of the bedrock leading to the isolation of a stack linked to the cliffs by a sea arch. The eventual collapse of this arch is a sudden event that is difficult to predict but the erosional process involved can take centuries. In places, dramatic changes have happened suddenly, as in the St Margaret's Bay Chalk cliff failure in the south of England on the 24/03/2013 (Nolan, 2013). The erosion rate of rocks varies according to the lithology and internal structure but also to the local coastal energy with the fastest erosion rates recorded in wave-dominated environments (Woodroffe, 2002). A range of erosion rates for different types of lithology has been recorded worldwide through cliff retreat from early maps and/or photographs and thanks to erosion meters fixed on platforms and cliff faces. This work was undertaken at first by Emery and Kuhn (1982), was revisited by Sunamura

(1992) and has been updated recently by Dasgupta (2010). The global mean rate of platform erosion as measured by instruments is 1.486 mm/year (Stephenson and Finlayson, 2009). Although these rates were measured on a short term basis (up to 5 years), Stephenson et al. (2010) have suggested that they are more indicative than those measured for a longer term where rising uncertainties become an issue. The range of measured erosion globally goes from 0.004 mm/year for Granites and metamorphic lithologies from Sweden to 9.13 mm/year for sedimentary rocks in New Zealand and although the rates can be different for the same lithology from site to site reflecting the influence of local environmental constraints on coastal processes, clear distinctions are observed between different types of lithologies.

Of interest to the study area, the following values of erosion rates specific to local lithologies are taken from the latest review by Dasgupta (2010) and presented in figure 4.2. Basalt has an average measured erosion rate of 0.5 mm/year but no cliff retreats has been observed at the sites studied (Cape Reamur-Port Fairy, Victoria, Australia in Gill (1973)) which suggest an erosion rate of less than 0.01 mm/year. Chalk as measured has an erosion rate of 3.65 mm/year (English Channel coast, UK and France in Foote et al. (2006)) but shows a range of 10 to 3000 mm/year as recorded in cliff retreat (Sunamura, 1992). The chalk of this study area (the Ulster White Chalk Formation) possesses a much greater hardness and a much lower porosity than its other western Europe counterparts (Section 2.1.3) and despite the high energy waves the local cliffs are exposed, the local erosion rates are likely to be greater than the above mentioned value. Finally sedimentary and metamorphic lithologies globally have a measured mean erosion rate of 1.282 mm/year and 0.625 mm/year respectively (Dasgupta, 2010) but the erosion rate for sedimentary lithologies ranges quite dramatically from 0.01 to 1000 mm/year as recorded in cliff retreat (Sunamura, 1992). It is obvious from figure 4.2 that cliff-retreats cannot be used as a proxy for erosion rates as the measured average rates sit outside their range for most lithologies. This is likely due to structural control involved in the potentially rapid retreat of cliffs in chalk or Quaternary sediments. And as for basalt, the only measurement published (Gill, 1973) could not detect any cliff retreat. The measured rates are all contained in the order of 1mm/year but some variations linked with the rock resistance are visible.

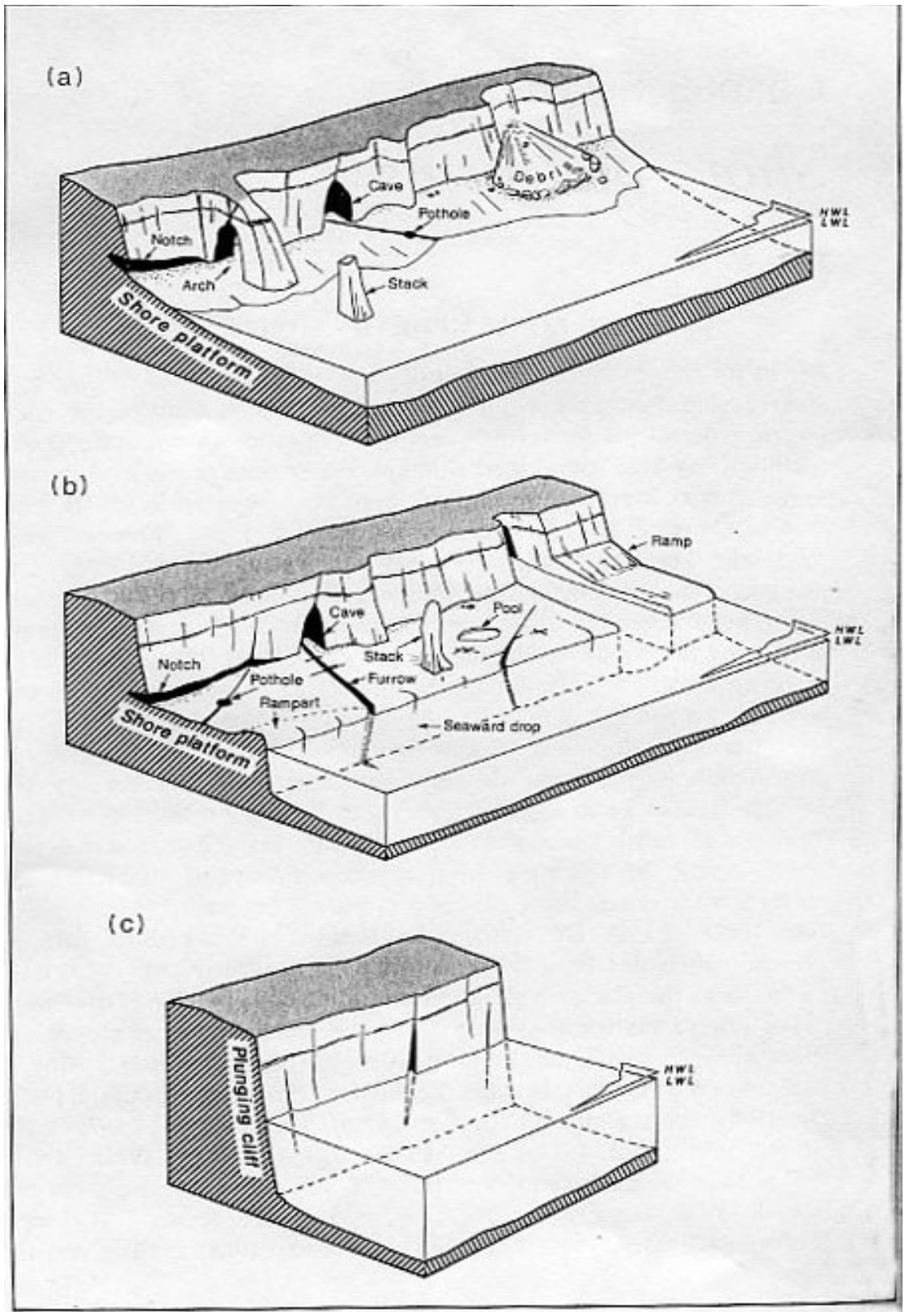

Figure 4.1: Diagram of the different types of rock coasts and their associated features: A) Cliff with a ramp or sloping shore platform; B) Cliff with a sub-horizontal shore platform; C) Plunging cliffs with no platform (from Sunamura, 1992).

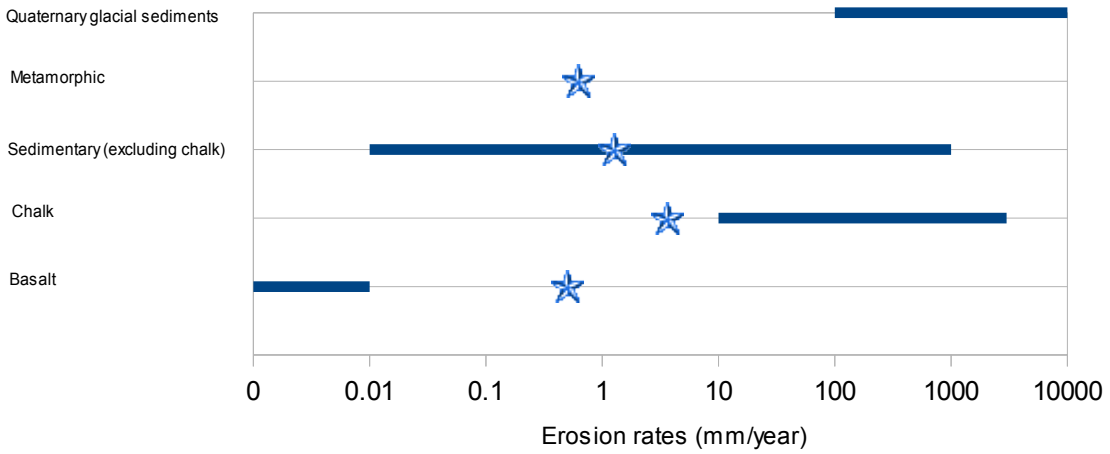

Figure 4.2: Global average of measured erosion rates (stars) and global range of recorded erosion rates from cliff retreats (lines) for various lithologies (adapted from Dasgupta, 2010).

4.1.1 Shore-platforms and marine terraces as RSL indicators

Shore-platforms develop in the intertidal zone where erosional processes, such as hydraulic quarrying caused by wave actions, operate at or near to the water surface (Trenhaile, 1997; 2000; 2012). Commonly gullies, narrow channels roughly perpendicular to the shoreline, and potholes are formed on the bedrock surface of shore platforms due to movement of pebbles and boulders in the swash zone (figures 4.1 and 4.3 and Woodroffe, 2002). The processes involved in the formation of shore-platforms occur at various rates dependent on the nature of the lithology and on the wave energy but also on other external factors such as thermal conditions and biological processes (Trenhaile, 2012). In particular, the influence of freeze-thaw processes in paraglacial conditions can lead to the rapid removal of frozen material and the formation of strandflats (Bird, 2000). Whilst the shore platforms are clearly linked to RSL and tidal range, mean platform elevation and the height of the junction between the cliff and the seaward shore platform (the cliff–platform junction) varies within the intertidal zone according to wave exposure, weathering intensity and the resistance of the rock (Trenhaile and Byrne, 1986; Trenhaile, 2002). Consequently, these features can constrain the height of RSL but only with vertical uncertainties of several metres (Carter, 1983; McKenna, 1990; 2002; McKenna et al., 1992).

Figure 4.3: Modern shore platform forming in Basalt from the study area. A gully is visible to bottom right of the picture (Kieran Westley).

With a change in RSL, shore platforms may be converted into subaerial or submarine terraces, or sloping erosional continental and island shelves. Similarly cliff notches can be recognised on the cliff face above or below the modern RSL (figures 4.4 and 4.5). Since they can rarely be dated directly, these erosional features are usually interpreted in the light of associated sedimentary deposits and/or by correlation with other features of inferred equivalent age, although this reasoning sometimes becomes circular (Devoy, 1983; McCabe, 2008b). Similarly the presence of ice striae on a platform in line with an identified ice stream associated with dated deposits on land could help constrain its formation to preceding the glaciation linked with this ice stream. One particular challenge is distinguishing whether a rock platform is genetically linked to the most recent phase of RSL change, or is in fact inherited from an earlier RSL phase (or phases) (Young and Bryant, 1993; Brooke et al., 1994; Stone et al., 1996; Trenhaile et al., 1999; Trenhaile, 2002; 2010; Blanco Chao et al., 2003; McKenna, 2008).

Figure 4.4: Cliff notch found above modern RSL in Chalk cliffs of the study area.

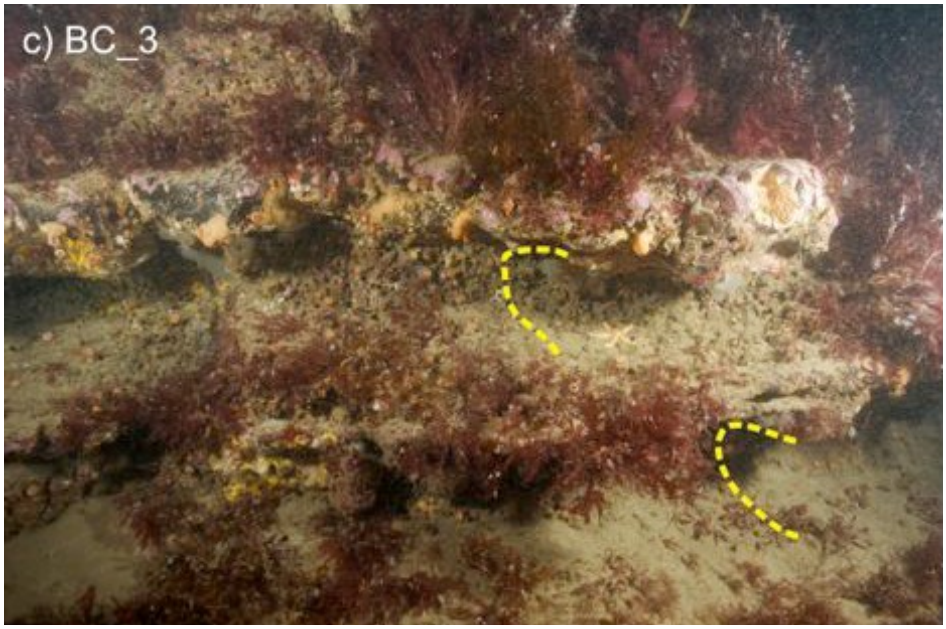

Figure 4.5: Submerged cliff notch found in the study area during ground truthing dives (from Quinn et al., 2010). Yellow lines have been drawn to emphasise the notches' profiles.

Wave erosion on hard rock coasts is accomplished mainly by the dislodgement and removal of joint blocks and other rock fragments, usually by broken waves (Trenhaile, 1987; Swantesson et al., 2006; Trenhaile and Kanyaya, 2007; Stephenson and Naylor, 2011). The processes responsible for wave quarrying, such as water hammer (impact) and the wave-induced compression of pockets of air in rock crevices, operate at or close to the water surface, which migrates up and down the foreshore with the tides and with changes in RSL. The evolution and profile development of a rock coast through mechanical wave erosion therefore reflects the amount of erosion accomplished at each elevation according to the resistance of the rock, the wave regime, the effect of submarine topography on rates of wave attenuation, and the amount of time that the waves have operated at each level (Trenhaile, 2000).

4.1.2 Raised shorelines recognised through depositional features

Coastlines composed of cliffs and platforms are also associated with bays where the accretion of wave deposited sediments creates beaches. As sediment accretion continues over decades to centuries, sediment is transported to the backshore and becomes inactive. It forms a long feature made up of sand and gravel parallel to the shore whose base marks the high water level (Woodroffe, 2002). Storm surges can also transport material such as rounded pebbles (shingles), shells and sand beyond the beach to form a ridge which can lie several metres above modern sea-level (figure 4.6). When RSL falls they are left behind and mark a high point with several metres of vertical uncertainties linked with the tidal and wave regime at the time of their formation. When RSL rises they are either eroded or pushed landward transgressively. This implies that raised beach and storm ridges are evidence of the last passage of RSL at that level as erosion linked with a hypothetical more recent storm surge of RSL rise would have destroyed them.

Figure 4.6: Modern shingle ridge from Rockstown, Co. Donegal on the west coast of the Inishowen peninsula. Its crest is approximately 3m above modern sea-level where the local MHWST is at +1.3m.

Glaciolacustrine deltas and glaciomarine fans are depositional mounds of coarse sediments from deglacial waters discharging in a lake or the sea (Bennett and Glasser, 2009). In country with high latitudes like Ireland, they have been used as raised shoreline features when their recognition on land implies a water level higher than their top level but with considerable uncertainty as to the water level actual elevation. It is important to note that they can not be directly linked to RSL as they can have formed in glacial lakes. They usually carry the mark of slumping due to the ice margin retreat and sometimes show sign of erosion from wave action of a subsequent transgression.

4.1.3 Potential relict shoreline features

Figure 4.7 displays two RSL curves extracted from Brooks et al. (2008) and showing various evolution of the RSL with highstands, lowstands and stillstands. The type of coastal features associated with such evolution are added. As described above, stillstands, or periods when the RSL is stable, will produce cliff notches or marine terraces depending on the resistance of the substrate (type of lithology or unconsolidated sediments). Highstands can leave behind beach or gravel ridges as well as washing limits (described in section 4.2.1 below). And lowstands can leave a channel cut, due to fresh water flowing into the lower level of the sea, or a break of slope on the coastal profile corresponding to the lowest level of wave action. Subsequent change in the RSL, in particular if wave erosion is once again active at the levels where the relict shoreline features have been formed, will rework, attenuate or even obliterate these features. In figure 4.7, features formed at L1 may potentially be overridden or eroded deeper by the subsequent wave action at L2 and so become unrecognisable. Similarly, beach ridges left behind by H1 can be obliterated by further transgression toward H2, in particular if the sea level rises slowly creating a ravinement surface (Cooper, 2007). Hence, the investigation of relict shoreline features in the offshore data presented below will be put in context of the type of RSL curve required for their formation and preservation.

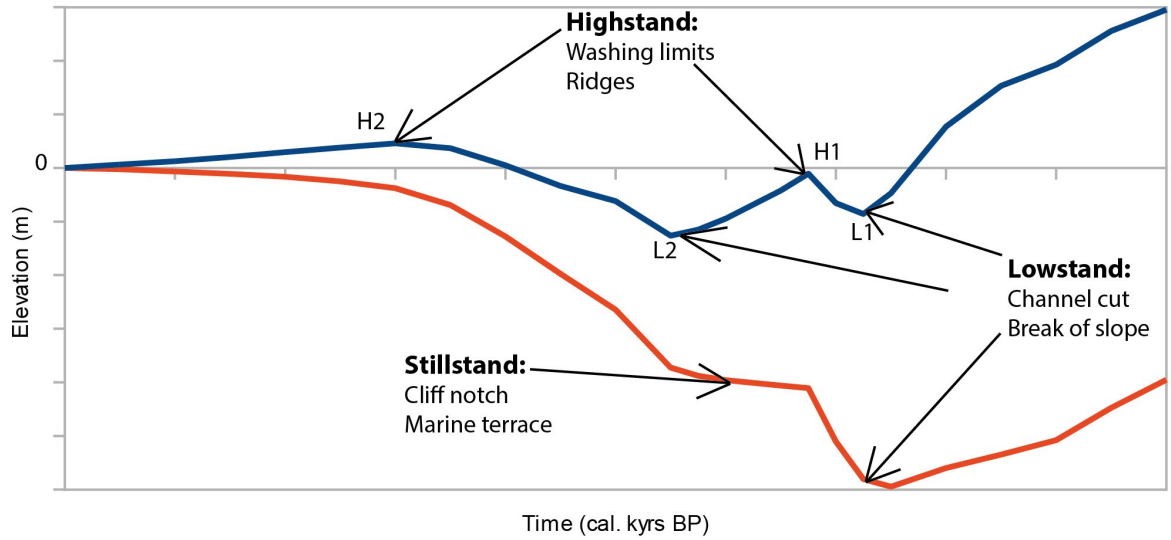

Figure 4.7: Schematic representation of potential relict shoreline features formed by evolving RSL. The RSL curves are extracted from Brooks et al. (2008).

4.2 Raised and submerged shorelines as recognised in the north of Ireland

4.2.1 Raised shorelines of the study area

The north coast of Ireland is not only famous for its geology but has been the subject of studies on raised shorelines for close to two centuries. In the first half of the 19th century, J.E. Portlock (1843) reports in his chapter on "detritus" on the gravel ridges around Lough Foyle in county Derry but only hints at their potential marine origin. By the end of the 19th century, the Geological Survey of Ireland's memoirs on the region (Hull et al., 1890; Symes and McHenry, 1886) discuss the raised beaches observed in North Donegal (the highest in Ireland at 15 to 23m elevation) and to the south east of the study area beside the town of Cushendall and R.L. Praeger (1895; 1896) reports on the raised beach's fauna from Inishowen and the north-eastern coast of Ireland. The term "raised beach" is then in use and appears to represent deposits found on raised terraces. These deposits had been recognised in Scotland as well and, although not forming a continuous feature, were generally considered synchronous when found at the same elevation. As the effect of isostasy was recognised in formally glaciated areas, this led to the recognition of shoreline series corresponding to various highstands of the RSL. Praeger relates the understanding of these features at that time: "Professor Hull (then head of the Geological Survey of Ireland) has pointed out that the elevation above present sea-level of the raised beaches of the east coast of Ireland increases as we pass northward, varying from high-water mark at Dublin to twenty feet (6m) above it on the Antrim coast; and he identifies this Irish series with the twenty-five-foot (7.5m +/- 2m) raised beach of Scotland. Into this suggestion [...] I need not at present inquire, but may remark that my observations bear out, on the whole, Hull's statement as to a general increase of elevation with increasing latitude" (Praeger, 1896, p 31). Unfortunately Praeger does not mention any of these features in detail north of Larne. His work forms the basis of a methodology for sea-level change reconstruction based on the fauna and flora found in archaeological deposits (Coffey and Praeger, 1904).

As radiocarbon dating of such features was carried out in the first half of the 20th century through the excavation of archaeological sites associated with these late glacial shorelines alongside the understanding of the local palaeobotanical stratigraphy, a general consensus emerged that the shorelines of the same series became younger with increasing distance from the proposed ice centre. This led W.B. Wright (1937) to develop the

isokinetic theory where a raised shoreline formed when the local rate of isostatic rebound corresponded to the rate of eustatic sea-level rise, i.e. a stillstand. In the early phases of deglaciation, the eustatic sea-level was rising rapidly and could keep up with the high rate of rebound found in areas closer to the former ice centres. As the rate of eustatic sea-level rise decreased, the crust was rising too rapidly so that the zone of active coastal processes shifted towards areas of lower isostatic rebound away from the centre of the ice sheet. This was the first theory to explain the tilt found on some of the highest raised shoreline series of Scotland and Ireland (McCabe, 2008b). The lower raised shorelines considered to be post glacial in origin were found to be flat for the most part with a slight tilt at the outer margins.

In his extensive work in the Firth of Forth, the Scottish academic J.B. Sissons (1963) showed that all the raised shorelines of the area presented a tilt away from the ice centre. His view was that, although this tilt varied with a higher angle (42cm per km) for the late glacial shoreline and a lower angle (7cm per km) for the later post-glacial series, every raised shoreline had a tilt. This conclusion prompted the work of several scientists in Ireland during the next decade (Stephens, 1963; Prior, 1965; Orme, 1966; Stephens and Synge, 1965; Synge and Stephens, 1966) who started to survey systematically the northern and eastern coastline of Ireland as well as the western coastline of Scotland for new raised shorelines and reassessed the earlier findings. Synge and Stephens (1966) examined the field relationships between marine forms, ice limits and sea-levels. In particular, the interactions of moving ice margins, isostatic adjustment and global eustatic sea level trends were recognised as the cause of low preservation potential of raised marine features and the difficulty of linking fragmentary evidence along narrow coastal strips.

Aware of the fragmentary nature of coastal morphological evidence, the range of raised shoreline features in the study area was then extended to include newly discovered erosional features such as terraces and notches and depositional features such as beach and storm ridges but also to include another type of raised marine evidence entitled “washing limits”. These are described by the authors as “the upper limits above which the effects of wave action cannot be detected” (Synge and Stephens, 1966). They give examples of these that can be described as erosional features (that were then undatable):

1. the upper limit of bare rock in cliffs or hills with shallow sediment cover,
2. the lower limit of perched rock as waves would have dislodged them,

3. the lower limit of shallow channels at the surface of deltas for instance as wave actions would have flattened them
4. the upper limit of "washed drift" which is recognisable in a section as a thin layer (about 1m) of reworked glacial sediments where the finest components have been removed.

All of these different features classified as washing limits would correspond to the highest water mark for a given RSL and so could have a similar relationship to sea-level as the crest of storm ridges. The recorded raised shorelines of Donegal (Stephens and Synge, 1965) and of Antrim and Derry (Synge and Stephens, 1966) are presented in figure 3.8 and table 4.1 where the height measured by the authors in feet comparing with the OD of Belfast at the time have been converted into meters compared to the modern OD of Malin Head. No case by case description of these features are given but Stephens and Synge (1966) explain that the raised beaches are composed of much more poorly sorted material than modern beaches (consistent with the view that they were formed from glacigenic sediments) and that they only considered strandline features that were cut into drift or other unconsolidated sediments (as rock cut strandline necessited a much longer period of stable sea-level for formation).

Place name	Easting	Northing	Elevation in meters	Feature
Drumnagreagh Port	335000	413000	20.29	cliff notch
Drumnagreagh Port	335000	413000	18.48	cliff notch
Drumnagreagh Port	335000	413000	15.45	cliff notch
Drumnagreagh Port	335000	413000	6.36	cliff notch
Drumnagreagh Port	335000	413000	3.94	cliff notch
Glenarm	331000	416000	18.48	cliff notch
Glenarm	331000	416000	15.45	cliff notch
Glenarm	331000	416000	6.36	cliff notch
Glenarm	331000	416000	3.94	cliff notch
Glenarm	331000	416000	8.48	shingle ridge
Garron point	330000	425000	16.66	cliff notch
Garron point	330000	425000	7.57	cliff notch
Carnlough	328000	418000	17.87	cliff notch
Carnlough	328000	418000	5.76	cliff notch
Carnlough	328000	418000	3.03	cliff notch
Carnlough	328000	418000	16.96	shingle ridge
Carnlough	328000	418000	7.57	shingle ridge
Tornamoney Point	326000	434000	16.05	cliff notch
Tornamoney Point	326000	434000	10.60	cliff notch
Tornamoney Point	326000	434000	8.48	cliff notch
Tornamoney Point	326000	434000	21.50	washing limit
Red Bay	325000	425000	18.48	cliff notch
Red Bay	325000	425000	8.48	cliff notch

Place name	Easting	Northing	Elevation in meters	Feature
Red Bay	325000	425000	4.85	cliff notch
Red Bay	325000	425000	16.96	terrace
Cushendun	325000	434000	15.45	cliff notch
Cushendun	325000	434000	8.48	peat deposits ?
Cushendun	325000	434000	6.36	shingle ridge
Cushendun	325000	434000	3.33	shingle ridge
Cushendun	325000	434000	10.91	terrace
Cushendall	324000	428000	10.00	shingle ridge
Cushendall	324000	428000	4.55	shingle ridge
Cushendall	324000	428000	6.06	terrace
Cushendall	324000	428000	18.78	washing limit
Torr head	324000	442000	21.20	washing limit
Rue Point	316000	447000	9.69	cliff notch
Rue Point	316000	447000	7.88	cliff notch
Rue Point	316000	447000	3.94	cliff notch
Rue Point	316000	447000	18.17	washing limit
Church Bay	315000	451000	18.78	shingle ridge
Ballycastle	312000	442000	12.42	terrace
Portballintrae	293000	442000	7.57	unknown
Portballintrae	293000	442000	8.48	washing limit
Portrush	286000	440000	7.88	shingle ridge
Portstewart	282000	439000	7.27	shingle ridge
Portstewart	282000	439000	4.85	shingle ridge
Dunagree Point	268000	444000	19.99	washing limit
Dunagree Point	268000	444000	17.87	washing limit
Greencastle	265000	440000	21.50	washing limit
Kinnagoe Bay	264000	447000	5.15	cliff notch
Roe mouth	264000	429000	6.36	terrace
Ballykelly	263000	423000	16.05	cliff notch
Ballykelly	263000	423000	6.67	cliff notch
Ballykelly	263000	423000	4.24	cliff notch
Ballykelly	263000	423000	2.43	cliff notch
Moville	262000	438000	21.50	washing limit
Tremone	259000	448000	7.27	cliff notch
Tremone	259000	448000	3.33	cliff notch
Tremone	259000	448000	12.42	terrace of gravel
Tremone	259000	448000	21.50	terrace of shingle
Gresteel	256000	423000	15.45	cliff notch
Gresteel	256000	423000	7.57	cliff notch
Gresteel	256000	423000	3.64	cliff notch
Gresteel	256000	423000	2.12	cliff notch
Donnybrewer	253000	424000	12.42	cliff notch
Donnybrewer	253000	424000	4.55	cliff notch
Drumskellan	251000	428000	4.55	cliff notch
Troma	251000	429000	14.24	cliff notch
Troma	251000	429000	4.85	cliff notch
Troma	251000	429000	2.73	cliff notch
Drumskellan	251000	428000	13.33	terrace
Drumskellan	251000	428000	2.12	terrace of shelly gravel
Drumskellan	251000	428000	5.76	washing limit
Culmore	247000	424000	4.55	cliff notch
Culmore	247000	424000	3.03	cliff notch
Culmore	247000	424000	13.33	terrace

Place name	Easting	Northing	Elevation in meters	Feature
Ballycramsy	244000	453000	5.15	cliff notch
Ballycramsy	244000	453000	16.66	shingle ridge
Doon	243000	458000	3.94	beach ridge
Doon	243000	458000	6.36	cliff notch
Doon	243000	458000	15.45	terrace
Doon	243000	458000	19.99	terrace of shingle
Rashenny	242000	448000	3.03	cliff notch
Rashenny	242000	448000	13.03	terrace
Rashenny	242000	448000	3.94	terrace
Rashenny	242000	448000	17.57	washing limit
Rashenny	242000	448000	6.97	washing limit
Malin Head	238000	459000	21.81	shingle ridge
Malin Head	238000	459000	6.97	shingle ridge
Malin Head	238000	459000	13.63	terrace
Malin Head	238000	459000	7.57	terrace of drift
Malin Head	238000	459000	19.99	washing limit
Pollan Bay	238000	450000	19.99	washing limit
Kindrohid	235000	448000	19.99	shingle ridge
Rockstown	234000	448000	15.15	cliff notch
Rockstown	234000	448000	10.00	cliff notch
Rockstown	234000	448000	4.24	cliff notch
Rockstown	234000	448000	6.97	terrace
White Castle	233000	433000	14.24	cliff notch
White Castle	233000	433000	4.55	cliff notch
White Castle	233000	433000	3.94	cliff notch
Dunaff Bay	232000	447000	9.39	cliff notch
Dunaff Bay	232000	447000	9.39	shingle ridge
Portbane	229000	439500	3.33	terrace of beach sediments
Portbane	229000	439500	10.00	washing limit
Fanad Head	223000	448000	9.69	cliff notch
Fanad Head	223000	448000	7.57	cliff notch
Fanad Head	223000	448000	17.27	shingle ridge
Fanad Head	223000	448000	15.45	washing limit
Glashagh Bay	220500	446500	14.84	cliff notch
Glashagh Bay	220500	446500	8.48	cliff notch
Glashagh Bay	220500	446500	5.76	shingle ridge
Rosapenna	212000	438000	5.45	beach ridge
Rosapenna	212000	438000	12.42	washing limit
Dunfanaghy	202000	438000	3.94	terrace

Table 4.1: List of recorded raised shorelines for the north of Ireland (Stephens and Synge, 1965, Synge and Stephens, 1966). Locations are in the Irish National Grid coordinate system (ITM) and elevations have been converted in meters above Malin OD.

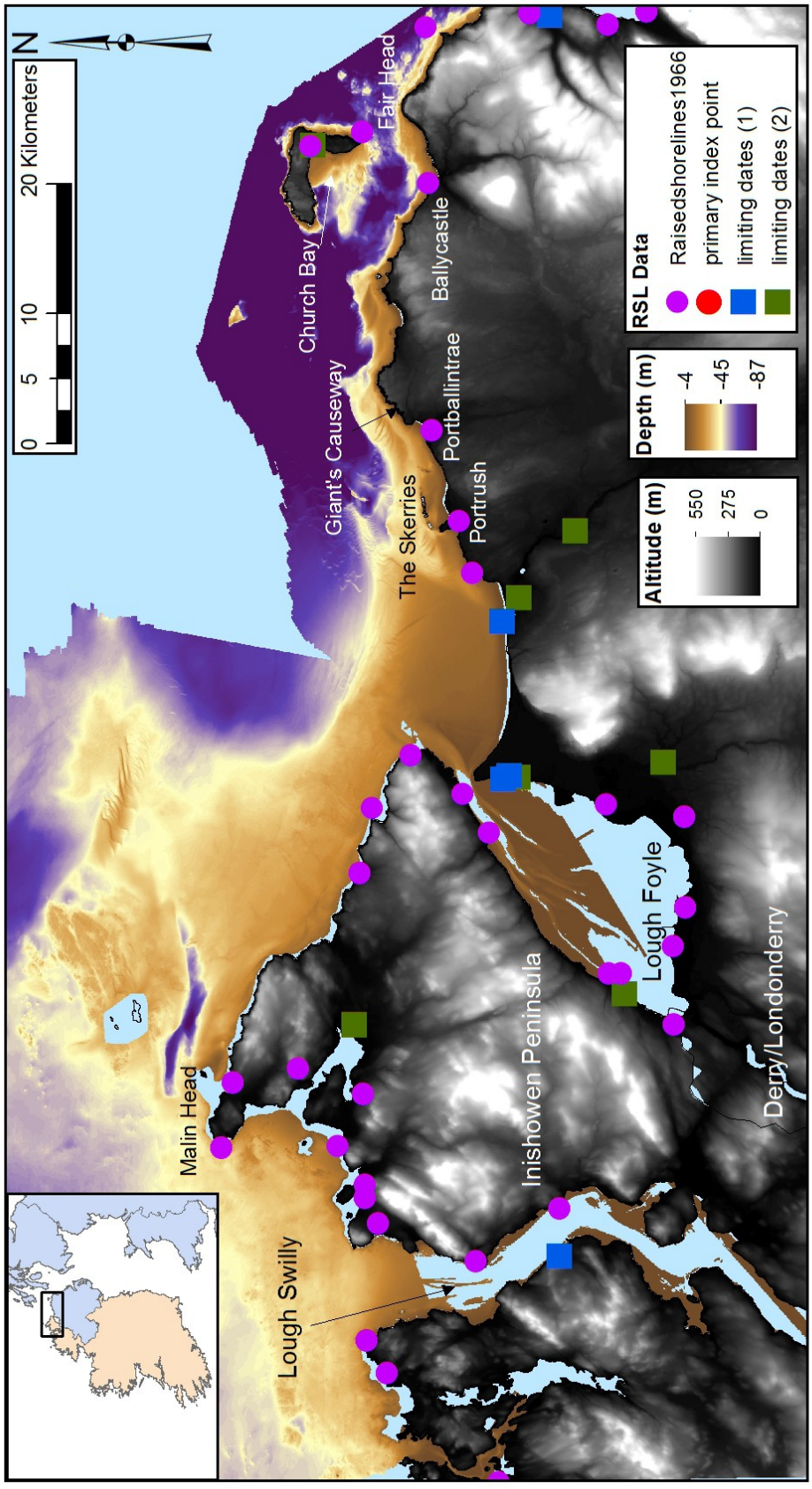

Figure 4.8: Location of recorded raised shorelines (Synge and Stephens, 1966) and sea-level data for the study area (Brooks and Edwards, 2006).

The data points from these surveys were presented on a strandline relation diagram (updated in figure 4.9) in order to relate raised shoreline series from the north of Ireland and Scotland. The shoreline series were dated roughly (Synge and Stephens, 1966) using the idea that the highest shorelines were older in age and on the basis of their location inside or outside known ice readvance extents which had been previously dated. This extensive body of work confirmed the isokinetic theory, that all raised shorelines are tilted and gave a quantitative angle for these tilts that differed from the ones that Sissons (1963) had recorded. Although the dating from these features was based mainly on height and location correlation to other datable depositional glacial features, they were used to build an understanding of the extent and thickness of the ice-sheets of Britain and Ireland and "confirmed" that no major faulting was active in the north channel during the late glacial period.

Later research on raised shorelines tended to highlight their many shortcomings as RSL indicators (Carter, 1982; Devoy, 1983; McKenna, 1990; McKenna et al., 1992). First of all, their fragmented and diverse nature makes the correlations of several unconnected raised shorelines and their relationships to ice limits very tentative. The validity of the RSL reconstruction based almost exclusively on the elevations and tilts of coastal landforms have been questioned. The fact that any direct dating of these erosional feature was impossible and that major uncertainties were associated with the dating of depostional features could not be ignored. Much of the often complex Pleistocene stratigraphy recording the various glacial events found around the coast were thought to correspond to regionwide events and the models created had no geochronological control (McCabe, 2008b). More recent research undertaken by R.W.G. Carter and J.McKenna (McKenna, 1990; McKenna et al., 1992) on the modern basalt shore platforms between Portstewart and Portballintrae in Co. Derry highlighted that the considerable height range of platform developments adds a vertical uncertainty for the corresponding RSL of the order of 5m above and below the cliff-platform junction. Furthermore, structural control from the lithology and local environment means that some modern shore platforms (for example at Seaport and Port Gallen in the study area) exhibit a tilt that is comparable in angle to those measured in the raised shorelines of Scotland and Ireland (McKenna, 1990).

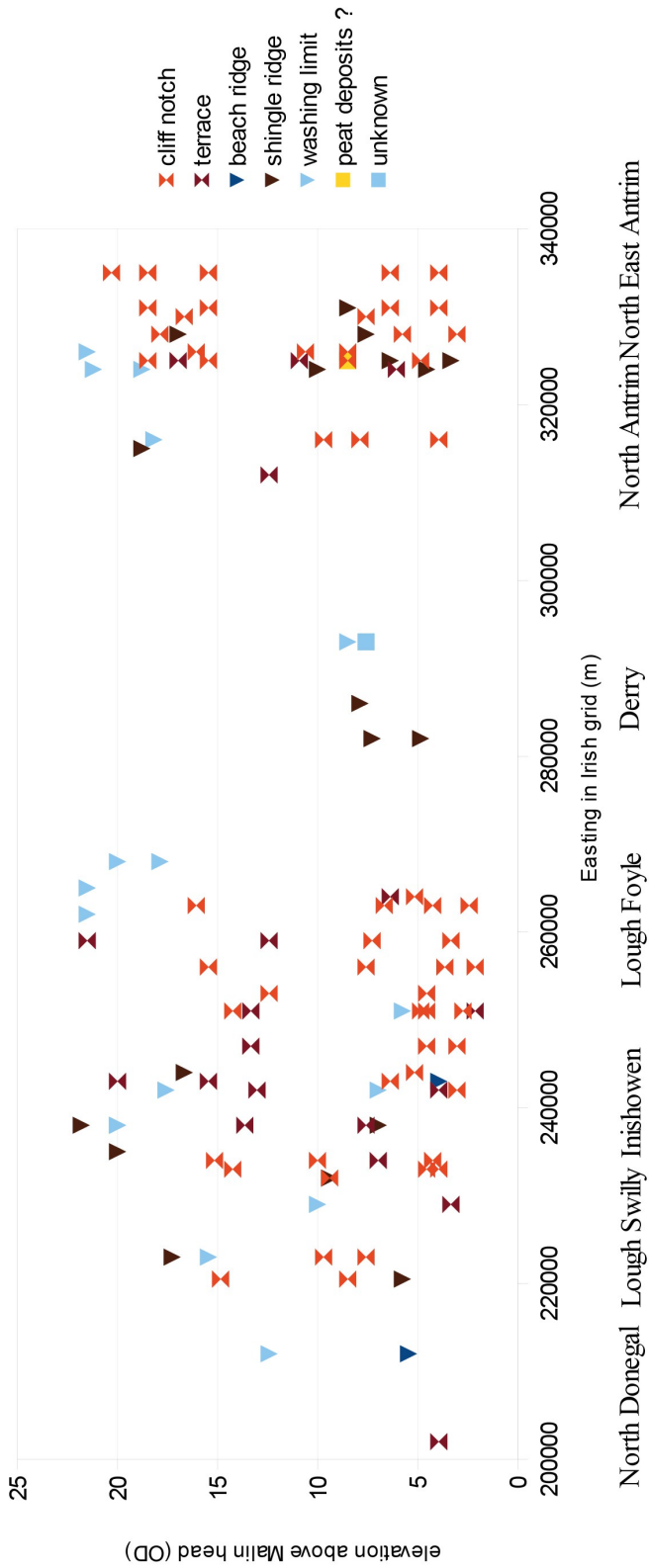

Figure 4.9: Comparison of raised shorelines elevation for the north coast of Ireland (adapted from Synge and Stephens, 1966).

Hence this has led modern research to resurvey the area in search of datable sea-level indicators from which an actual indicative meaning to the RSL at the time of their formation was well understood. Some of the above mentioned features were kept in mind and extensive work by M. McCabe on deglacial history, marine influence and RSL change have led to the development of a more comprehensive range of local models of RSL change for the North East of Ireland (McCabe et al., 2007; McCabe, 2008b). These were built from a corpus of intensely studied sites displaying various phases of transgression and regression linked with the complex deglacial history of the area. Raised shoreline surveyed and studied intensely during the 1960s are not completey discarded as their presence clearly indicates a range of periods of higher than present RSL but the construction of long shoreline series accross the length of the coastline has been abandoned. In some cases presented by McCabe (2008b) where these features are accurately described in their local context, they are still considered contemporaneous with ice sheet readvances that have been dated. Figures 4.10 and 4.11 display the location and meaning of some of these raised shoreline features for Inishowen and the North East coast of Ireland (McCabe and Clark, 2003; McCabe et al., 2007 and Chapter 2).

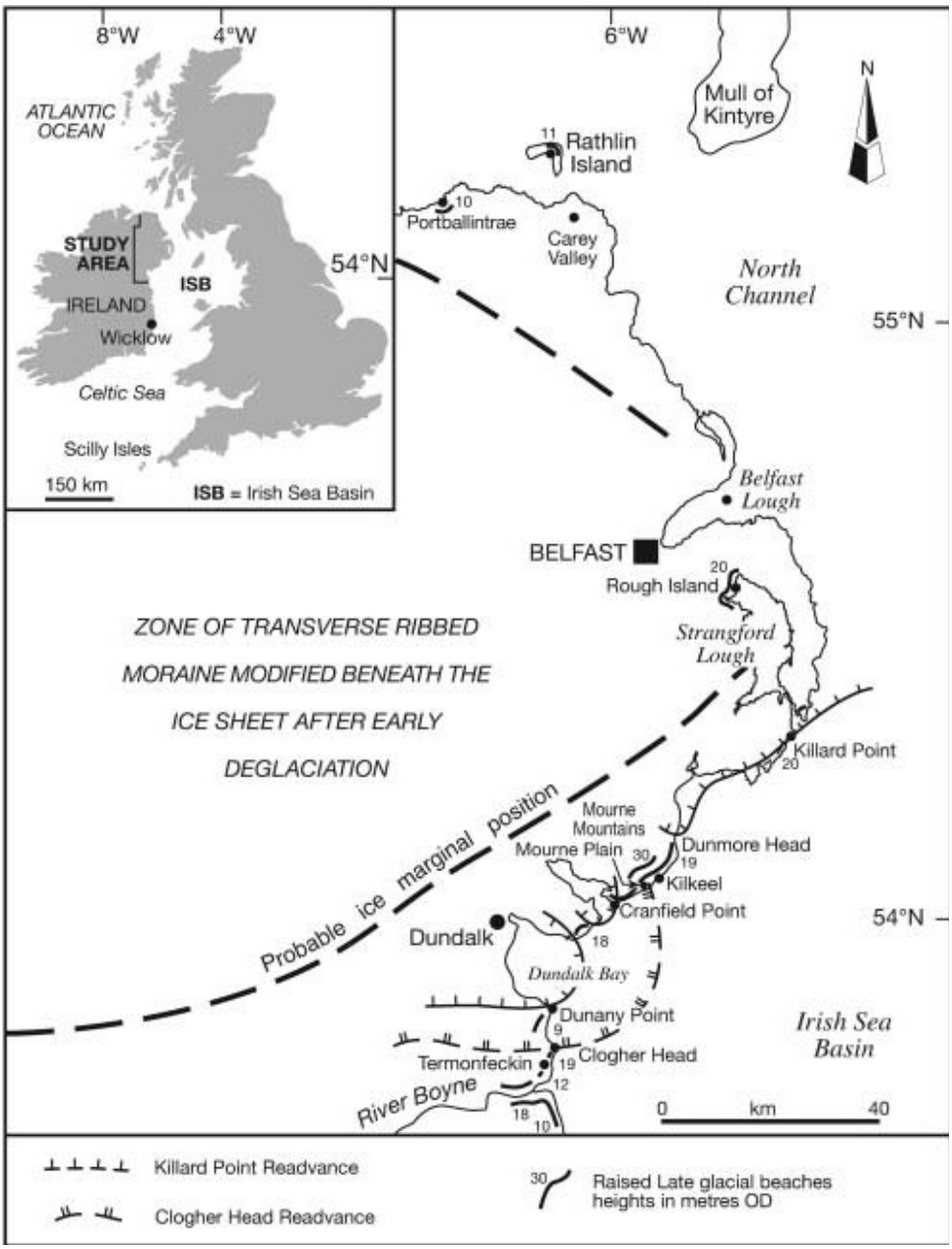

Figure 4.10: Location of raised shorelines in relation to the ice mass during deglaciation. (from McCabe et al., 2007)

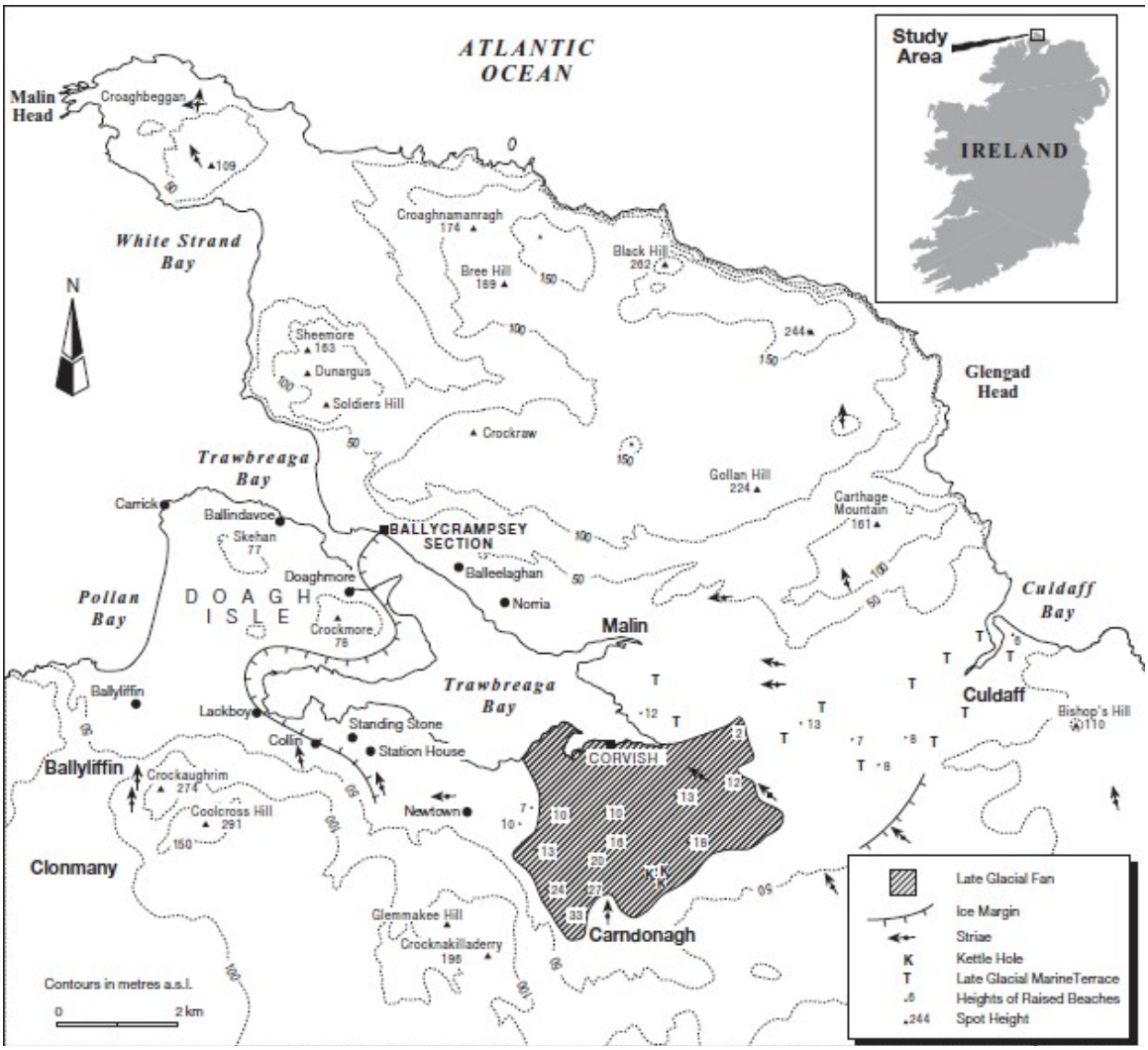

Figure 4.11: Location of raised shorelines in the north of the Inishowen peninsula (from McCabe and Clark, 2003)

Additionally in Lough Foyle, work by Carter (1972, 1975 and 1982) depicted the formation of the Magilligan peninsula from a gravel barrier nucleus (the Giant's Walk) sometime after 7000 BP to a series of raised beach barriers (figure 4.12). This date corresponds to the generally accepted Holocene highstand for the north of Ireland (Chapter 2). The higher shoreline formed by drift deposition to the north of the gravel barrier (at +7m O.D. and still visible in parts around Lough Foyle) was eroded away and reworked to allow the formation of a large inland bay. Up to 30 swash aligned beach ridges were formed from reworked sand of offshore origin to develop the modern foreland with inter-ridge peat overlying the ridges at heights of +2.2m to +3.9m O.D.. The peninsula seaward extension terminates in a high dune barrier (up to +17m O.D.).

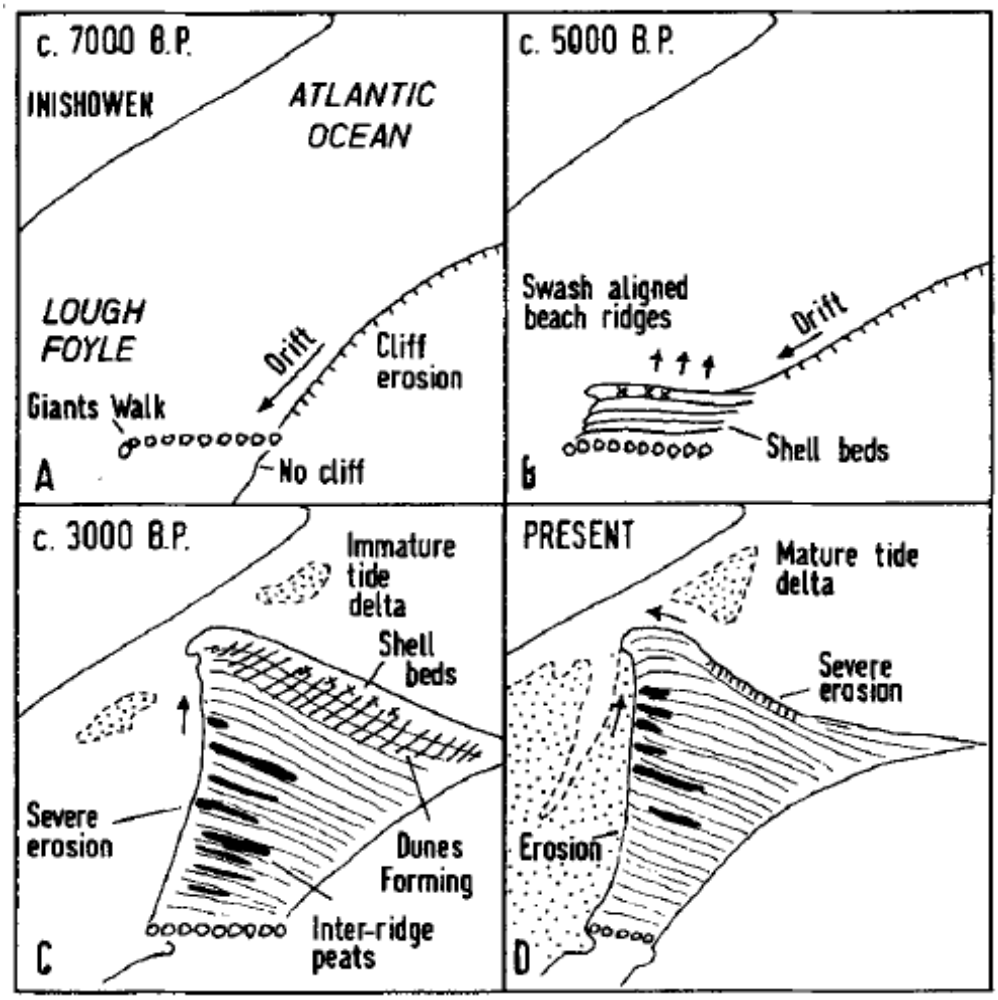

Figure 4.12: Geomorphological evolution of the Magilligan Foreland since 7000 BP (from Carter, 1982).

Today, raised terraces are still used for RSL change reconstruction away from ice sheet influences and in particular for the evaluation of the tectonic uplift which was inflicted on the localities in question (Ferranti et al., 2006; Pedoja et al., 2011). All of these studies use the raised terraces as a depositional level and use the sediments deposited for actual RSL data reconstruction. Some such studies use the cosmogenic nuclide approach to date the length of exposure of the erosional surface (Alvarez-Marron et al., 2008), others use radiocarbon dating from microfossils or finds from archaeological sites at various elevations (Smith et al., 2010; Strasser et al., 2011) or Uranium-series dating from fossils (Muhs et al., 2012).

4.2.2 Geomorphological study of the offshore data

Coastal researchers have understood the potential of finding preserved relict shorelines not only above modern sea-level but below as well. The wave action during a transgression from a lowstand will have the main effect of destroying depositional features of unconsolidated sediments from relict shorelines if these are not buried under other sediments. Hence erosional features and buried marine terraces in particular have been the focus of recent research especially when looking for eustatic lowstands in far field locations away from the influence of ice sheets on isostasy (Rohling et al., 1998; Collina-Girard, 2002; Beaman et al., 2008; Leroy et al., 2008; Rovere et al., 2011; Zecchin et al., 2011). These studies use a methodology called sequence stratigraphy, a multidisciplinary methodology developed in the early 1980s (Abbott and Carter, 2007). It was based on the understanding that the major unconformities recognised in basins worldwide were controlled by RSL changes that could also be found in well logs and outcrops at local, regional and global scale.

In the study area, the early recognition of a consistent break of slope in the Victorian hydrographic chart at the 30m depth contour suggested a potential late glacial lowstand at that level (see Quinn et al., 2008 for a review). Similarly, early investigation of the inner shelf through seismic data and limited coring survey has identified potential beach and terrestrial deposits now submerged by several tens of metres of water, suggestive of periods during which RSL was below present (Cooper et al., 2002; Kelley et al., 2006). Further studies can only be undertaken with the help of very high resolution bathymetric data in order to recognise features a few meters wide or to detect the abruptness of underwater cliffs. The study area did not allow any such investigation until recently when the Joint Irish Bathymetric Survey was undertaken.

4.3 Results from the exploration of the JIBS data

4.3.1 Findings from the histograms

The potential evidence for submerged shorelines in the geomorphology of the seabed was investigated. Initial inspection of the data revealed clear evidence of buried marine terraces and interesting lines of break of slopes and bathymetric histograms were studied for their potential at uncovering submerged shorelines at comparable depth along the study area using the JIBS dataset (section 3.2.1). Figure 4.13 shows the curves obtained for the Northern Irish dataset and the Republic of Ireland datasets over the first 100m depth. The JIBS datasets has been separated into two due to the different institutions in charge of their compiling; i.e. the Marine Institute for the Republic of Ireland and the Maritime and Coastguard Agency for Northern Ireland (see section 3.1.1). Due to the inner programming of ArcGIS, differences in the total depth range of each area's dataset translates into bin-size differences (a depth range of 0 to 277m for Northern Ireland induces a bin size of 1.09 m and a depth range of 3 to 87m for the Republic of Ireland induces a bin size of 0.33 m). In light of the potential influence of bin-effects outlined in section 3.2.1, fine discrete peaks of data at particular depths can be displaced or overridden from one histogram with a smaller bin size to another histogram with a larger bin size. Hence, analysis is restricted to a consideration of the first-order features of each curve rather than on the finer characteristics of particular depth intervals.

The Northern Irish curve reveals spikes at depth of 4m, 13m, 38m, 42m, 47m and 67m. The main spike is recognised at 13m depth +/- 3m making the rest of the curve appear somewhat flat. This is due to the large flat expanse of seabed covered by modern sediment to the north east of the mouth of Lough Foyle visible as a spread of low backscatter values in figure 3.2. It prevents the recognition of spikes of erosional origin that could be related to relict buried shorelines below this depth. The range of depth between 24 to 30m shows a drop in the number of bathymetric points which corresponds to the previously cited main break of slope at these depths (Quinn et al., 2008; 2009; 2010).

The curve for the Republic of Ireland dataset is much more limited in extent from 8m to 53m depth and presents three main concentrations of points with a number of smaller spikes at 20m, 28m, 30m, 34m and 43m.The main concentration of points is between 23m and 39m depth which correspond to the depth range of the mainly bare near shelf around the Inishowen peninsula.

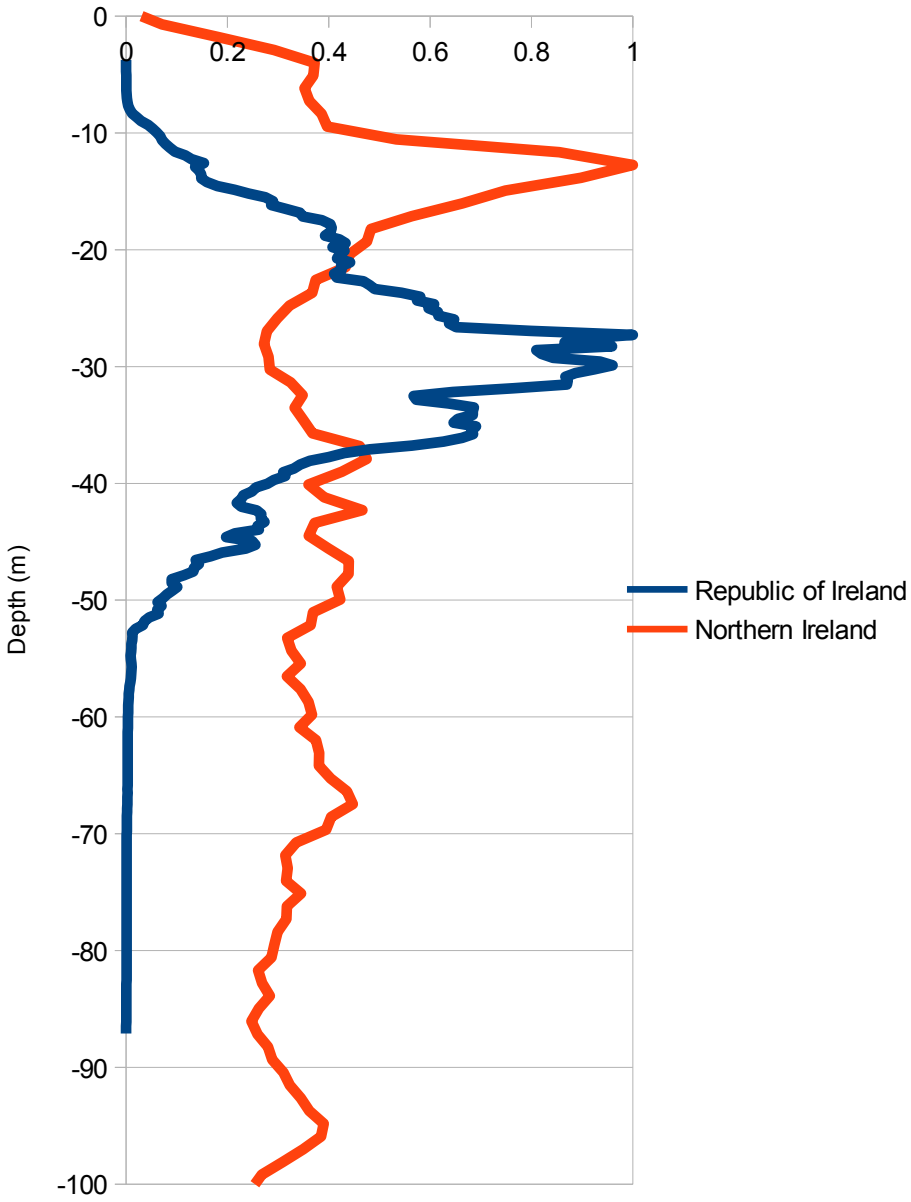

Figure 4.13: Bathymetric histograms for the 2 JIBS datasets.

These two curves are very different and no spike from one of them can be followed or recognised in the other. Hence, these datasets have been subdivided in smaller regions mapped on figure 4.14 in order to recognise more localised spikes and test whether some of these could be followed from one area to the next. If a spike can be followed along the coastline, a potential dipping angle in the relict shoreline could be measured and compared to the one visible on the onshore evidence (sections 1.2 and 2.4.3). Figure 4.15 presents sub divisions of the Northern Irish dataset extracted along the coast from east to west and around Rathlin island. More spikes are apparent and some can be related from one area to the other.

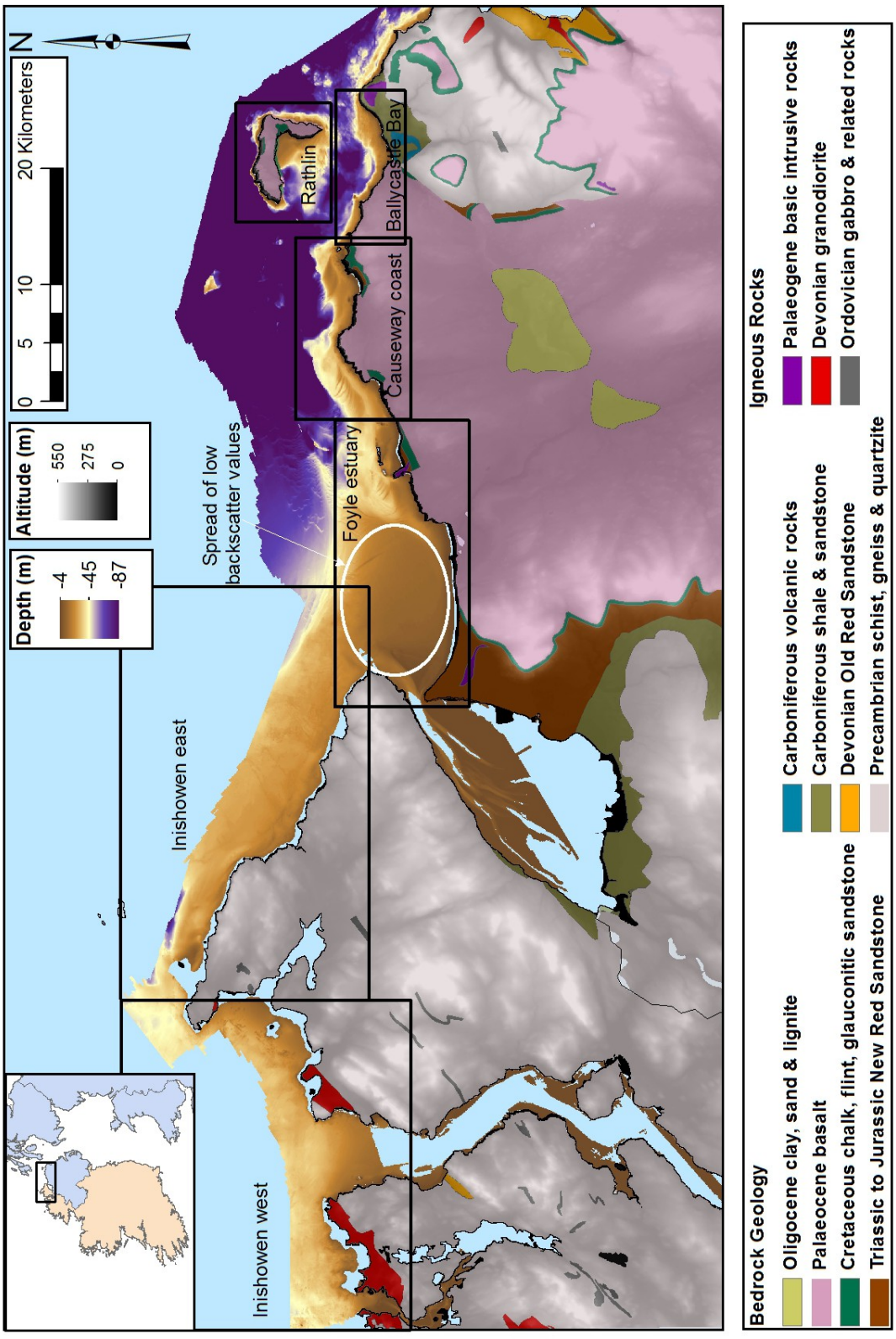

Figure 4.14: Location map of the localised areas of the two datasets used for bathymetric histogram investigation in figure 4.15 and 4.16.

The Foyle estuary area displays the main spike found before for the larger dataset at 13m depth. Similarly to this earlier curve, this spike is so preponderant that the rest of the curve is roughly flat beside a lack of points at depth ranging from 25 to 30m. Of interest, smaller spikes are detected at 5m, 38m and 43m depth.

The Causeway coast displays a quite different bathymetric evolution with a concentration of points between 15 and 50m depths. Again this corresponds to the near shelf as a whole and is mainly controlled by an extensive Basalt lava flow hardly covered by modern sediments and terminating offshore with underwater cliffs. In this range, more minor spikes are observed at depths of 22m, 25m, 32m, 36m and 43m. Outside of the main concentration of points, a large spike is observed at 7m depth +/- 1m.

The Ballycastle Bay bathymetry appears to be bimodal with a first concentration of points between 16 and 29m depth, with a series of more minor spikes at 16, 19 and 25m depth, and a second deeper one between 55 and 75m depth centered around two main spikes at 62 and 68m depth. We can recognise the first concentration of points as the near shelf first appearing mainly as bare rock followed by a rapid drop between 30 and 40m depths. The second concentration of points is recognised to be due to a step in the bedrock towards the basin floor of the area. Outside of these two ranges, another very discrete and prominant spike is detected at 7m depth.

The Rathlin island curve is comparable in shape to the Ballycastle Bay one. Going deeper, a minor spike is recognisable at 6m depth. Then a rather large spike is detected at 15m depth +/-2m, corresponding to the sediment covered near shelf of Church Bay, with a further minor spike at 20m depth, corresponding to the mainly bare bedrock near shelf around the southern part of the island. Finally a wider concentration of points appear between 41 and 53m depths with minor spikes at 42 and 50m depth. Another spike is visible at 60m depth +/-2m.

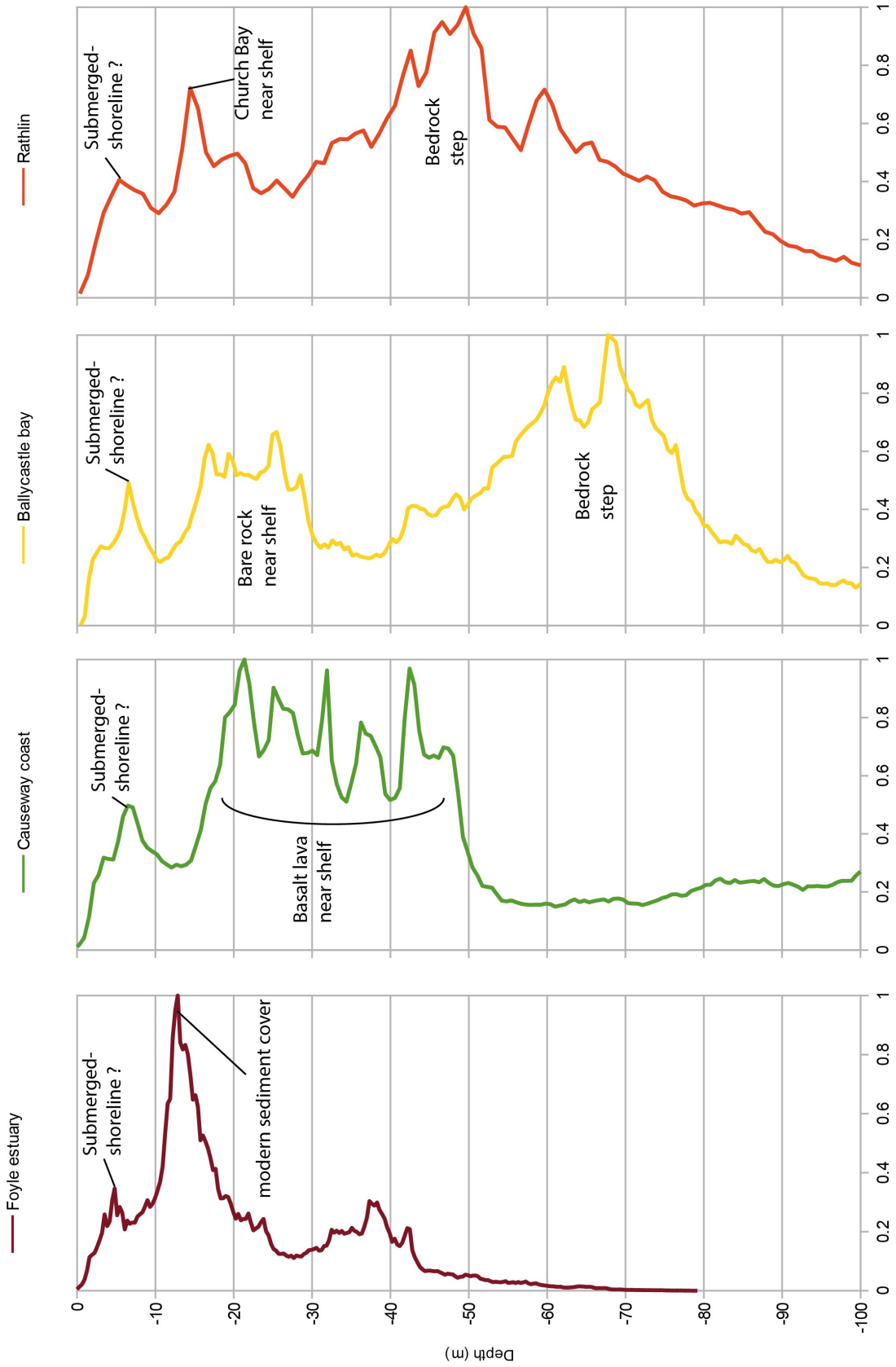

Figure 4.15: Bathymetric histograms for subdivision of the Northern Irish coast.

These four regional curves are more indicative of the depth of potential relict shorelines as each spike can be more directly related to flatter area on the bare bedrock substrate. Of note, the break of slope at 30m depth (see section 2.4.3) is not present in every stretch of the coastline and actually sits in the main concentration of points for the Causeway coast. Beside the main spike in the Foyle estuary linked with modern deposition, the other main concentration of points vary in depth median and depth range from one area to the next and appear controlled by the local lithology in particular the lava flows around the Giant's Causeway coastal area. The evidence of bare rock zones in the bathymetry appears linked with modern sediment deposition pattern where little or no deposition occurs in zones outside the main embayments of the North Antrim coast (Church Bay in Rathlin is an exception) and a large amount of sediment is deposited around the mouth of the Lough Foyle. It is quite unlikely that any major past RSL signal is contained in these lithologically and environmentally controlled concentrations of points. The most interesting spike that can be followed from one zone to the next lies at 5m depth for the Foyle estuary, 6m depth for Rathlin Island and 7m depth for the Causeway coast and Ballycastle Bay.

Similarly, figure 4.16 displays the subdivision of the Republic of Ireland datasets between the east coast of the Inishowen peninsula and the west coast of it with the mouth of the Lough Swilly.

The western zone shows the main concentration of points to be located between 33 and 37m depth corresponding to the main bare bedrock shelf. The sudden drop in the number of bathymetric points following is due to the limited geographical coverage of the survey preventing a correct representation of the range of depths of the shelf. Of note is a more minor spike at 18m depth.

The curve for the eastern coastline of the Inishowen peninsula presents many similarities with the curve for the two datasets combined (Republic of Ireland in figure 4.13) with the main concentration of points located in the range of 27 to 33m depth. A minor spike in the data at 19m depth appears as a potential correlation for the minor spike at 18m on the west side.

The limited extent and depth range of the Republic of Ireland dataset precludes a more general comparison of the bathymetric signal along the whole length of the JIBS

study area. Some particular depths associated with isolated spikes indicate areas of interest where further studies can be concentrated. These associations are made on the basis of significant spikes outside the main depth range with concentrations of points for the various areas that appear to be structurally controlled. The shallowest spikes in our curves were deemed more likely to be associated with potential relict shorelines as they can be traced consistently throughout the subdivision of the dataset with depth sensibly similar and no lithological or structural control was detected for them. Based on these, a continuous "western dip", an east to west gradient due to the proximities of the ice centre in Scotland and Fennoscandia influencing a differential isostatic rebound, is not obvious on the shore platform record (sections 1.2 and 2.4.3). In Northern Ireland, the record for the Foyle estuary shows the shallowest spike (5m depth) in comparison to the areas west of it. A possible correlation is made around the Inishowen Peninsula between spikes observed in the two areas but again it is slightly deeper in the east than in the west. Further precise identification of shoreline features such as marine terraces can help decipher the origin and potential association of these spikes.

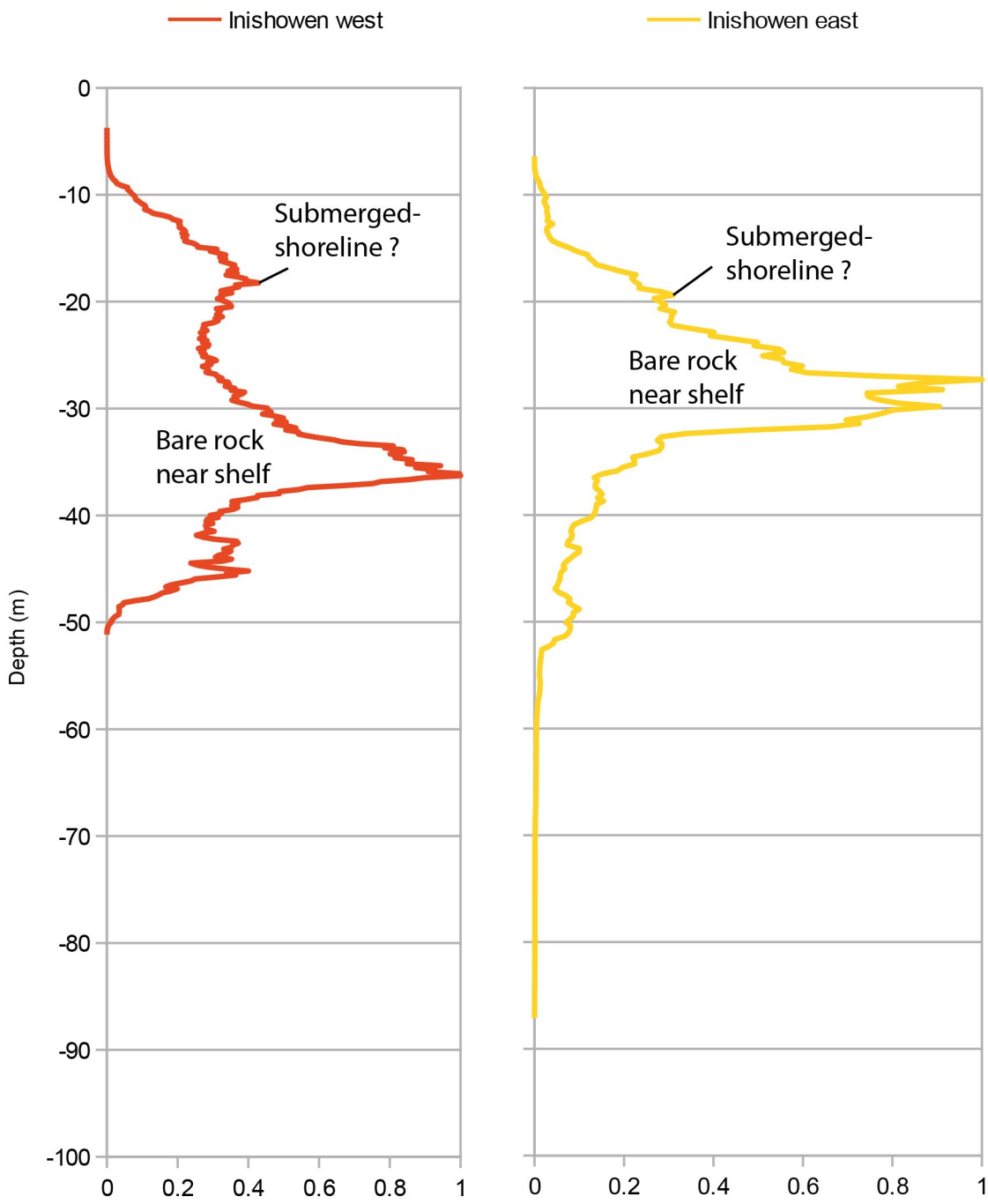

Figure 4.16: Bathymetric histograms for both sides of the Inishowen peninsula.

4.3.2 Evidence from the recognised marine terraces

Out of the 502 recorded features, 213 terraces were formed in metamorphic rocks, 164 in basalt and 122 in sedimentary rocks. This distribution allows for a comparison of these 3 lithology categories with the main caveat being the lack of bathymetric data for depths shallower than 15 to 10m for the western part of the data where all features were formed in Metamorphic rocks.

Figures 4.17 to 4.20 show examples of identified platforms for various environments of the study area. Terraces formed in the chalk in Ballycastle Bay (figure 4.17) and Church Bay (figure 4.18) are elongated and follow the coastline whereas terraces formed in basalt (figure 4.19) or metamorphic rocks in Trawbreaga Bay (figure 4.20) are much smaller with diverse shape and orientation. This contrast appears to be linked with the lithologies' structural constraint as exemplified in the offshore terraces in Trawbreaga Bay where two perpendicular faults appear distinctly as terraced outcrops. Furthermore, the contours of basalt or metamorphic terraces are sharper than those of chalk terraces.

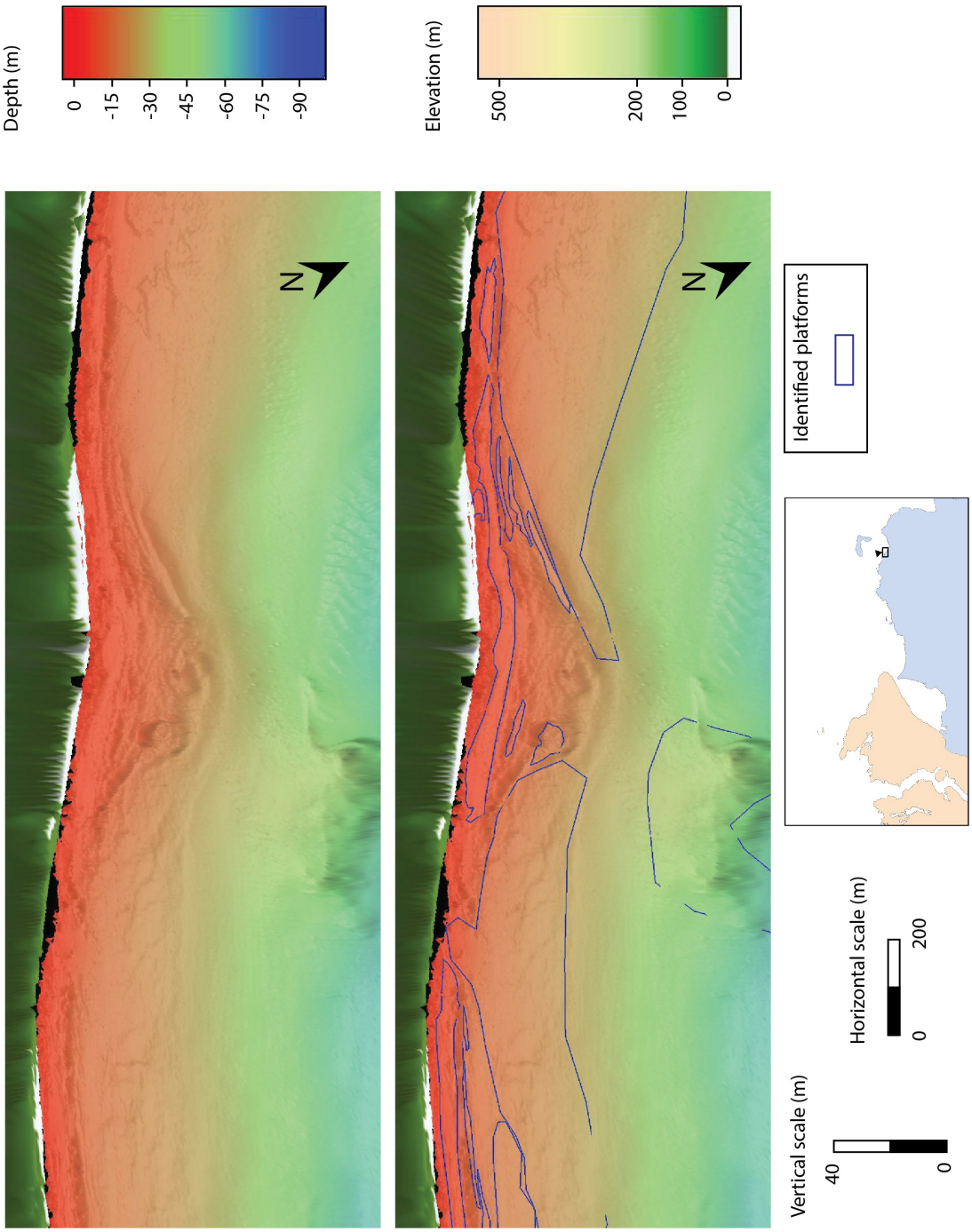

Figure 4.17: Oblique view of identified platforms formed in local chalk for stretch of coast on the western side of Ballycastle Bay.

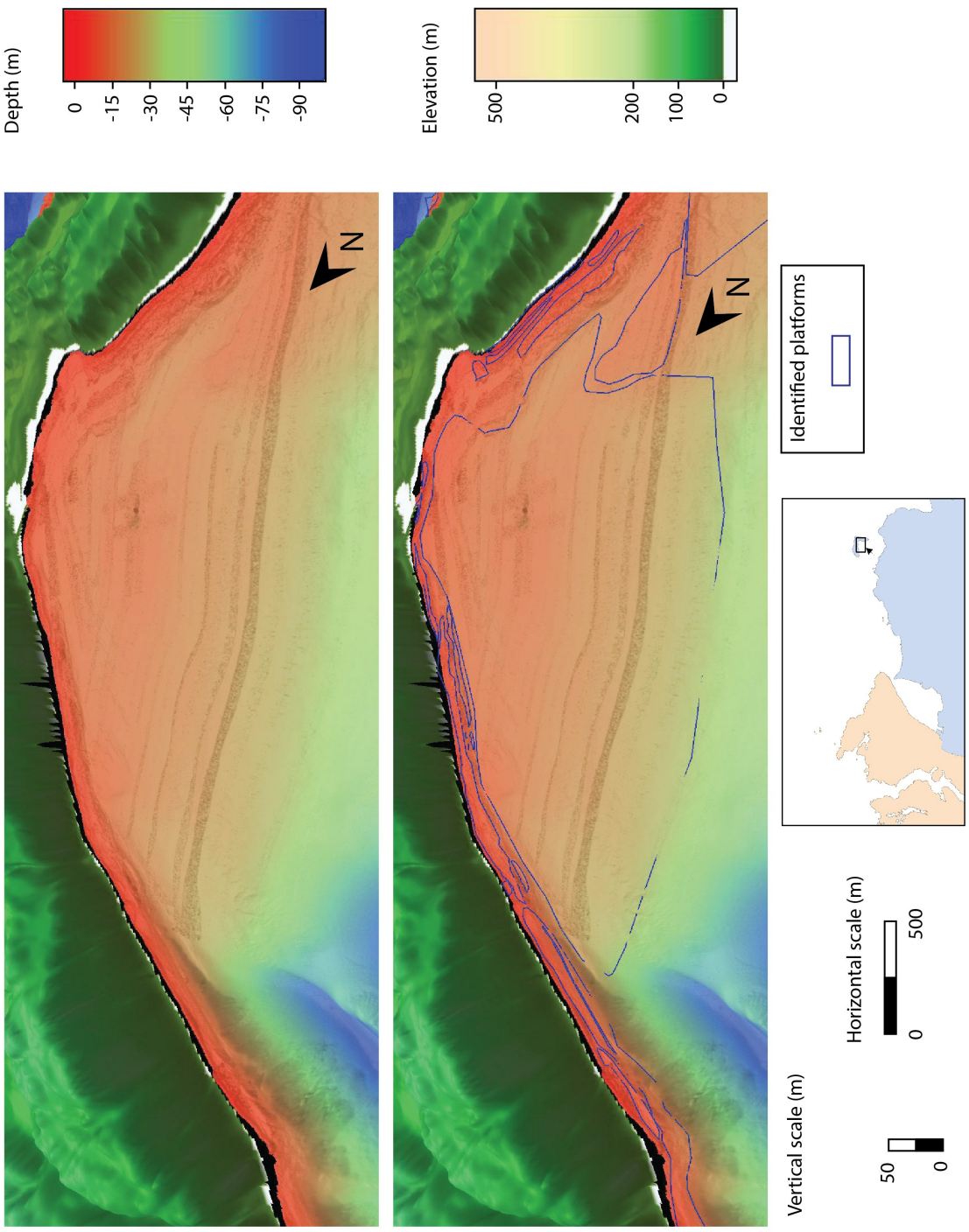

Figure 4.18: Oblique view of identified large platform in the centre of Church Bay with associated smaller platforms formed in local chalk along the coast.

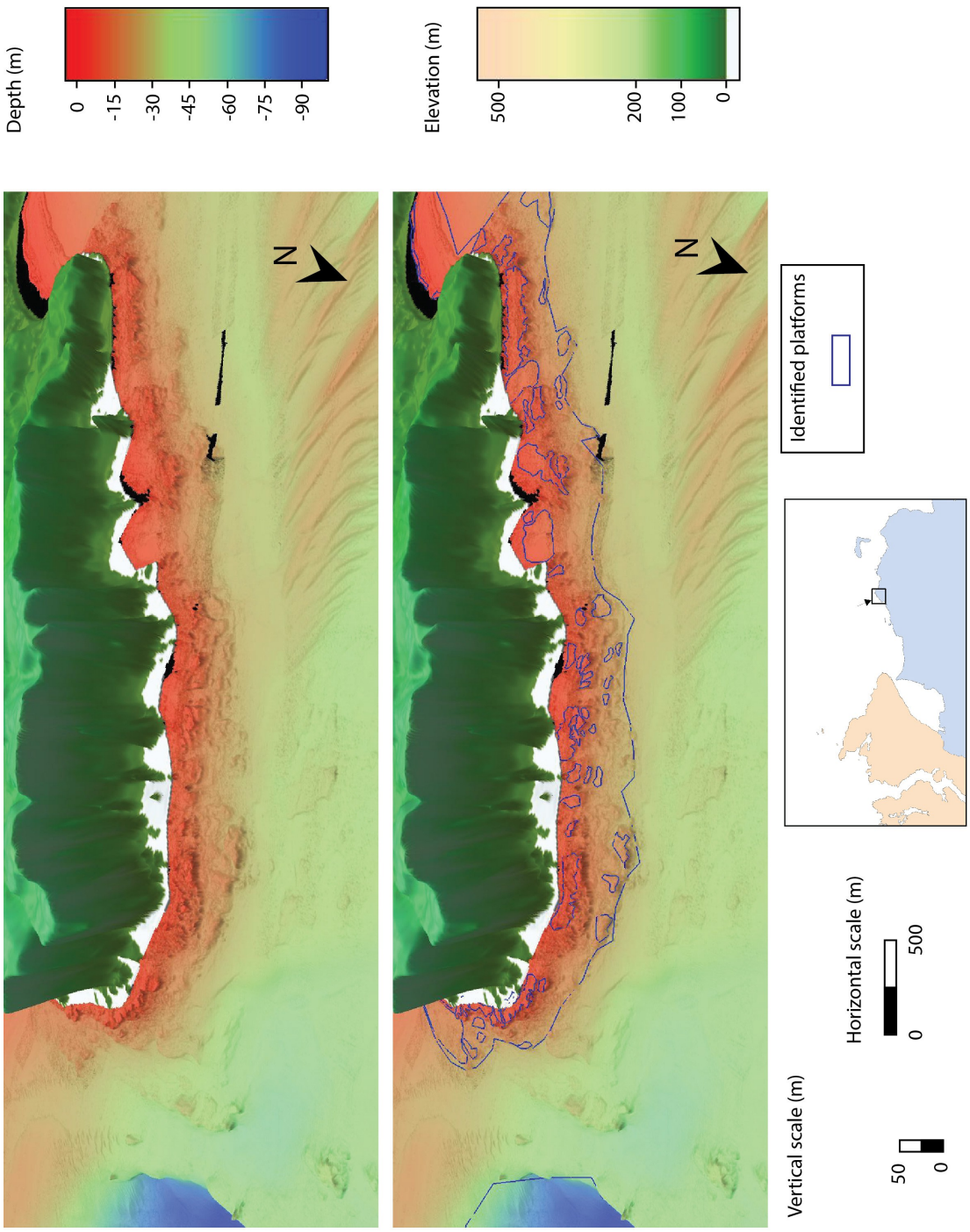

Figure 4.19: Oblique view of identified platforms formed in local basalt for the Giant Causeway coastline.

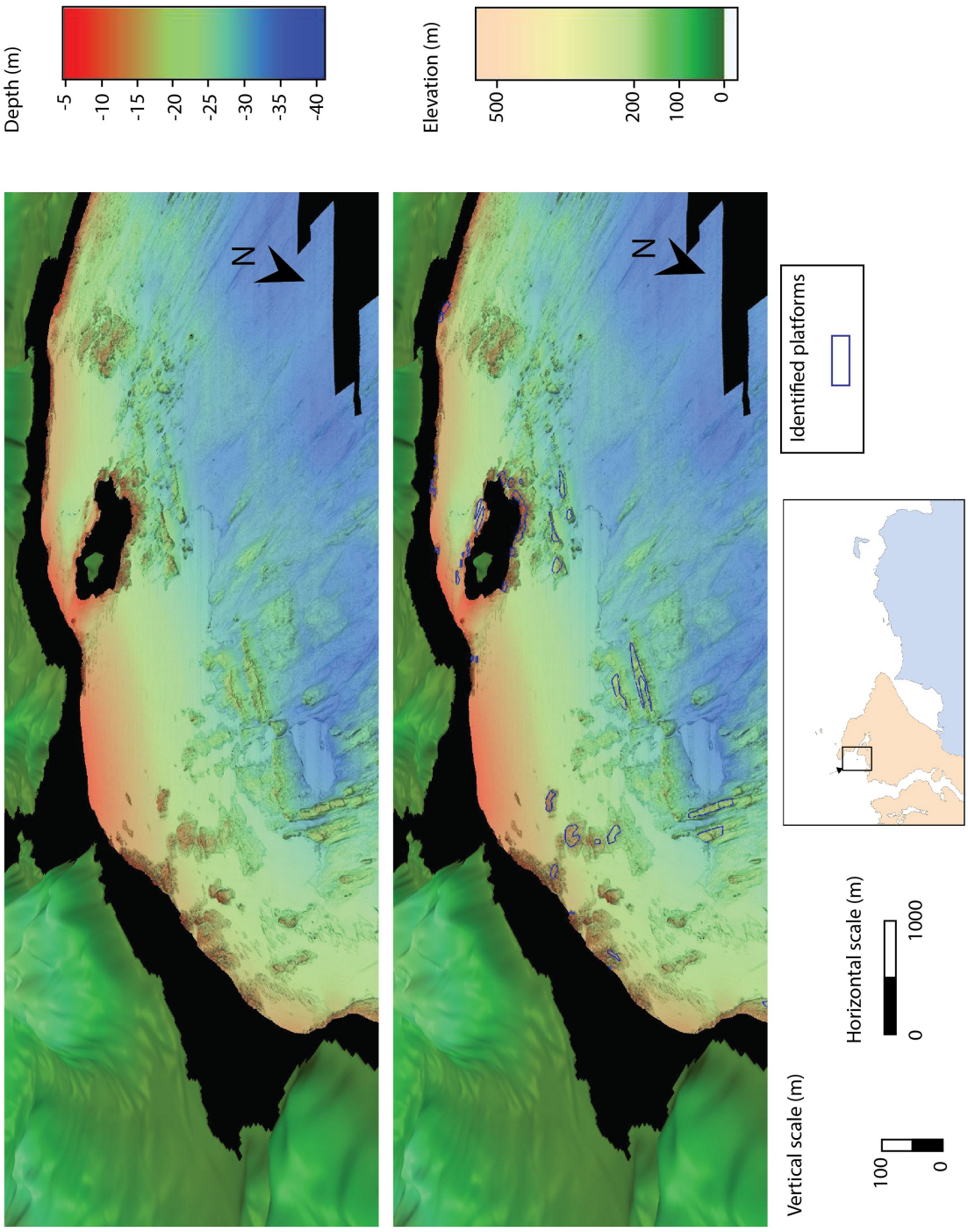

Figure 4.20: Oblique view of identified platforms formed in local metamorphic rocks for Trawbreaga Bay, on the west side of Inishowen.

4.3.2.1 Location and depth of marine terraces

Figures 4.21 and 4.22 display the features recognised colour coded by their average depth for the Ballycastle Bay area and for the Lough Swilly area respectively which allows a rapid overview of their morphologies in respect to their location. The lithological control on the shape and depth of these features can be inferred in parts from the display of the onshore rocks in close proximity to them. The range of average depth recorded for these features is from 2 to 80m with a range of minimum depth from 0 (modern forming shore platform) to 55m. Most features have been recorded between 2 and 24m of average depth and terraces deeper than this range were usually much larger in surface area. These deeper terraces showed a less obvious relationship with the modern coastline and their nature as former shore platforms was deemed less likely (lower recognition confidence index). Hence for the interest of this study only the features recorded with an average depth above the 30m mark were considered for further analysis.

We can recognise at this stage some correlation between the results of the bathymetric histograms and some of the features displayed. In Ballycastle Bay and around Rathlin Island (figure 4.21), a concentration of relatively long shore-parallel features were detected at median depths between 5 and 8m and corresponding to isolated spikes at these depths (figures 4.17 and 4.18). As recognised before, the large near shelf marine terrace of Church Bay is recorded here with a median depth of 15m and will be labelled CB-15. The extensive flat basaltic lava flow (Fyfe et al., 1993) recorded as a marine terrace at 35m median depth to the west of Ballycastle Bay corresponds to the concentration of points described for the Causeway Coast histogram (figure 4.15).

In comparison, the minor spike observed at 18m depth on the western Inishowen histogram can not be correlated to any concentration of terraces at that level (figure 4.16).

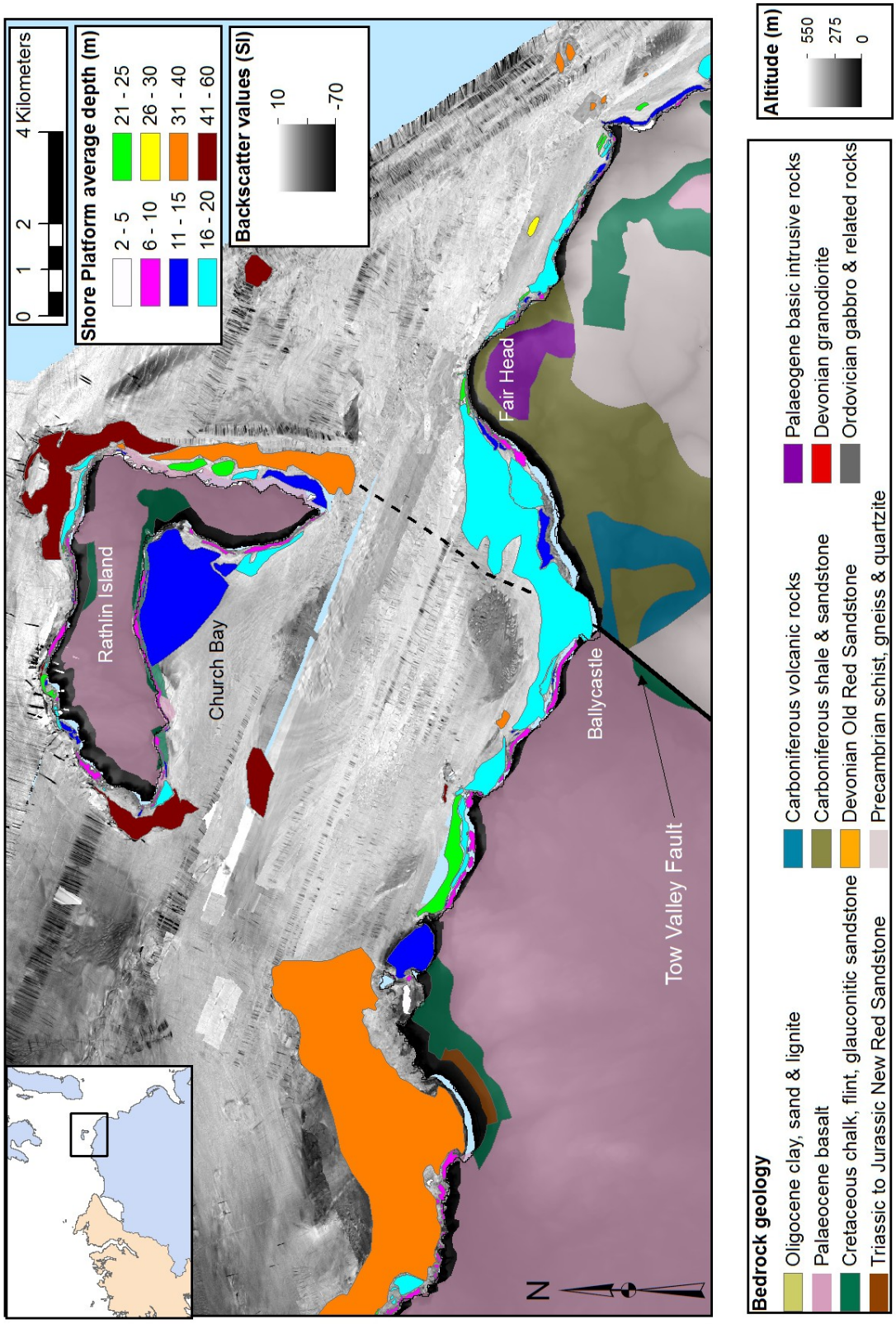

Figure 4.21: Median depth of recognised features for the Ballycastle Bay/Church Bay area.

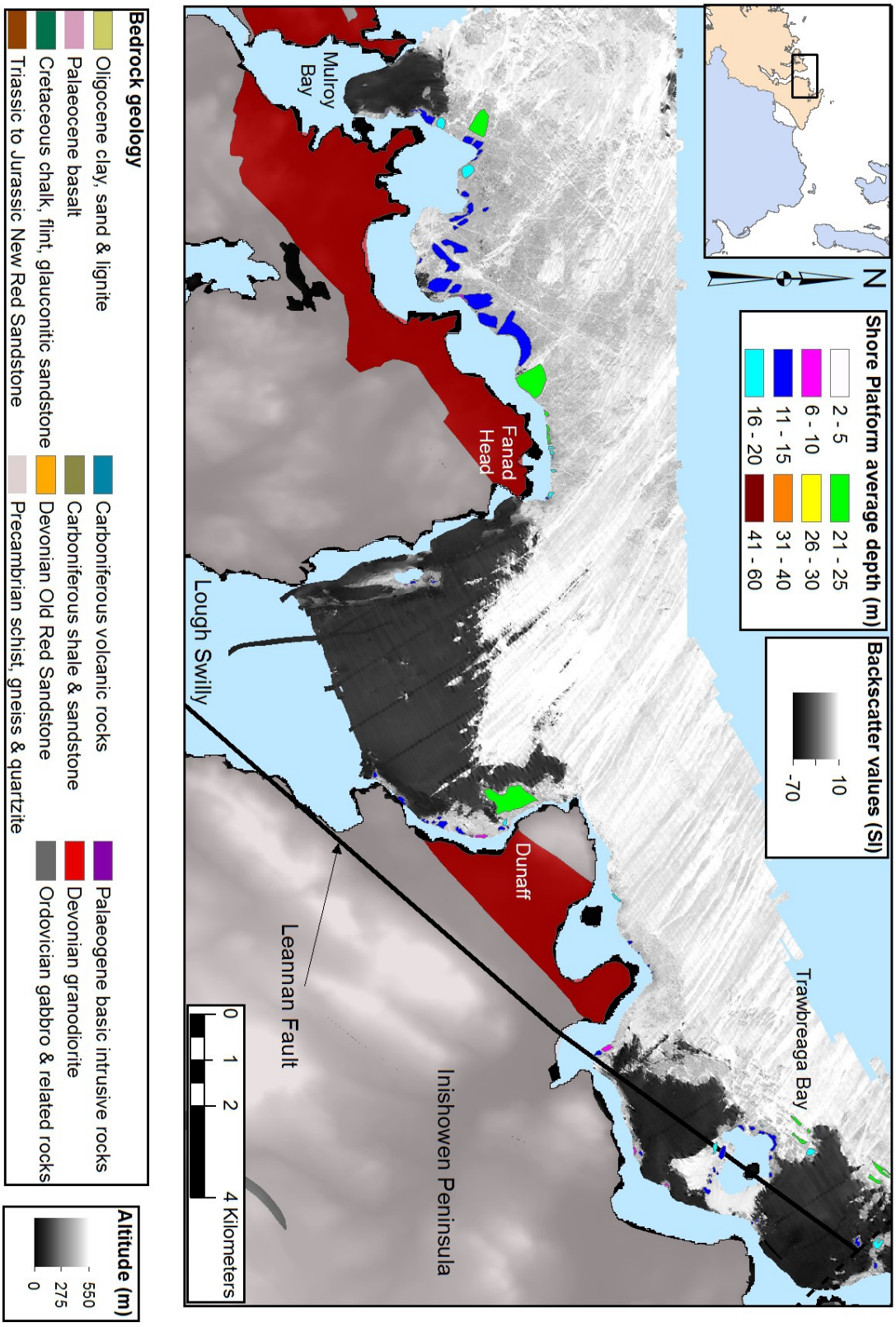

Figure 4.22: Median depth of recognised features for the area around the mouth of Lough Swilly.

Figure 4.23 displays the number of features recorded per median depth for each lithology ;

- Basalt terraces have a main range of median depth between 4 and 22m with some particular depths showing a concentration of features at 5-6 and 9m. The main concentration of features appear between 4 and 9m.
- Sedimentary terraces have a main range of average depth between 5 and 20m with a concentration of features at 7m.
- Metamorphic terraces have a main range of average depth between 9 and 21m with some particular depths showing a concentration of features at 9 and 14-15 and 20m.

These concentrations may highlight structural control on the depth of formation and continuity of terraces. As we could see when comparing figures 4.17 and 4.19, basalt terraces are much less continuous and so will show a concentration in numbers at particular depths over one long chalk terrace. Hence the comparison of the morphological parameters of the recorded features, in particular their width, is necessary to draw any kind of information relating to former RSL.

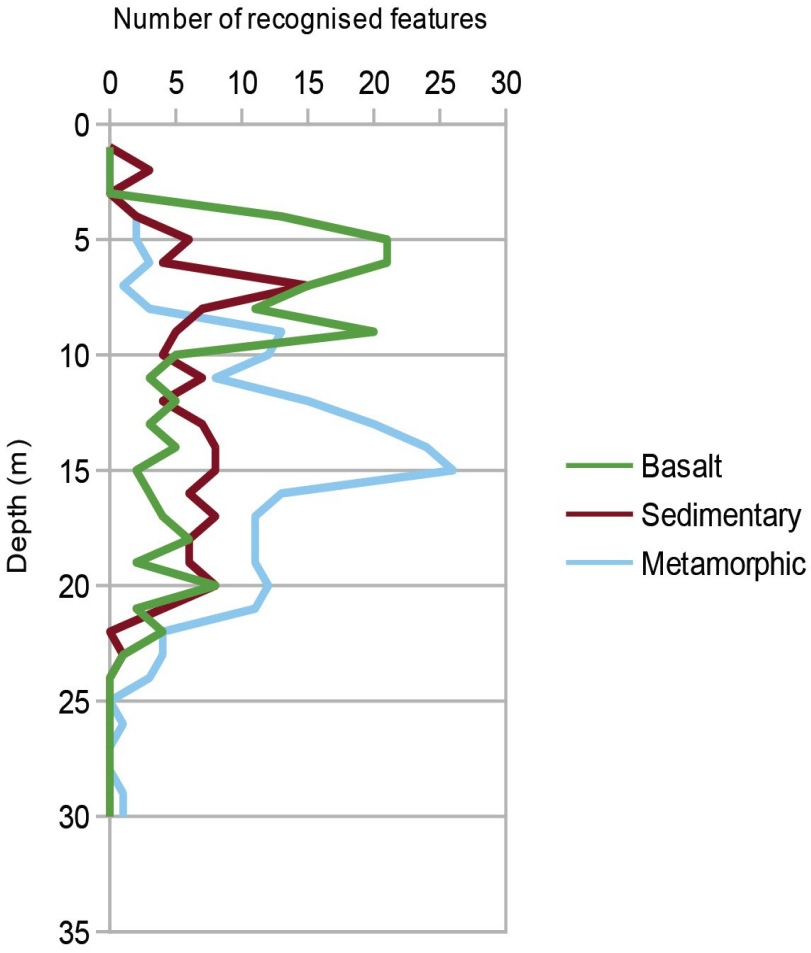

Figure 4.23: Distribution of recognised features per mean depth for the 3 main lithologies.

4.3.2.2 Main morphological parameters

When considering width, figure 4.21 shows that features in the Ballycastle Bay area formed in a shoreline oriented to the north west, which is the direction of main wave inducing winds for the region (see chapter 2), and are wider than the ones oriented to the north or north east. CB-15 appears as an exception being formed in a very sheltered zone but much larger than the other terraces of the study area (with an average width of 1.75km). This feature is hinted to be formed in unconsolidated sediment as such a substrate requires much less wave action for its erosion. Similarly the influence of the orientation of the coastline on the width of the terraces is clear along the whole study area.

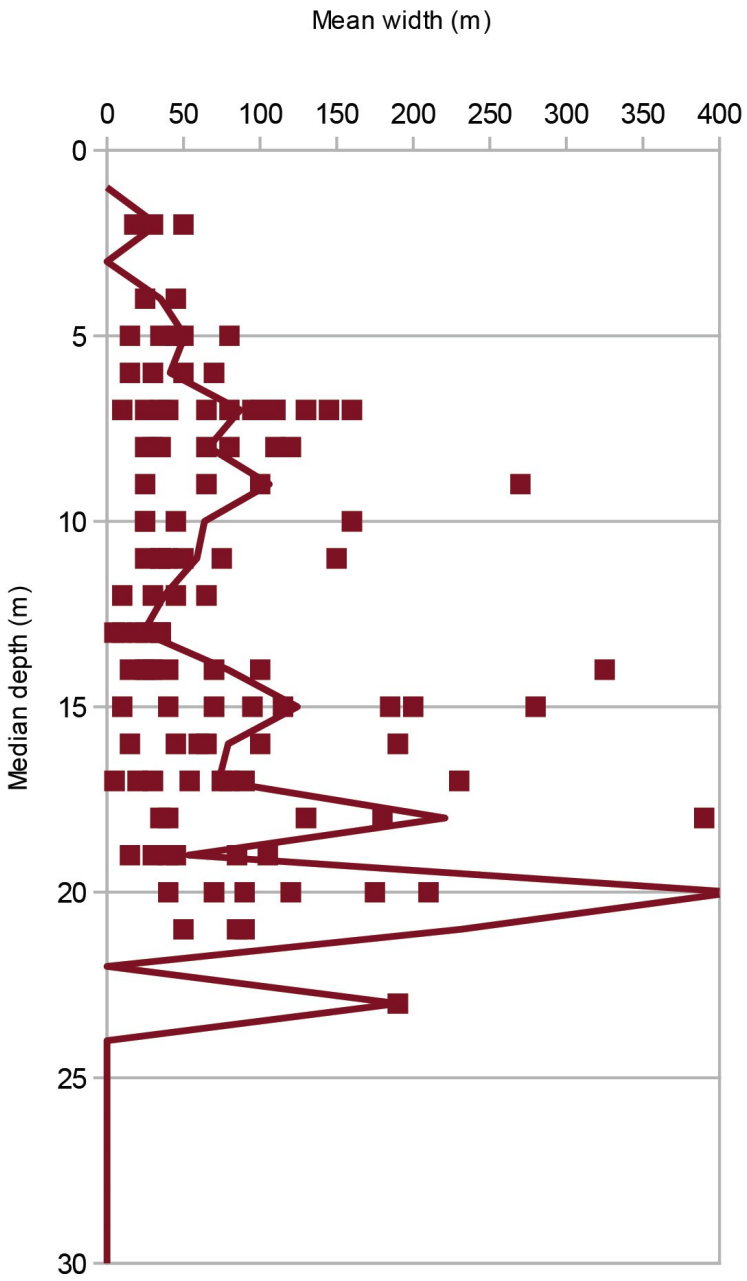

Figure 4.24: Mean width of the terraces formed in sedimentary rocks along their median depth. The continuous line represents the average per depth.

Figure 4.24 displays the cloud of data points for every feature formed in sedimentary rocks in their median depth to average width space. This figure gives a quick overview of the evolution of the range of width for platforms according to their median depth. Similar graphics were produced for the two other types of lithologies and shown in appendix 4.1. They were explored for any cluster of points corresponding to a particular depth linked with their lithology. In other words, do terraces formed at a particular depth in either of the lithologies have a similar width ? The range of width recorded varies greatly for each depth with the majority of terraces found to be less than 100m wide in all lithologies. No particular cluster was observed and these graphics do not contain more information beside the fact that wider terraces only appear at particular depths.

4.3.2.3 Lithological control on morphology

Figure 4.25 displays all the recorded terraces according to their median depth and their easting and according to their lithology. This figure highlights the lack of bathymetric data at shallower depth for the western part of the study area. It also recognises the main lithological zones described in chapter 2. For each lithology, no clear geographical control is visible on the median depth of formation of these features.

The computed average for all features of the 3 main lithology categories recognised at depths shallower than 30m show that terraces formed in basalt are on average narrower with 92.08m followed by terraces formed in sedimentary rocks with 106.25m and finally those formed in metamorphic rocks are the widest with 107.17m average width. Stretches of the study area's coastline that are either oriented to the north west or the north east are formed rather equally in the three types of lithology. If we assume the wave conditions were similar throughout the study area as RSL was changing, this result would indicate that basalt is locally the more resistant lithology.

Figure 4.26 presents the average of the mean width of all the platforms found at a particular mean depth per lithology. It appears marine terraces are on average wider at greater depth as was hinted in figure 4.24. As some of these values can be greatly influenced by one large feature, it was deemed of more interest to describe the general trends rather than the spikes of the curves.

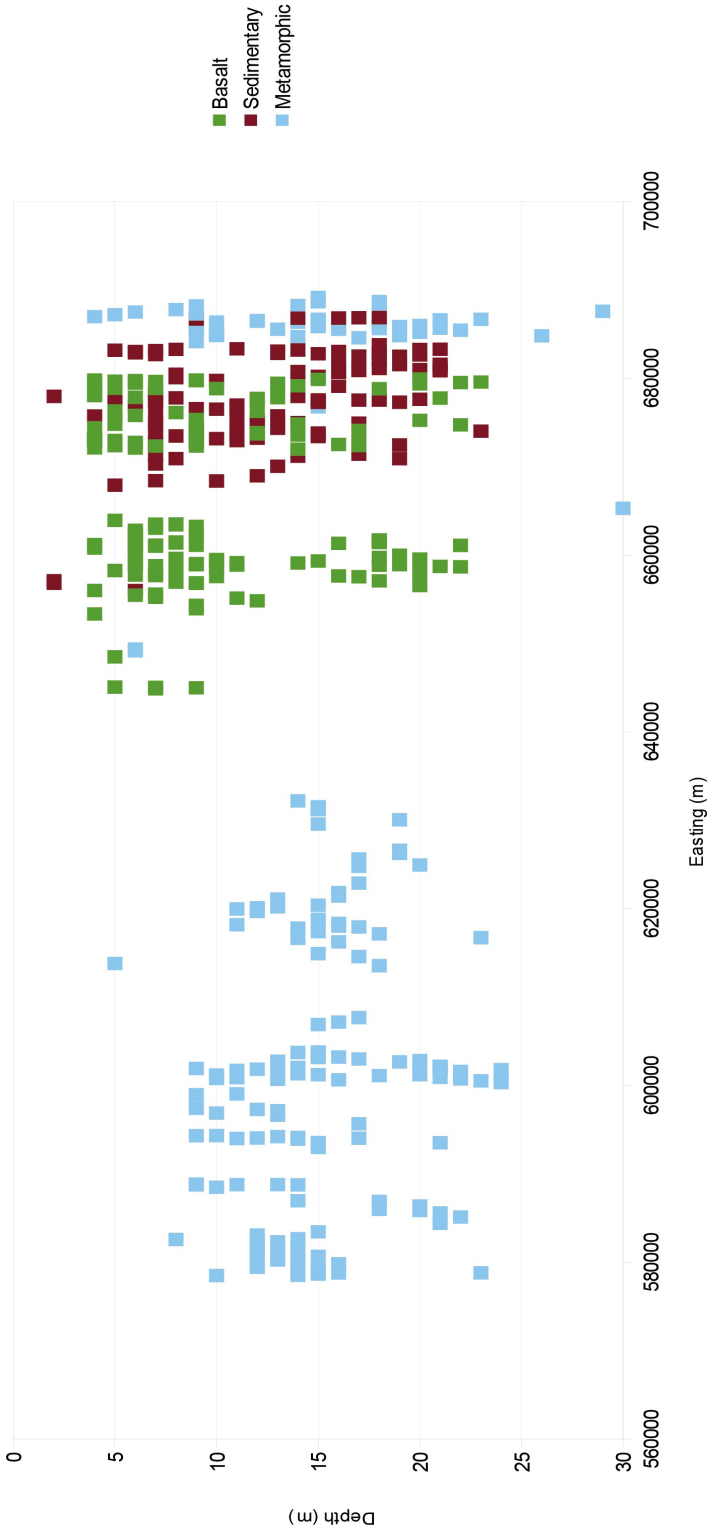

Figure 4.25: Location of each of the recognised features for the study area based on their easting of their central point and their median depth. They are represented according to their lithology.

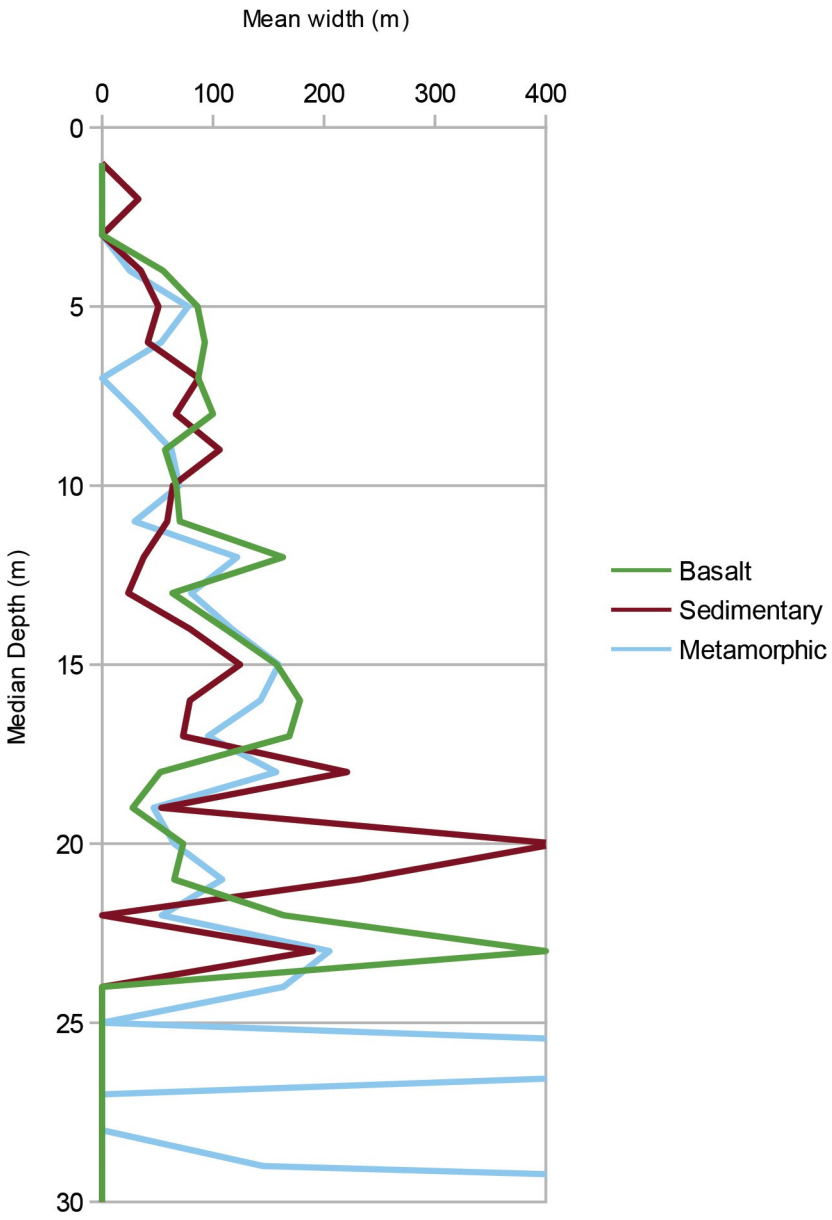

Figure 4.26: Comparison of average width of platforms recognised at particular depth for the 3 lithologies.

These curves share a similar evolution with very similar values at shallow depth and appear to differ only due to some large features at some particular depths (spikes on the curves). Basalt terraces are on average about 90m wide for depths between 4 and 8m, sedimentary rock terraces are on average 70m wide between 5 and 10m and 80m wide for depths between 14 and 16m and metamorphic rock terraces are on average 120m wide for depths between 12 and 18m.

Thornton and Stephenson (2006) concluded that there was no significant correlation between the mean depth of a platform and its location in a bay or a headland. This conclusion was tested by plotting the number of terraces recognised in a bay or a headland against their median depth. About 70% of features were found on headlands rather than in bays in the study area and this ratio hardly changes according to depth (figure 4.27) which is consistent with earlier findings. This was plotted assuming that locations in bay and headland do not vary with depth, a notion that is corresponds to observation of the JIBS datasets.

The average mean width of the terraces formed at a headland is smaller (91.05m) than for the ones found in bays (128.56m). This difference is consistent with bays being formed in areas of least resistance to erosion and so this is reflected in the platforms formed at these locations. Beside, this can be further analysed in view of the average width varying according to the three main lithologies of the study area (figure 4.28). This difference in width is very clear in platforms formed in basalt or sedimentary rocks but not for platforms formed in metamorphic rocks.

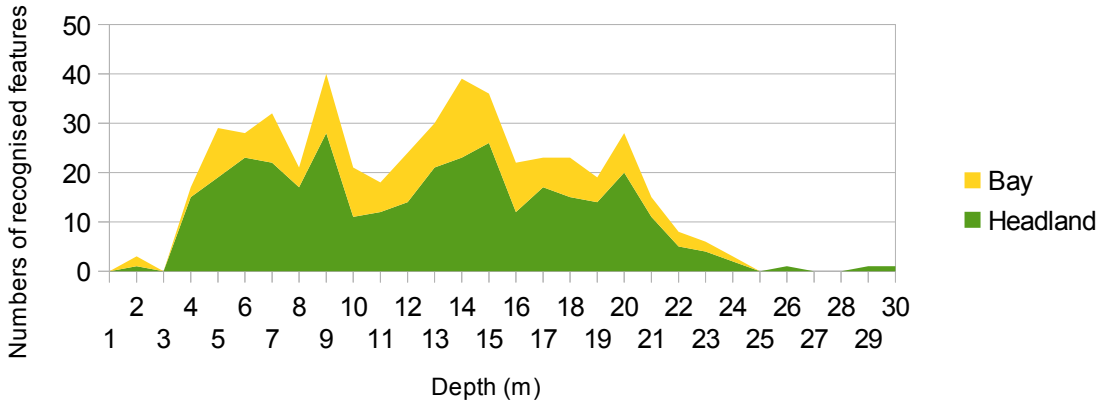

Figure 4.27: Evolution of the relative proportion of features located in a bay or off a headland along their median depth. The depth is here plotted along the X axis.

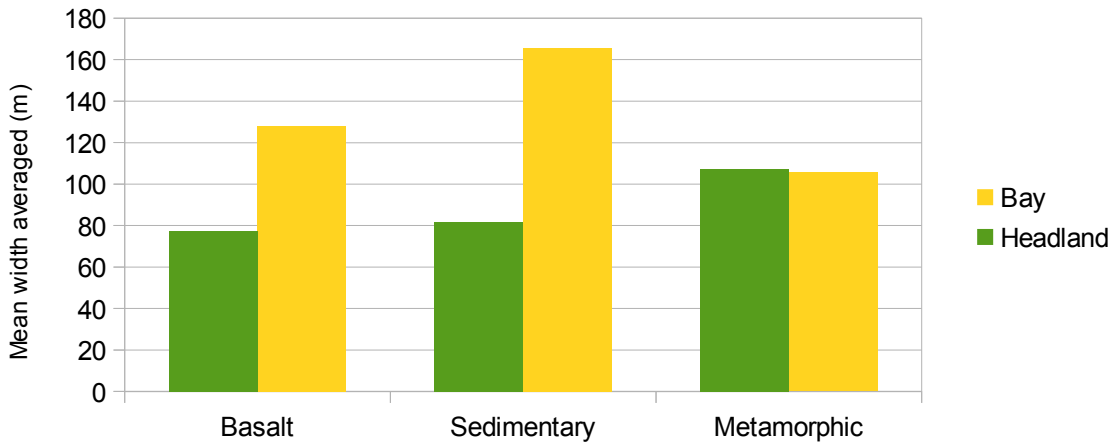

Figure 4.28: Variation of the average width of features located in a bay or off a headland at depth above 30m for the 3 main lithologies.

This section illustrated the basic control expressed by Sunamura (1992) on a terrace width which are its exposure to wave action and the rock resistance to it. Orientation of the coast and situation on a bay or headland offer some clear correlations with the mean width of terraces. And differences are observed for the three lithologies of the area with basalt appearing as the most resistant rock. Some previous studies had hinted at potential influences of such control on the median depth of the terraces (Thornton and Stephenson, 2006; Dasgupta, 2010). These do not appear in the study area and allow to constrain the influence of contemporary RSL on the formation of these features further.

4.3.2.4 Lithological control on the angle of slope

Several studies state that one of the main controls on the angle of slope of a shore platform, beside the structural control of a bedding dip, is the rock strength: sub-horizontal type B features are more likely to form in more resistant rocks (Sunamura, 1992; Thornton and Stephenson, 2006; Dasgupta, 2010). Figure 4.29 shows the relative proportion of features recognised along the whole study area of either type A or B for the 3 main lithologies. This displays the preponderance of type B sub-horizontal platforms over type A ramp-like platforms in basalt (70%) and in sedimentary rocks (65%) compared to an almost equal amount (55%) for the metamorphic rocks. If we accept the hypothesis postulated above, basalt would appear to be the most resistant lithology for the study area

before sedimentary rocks and metamorphic rocks respectively which is supported by the previous evidence from the average width of our features (section 4.3.2.3). It is necessary to take into account other controls such as the age of these lithologies and the age of the features recorded which can not be known and would very likely have an effect on their angle of slopes. For instance, the local metamorphic rocks are much older (Precambrian; before 540 Ma) than the other two types of lithologies (late Mesozoic-early Tertiary ; 70 to 60 Ma). Similarly, subglacial erosion was significant for the area and very significantly visible in the metamorphic near shelf in Donegal. Such processes tend to smooth the surface and in particular the potential breaks of slope present and so limit the preservation and/or recognition of sub-horizontal terraces.

Figure 4.30 displays all the recorded terraces according to their median depth and their easting and according to their type. It is important to note that some of the larger features recognised are recorded as type B due to the fact that their angle of slope is less than 0.9° even though there is a considerable difference between their mean depth and their minimum depth recorded at their Cliff Platform Junction (CPJ). The two types of terraces are distributed rather equally in depth along the study area and no direct control from their locality is detected.

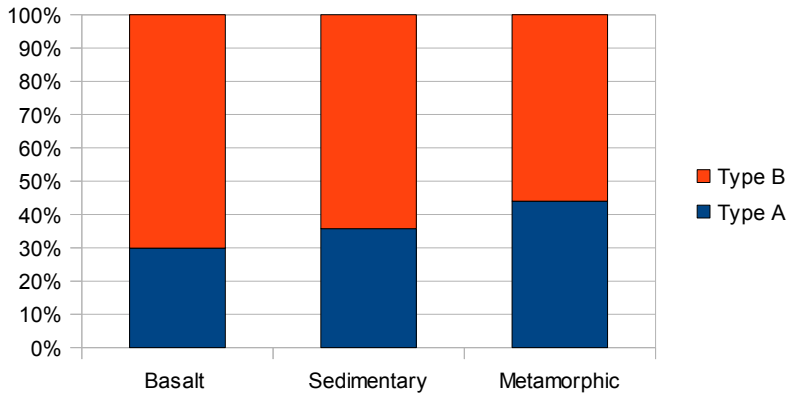

Figure 4.29: Relative proportion of recognised features of either type in the 3 main lithologies.

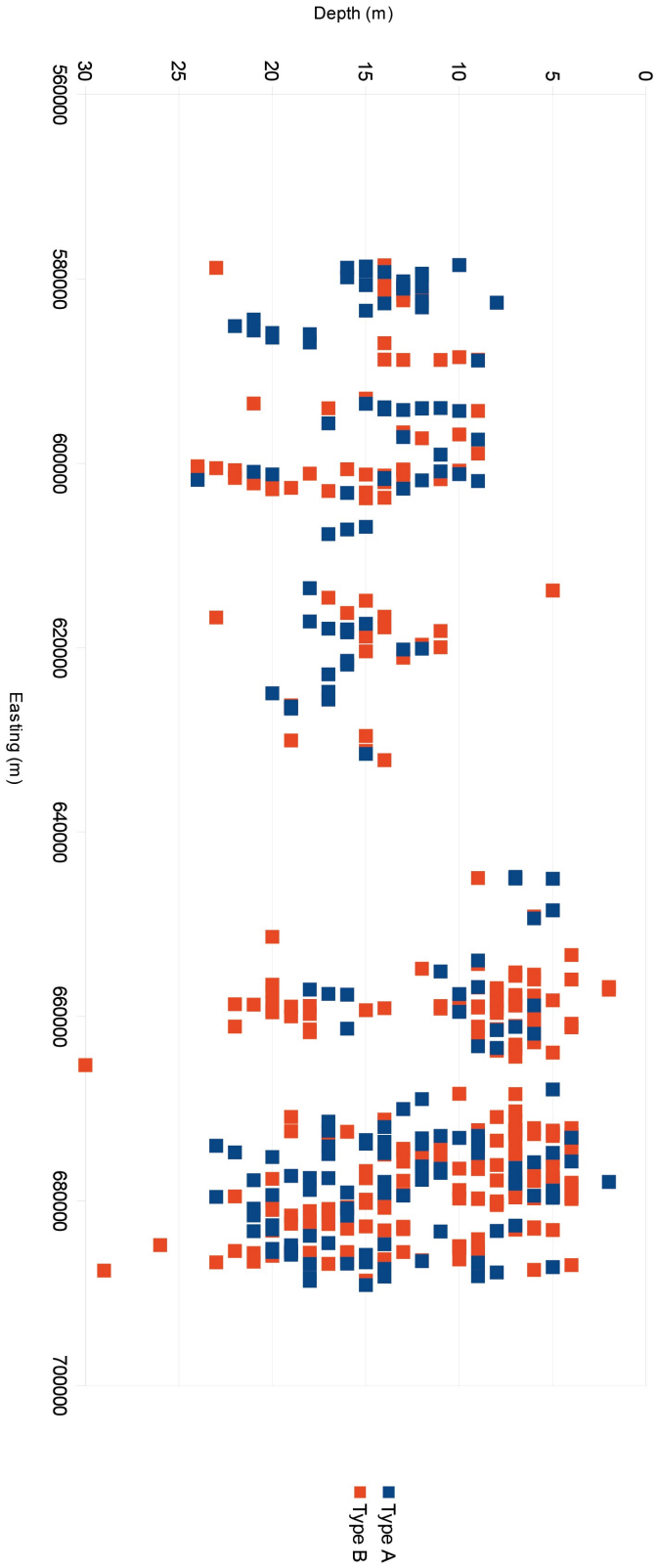

Figure 4.30: Location of each of the recognised feature for the study area based on their easting of their central point and their median depth. They are represented according to their angle of slope's classification as type A or B (Sunamura, 1992).

Type A platforms in the study area have an average mean width of 133.56m which is very slightly higher than the average for type B platforms at 129.06. We could consider then that in the study area, the angle of slope of a feature does not affect its width significantly although when looking only at terraces found at depths shallower than 30m, we find that type B platforms are significantly narrower (89.72m) than type A platforms (124.14m). This could be due to the extended period of stable RSL needed to erode wide sub-horizontal platforms (type B) compared to ramplike platforms (type A).

Furthermore, the mean width of terraces found below 30m depth of each type for each of the 3 main lithology categories have been averaged and presented in figure 4.31. Type A platforms are wider than type B in all lithologies and this difference is accentuated in basalt with type A features being almost twice as wide as type B. The reason behind this difference in basalt platforms is unknown but is likely to be due to structural control.

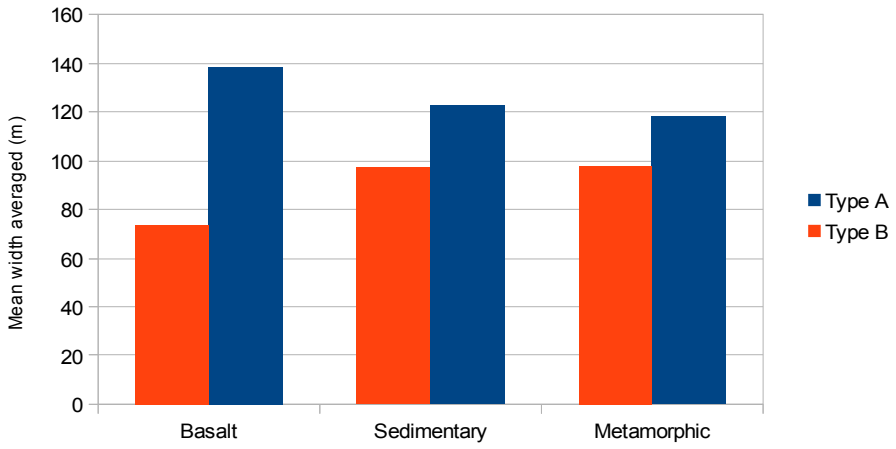

Figure 4.31: Average width of platforms recognised in each of the 3 main lithologies at depth below 30m.

4.3.2.5 Rugosity of the terraces

The rugosity (roughness) of shore platforms is a rarely mentioned topic in the associated literature (Dasgupta, 2010). It is associated with the degree of weathering of a platform and could give an indication of a platform's age (Trenhaile, 2002). It is generally measured in the micro-scale (mm to cm) but as clear differences were visible at the DEM's resolution, macro-scale (cm to m) rugosity was investigated in relation to the geographic location, the depth and the type of lithology the terrace was formed in. Figure 4.32 displays all the recorded terraces according to their median depth and their easting and according to their level of rugosity recognised and classified through visual inspection. The presence of modern sediment over these erosive features would prompt their surface to be classified as presenting very low to medium rugosity whereas bare rocky surfaces would be recorded with a rugosity between medium to very high. The “extreme” level of erosion corresponded to surfaces criss-crossed by grooves several meters deep (see figure 3.8). In general, features recognised in Northern Ireland present a generally low level of surface erosion. In contrast, most features found in the Donegal part of the dataset have a high to very high level of erosion.

On of the plausible causes of a high macro scale rugosity on a terrace could be that it is subjected to high energy currents and/or past wave action preventing sediment to accumulate. In that sense, it can not be linked directly to the level of weathering of the terrace but can highlight some depth zones of higher energy. When we look at the recent glacial history of the study area, such zones of higher rugosity can be equally due to the subglacial erosion with ice flowing out on the shelf from either mainland Ireland or Scotland. Additionally, it is conceivable that recent RSL change might have accentuate the level of surface erosion of such features. A concentration of features with a higher level of rugosity was found for depths between 5 and 16m with lower rugosity recorded at deeper depths throughout the study area.

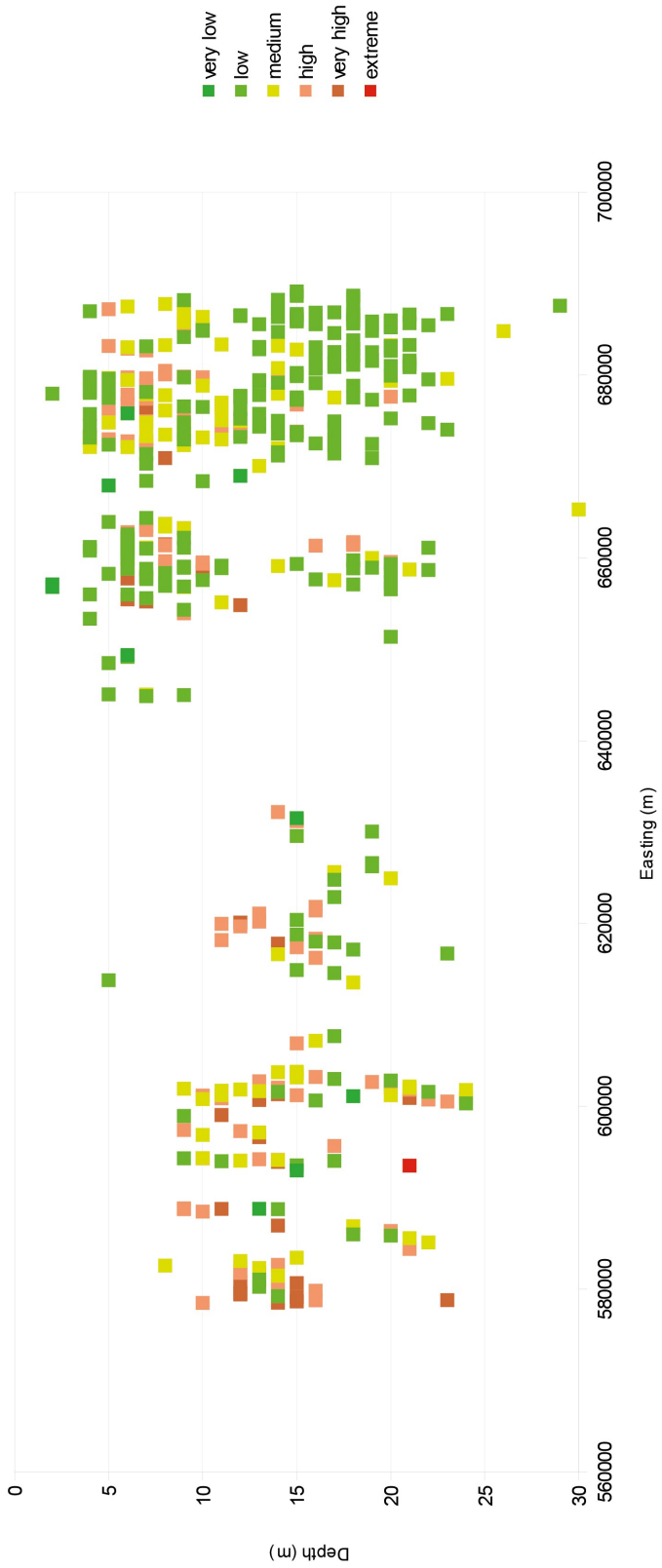

Figure 4.32: Location of each of the recognised feature for the study area based on their easting of their central point and their median depth. They are represented according to their rugosity class.

4.3.3 Accretional features

Less than 20 accretional features were recorded in the study area including only 3 sand bars. A number of beach ridges (see section 4.1.2) were located mainly in the Bann Estuary/Portstewart area (figure 4.33). All beach ridges were located at depth of less than 6m and the sand bars size and depth varied significantly. A groundtruthing survey of the beach barrier detected at Runkerry Bay to the east of Portballintrae was unable to locate it. This could be due to the fact that these "beach barriers" are associated with modern processes and so are regularly displaced or eroded altogether. But it could also be the result of a processing error in the raw bathymetric dataset as all the potential features detected follow the track of the vessel during the survey.

The recorded sand bars appear to be more definite features. These could be assimilated as longshore bars due to their west to east alignment and could be the result of modern underwater current meeting the break point of the large waves hitting this strech of the coast (section 2.3.1).

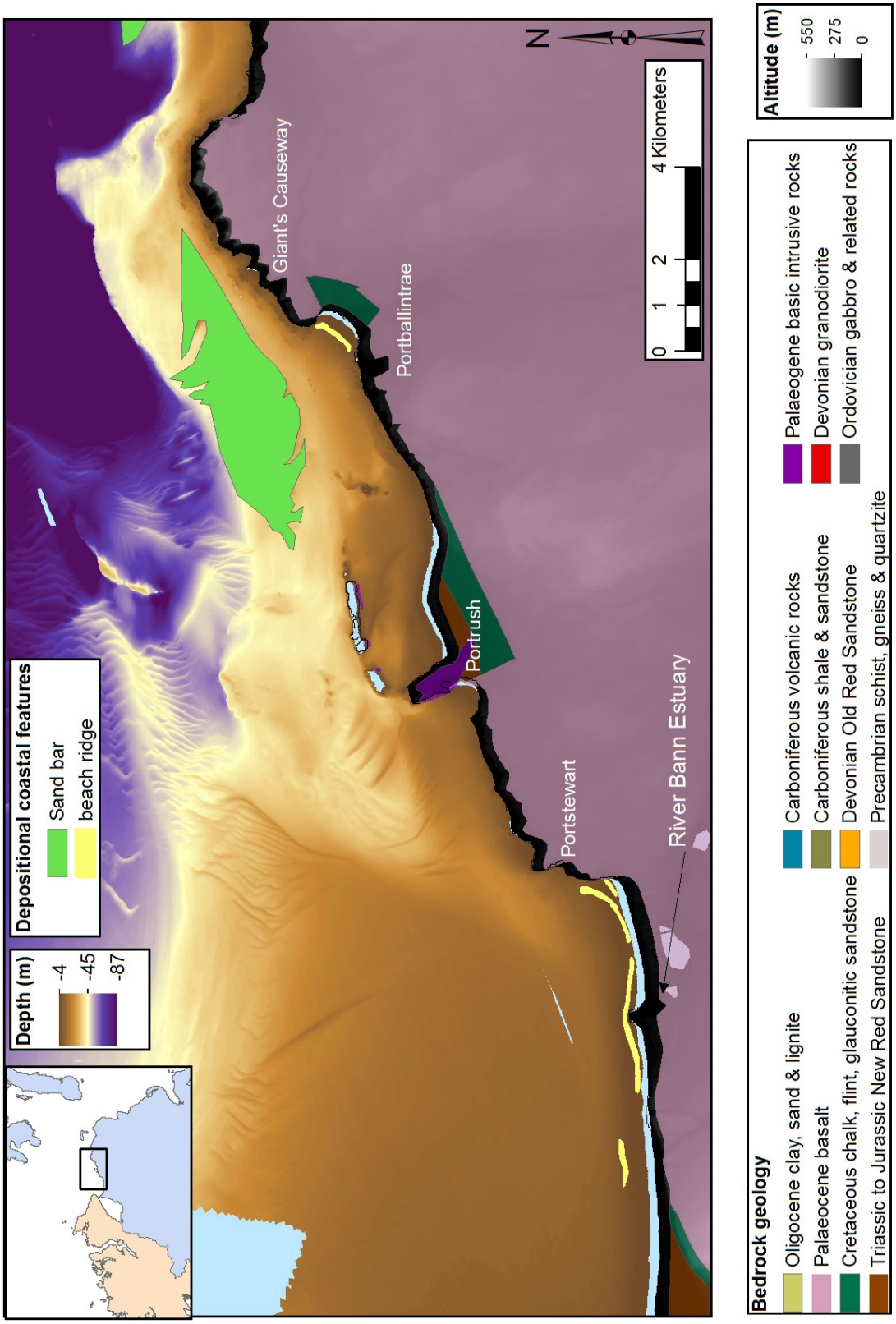

Figure 4.33: Classification of accretional features recognised in the area around Portrush.

4.4 General conclusions on the recognition of submerged erosional coastal features on the bathymetric data

The JIBS datasets allowed the recognition of more than 500 submerged marine terraces, of which the majority appear to have been formed from the erosion of bedrock (or unconsolidated sediments) due to the wave action and as such are related to previous RSL lower than present. The terraces identified were found at a wide range of depth but this range varies according to the lithology of the rock where the terrace has formed and its location. The early study of the histograms from the bathymetric data of particular stretches of the coastline highlighted ranges of depths where potential relict shorelines could be identified. In particular, a preponderance of narrow terraces were identified in the range of 5 to 8m depth on the Northern Irish coast with an average width of 80m over the three lithologies.

The notion of lithological control on the morphology of the local terraces was tested and brought to light some interesting characteristics for the study area. In general, terraces were found to be wider when they are deeper, ramp like (type A), located on a shoreline facing the highest wave energy (the North West for the study area) and formed in bays.

Basalt was found to be the most resistant lithology present in Northern Ireland in the study area with terraces formed predominantly at shallower depth (less than 10m) based on their average width. Following the findings of Sunamura (1992), this was further confirmed by the preponderance of type B platforms formed in this lithology. Sedimentary rocks, found in Northern Ireland, and metamorphic rocks, found throughout the study area, were found to be on average of comparable resistance based on their average width but the higher preponderance of type B platforms in sedimentary rocks could indicate a higher rock resistance. No relations were found between the lithology and the median depth of the features at the macro scale of our study (Thornton and Stephenson, 2006). Rugosity of the terraces surface was also investigated and showed to vary according to the geographical location although for the study area, that correlates to a strong lithological control and so could be an age or weathering artefact.

Accretional coastal features were also investigated. The limited presence of potential beach barriers at very shallow depth implies that modern processes are very likely to be responsible of their formation. The same can be said of the recognised sand banks of

the study area. The high energy of modern coastal processes appear to have eroded any accretional evidence of past RSL offshore on the seabed but some of these features might have been preserved below more recent sediment deposition.

4.5 Age of these recorded features based on recorded rates of erosion

As we cannot date the formation of the recorded erosional features, we cannot know the period of stable RSL stillstand needed for their erosion (figure 4.7). But based on recorded and measured rates of erosion globally on similar lithologies, it is possible to give an estimate. The global average measured erosion rates of modern shore platforms are 0.5mm/year for basalt, 3.65 mm/year for chalk (although the local chalk is harder than most chalks where measures were made), 1.282 for sedimentary rocks excluding chalk and 0.625 for metamorphic rocks. As such, a general rate of erosion of 1mm/year was chosen as a mean value for the study area. This was used to compute a first assessment of the stillstand (stable RSL) time period needed for the formation of terraces at each depth, assuming these terraces were formed by wave action only. In figure 4.34, the average width of all platforms found at a particular depth were used to compare the time length needed for the 3 zones delimited in the recently published GRMs for the study area; North Antrim, Derry and Lough Swilly (see chapter 2). Furthermore, it has been noted that modern shore platforms can be inherited from previous interglacial stages and this process could have occurred at any elevation (Trenhaile, 2001; McKenna, 2008). As such, the length of time required for the erosion of a platform does not have to happen in one continuous period and can be divided in several as in the case of comparable RSL change following comparable glacial cycles in the Quaternary.

At this average erosion rate, the main range of time period needed would be between 20,000 and 200,000 years. In particular, the set of narrow terraces recognised from the spikes on the bathymetric histograms would have required 80,000 years of stable RSL at 5 to 8m depth. This time scale fits the idea of inherited features whose formation required several discontinuous period of erosion during the Quaternary. This strongly suggests that these features can not find their origin in the last period of deglaciation since the Last Glacial Maximum about 20,000 years ago or that processes like wave quarrying or periglacial weathering were much more vigorous than expected leading to the formation of strandflats (Bird, 2000).

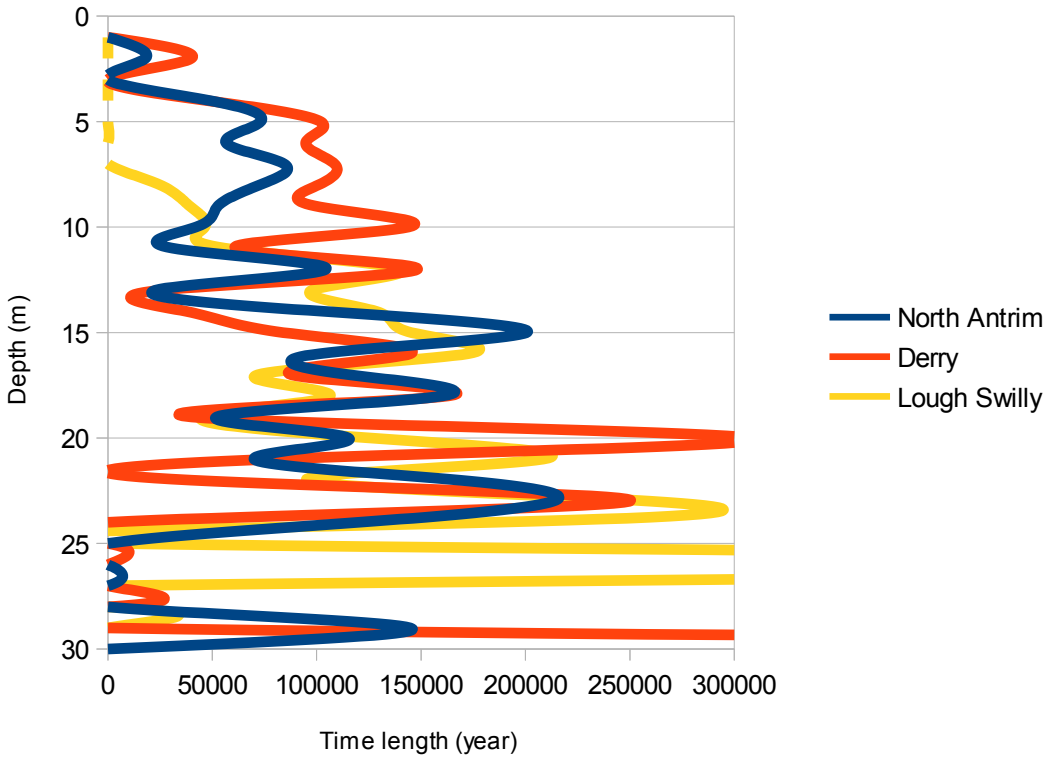

Figure 4.34: Time length of stable RSL lowstand needed for the formation of recorded marine terraces for the 3 zones used in recent GRMs (average erosion rate of 1mm/year).

Similarly, if we look at the modelled RSL curves for the study area from the recent GRMs (Brooks et al., 2008; Bradley et al., 2011; Kuchar et al., 2012), they display a relatively fast changing RSL. This implies that erosional features that were formed due to the wave action at lowstands would only be very narrow. For the three locations of the study area, the lowstands appear to only be stable for about 1,000 years which would only be responsible for terraces of 1m width, or cliff notches, according to our average local erosion rate. In comparison, for the North Antrim area, the highstand modelled during the Holocene is stable between 1 and 2 m above m.s.l. for 5,000 years bearing the potential of rocky erosional features up to 5m in width. However, this elevation being so close to the modern RSL, any platforms formed would be likely to be confused with the topographical dataset with features formed due to modern coastal processes. And so these features would not be recognised among the wealth of buried marine terraces of much larger width. It is important to recognise that the RSL change of the last deglaciation is modelled to be responsible to some small extent to the erosion of some of these features.

4.6 Strandline relation diagram for the newly recognised marine terraces

Figure 4.35 plots all the cliff-platform junctions for all the recognised marine terraces according to their depths and from West to East along the coastline of the study area. This diagram was created in order to emulate the similar diagrams from the main studies of the 1960s (figure 4.9 and Stephens and Synge, 1966 for the main point of reference) that were used to reconstruct the Late glacial and Post glacial shorelines and their angle of dip from the ice centres based on surveyed raised shorelines. For each CPJ, an error bar of 5m over and below was added following subsequent work on the actual indicative meaning of such erosional coastal features (McKenna et al., 1992). The erosional notches found on ground truthing dives in Ballycastle Bay and Church Bay (Quinn et al., 2010; Westley, pers. Comm.) were added to this plot with no error bar as their indicative meaning is closer to the mid-tide level.

All of these features are erosional features with most of them carved in rock and as such can not be dated and most likely correspond to RSL evolution over periods of time much longer than the last 20,000 years whereas the raised shoreline features were all thought to correspond to the last transgression (Synge & Stephens, 1966). Nevertheless, the range of lowstands modelled from recent GRMs developed for Ireland (Brooks et al., 2008, Bradley et al., 2011 and Kuchar et al., 2012) were added to this plot in order to test the relative abundance of these features at this range of depths. No particular preponderance of recognised features is visible at the modelled lowstand depth of the CPJ but it is interesting to note the concentration of notches found in Ballycastle Bay and Church Bay to correspond to the lowstands modelled for both the Brooks et al. (2008) model and the Hub-min (Kuchar et al., 2012) model (figure 4.35). Similarly, the highstands from the recent models were added to figure 4.9, displaying the raised shoreline evidence from the study area, and presented in figure 4.36. Again no major correlation is visible beside some of the lower cliff notches, terraces, beach and shingle ridges from the area from the Lough Foyle to the Lough Swilly.

These plots highlight the inherent difficulty in linking these features from one bay to the next to build hypothetic shorelines and confirm the recent literature reluctance to use such diagrams.

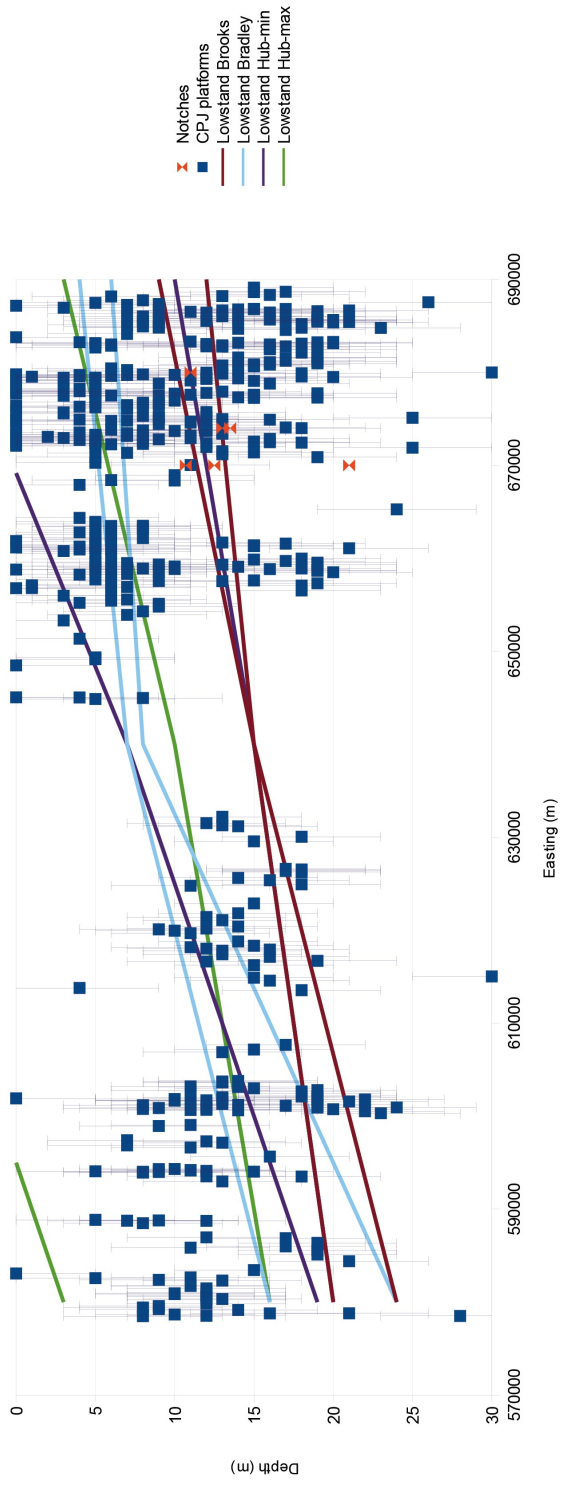

Figure 4.35: Comparison of the depth of the CPJ of the recorded marine terraces for the whole study area from west to east. That depth was given an uncertainty of +/-5m as for its indicative meaning (McKenna et al., 1992). Records of the depths of cliff notches found on ground truthing dives have been added (Quinn et al., 2010; Westley, pers. comm.). The range of lowstand depth predicted by each of the recent GRMs is located between the 2 continuous lines of each colour (see chapter 2 for RSL curves).

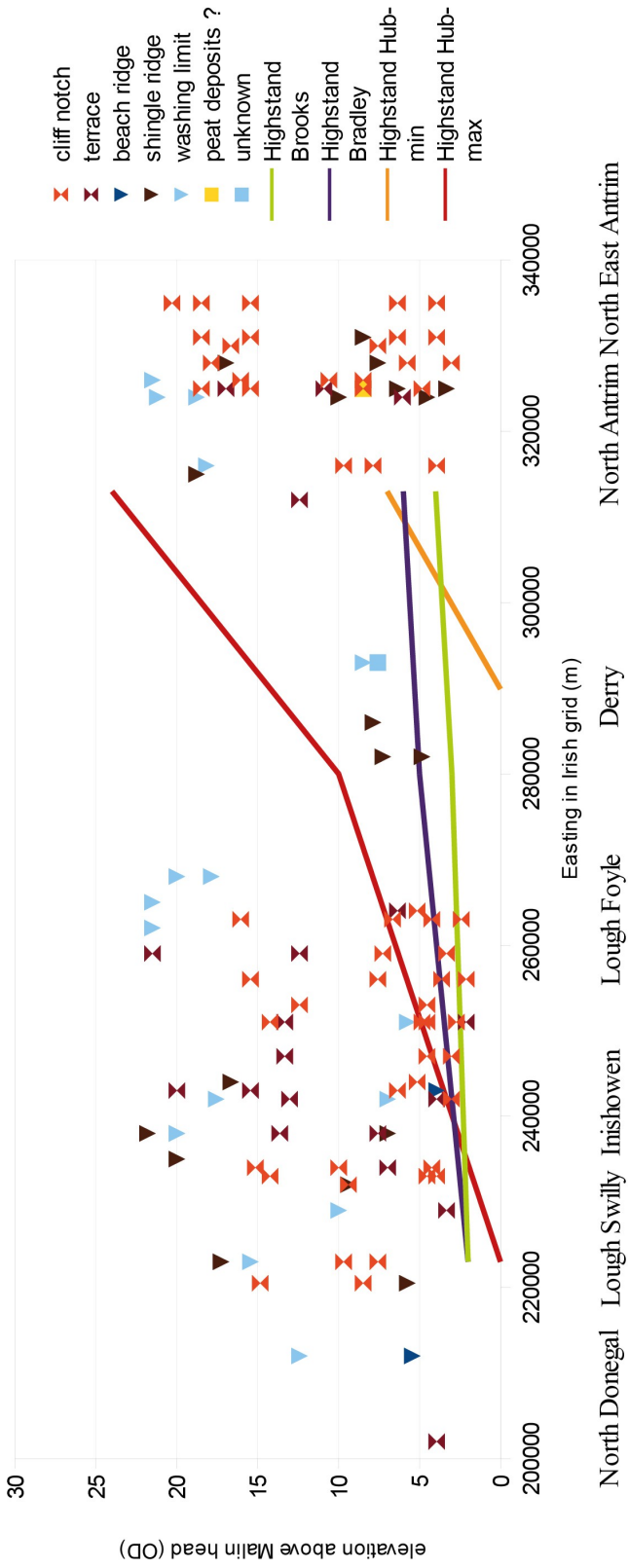

Figure 4.36: Comparison of raised shorelines elevation for the north coast of Ireland (after Synge and Stephens, 1966). The highstand elevation predicted by each of the recent GRMs is shown with the continuous lines.

4.7 Conclusion

This chapter explored the range of coastal features indicative of past RSL both on land and offshore. The evidence on land has been studied for almost 200 years and was used to build the original understanding of the process of glacial uplift. Extensive work in the 1960s (see Synge and Stephens, 1966) were used to reconstruct the evolution of RSL during the last deglaciation. Most of their findings have been reassessed recently. McCabe et al. (2007) and McCabe (2008b) show a refinement in the techniques, in terms of the use of more detailed stratigraphical constraints, used in order to draw some limited conclusions on the RSL evolution.

The recent availability of the extensive JIBS dataset allowed the exploration of the bathymetry for relict shorelines visible as erosional or accretional features. After initial inspection of the evidence from the histograms of the data, a marine terrace database was developed in order to record and test the correlation between several physical parameters on the morphology of these features. A large range of features were detected throughout the study area and at various depth. Lithological control was clearly observed over the width of the features formed (extent of erosion), their angle of slope and the rugosity of their surface. Finally, basalt appeared locally as the more resistant lithology followed by the local sedimentary rocks and the local metamorphic rocks respectively. This could be due to the extensive structural control of lava flows on the resulting terraces.

The potential for RSL information contained in these features was finally investigated. Based on global average rates of erosion for various lithologies, it was concluded that most of the features detected here were formed over large periods of time, longer than the last deglaciation period. However this last period of RSL change is likely to have had an influence on the terraces although limited. The issue of inheritance of the terraces of the study area will further be explored using erosion models in the next chapter where a quantification of the influence of recent RSL change will be sought.

Chapter 5

Modelling the development of the coastal profiles of the study area

With a change in RSL, shore platforms may be converted into subaerial or submarine terraces, or sloping erosional continental and island shelves. Since they can rarely be dated directly, these erosional features are usually interpreted in the light of associated sedimentary deposits and/or by correlation with other features of inferred equivalent age, although this reasoning sometimes becomes circular (section 3.2.1 and Devoy, 1983). One particular challenge is distinguishing whether a rock platform is genetically linked to the most recent phase of RSL change, or is in fact inherited from an earlier RSL phase (or phases) (Young and Bryant, 1993; Brooke et al., 1994; Stone et al., 1996; Trenhaile et al., 1999; Trenhaile, 2002; 2010; Blanco Chao et al., 2003; McKenna, 2008).

The possibility that many shore platform features in the study area are metachronous or inherited is widely acknowledged in the literature (Orme, 1966; Carter, 1982; McKenna, 2002; 2008), although difficulties in developing reliable chronologies have commonly frustrated attempts to distil more precise information. The simulations presented in this chapter permit a first order assessment of the extent and distribution of potentially inherited features to be made. The basis of this chapter has been published as Thébaudeau et al. (2013) – see Appendix 4.1.

5.1 Selection of target profiles

Analysis of the study area was focussed on three specific localities along this stretch of coast which are selected to provide a representative range of lithology, tidal range, aspect and morphology (figure 5.1).

Study area 1 (North Antrim) comprises Ballycastle Bay opening to the north, and Church Bay on Rathlin Island opening to the south west. The western half of Ballycastle Bay and the whole of Church Bay are etched into a Palaeocene basalt plateau that overlies Cretaceous chalk and greensand. The eastern half of Ballycastle Bay is composed of Carboniferous limestone with a Tertiary dolerite sill, and it is separated from the western half by the Tow Valley fault which reaches the coast at the town of Ballycastle.

Study area 2 (Derry), comprising the north westerly facing coastline of Portrush and Portballintrae is situated to the west of study area 1 and adjacent to the Giant's Causeway World Heritage Site. In this area, the Palaeocene basalt plateau is close to modern sea-level with active shore platform development. The Tertiary dolerite sill of Ramore Head and the Skerries divides the area in two and forms a sheltered 'inner sea' to the east of Portrush.

Study area 3 (Donegal) is situated at the mouth of Lough Swilly and presents a strong contrast to the other study areas in terms of its morphology and underlying geology. Here, the rocks are Precambrian quartzites and pelites, with a Devonian granodiorite pluton. The north westerly facing coastline lacks the prominent cliffs of North Antrim or Derry, and instead comprises exposed sloping rock surfaces that are mantled in places by sand or gravel beaches and windblown deposits.

Six shoreline profiles were selected to represent the main morphologies of this stretch of coast and compiled from the bathymetric mapping and topographic DEM are presented in figure 5.2. These profiles are actual profiles taken at the locations plotted in figure 5.1 and are characteristic of the stretch of coast where they are located.

In area 1, three profiles are constructed representing the contrasting lithologies within Ballycastle Bay (profiles 1 and 2), and the more sheltered environments within Church Bay on Rathlin Island (profile 3). Profile 1, representing the eastern half of Ballycastle Bay, comprises three main elements: the sill in the cliff face of Fair Head which extends from the intertidal zone to an elevation of 80m without any marked breaks of slope; a sloping (~ 2°) terrace about 250m wide extending from the intertidal area to a

depth of approximately 8m depth; and a second sloping terrace (~ 1°) about 1000m in width and extending from 15m to 30m depth, that is backed by a small submerged cliff face (figure 5.2, profile 1). In the western portion of Ballycastle Bay (profile 2) the cliff section is similar to that of profile 1, but there are consistent differences in the submerged terrace profiles which are cut into Cretaceous chalk and greensand. Here, a sloping (~ 3°) terrace surface between 20 and 200m wide extends from the intertidal zone to a depth of −7m. This gives way to a subhorizontal platform between 15 and 70m wide. A second subhorizontal platform up to 150m in width is intermittently recorded at a depth of around −17m, below which the gradient of the seafloor increases to ~ 1.8°. Both submerged terraces are carved in Carboniferous limestone whilst the cliff face is formed by the basalt plateau. In Church Bay (profile 3), the same general morphology is observed except that the sub-horizontal platform at −7m is absent. Instead, the upper sloping terrace surface terminates in an abrupt cliff face at −10m.

In study area 2, there are Cretaceous chalk cliffs up to 45m in height to the west of Portballintrae, rising from a 20m wide sub-horizontal platform at around +6m (figure 5.2, profile 4). Sand dunes cover Jurassic sedimentary rocks up to the town of Portrush (figure 5.2, profile 5), where the Tertiary dolerite sill of Ramore Head and the Skerries protrudes from the modern coast. West of Portrush, cliffs of Palaeocene basalt extend from the intertidal zone to around 20 to 25m in height. Whilst there are no bathymetric data between the intertidal zone and −10m along the chalk coast (profile 4), a sloping terrace (~ 2°) is present from the intertidal zone to a depth of 15m on the basalt coast to the west of Portrush (profile 5). There is a sloping terrace (~ 1.3°), about 300m wide, from 10m to 16m depth in the chalk (Figure 5.2, profile 4), and a subhorizontal platform, up to 1000m wide, from 15m to 20m depth in the basalt (figure 5.2, profile 5). Around the Skerries, a sub-horizontal platform forms a flat seabed at a depth of 20m.

In the study area 3 (figure 5.2, profile 6), there is a wide (150m), gently sloping (~ 3°) terrace extending from the intertidal zone to a depth of 20m. This is succeeded by a sub-horizontal platform with an uneven surface up to 1000m wide, which terminates in a short drop to the Malin shelf.

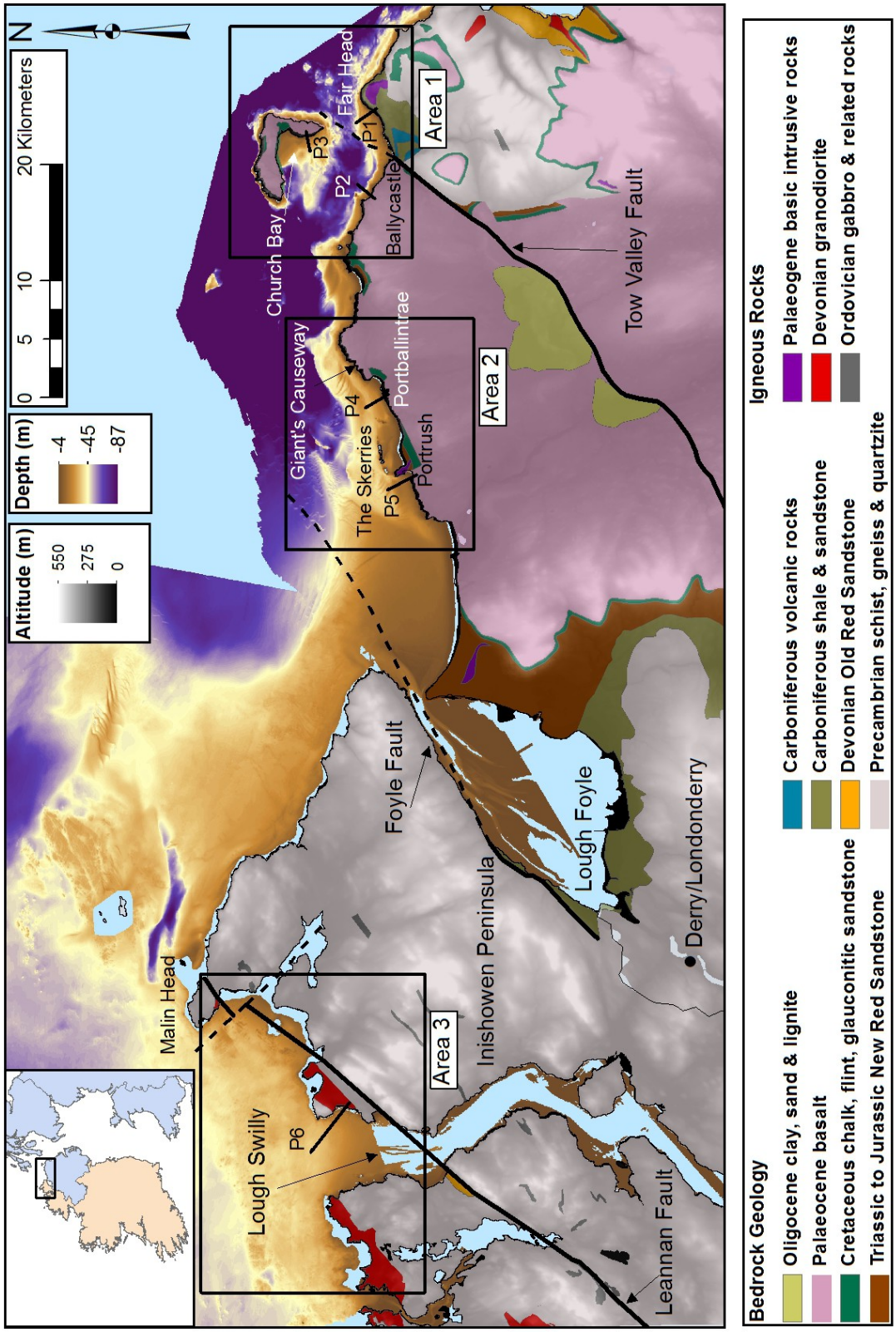

Figure 5.1: Location map of the 3 specific areas and the shoreline profiles used for analysis plotted against the JIBS swath bathymetry dataset (offshore) and the bedrock geology (onshore).

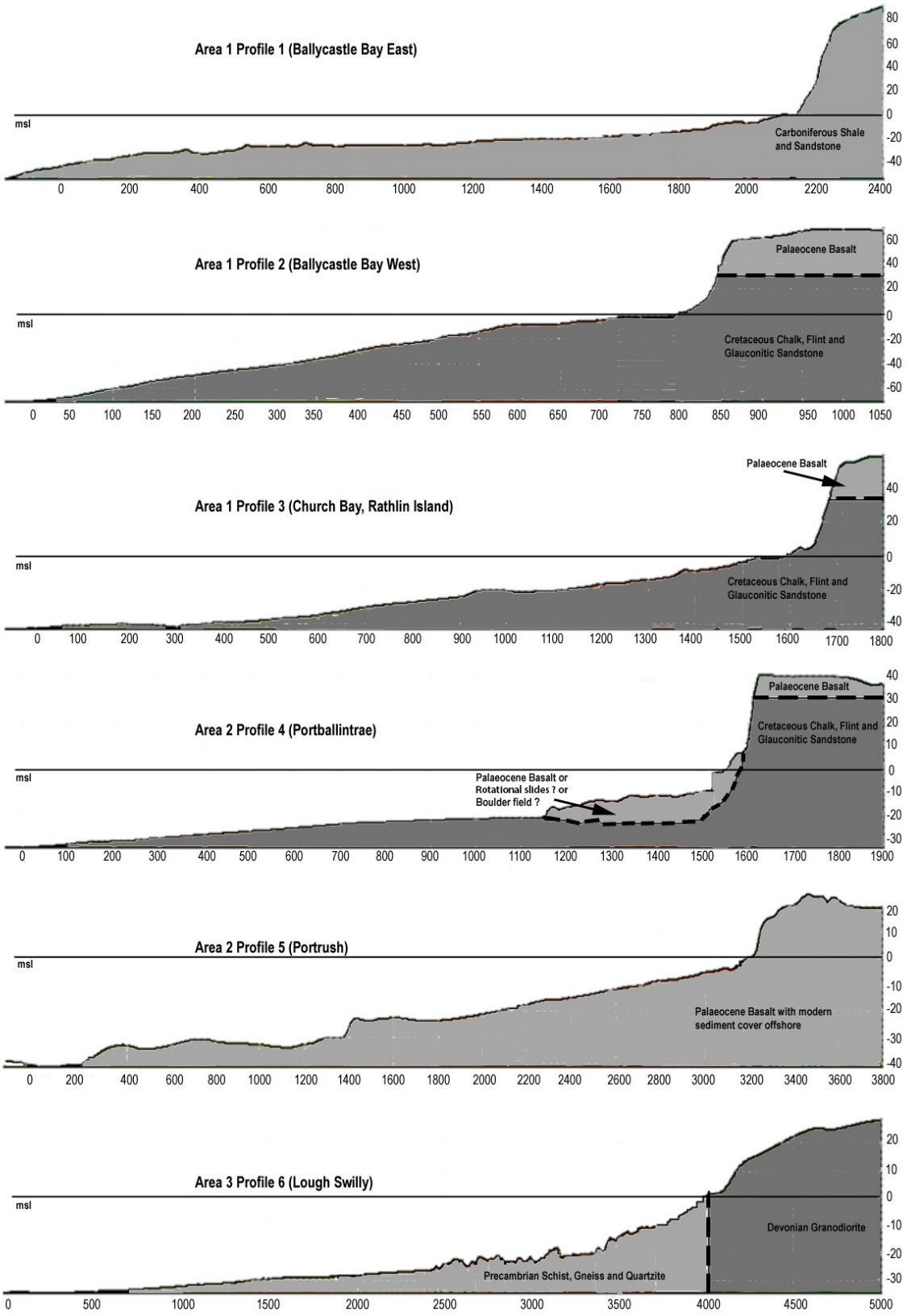

Figure 5.2: Composite coastal profiles derived from high resolution swath bathymetric data. Major changes in lithology are indicated on each profile for reference. MSL = mean sea level.

5.2 Output of the wave erosion model

No erosion occurs in any of the three study areas during runs with both highly resistant rocks ($SF_{cr} \geq 1000$) and very low initial gradients (2.5°). Preliminary model runs on linear slopes (not shown) revealed that erosion increases with increasing initial slope gradient due to diminished wave attenuation. Consequently, for model runs with two slope elements (simulating inherited morphology), no erosion occurs on the gently sloping shelf below the modern low tidal level (figure 5.3). However, the steep, previously uneroded hinterlands (slope 35°) experience substantial erosion, especially during the early periods of the model runs (figure 5.3).

The degree of erosion increases with decreasing rock resistance. In model runs with moderately resistant rock ($SF_{cr} = 500$), considerable modification of the shelf occurs, extending in some cases to depths of 20 m or more, and resulting in cliff recession of up to several hundreds of metres (figure 5.4). The amount of erosion for a given rock type increases from east (Area 1) to west (Area 3) reflecting differences in tidal regime (table 2.2) and RSL history.

Cliff–platform junction height decreases to the west and is generally between 0.25 and 0.5m lower in runs using less resistant rock. With the exception of runs driven by the Hub-min model RSL curve, which produces cliff–platform junctions in the upper portion of the modern intertidal zone, cliff bases are usually produced that are up to several metres above the present high tidal level in all three areas (table 4.1). The formation of sub-horizontal shore platforms and terraces is strongly associated with the slowest rates of RSL change (see Section 4.1.3).

To explore these general features in more detail, the evolution of the subtidal, intertidal and supratidal components of profiles from each study area are considered. These were produced by multiple runs employing different RSL scenarios for both high and low resistance rock (figures 5.3 and 5.4).

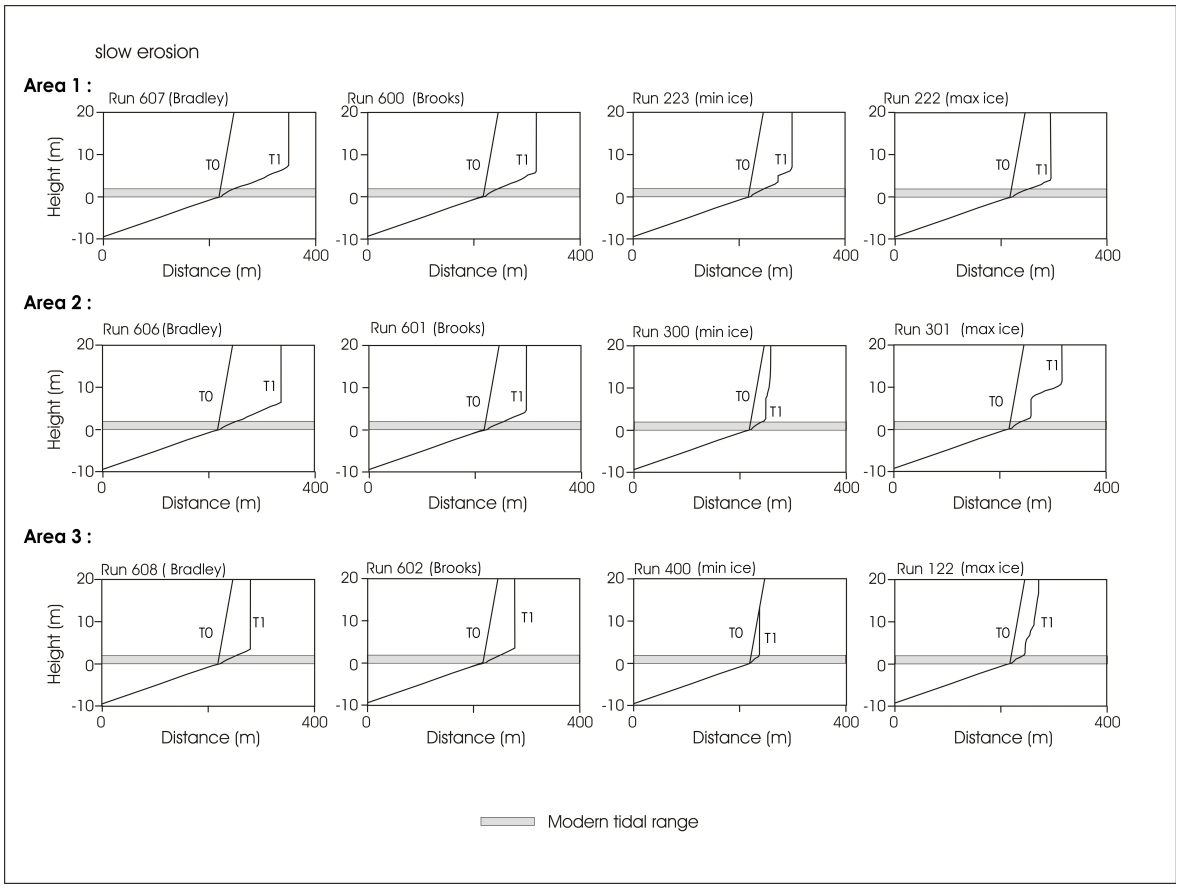

Figure 5.3: Slow Erosion (SFcr = 1000): Modelled shoreline profiles showing the modification by waves of a slowly eroding coastline with inherited morphology for each of the three study areas and four relative sea-level scenarios. The initial profile (T0) comprised a linear surface with a 5° slope below mean low water spring tides (MLWS) and a steeper surface of 35° above MLWS. T1 = the resulting profile. The modern tidal range is plotted as a shaded area.

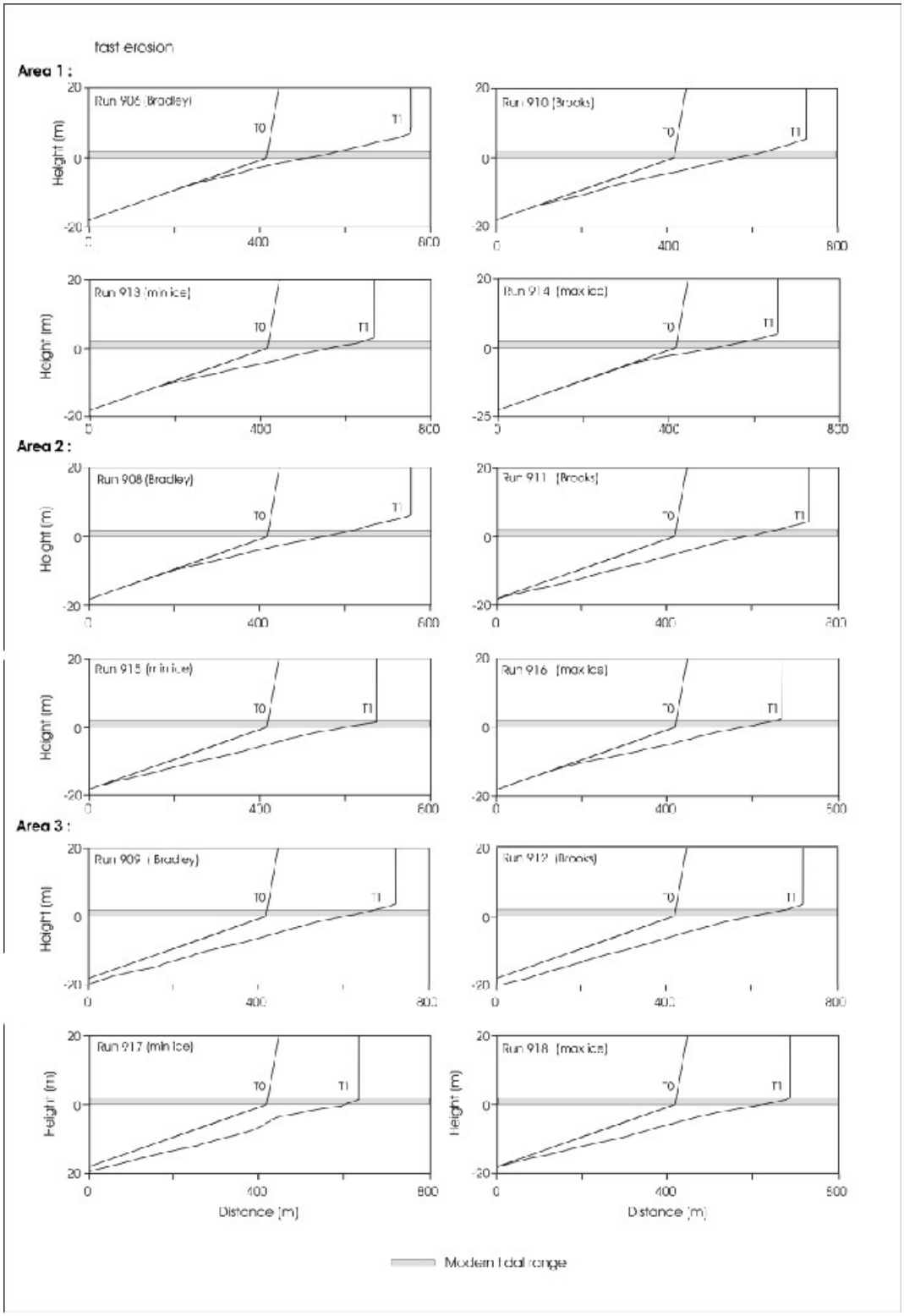

Figure 5.4: Fast Erosion (SFcr = 500): Modelled shoreline profiles showing the modification by waves of a rapidly eroding coastline with inherited morphology for each of the three study areas and four relative sea-level scenarios. The initial profile (T0) comprised a linear surface with a 5° slope below mean low water spring tides (MLWS) and a steeper surface of 35° above MLWS. T1 = the resulting profile. The modern tidal range is plotted as a shaded area.

Area	Cliff–platform junction	Bradley	Brooks	Hub-Min	Hub-Max	Measured
(1) N. Antrim	Mean	6.6	3.9	2.6	4.1	
	Max	7.1	4.1	3.6	4.6	1.8–2.3
	Min	6.1	3.6	1.6	3.6	
(2) Derry	Mean	5.7	3.4	1.4	1.7	
	Max	6.2	3.7	1.7	2.2	0.2–2.2
	Min	5.2	3.2	1.2	1.2	
(3) Donegal	Mean	1.3	1.1	−0.4	−0.2	
	Max	2.3	1.3	−0.2	0.3	−1.3 to −0.2
	Min	0.8	0.8	−0.7	−0.7	

Table 5.1: Simulated altitude of the cliff–platform junction (in meter OD Malin Head) for each study area and relative sea-level scenario (see text for details), compared with the observed altitude from the topographic data.

5.2.1 The subtidal zone

In all runs, erosion of the submarine shelf tends to produce surfaces extending down to depths of about 5–7m that are slightly convex upwards, with mean gradients which increase with rock resistance and range from about 1.5° to 3.5°. No step-like submarine terraces backed by very steep scarps are formed, but one or more subtle increases in gradient (typically of less than 2° extending over elevations of only a few metres) do occur in a number of runs. These changes are generally within depths of less than 15m of the present low tidal level, and in runs with moderately resistant rock (figure 5.4, Area 1 and Area 2). Erosion at the lowest postglacial RSL in Area 3 also produces some terraces at depths ranging from about 23 to 15m depth (figure 5.5, Area 3). Some more prominent terraces with gently sloping surfaces (gradients 1–2°) backed by slopes of as much as 10 to 15° (figure 5.4, run 917) generally develop in runs with resistant rocks ($SF_{cr} \geq 700$). These are found at around 6m depth in Area 2, and at about 20m and 14m depth in Area 3 when using the Bradley model RSL curve. Terrace formation is less frequent in the three study areas when employing the Brooks and Hub-Min model RSL curves (figures 5.3 and 5.4).

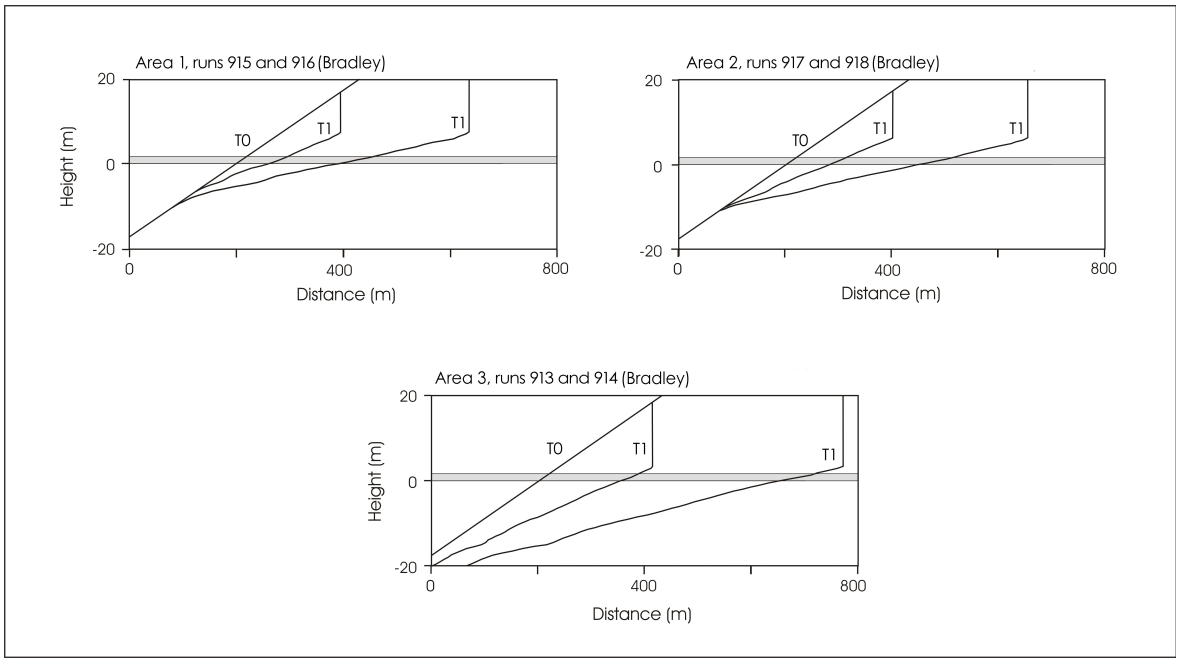

Figure 5.5: Modelled shoreline profiles for each study area illustrating the formation of sub-tidal terraces and breaks in slope in an initially linear surface under moderate erosion ($500 < SF_{cr} < 1000$) when driven by relative sea-level curves produced by the Bradley glacial rebound model (Bradley et al., 2011).

5.2.2 The intertidal zone

In most runs, the modern shore platforms, extending from the MLWS to the MHWS tidal levels, range from about 50 to 150 m in width, with corresponding mean gradients of 2.3° to 0.75°. The widest platforms and terraces with the lowest slope gradient develop in the least resistant rocks. The platforms are generally broadly linear, although some are gently concave or convex in shape. Varying the RSL curve elicits an array of contrasting responses, although in general platforms produced during runs driven by the Hub-Min and Hub-Max RSL models are, respectively, about 10 to 15m narrower and wider than those produced by the Brooks and Bradley RSL curves.

5.2.3 The supratidal zone

Erosion above the modern low tidal level generally produces a single vertical cliff, both in runs that commence with a single linear, sloping surface, and those with an inherited cliff in the initial profile. As noted previously, the absence of erosion in runs with a very low initial gradient and resistant rocks means that the supratidal zone consists entirely of the initial surface. In most runs, however, erosion creates a cliff that extends up to a point above the highest RSL represented in each of the curves, where the initial surface is unmodified. In a few runs for area 1, using the Hub-Min and Hub-Max RSL curves and resistant rocks, the top of the cliff is lower than the highest RSL and the surface above the cliff top is modified by wave erosion to produce irregular slopes with elements that are both steeper and gentler than the initial slope (figure 5.3, Run 223). In a few runs with cliffed initial profiles and resistant rocks ($SF_{cr} \geq 750$), profiles comprising two vertical cliffs separated by a gently sloping terrace are generated when driven by the Hub-Min and Hub-Max RSL curves. Most of these subaerial terraces occur in runs for area 1 and range from 1 to 27m in width and, depending on their width and gradient, are about 5 and 8m above the modern high tidal level (MHWS) (figure 5.3, run 223). Other, well defined, gently sloping subaerial terraces several tens of metres in width are produced less frequently in runs for area 2 (figure 5.3, run 301), where they develop between 7.5 and 11.5 m above the present high tidal level (MHWS).

5.3 Comparison of modelled and measured profiles

The simulated profiles provide a first order assessment of the wave erosion experienced along the north of Ireland coast since it became permanently ice free around 16,000 years ago (Clark et al., 2012). By holding wave and tidal regime constant, the influence of differences in rock resistance, profile gradient and RSL history can be examined. As rock resistance increases, the mean profile steepens and becomes narrower. However, profile shape is also controlled by wave efficacy and the duration of erosion at a given height. Consequently, changes in shoreline slope in space and through time, coupled with the shape of the RSL curve will modify this general relationship.

5.3.1 Mean profile gradients

Comparison of modelled and mapped shoreline profiles from each area permits some general conclusions to be drawn. The overall mean gradient is most meaningfully compared across the intertidal to subtidal portions of the profiles extending down to around 15m water depth (figure 5.6). As RSL only briefly occupies heights below this range, significant modification of the initial profile can only be accomplished with extremely rapid rates of erosion which, in turn, result in poor fits between modelled and mapped profiles across the remainder of the height range. Best overall fits are predominantly found in runs with moderate to slow rates of erosion (SF_{cr} =500 to 1150). Generally good agreement in mean gradient is observed for profile 1 (limestones, shale and sandstone) and profile 3 (chalk) in Area 1, and profile 6 (quartzites and pelites) in Area 3. It is noteworthy that the breaks in slope at c. 10m, 15m and 20m depth for the measured profiles 1, 3, and 6 respectively, correspond to the RSL minima for each of these areas as simulated by the Brooks and Hub-Min models. This is consistent with the idea of only minimal modification of the seafloor below c. 20 m by RSL change during the last 16,000 years.

Reasonable fits are also obtained in Area 2 for profile 4 (chalk) at Portballintrae and, to a lesser extent, the slightly concave up profile 5 (basalt) at Portrush. The backscatter and bathymetric data reveal a highly irregular, sloping surface from about 10 to 20m depth in profile 4. Whilst groundtruthing will be required to establish its composition, it could represent outcropping basalt below the chalk, or a boulder field, perhaps associated with the submerged glaciogenic sediments reported from the region (Kelley et al., 2006; Dunlop et al., 2010). In any event, the different lithology and surface roughness of this

feature in comparison to other parts of the profile which are incised into chalk, may account for some of the mismatch between modelled and measured profiles at this location. For example, McKenna et al. (1992) highlight the role of basalt flow structure and weathering horizons in promoting irregular, stepped shoreline profiles along the Causeway coast.

In contrast to the other sites, at Portrush the closest agreement between modelled and measured profiles is obtained with a comparatively low critical surf stress value (SF_{cr} = 240) corresponding to much more rapid erosion. The measured profile is also influenced by a covering of modern surficial sediments. One possible explanation for the required low resistance in this area would be incision into glacial diamict rather than underlying basalt. Kelley et al. (2006) report glacial sediments and gravel deposits beneath a cover of Holocene sand in the Portrush area.

Despite good agreement between modelled and measured profiles in the eastern portion of Ballycastle Bay, the wide sub-horizontal platform at 7 to 8m depth in the western part of Ballycastle Bay could not be simulated satisfactorily. In some runs, a slight reduction in slope gradient is observed at these depths corresponding to brief still-stands in the Brooks and Bradley RSL curves. The available data provide no indication that this feature is lithologically or structurally controlled. Whilst the underlying geology is similar to that of the adjacent profile in Church Bay (profile 3), the aspect of the two stretches of coastline is contrasting, with the western portion of Ballycastle Bay being more sheltered from wave action. Whilst a reduction in wave energy cannot account for enhanced formation of a shore platform, it is consistent with the increased preservation potential of an older featured inherited from a previous phase or phases of lower than present RSL.

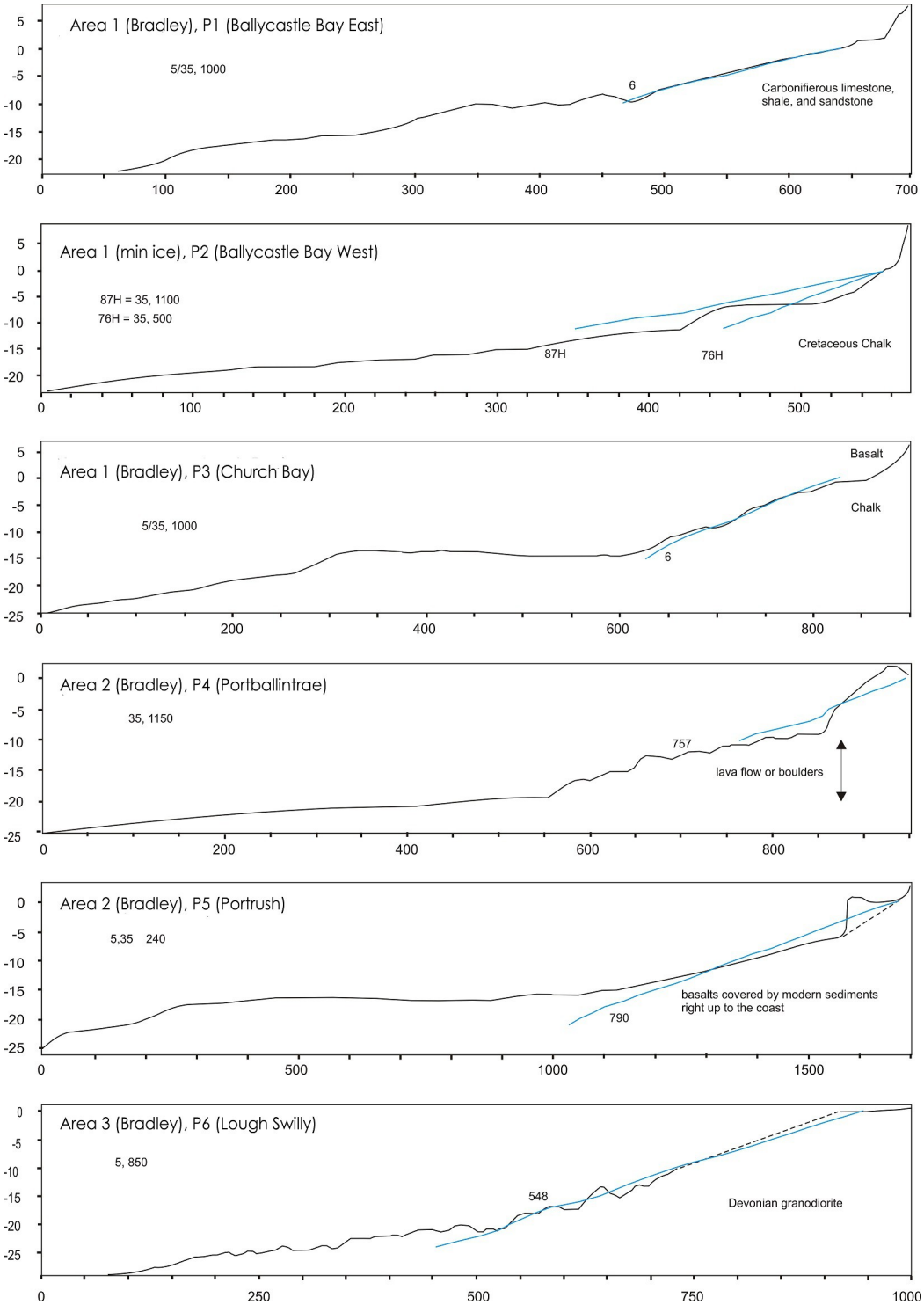

Figure 5.6: Simulated mean profile gradients (blue lines) plotted against the measured composite profiles for each of the study areas (black lines). Figures refer to the initial profile gradients (linear 5° slope or composite 5° slope with a 35° inherited cliff) and the rock resistance (SF_{cr}) used in each run. For clarity, the simulated profiles are only plotted for the height range over which modification of the initial surface occurred. These best-fit profiles are produced by the relative sea-level curves generated from the Bradley model (Bradley et al., 2011) with the exception of Profile 2 which is derived from the Hub-Min scenario (Kuchar et al., 2012).

5.3.2 Platform features, cliff-platform junction height and relative sea-level

Whilst the bathymetric data contain abundant evidence for submerged sub-horizontal platforms at a range of depths, the model simulations fail to reproduce similarly sized features anywhere within the subtidal zone. Whilst platforms can be created at lowstands by lowering the resistive strength of the rock, this causes them to be removed during subsequent RSL rise. In more resistant rocks, the duration of lowstands is insufficient to create features of comparable scale. Hence, to form and subsequently preserve these features, RSL is required to occupy lower elevations for more extended periods of time than in any of the simulations. By definition, and based on the RSL scenarios used in this study, any feature below the minima of the simulated RSL curves (c. 12m, 15m and 25m depth for Areas 1, 2 and 3 respectively) predates 16,000 BP.

Similarly, whilst raised terrace features are produced in some of the model runs with a steep inherited cliff etched in resistant rock, no single RSL curve or combination of parameters replicates the terrestrial shoreline features reported from this region (section 4.2.2). The most pronounced raised features are generated in runs driven by the Hub-Min and Hub-Max RSL models, since these have intervals of quasi-stable higher than present RSL associated with Meltwater pulse 1a. Cliff-line retreat precludes the preservation of raised shoreline features in scenarios with low rock resistive strength. Whilst detailed comparison between simulated terraces and recorded 'raised shorelines' is premature, simulated terrace heights show broad agreement with the elevations of some inferred postglacial shorelines. For example, modelled terraces are found between +8 and +14m in Areas 1 and 2, compared to a general upper limit of postglacial raised shorelines across the region of between c. +7 to +13m (section 4.2.2). More detailed field mapping to separate composite shoreline features, coupled with improved constraints on model parameters is required before more specific comparisons can be made.

Since consideration of the overall mean profile gradients indicates shorelines are cut into resistant rock with moderate to slow rates of erosion, the formation of numerous platforms or terraces requires RSL to occupy certain height ranges for more extended periods of time than in the simulated RSL curves. Providing the modelled parameters give a reasonable approximation of conditions since deglaciation, these results suggest that some of the raised platforms and most of the submerged platforms are inherited from an earlier phase or phases of RSL which confirms the initial findings from the marine terraces

database for the study area (section 4.5).

As with all modelling studies, these interpretations are associated with some caveats relating to parameter/variable choice. Firstly, the models are run using modern hydrographic data. Changes in wind-wave climate through time are likely and may alter the rate of erosion (Neill et al., 2009; 2010), although to some extent any deviation in erosive power is offset during selection of rock resistance in order to minimise the misfit between modelled and measured mean profile gradients. Similarly, previous numerical modelling indicates that tidal range changes are likely to have occurred since deglaciation (Uehara et al., 2006). Whilst a larger tidal range could potentially alter the height at which simulated shore platforms are formed, it would not induce widespread shore platform formation at the range of elevations apparent in the DEM.

Secondly, whilst rock resistance is varied between runs and simulated profiles, critical surf stresses were not modulated within an individual profile (to simulate vertical differences in rock strength) or through time. The latter could be significant where recently deglaciated terrains are exposed to extreme freeze-thaw action, initially rendering the surface weaker and more easily eroded (Robinson and Jerwood, 1987; Fournier and Allard, 1992; Trenhaile, 2002). The high levels of saturation and salinity associated with the intertidal, spray and splash zones are certainly conducive to frost weathering (Trenhaile and Mercan, 1984), whilst the action of glacial or drifting ice itself are also potentially significant erosive agents (Dionne and Brodeur, 1988; Hansom and Kirk, 1989). Conceivably, these combined effects could promote rapid shore platform development immediately following deglaciation as in the case of the formation of strandflats in the North Atlantic (Bird, 2000), although this will tend to be offset by the comparatively rapid rate of RSL fall associated with the early phase of glacioisostatic rebound. Whilst the study locations were selected to avoid major within-profile lithological changes, more detailed, location specific analyses would benefit from incorporating any known vertical variations in rock resistance revealed by fieldwork, diving or drop-camera surveys. Similarly, previous modelling studies have considered both wave and weathering effects on shore platform genesis (Trenhaile, 2008; 2010), and inclusion of a time-variable weathering term would also be a useful addition to future work in this region.

Finally, the models are driven by simulated RSL curves which, whilst representing the current state of the art, are comparatively poorly constrained by field data in the study

area (especially during the early stages of deglaciation). Modification of the RSL curve to promote lengthier still-stands at certain heights would produce more terrace and shore platform features. For instance, the possible highstand around +19m in McCabe et al. (2007) (see section 2.4.2) would imply 2,500 years of stable RSL which has the potential to produce platforms of 2.5m in width (using the global average rate of erosion of 1mm/year). However, there remains a finite amount of time within which to accommodate RSL change, hence extending the duration of still-stands, or expanding RSL maxima/minima, requires concomitantly more abrupt RSL rises and falls, ultimately producing a step-like RSL curve that is physically implausible.

The height of the simulated cliff–platform junction is particularly sensitive to the choice of RSL curve used to drive the wave-erosion model. In areas experiencing RSL rise during the Holocene, cliff–platform junctions typically occur between mid-tide and spring high tide level, with higher levels corresponding to more resistant rocks (Everard et al., 1964; Wright, 1970; Trenhaile, 1972; 1978; 2010). In the study area, the cliff foot is typically above present high tidal level, consistent with formation during higher than present RSL. The approximate height of the cliff–platform junction determined from the topographic data ranges from between c. +1.8m and +2.3m OD in Antrim (MHWST = +0.5m OD) to between c. −1.3m and −0.2m OD near Lough Swilly (MHWST = +1.3m OD) (table 5.1 and 2.2). This height trend reflects the widely recognised westward tilt in shoreline features resulting from increased isostatic rebound toward the northeast of Ireland. This general geometry is reflected in the simulated RSL curves although, with the exception of the Hub-Min model, the simulated height of the cliff base is over-predicted (table 5.1). The sensitivity of cliff base height to differences in simulated RSL suggests that more detailed work compiling field measurement of cliff–platform junction height, lithology and wave climate could provide useful additional constraints on modelled RSL curves.

5.4 Conclusion

The objective of this study was to provide a broad, first assessment of rocky shoreline profile development at the regional scale. Rocky shoreline profiles generated from a wave-erosion model driven by simulated RSL curves for the past 16,000 years, approximate the overall mean gradients of most measured shoreline profiles in the study

area. In these profiles, breaks in mean slope are observed at depths comparable to the RSL minima in several of the RSL scenarios, with shallower depths being erosively modified since deglaciation. All RSL scenarios replicate the observed geometry of changes in cliff–platform junction height along the coast, although several overestimate the actual elevations inferred from the topographic data. Whilst some of the RSL scenarios produce a limited number of raised shore platforms at comparable heights to similar features reported in the literature, no single curve or combination of parameters is capable of generating the range of platform and terrace features present in the bathymetric and topographic data (chapter 4). This is consistent with the idea that many of these features are inherited from an earlier phase or phases of RSL change.

The best parameters used to fit the model output to measured profiles, in particular the rock resistance, is associated with varying lithologies (figure 5.6). As was presented in chapter 4, lithology is the preponderant control on the morphology. Chapter 7 will further integrate these findings in order to make further inferences on the formation process and age of the recognised marine terrace and extract the ones potentially linked with postglacial RSL change.

Although no direct comparisons of the level of contemporary shorelines made of marine terraces can be traced, cliff-platform junction evidence data indicate a local variation in level which indicates general agreement with the modelled RSL curves. This will be further analysed in chapter 7.

Whilst the geomorphological analysis of the study area coupled with modelling gave an insight into the processes and time scale involved in the formation of erosional features in hard rock, they emphasized the limited influence of the postglacial RSL changes on them. The following chapter will deal with the modern sediment stratigraphy for the study area and devise a depositional scenario linked directly to the RSL evolution of the deglaciation period.

Chapter 6

Sub bottom investigation of RSL change evidence

Chapters 4 and 5 presented the analysis of erosional coastal features found in the study area. This chapter will investigate the depositional history of the study area in order to draw inferences concerning RSL change. The stratigraphical sequences at various locations of the study area were identified by exploring their seismic data and suitable targets to ground-truth by coring were selected. Acoustic-lithological correlations made at cored locations were then extrapolated to provide a general description of sediment deposition in the study area.

6.1 Seismic stratigraphy

In this section, the regional seismic data is presented and analysed in order to identify suitable targets for ground-truthing. The presentation of published findings on the seismic units from adjacent offshore basins identified by the British Geological Survey (BGS) from their regional marine exploration programme will be introduced first (section 6.1.1) followed by a presentation of the extensive published work on the Skerries and Portrush area (section 6.1.2). The investigation of unexplored zones of the study area will start with the areas where Chirp data (figure 3.11) were collected and some of the results were already published in the literature; Runkerry Bay and the Bann estuary (sections 6.1.3 and 6.1.4). The bays (Whitepark Bay, Church Bay and Ballycastle Bay) and the one seismic line for each Lough Foyle and Lough Swilly where more recent Pinger data was collected are presented next (sections 6.1.5 to 6.1.9). Each of the seismostratigraphies will be presented using a single line (or lines when deemed necessary) displayed from the SMT Kingdom software with highlighted recognised units (with associated map for location) and a summary table. The line (or lines) displayed were selected based on their ability to represent most of the seismic units and their relationships to each other. All depths presented below are actual depth of the reflectors and thickness of the seismic units (calculated with the previously mentioned rapid conversion from the velocity of Pwave in water : 1500 m/s (section 3.4.2)) and not sub-bottom depth. As such there are no bathymetric effects, meaning that the representation of the thickness of a unit on a map does not vary with the depth or morphology of the seabed

6.1.1 Offshore basins stratigraphy

The following information is mainly extracted from the British Geological Survey (BGS) regional marine reports (Eden et al., 1971; Fyfe et al., 1993).

The main legacy for the Quaternary ice sheets action in the Malin and Hebrides sea (north of the study area) are glaciomarine deposits corresponding to the last glaciation up to 300m thick and numerous moraines and glacial striae on the sea floor (Eden et al., 1971; Fyfe et al., 1993; O'Cofaigh et al., 2010). Part of the relief appears to be Tertiary in origin (Evans et al., 1982) but the overdeepening of many of the basins and their general orientation along the ice flows recognised on terrestrial evidence clearly shows the

predominance of glacial erosion in the development of the rock head morphologies for the area. Most of the sediments that infill the basins and cover the inner shelf appear to be of late Devensian age (post 30000 BP) although some underlying layers, notably in the Hebrides north of the study area, have been shown to predate this (Davies et al., 1984; Fyfe et al., 1993) but more work is required, in particular for Quaternary sediments in the Malin sea. The majority of this study area has Quaternary deposits of unconsolidated sediments of less than 20m thickness with only 2 areas of thicker deposits found to the west of Malin Head and north of Portrush (figure 6.1). The east side of the study area, North Antrim, has the thinnest sediment cover with places with less than 5m thickness of Quaternary deposits (see section 6.1.7).

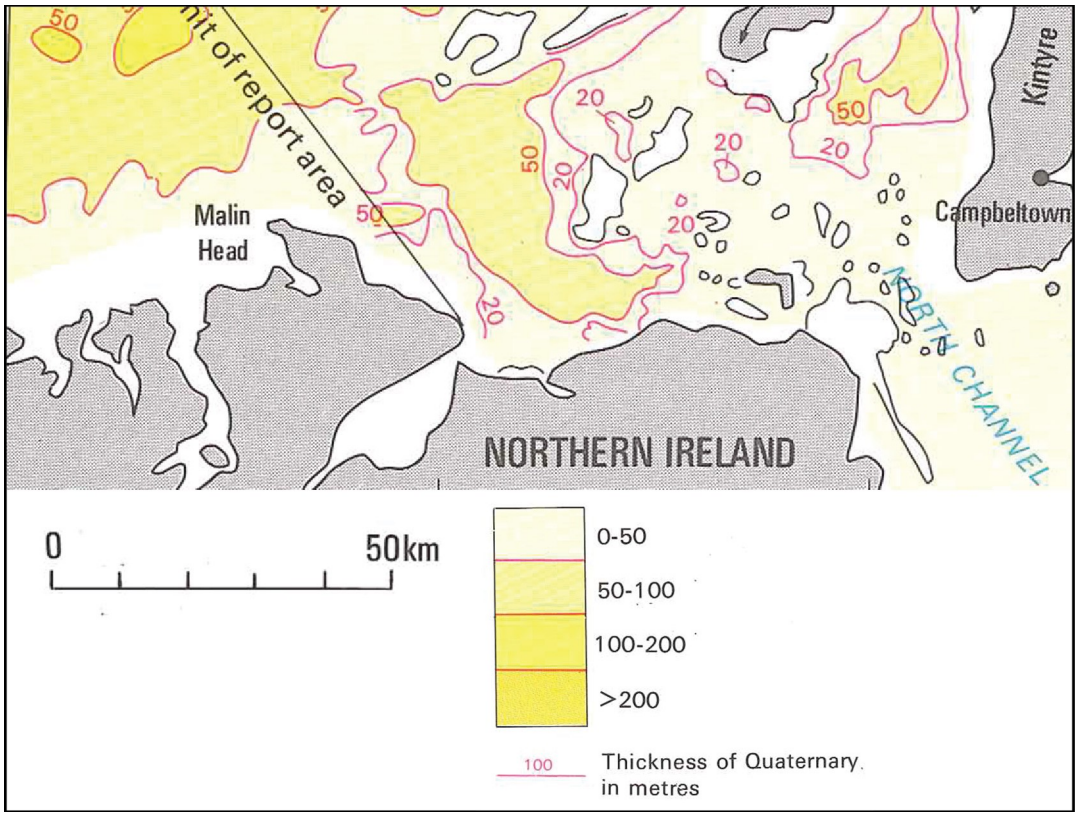

Figure 6.1: Contour map of the thickness (in meters) of Quaternary sediments for the study area (from Fyfe et al., 1993).

Further south east of the study area lies the Irish sea which similarly has a limited number of basins where Quaternary deposits are thicker than 100m; the main one being the north channel (figure 2.11) forming the northern part of the Celtic trough running along the centreline of the Irish sea and the others are several elongate incisions thought to have a glacigenic origin (Wingfield, 1990). The Irish sea presents a complex Quaternary

depositional history with evidence for up to 3 different glaciations in places (Jackson et al., 1995).

The various Quaternary formations for the Malin and Hebrides seas are presented in table 6.1 (Fyfe et al., 1993) and most have been sampled through boreholes in the Hebrides sea, north of the study area (figure 6.2 for their location). The glaciomarine sequences are composed of silty to sandy clays with dropstones and appear as transparent to very well stratified seismic units. Most of the top sediments that appear to be deposited mainly in the early Holocene (Graham et al., 1990) have a maximum thickness of 25m and are composed of muddy sands.

The oldest Quaternary sediments identified in the Malin-Hebrides sea area are stiff silty clays up to 45m thick with a transparent acoustic signature overlain confromably by an unsampled unit up to 25m thick with faint horizontal internal reflectors and diffraction hyperbolae which were interpreted as dropstones (Fyfe et al., 1993). These two units are termed the Skerryvore Formation and the micropalaeontological study of the lower unit (Skerryvore L) indicated deposition in a temperate environment (Davies et al., 1984). In comparison, the unsampled upper units (Skerryvore U) has been interpreted as a glaciomarine sediment due to the inferred presence of cobbles or boulders (Davies et al., 1984).

Sitting unconformably above the Skerryvore Formation is the Malin Formation up to 75m thick in the Malin sea and composed of two distinct and laterally equivalent units that were termed Malin A and Malin B (Davies et al., 1984). Malin A has a chaotic acoustic signature with discontinuous relfectors, point-source diffraction patterns and a hummocky upper surface. The samples recovered for this formation comprised of stiff gravelly, sandy clay and indicated a glaciomarine origin for this deposit. Malin B, on the other end, is characterised acoustically by parallel sub-horizontal internal reflectors and no diffraction hyperbolae. It occurs in isolated pockets within or adjacent to Malin A and has been interpreted as a fluvioglacial deposit or possibly as a proglacial, lacustrine deposit (Davies et al., 1984). In places, an erosional surface has been detected on top of the Malin Formation which has prompted its interpretation as a representative of a glaciation older than MIS 2.

The Canna Formation is a single unit with an average thickness of about 10m but that reaches 50m in thickness in places. It was deposited disconformably above the Malin

Formation as well as directly on bedrock. Its acoustic signature is either transparent or characterised by short, discontinuous randomly spaced internal reflectors. It has been sampled and comprised of stiff silty, sandy clays with numerous pebbles and cobbles. Davies et al. (1984) suggested the Canna Formation is a rapidly deposited glaciomarine sediment.

The Stanton Formation, up to 160m thick, is characterised by extremely well-stratified reflectors (commonly draped over irregularities in the rockhead) with point-source diffraction hyperbolae. It is a complex formation with a distinct member termed Uist (Fyfe et al., 1993) appearing as an acoustically transparent wedge. Both the formation and the member have been sampled and were found to be stiff laminated clays with lignite debris, shell fragments and dropstones. Micropalaeontological analysis of the recovered deposits indicated a glaciomarine origin. The upper surface of the formation represents an unconformity which is relatively smooth with wide open valleys tens of kilometers in length and oriented north-easterly. Both the morphology and areal extent of this surface preclude a fluvial or marine origin and it is thought to be the expression of glacial erosion during the LGM which would constrain the deposition of the Stanton Formation as pre-LGM (Davies et al., 1984).

This major unconformity is overlain by a thin acoustically chaotic unit (up to 20m) with hyperbolic reflections. This unit was called the Hebrides Formation and though unsampled is thought to correspond to the till left by the glaciation due to its association with the Minch Formation found to the south of the Isle of Skye which was sampled as a coarse grained diamicton up to 10m thick (Davies et al., 1984).

The Barra Formation is an almost transparent unit acoustically deposited above all earlier Quaternary formations as well as bedrock over a maximum thickness of 130m. It has been sampled as silty clays and micropaleontological analysis indicate a complex glaciomarine origin (Davies et al., 1984). It is thought to have been deposited under stadial conditions following the LGM with quickly rising RSL. A correlation between the Barra Formation and shoreline and glaciomarine deposits on Islay have been suggested by Benn and Dawson (1987).

The Jura Formation is a unit with an acoustic signature of well layered internal reflectors filling deep hollows in either rockhead or Quaternary deposits. It tends to be thicker close to the Inner Hebrides where it locally exceeds 300m. The Jura Formation

comprises of firm silty clays with isolated pebbles and shell fragments and micropalaeontological analysis show that both cold and warm faunas are represented suggesting fluctuating conditions, perhaps corresponding to the interstadial and stadial fluctuations from the LGM to the Holocene (figure 1.2 and Fyfe et al., 1993). This formation is of particular importance for this study as its base has been dated to 16,470 BP in borehole 71/09 which suggests a very rapid ice retreat after the LGM (Fyfe et al., 1993) for the North East area of the British Isles. However, it has been proposed that some dead carbon was used in the dated sample and a date of 13,500 BP was suggested by Davies et al. (1984) for the base of the formation based on palaeoclimatic considerations. The older date allows a longer period of deposition through known climatic fluctuations (figure 1.2) and is here thus preferred. This date added to the lithological description suggests a correlation with the glaciomarine sequence of Portballintrae (McCabe et al., 1994) which was identified as unit GM in Cooper et al.(2002) (section 6.1.2). Although its context is not coastal but clearly more marine, the environmental conditions it suggests will be used to understand the general deposition environment for the study area.

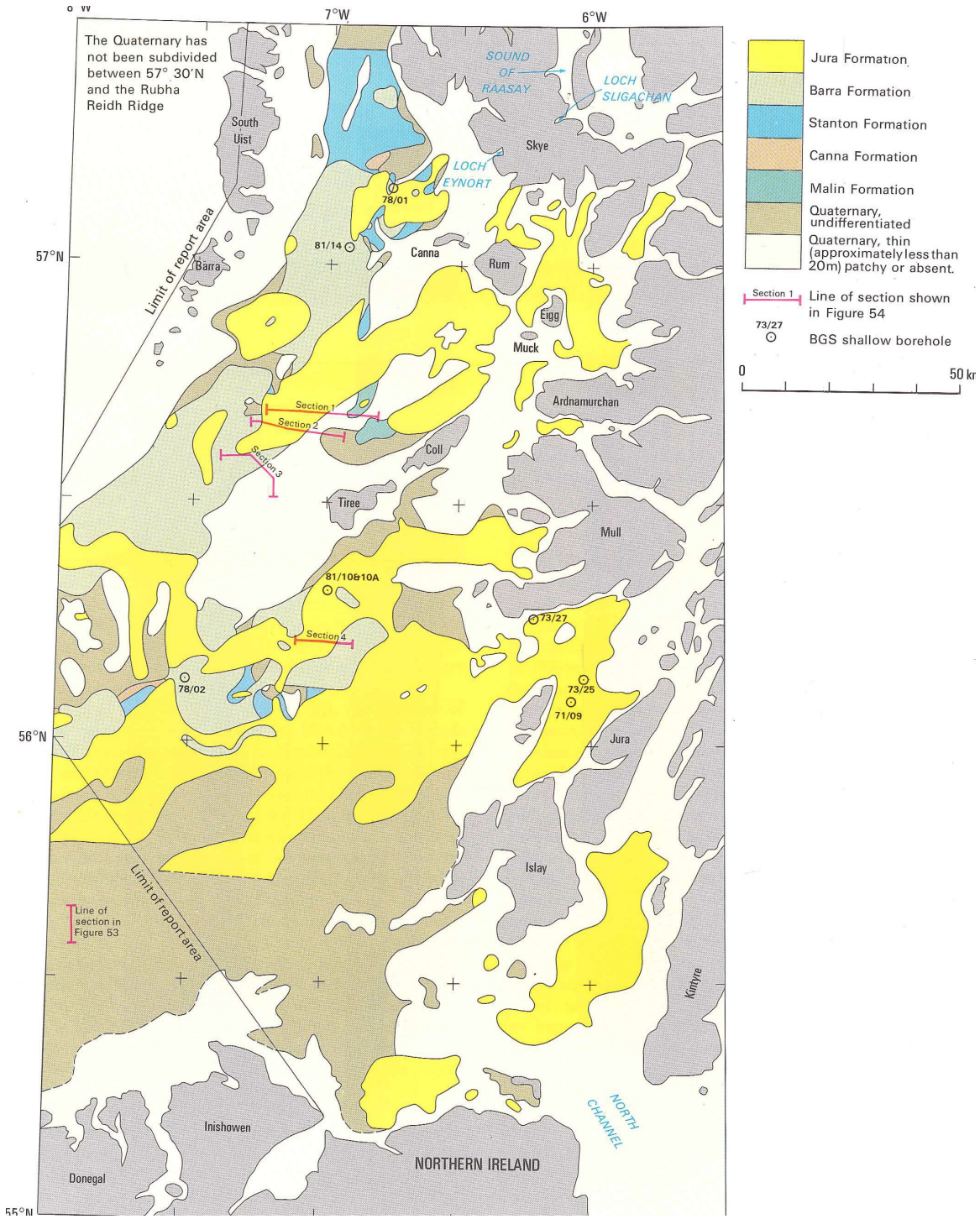

Figure 6.2: Location of Boreholes used for the sampling of seismic units for the Hebrides/Malin sea area (from Fyfe et al., 1993).

Age or dating evidence	Name	Thickness	Acoustic signature	Lithology	Depositional conditions	Upper surface	Comments
Early Holocene	Surface sands	Thin but up to 25m		Muddy sands	Temperate marine		
Base dated to 16470 yrs BP (but suggested at 13500 yrs BP by Davies et al. (1984))	Jura	10 to 30m (up to 300m)	Well layered reflectors	Silty clay with pebbles	Fluctuating conditions of warm and cold		Link with Clyde Beds (Peacock, 1981) and GM of Portballintrae ? (see section 6.1.2) High organic contents inferred from gas
	Barra	Up to 130m	Almost transparent with short, discontinuous reflectors (like Canna)	Silty clay with dropstones	Glaciomarine	conformable	Link with Islay (Benn & Dawson, 1987)
LGM ?	Hebrides/ Minch	20m	Transparent with hyperbolae	Unsampled but till for Minch	subglacial	conformable	Tenuous link between the two formations (different basins)
	Stanton (Uist)	160m (Uist up to 90m)	Very well stratified reflectors with some hyperbolae (transparent)	Laminated silty clay with debris, shell fragments and dropstones	Glaciomarine (severe)	Major unconformity	Late glacial erosion (Davies et al., 1984)
	Canna	10m	Short discontinuous reflectors on transparent	Silty sandy clays with pebbles	glaciomarine	unconformity	
Early glaciation ?	Malin A/B	75m	Discontinuous reflectors with diffractions, hummocky surface/ parallel sub-horizontal	Sandy clay/ unsampled	Glaciomarine/fluvioglacial ?	disconformity	
Deteriorating climate	Skerrivore L<U	45m < 25m	Transparent < faint horizontal beds with diffraction	Silty clays < unsampled (dropstones ?)	Temperate marine < glaciomarine	unconformity	Hebrides mainly but possibly in Malin

Table 6.1: Summarising table for the seismic units of the Hebrides/Malin sea area (Fyfe et al., 1993).

6.1.2 Skerries and Portrush area

Probably the most studied and best known of the coastal region in the JIBS, the "inner sea" formed by the coastline to the south, Portrush Head to the west and the Skerries islands to the north is a particularly sheltered bay in the study area. Besides, the presence of inter tidal peat on the west side of Portrush Head at Mill Strand (or West Strand) has been known for over 100 years (see Wilson et al., 2011 for a review).

Early work by Cooper et al. (2002) provided a first look at the seismic stratigraphy for the area from Portrush to the west to Runkerry Bay to the east and identified a potential "peat" reflector extending in places to 24m depth. It was observed in the first seismic unit interpreted as modern sand deposit (S). This sand unit is less than 5m thick, dips seaward and abruptly thins and terminates at around 30m depth. It overlies a unit interpreted as glaciomarine mud unit (GM) of 3 to 5m thickness. The final observable complete unit has been interpreted as a glacial till (T) and extends under the glaciomarine muds and over the bedrock and is characterised by a dense acoustic reflection with poor penetration of the signal. The seismic survey also identified a palaeochannel cut into the unit GM or T (figure 6.3) which can be traced over 1km alongshore. At its largest extent, this channel is 80m wide and 1m deep with its base at 15m depth. Furthermore, the internal high-amplitude reflector detected inside the channel was interpreted as peat indicating a subaerial origin for the channel. The interpretation of these seismic units were based on a comparison with the Portballintrae emergent sequence (McCabe et al., 1994) and intertidal peat at Portrush (Wilson et al., 2011). In the Portballintrae emergent sequence, three units were described; first overlaying the bedrock, a glacial diamict which base was radiocarbon dated using foraminifera to 17000 years BP, then a layer of rhythmically bedded sands and muds interpreted as a shallow marine deposit and finally a layer of gravel and sand truncating the underlying unit and identified as regressive in nature.

This study was followed by a coring survey described in Kelley et al. (2006) which aimed to hit the internal reflector of the upper sandy unit and describe it. This was achieved for core SK9 and the internal reflector postulated earlier on as peat was found to be a gravel bed. The logs of the recovered cores are presented in figure 6.4 and their location in figure 6.5.

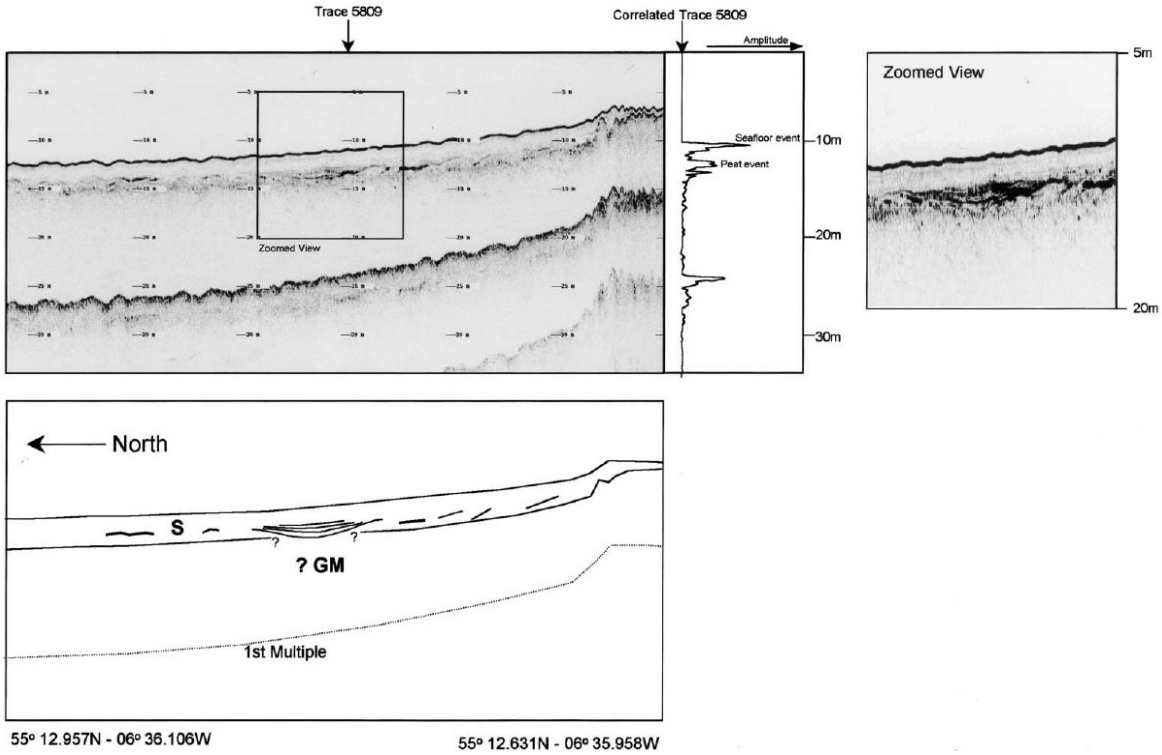

Figure 6.3: Palaeochannel identified on one of the seismic line in the Skerries area with authors' interpretation (from Cooper et al., 2002).

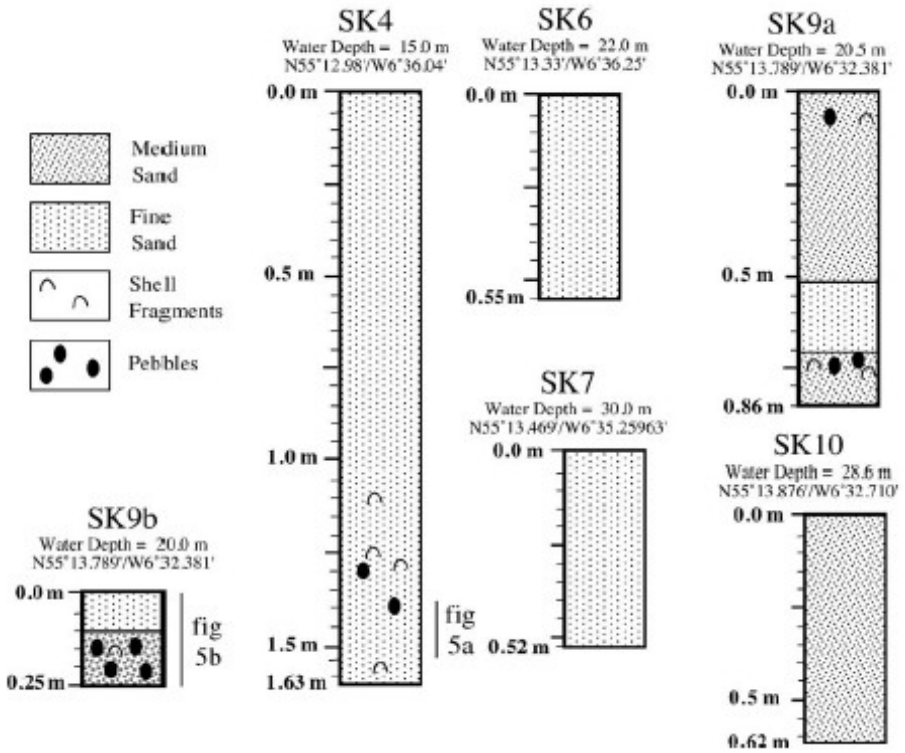

Figure 6.4: Logs of cores retrieved from the Kelley et al. (2006) survey.

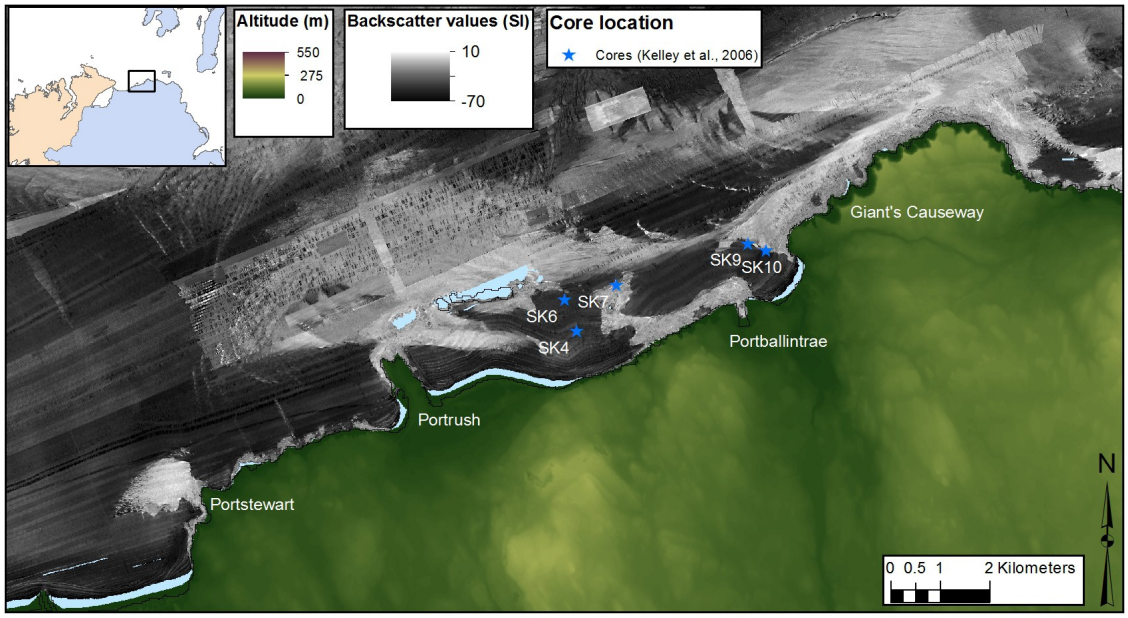

Figure 6.5: Location of cores retrieved from the Kelley et al. (2006) survey.

The reports on the archaeological applications of the JIBS Phase 2 and 3 (Quinn et al., 2009 and 2010) produced by the Centre for Maritime Archaeology at the University of Ulster described 7 seismic units (figures 6.7 and 6.6, table 6.2) based on their study of the seismic lines in the region, the previous works of Cooper et al. (2002) and the same sedimentary sequence from onshore Portballintrae described in McCabe et al. (1994).

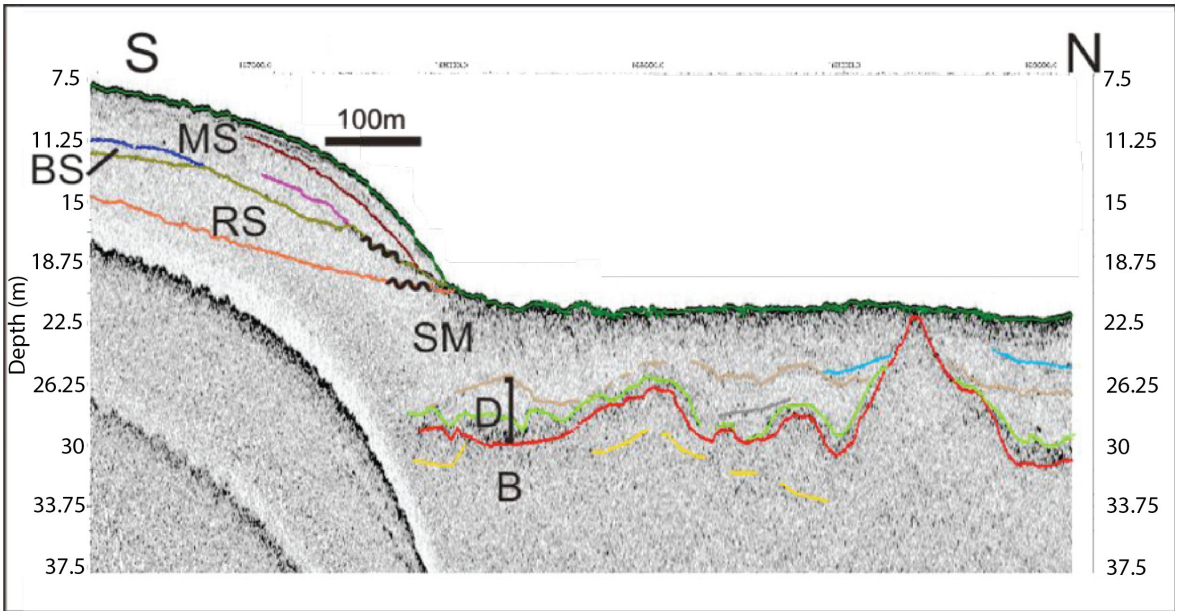

Figure 6.6: Seismic data and highlighted reflectors and seismic units recognised (after Quinn et al., 2009).

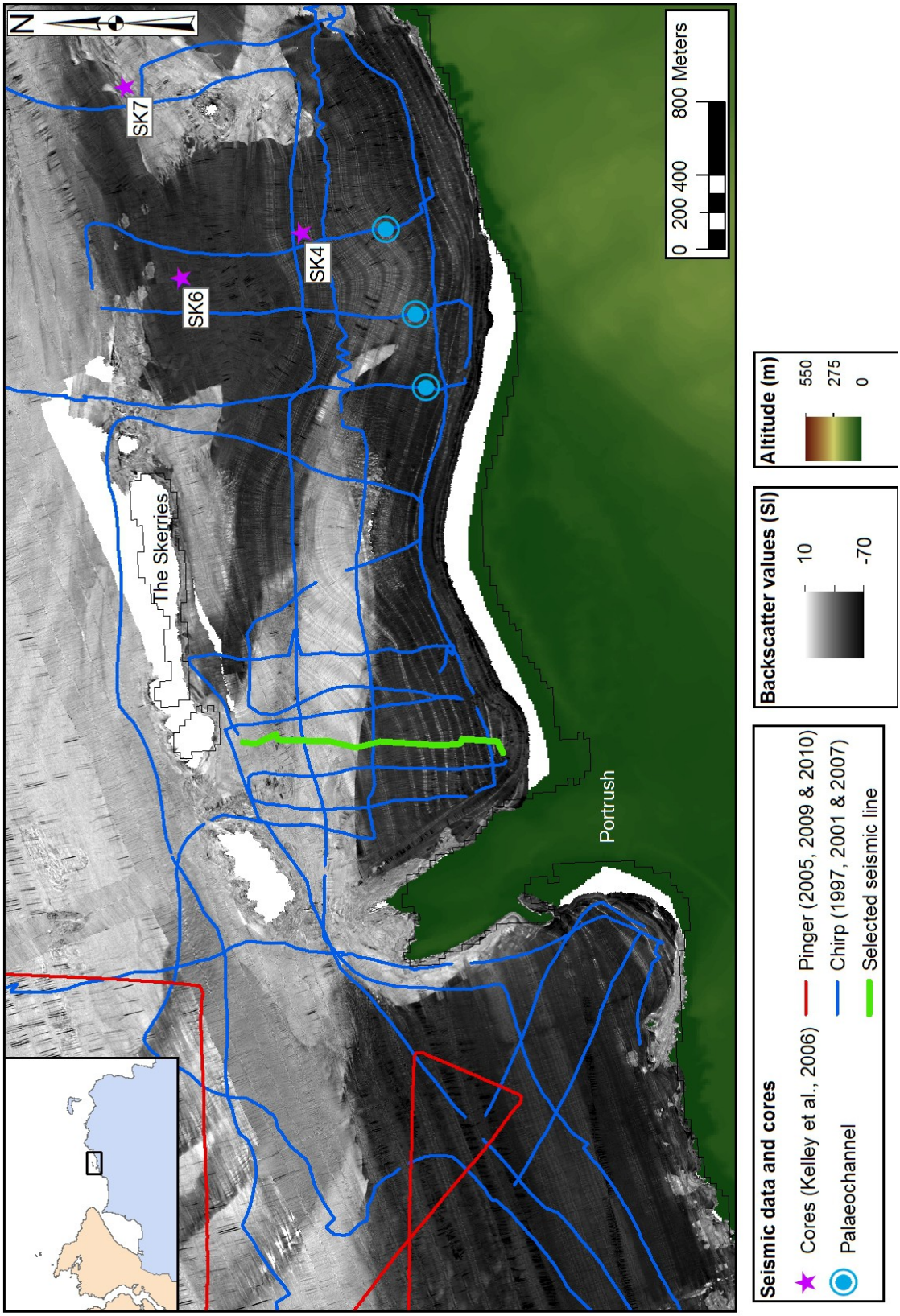

Figure 6.7: Location the seismic line used for the presentation diagram (figure 6.6) with location of the identified palaeochannel in the Skerries area.

Unit	Thickness	Acoustic signature	Interpretation	Lithology	Age
MS	Less than 5m	Moderate amplitude, parallel reflectors downlapping onto RS. Two higher amplitude reflectors within.	Marine sand	Fine to medium sands with occasional pebbles and shell fragments (Kelley et al., 2006)	
BS		Thin unit with wavy parallel reflectors draping over RS.	Beach Sand	unsampled	
T		Strong continuous upper boundary truncating RS.	Terrestrial deposit (with possible channel cuts)	Unsampled but associated with inter-tidal peat from the west strand of Portrush (Wilson et al., 2011)	Between 7960-8,340 and 6,563-6,737 cal. yrs BP (Wilson et al., 2011)
RS	3-4m	Relatively weak, sub-parallel, continuous reflectors.	Regressive sand (coarse sand)	Interbedded sands and sandy gravels (0.1-0.2m). Sands are massive to weakly laminated with isolated pebbles and cobbles set in coarse sands to granules. Gravels are massive and very poorly sorted. Clasts are mainly chalk. Deposition thought to result from wave erosion during a fall in RSL (McCabe et al., 1994)	
SM	2m (on land) 3 to 5m	Low amplitude, mainly sub-parallel reflectors at base. Where unit outcrops at seabed: chaotic, strong point reflectors. Where unit is buried: relatively strong continuous upper reflector.	Shallow marine coarsening upwards sequence (mud-silt-sand-coase sand/gravel)	Rythmically bedded sands and muds divided in 4 lithofacies each 0.1-0.3m in thickness going from sandy muds, muddy sands, ripple sands and laminated muds. Contains wave diagnostic features. The cyclical deposition is thought to be due to storm events (McCabe et al., 1994)	
D	2m (min.)	Two units. Lower Unit: strong chaotic reflectors draping over B; some point reflectors. Upper Unit: drapes unconformably over lower unit; some point reflectors. Relatively strong, continuous upper reflector.	Diamict (lodgement till overlain by waterlain till)	Stacked beds (0.3m-0.5m) of muddy diamict with dispersed pebbles, cobbles and occasional boulders (85 to 95% basalt, 1% chalk and flint). Thought to originate near ice margins (McCabe et al., 1994).	17,000 yrs BP based on microfaunal assemblage for the base of the unit (McCabe et al., 1994)
B		Relatively high amplitude, discontinuous reflector. Little penetration beneath.	Bedrock	Basalt with s-forms striated from south to north on the shore at Portballintrae (McCabe et al., 1994).	

Table 6.2: Seismic units description and interpretation for the Skerries and Portrush area (Quinn et al., 2009). Unit S from Cooper et al. (2002) correspond to MS, GM to SM and T to D.

In addition to the previously recognised units (Cooper et al., 2002), a unit visible only as a strong reflector below Modern Sand and above Regressive Sand or GlacioMarine (Shallow Marine) was interpreted as a terrestrial surface based on its association with the palaeochannels identified in the area (figure 6.3). Furthermore, a unit interpreted as Beach Sand (BS) was identified between the units RS and MS but only toward the shore. This interpretation is based only on its acoustic signature indicating a lithology similar to unit MS, i.e. sand, and its location over the interpreted terrestrial surface and toward the coastline. The lowest depth of unit BS appears as a ravinement surface and is found at 12m. This unit's restricted observation and lack of sampling puts this interpretation in question and this unit could be the results of more modern marine depositional conditions.

The two main stratigraphical levels of interest for RSL change were then identified by the unconformity they present as the upper limit of the unit SM and the lower limit of the unit MS (Quinn et al., 2009; 2010). Indeed these two erosional surfaces have been interpreted as being the results of wave action hence marking a regressive contact (top of SM) followed by transgressive contact (top of RS). These two reflectors were digitised, interpolated and mapped by the author for this study (figures 6.8 and 6.9).

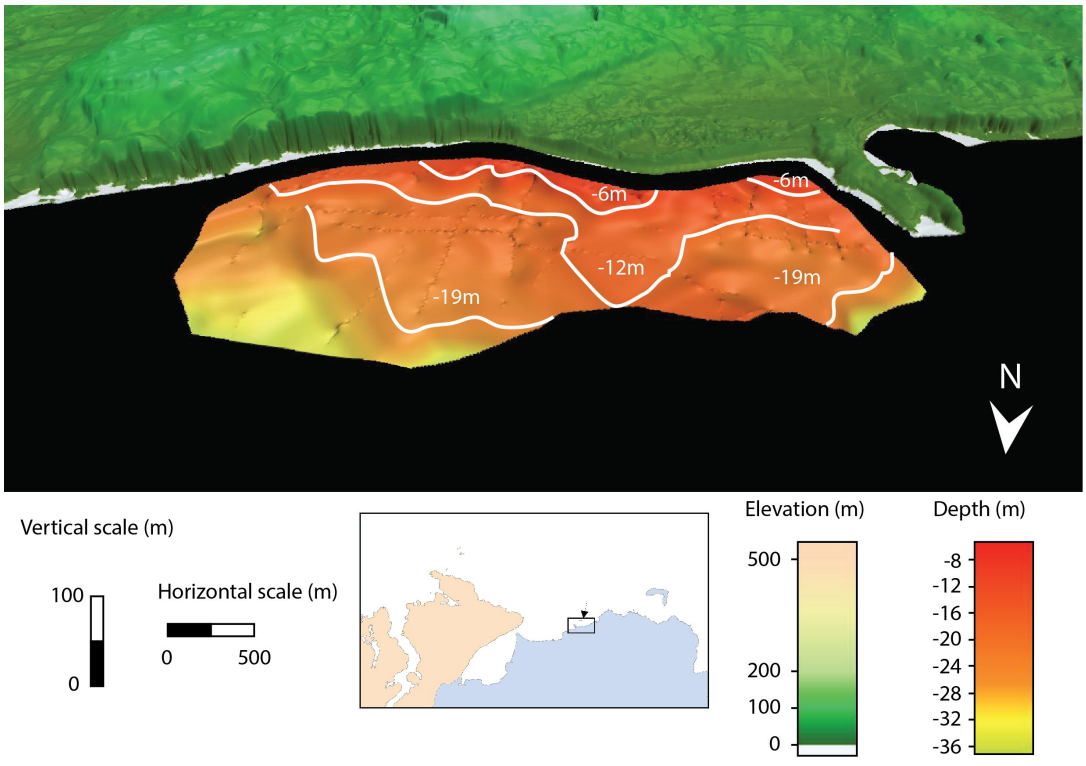

Figure 6.8: Oblique view of the interpolated surface of the top reflector of unit RS.

The top reflector of unit RS shows a general seaward slope with a series of plateau at about 6m, 12m and 19m depth.

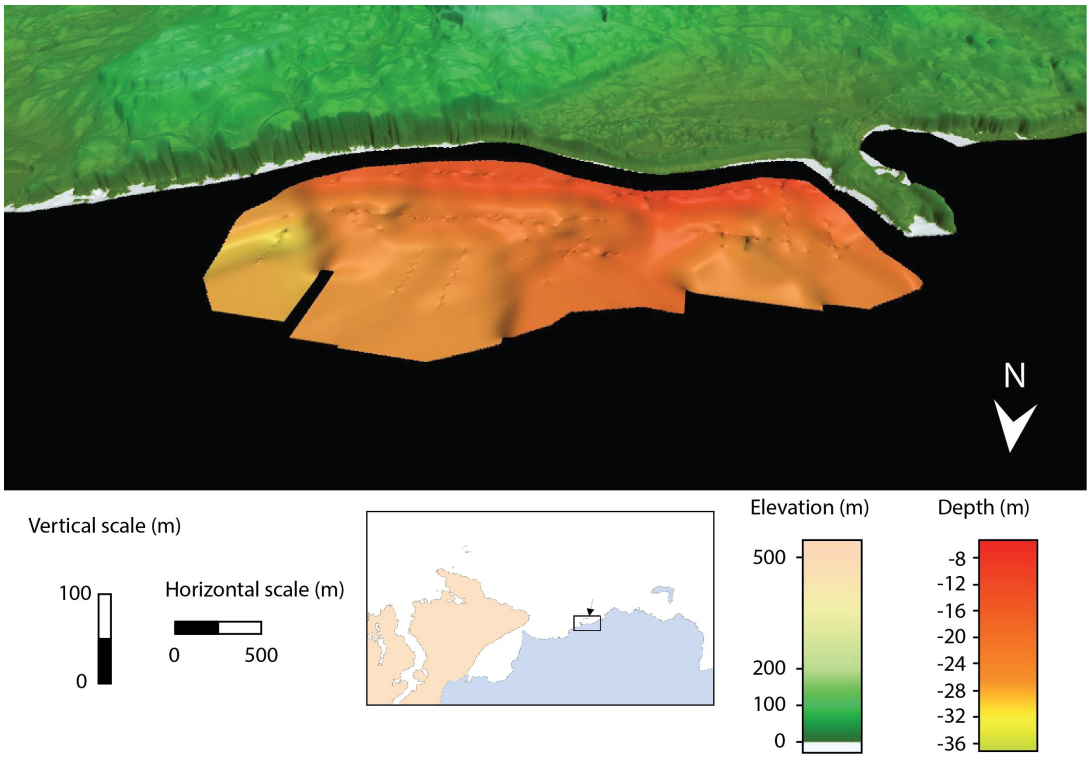

Figure 6.9: Oblique view of the interpolated surface of the top reflector of unit SM.

The top reflector of unit SM shows a similar morphology lying 3-4m below the top reflector of unit RS but disappears in the western central bathymetric trough of the Skerries inner sea.

Recent work has developed a strategy for the identification of the sea-bed substratum from bathymetric and backscatter data (Plets et al., 2012). Bathymetric data were used to generate terrain-indices (slope, rugosity, etc...) which were combined with a visual classification of the substratum using the backscatter data to classify the sea-bed into acoustic classes. The results imply that modern conditions show rapid movements of sediments over the inner shelf with some accumulation of reworked sands in protected bays and an absence of deposition on some exposed bedrock reefs of the coast.

6.1.3 Runkerry Bay

Just to the east of the Skerries "inner sea" is the area of Runkerry Bay where the aforementioned studies on the seismic datasets and sedimentary stratigraphy were undertaken (Cooper et al., 2002; Kelley et al., 2006). Although these two areas have been

previously presented as a whole, they have been separated here as their modern depositional environments are different; with Runkerry Bay being an open bay to the north west whereas the Skerries islands create much more sheltered conditions of deposition.

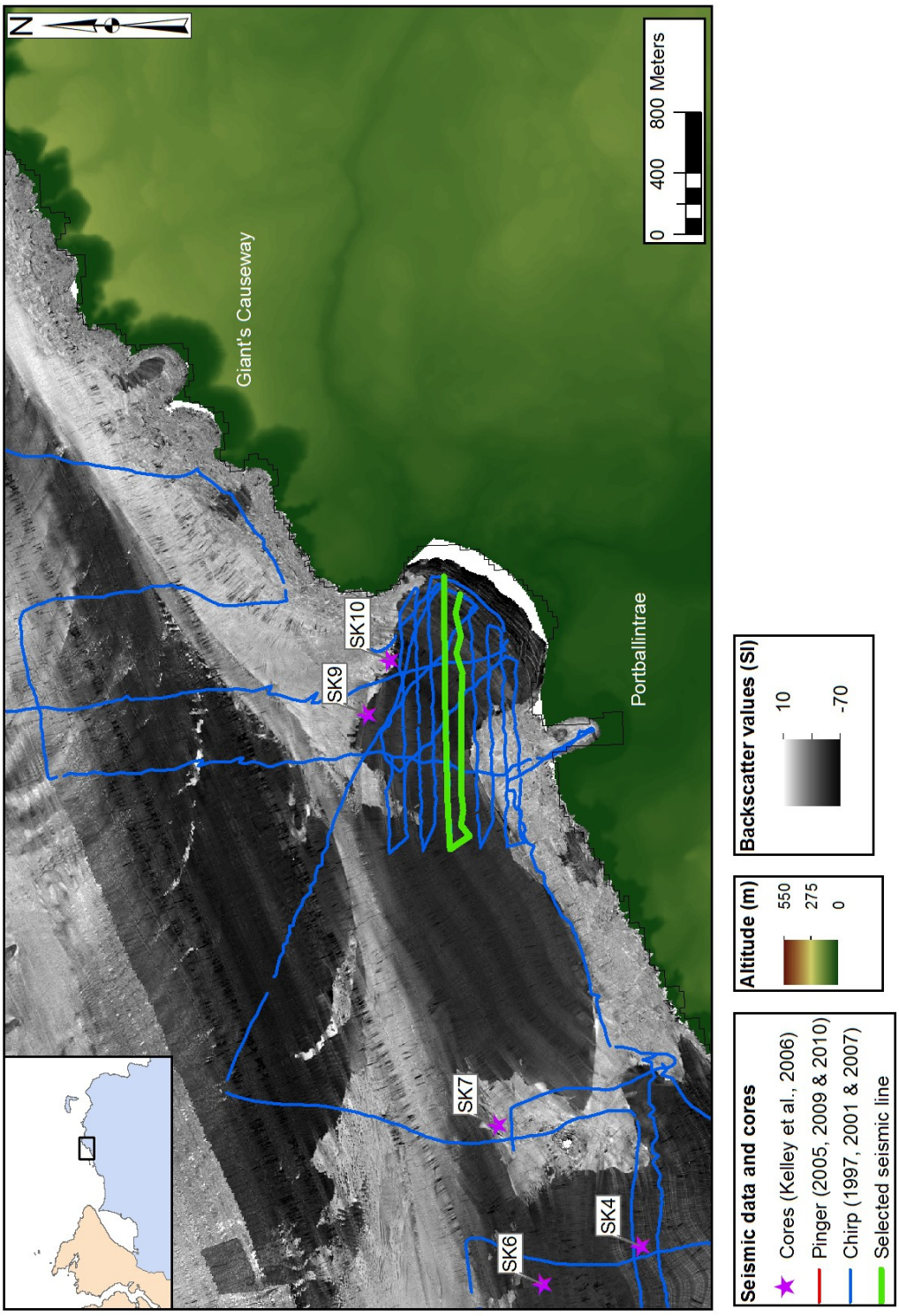

Figure 6.10: Location of the seismic line used for the presentation diagram (figure 6.11) in Runkerry Bay.

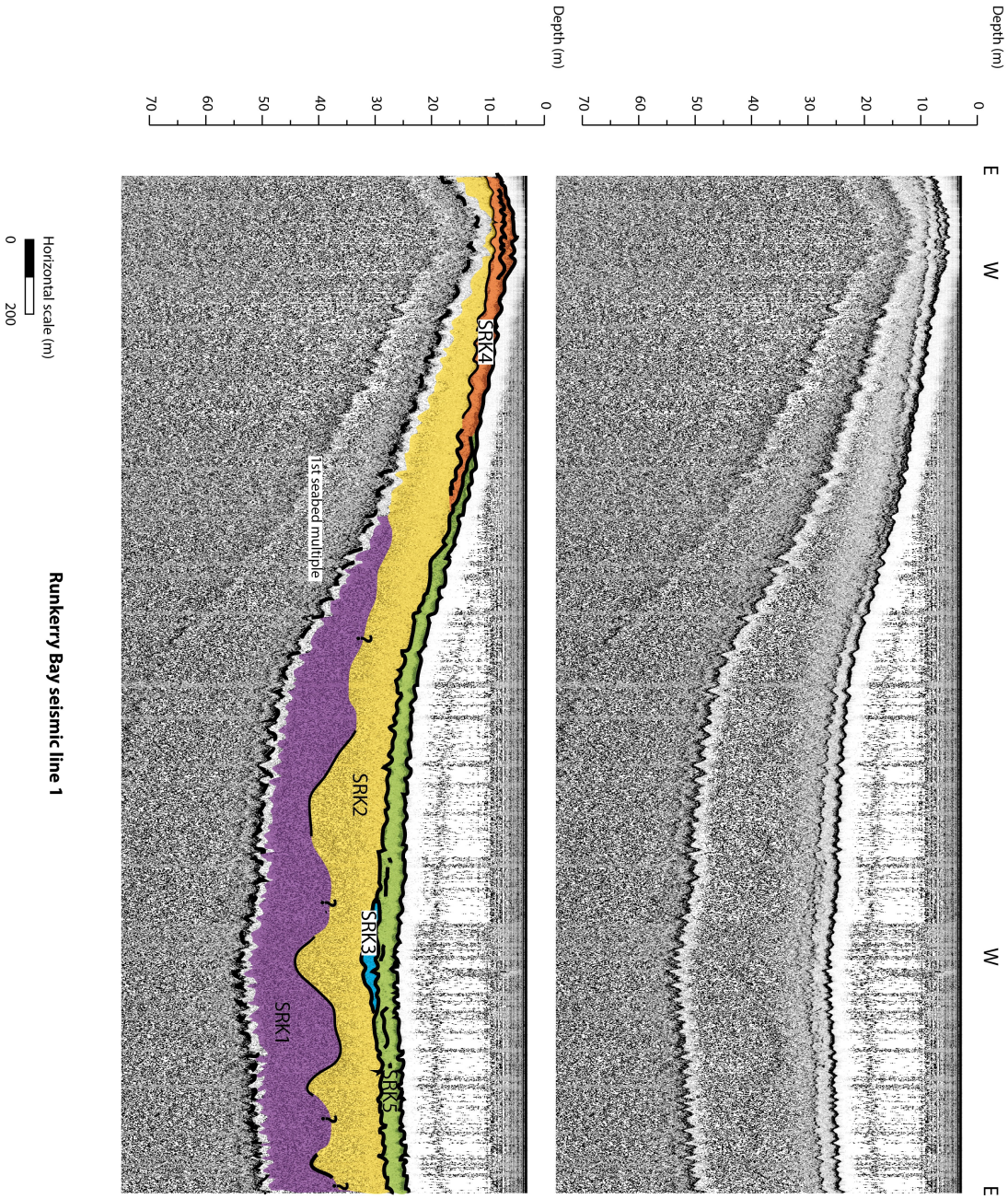

Figure 6.11: Seismic data line located in figure 6.10 with highlighted seismic units for Runkerry Bay described in table 6.3.

Unit	Top Reflector	Acoustic signature	Thickness
SRK5	Continuous strong	Characterised by a strong continuous bottom reflector and acoustically tranparent throughout. This units drapes over the underlying units as a slope front fill and contains some strong discontinuous reflectors that were interpreted as peat in Cooper et al. (2002) but when hit through coring were correlated with gravel beds (Kelley et al., 2006).	Up to 4m
SRK4	Continuous strong	Unit SRK4 appears in the higher ground and sits unconformably over unit SRK2. The unit is mainly transparent with weak parallel reflectors and some point reflectors concentrating upwards. This unit is truncated by SRK5.	Up to 2m
SRK3	Discontinuous medium to weak	This unit only appears at deeper depth and has a somewhat transparent signature showing less contrast with SRK2 than with SRK5.	Up to 3m
SRK2	Continuous medium to weak.	Strong top reflector appearing mostly parallel to the sea-floor draping unit SRK1. This unit is chaotic at depth and more transparent towards the seabed.	6 to 12m
SRK1	Continuous, broad and weak to medium	Weak top reflector showing a discontinuous surface of high rugosity and outcropping in places.	Unknown

Table 6.3: Description of seismic units highlighted in figure 6.11 for Runkerry Bay.

The acoustic basement forms here the upper reflector of Unit SRK1. This reflector is continuous, broad and weak to medium in intensity. The seismic unit's acoustic signature is chaotic. SRK1's top reflector slopes down seaward with a distinct break of slope at around 18m depth until a sub-horizontal plateau at an average depth of 40m (figure 6.12). It outcrops in the shallower waters and in the form of peaks toward the middle of the bay. A change in backscatter values from the lower value of -70 (SI) for the modern sediment to -10 (SI) is visible at these outcropping locations which is indicative of either a gravel bed or rock outcrop.

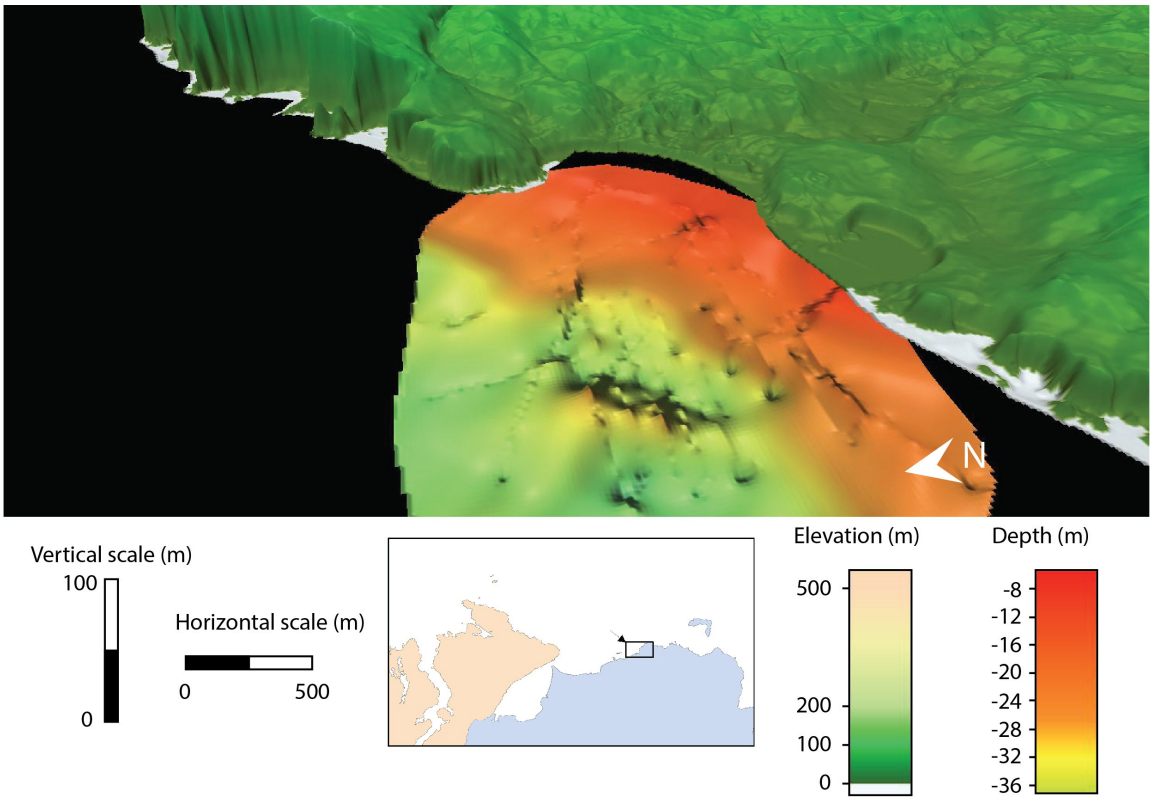

Figure 6.12: Oblique view of the interpolated surface of the top reflector of unit SRK1.

Unit SRK2 is also chaotic in acoustic signature and virtually indistinct to unit SRK1 at depth. This signature becomes more transparent towards the seabed with a continuous top reflector of medium to weak intensity. Unit SRK2 drapes unit SRK1 and has a thickness of less than 2m in the shallower waters where it is truncated by unit SRK4 but is thicker in the deeper plateau with an average of 10m (figure 6.13).

Unit SRK3 only appears in the deeper part of the bay and the extent of the survey limits our understanding of it. Its acoustic signature is somewhat transparent and makes it virtually indistinct to unit SRK2. Its top reflector is discontinuous and medium to weak in intensity. Unit SRK3's top reflector appears at about 15m depth and is likely to extend deeper down. This unit's maximum observed thickness is 3m.

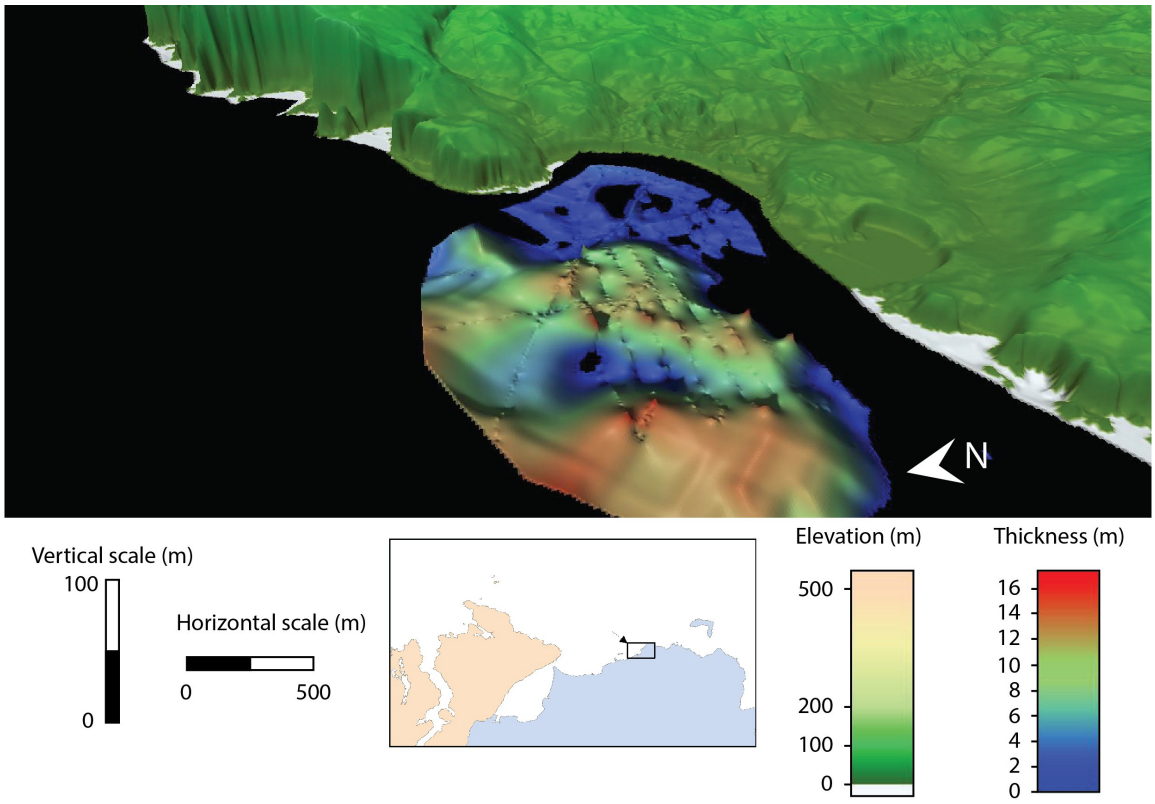

Figure 6.13: Oblique view of the interpolated thickness of unit SRK2.

Unit SRK4 displays a transparent acoustic signature with some weak parallel reflectors and some point reflectors towards its top. This unit is bound by a continuous and strong top reflector which appears in shallower zone and slopes down seaward from the centre of the bay. SRK4 sits unconformably over SRK2 and is itself truncated by unit SRK5 at depths from 9 to 20m. Its thickness is roughly constant at about 2m.

Unit SRK5 is acoustically tranparent throughout. This units drapes over the underlying units as a slope front fill and contains some strong discontinuous reflectors that were interpreted as peat in Cooper et al. (2002) but when hit through coring were correlated with gravel beds (Kelley et al., 2006) (see section above). This unit's top reflector at the seabed is continuous and strong. It is sloping seaward until a plateau at about 24m (figure 6.14). It presents a slight depression from the west of the bay towards the north of the bay that corresponds to one visible on the seabed. Unit SRK5 has a thickness roughly consistent at about 4m (figure 6.15).

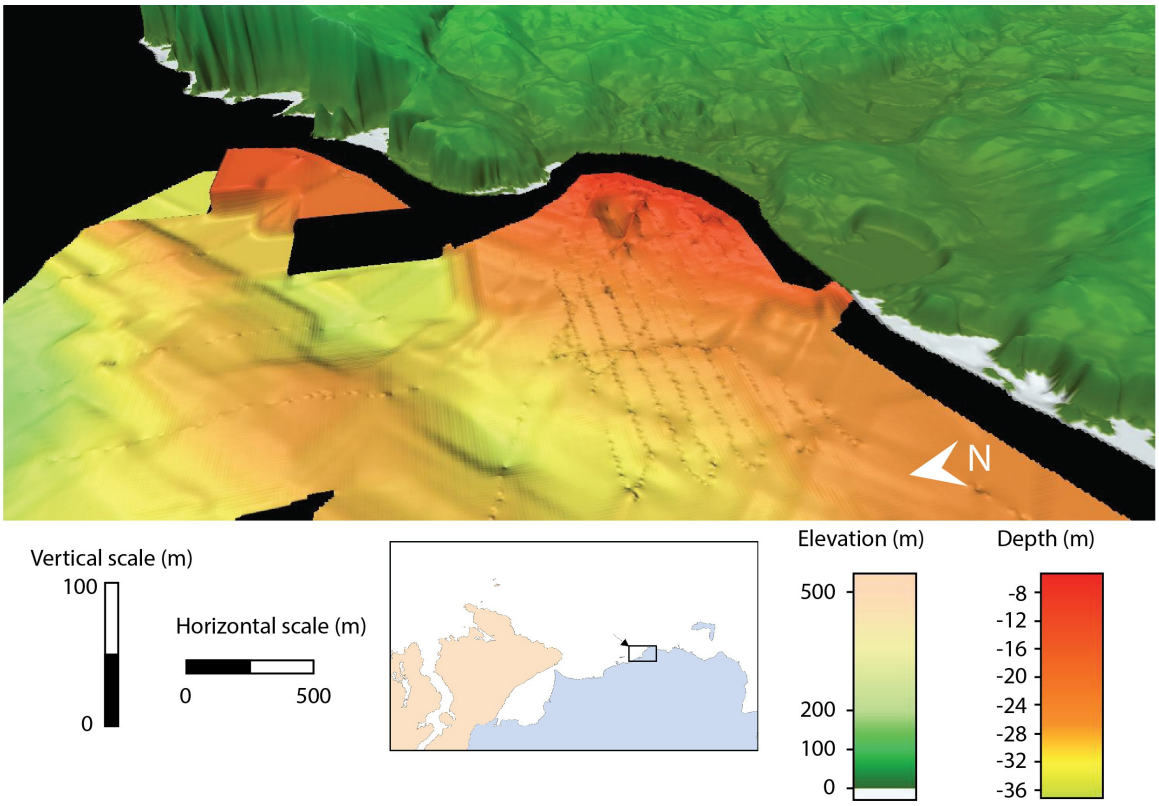

Figure 6.14: Oblique view of the interpolated surface of the bottom reflector of unit SRK5.

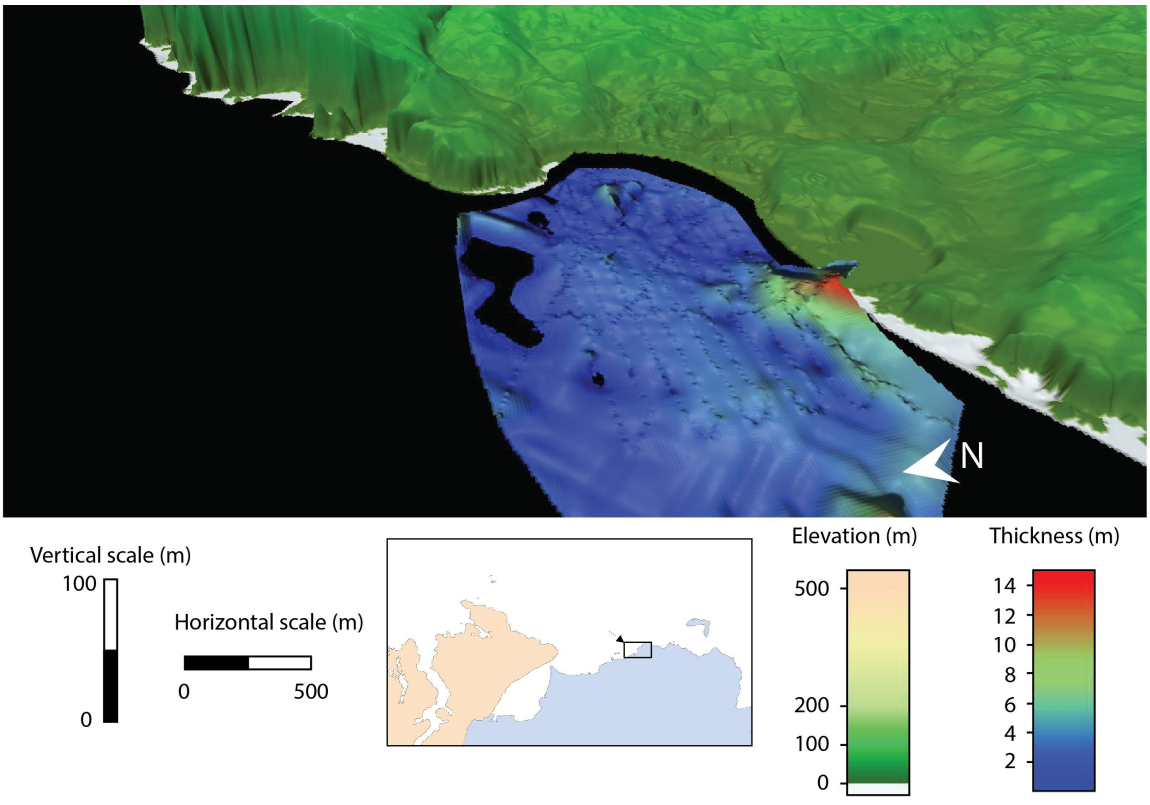

Figure 6.15: Oblique view of the interpolated thickness of unit SRK5.

6.1.4 The Bann estuary area

Quinn et al. (2009; 2010) presented a brief interpretation of the seismic data from the Bann estuary, west of Portstewart and east of the mouth of Lough Foyle. They identified the main reflector, consistent and laterally continuous, as a subaerial surface cut during the last regression and lowstand where a palaeochannel is clearly visible (figure 6.17). This sub-horizontal subsurface appears from about 7m depth and outcrops at about 30m depth almost 7km offshore. The upper limit of the channel infill is at 12m on average and its base is at 18m below msl. The upper unit of sand and gravel is about 5m thick. The authors have postulated that this represented the former bed of the river Bann before the formation of the dune system at Portstewart, circa 4000 BP.

Strangely, this inferred channel is visible in only one of the local seismic lines which presents a problem with the interpretation. There are several seismic lines around this first location (figure 6.16) and yet there is no other evidence of it, in particular to the south of it toward the modern course of the river Bann. The most likely reason is a seismic penetration problem due to the shallower waters and thicker sands inshore where the next seismic line south of the original location was measured creating multiples of the seabed before another boundary is hit by the signal. Indeed the depth of seabed is only 3 to 4m along the coastline and the main reflector mentioned above disappears for the zone directly south of the palaeochannel location. Similarly, no further evidence of the channel is visible north of the first location. The most likely explanation here is the fact that the channel would have reached the former shoreline close to that location as the main reflector (ravinement surface) slopes down seaward. However no deltas were identified that could help constrain the depth of this channel further. Erosion linked with a rise of RSL might also be responsible for the uniqueness and isolation of the section preserved for such a channel.

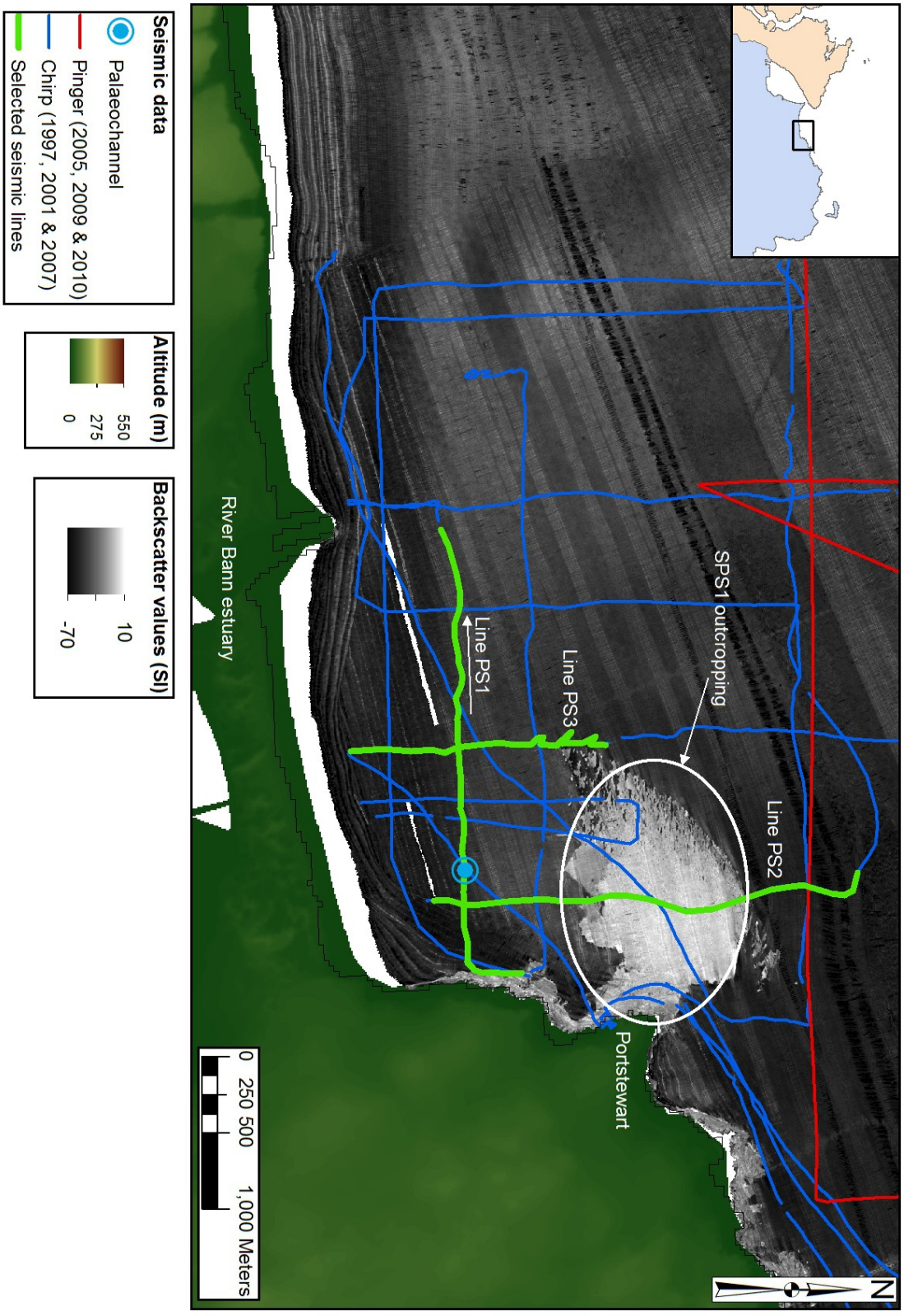

Figure 6.16: Location of the seismic line used for the presentation diagrams (figures 6.17 to 6.19) with location of the identified palaeochannel in the Bann estuary area.

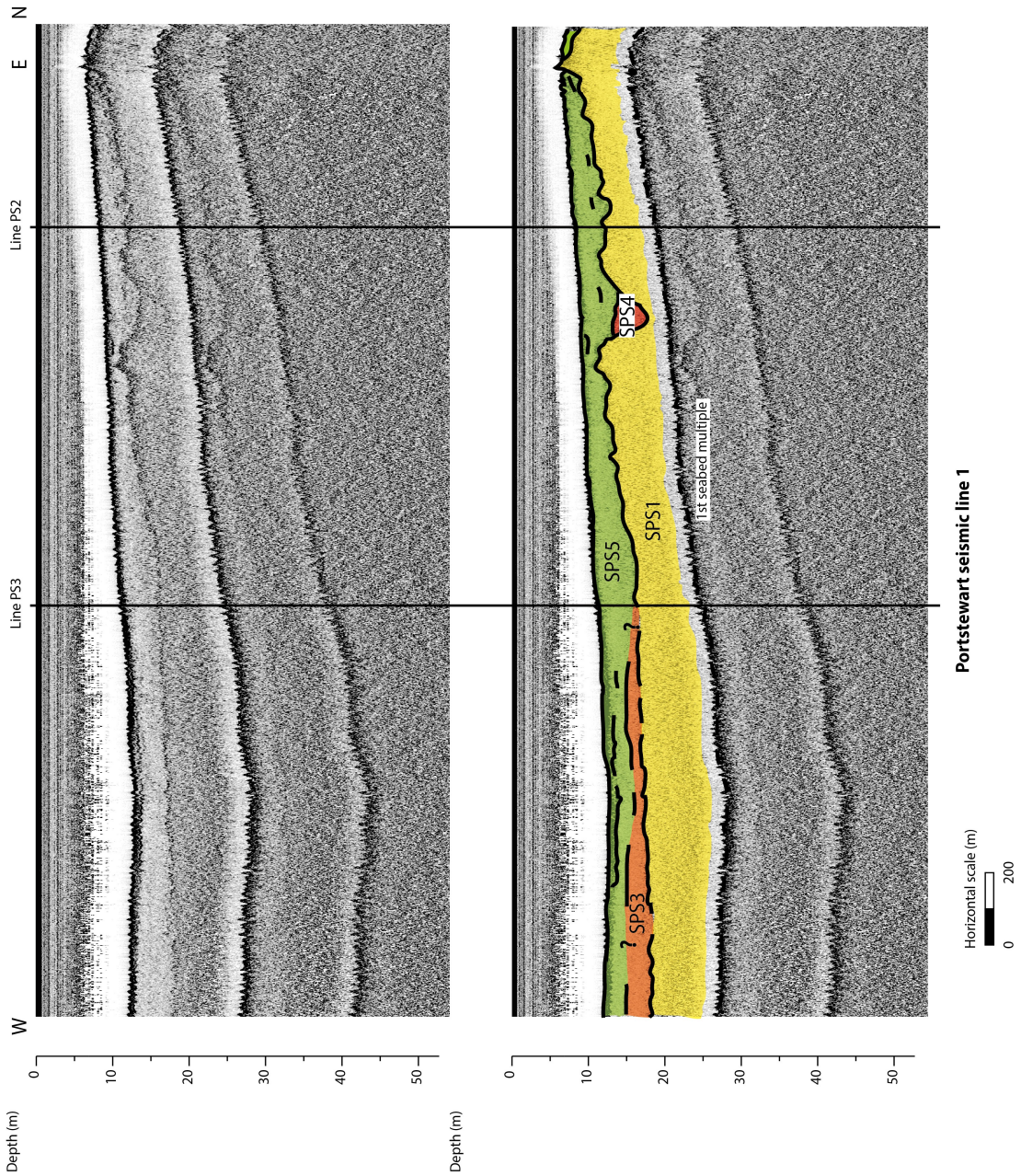

Figure 6.17: Seismic data and highlighted seismic units (described in table 6.4) for line PS1 (located on figure 6.16) in the Bann estuary area. The intersections with lines PS2 and PS3 are displayed.

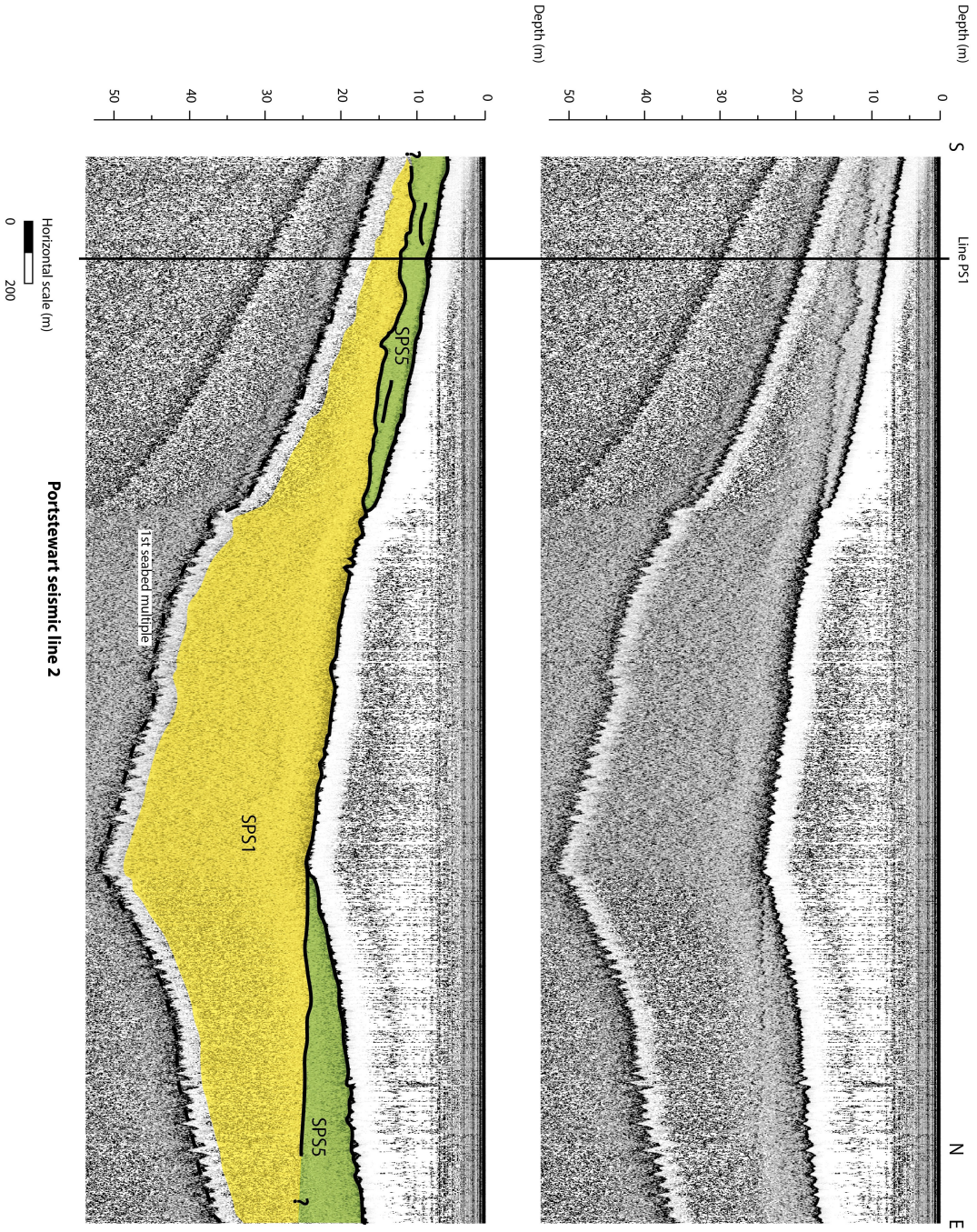

Figure 6.18: Seismic data and highlighted seismic units (described in table 6.4) for line PS2 (located on figure 6.16) in the Bann estuary area. The intersection with line PS1 is displayed.

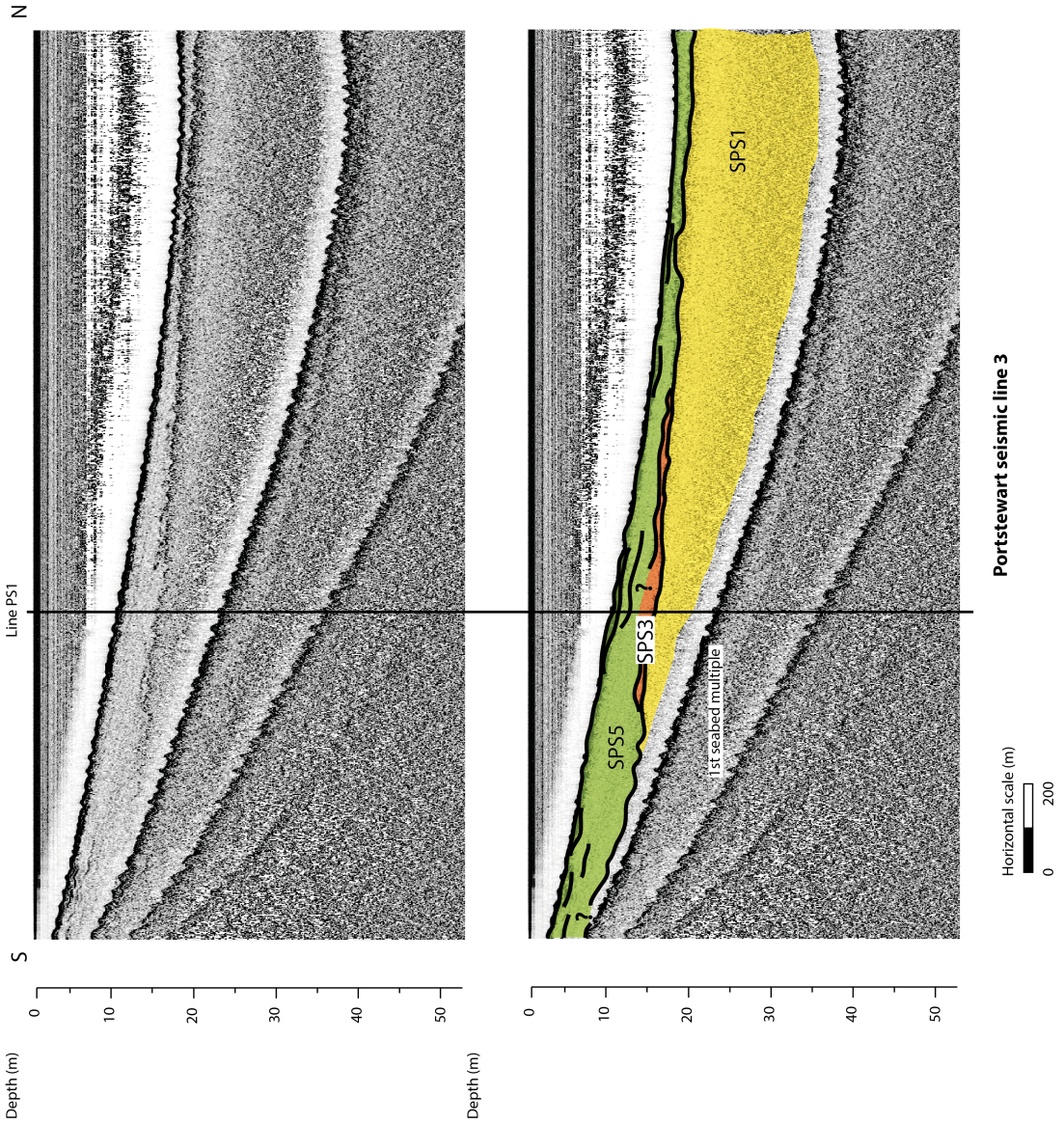

Figure 6.19: Seismic data and highlighted seismic units (described in table 6.4) for line PS3 (located on figure 6.16) in the Bann estuary area. The intersection with line PS1 is displayed.

Unit	Top reflector	Acoustic signature	Thickness
SPS5	Continuous strong	This units drapes over its underlying units and contains some strong sub-parallel discontinuous reflectors similar to those seen in runkerry bay. It appears to be coarsening upward.	Up to 3m
SPS4	Discontinuous chaotic strong	Medium to strong parallel reflectors with a chaotic appearance. This unit sits inside a definite palaeochannel from unit SPS1.	5m
SPS3	Discontinuous weak	Unit SPS3 appears in the lower ground and sits unconformably over unit SPS1. The unit is acoustically transparent.	Up to 3m
SPS2	Discontinuous medium to strong	Appearing only in some places, this unit forms a mound of material over SPS1. It is transparent throughout.	Up to 1.5m
SPS1	Discontinuous medium to strong	Strong top reflector appearing mostly parallel to the sea-floor but with a distinct unconformity with its overlying units and a hummocky surface. The top of this unit contains some point reflectors particularly in the higher ground and the unit is mainly chaotic throughout.	unknown

Table 6.4: Description of seismic units highlighted in figures 6.17 to 6.19 for the Bann estuary area.

The top of unit SPS1, the acoustic basement for this area, is the most obvious reflector observed here and mentioned previously in Quinn et al. (2010). It is discontinuous, medium to strong in intensity and appears to be mostly parallel to the sea-floor. The unit itself is chaotic and some distinct point reflectors appear toward its top, particularly in the shallower waters. The bathymetry of its top reflector shows a clear seaward slope with a plateau at about 22.5m (figure 6.20). Its top surface is clearly an erosion surface and a palaeochannel cut on its upper surface appears in one seismic line. This unit outcrops to the north east of the area where a lower backscatter signal has been observed (figure 6.16).

Unit SPS2 is only detected in places as a small mound of material up to 1.5m in thickness at a depths of 19m. Its acoustic signature is transparent and its top reflector is discontinuous and medium to strong in intensity.

Unit SPS3 appears mainly at lower depths and presents a roughly constant thickness of 1m except in the main depressions of unit SPS5 where its thickness averages 3m. It has a transparent acoustic signature with a discontinuous and weak top reflector. SPS3 drapes over unit SPS1 and SPS2 and has been truncated at shallower depth by unit

SPS5 at a depth of 15 to 18m.

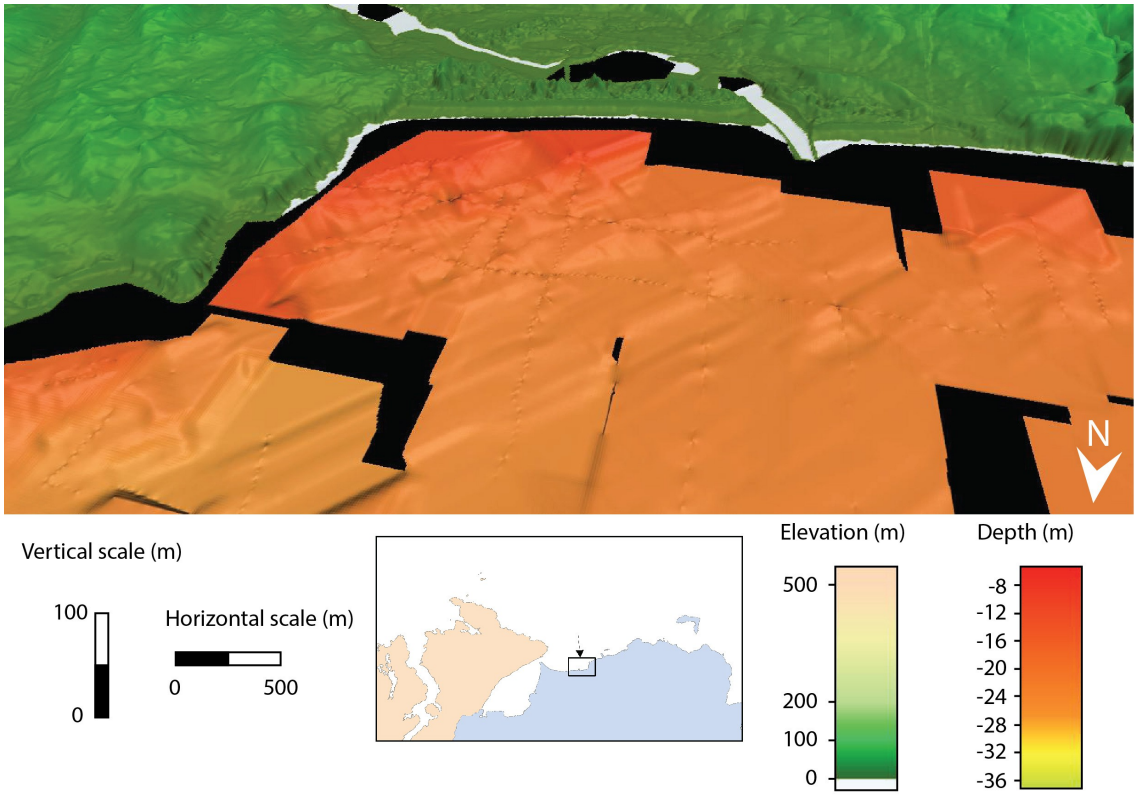

Figure 6.20: Oblique view of the interpolated surface of the top reflector of unit SPS1.

Unit SPS4 only appears in the only one seismic line clearly showing a palaeochannel and is laid over unit SPS1. It has a chaotic signature with medium to strong parallel internal reflectors. Its top reflector is discontinuous and somewhat chaotic but strong in intensity. The channel where this unit is found is 170m wide with a maximum depth of 7m. The base of this channel is at 18m which gives a thickness of 4.5m to the unit.

Unit SPS5 drapes over its underlying units and contains some strong sub-parallel discontinuous reflectors similar to those seen in Runkerry Bay (section above). Its acoustic signature is transparent but with point reflectors appearing toward its top. Unit SPS5's top reflector at the seabed slopes down seaward to a depth of about 15m and appears sub-horizontal thereafter (figure 6.21). Its average thickness is 2.5m in the nearshore but the unit gets thicker towards the aforementioned depression with an average of 4.5m and a maximum of 7.5m (figure 6.22).

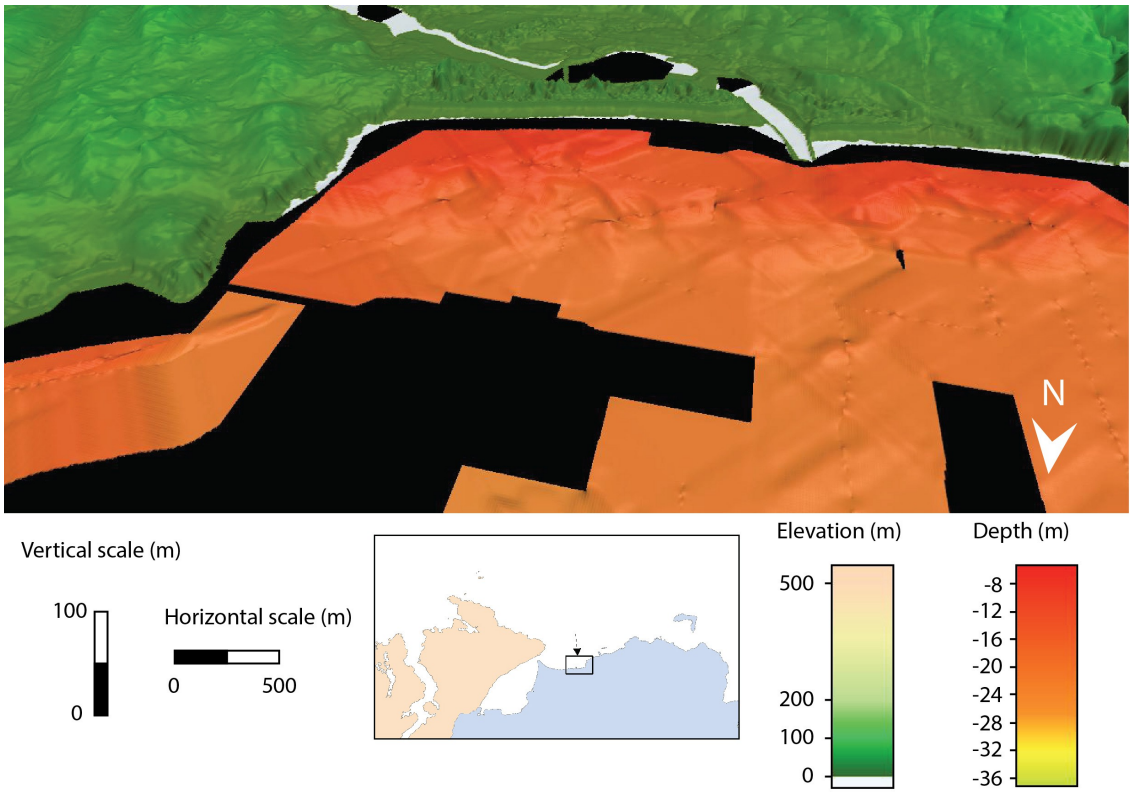

Figure 6.21: Oblique view of the interpolated surface of the bottom reflector of unit SPS5.

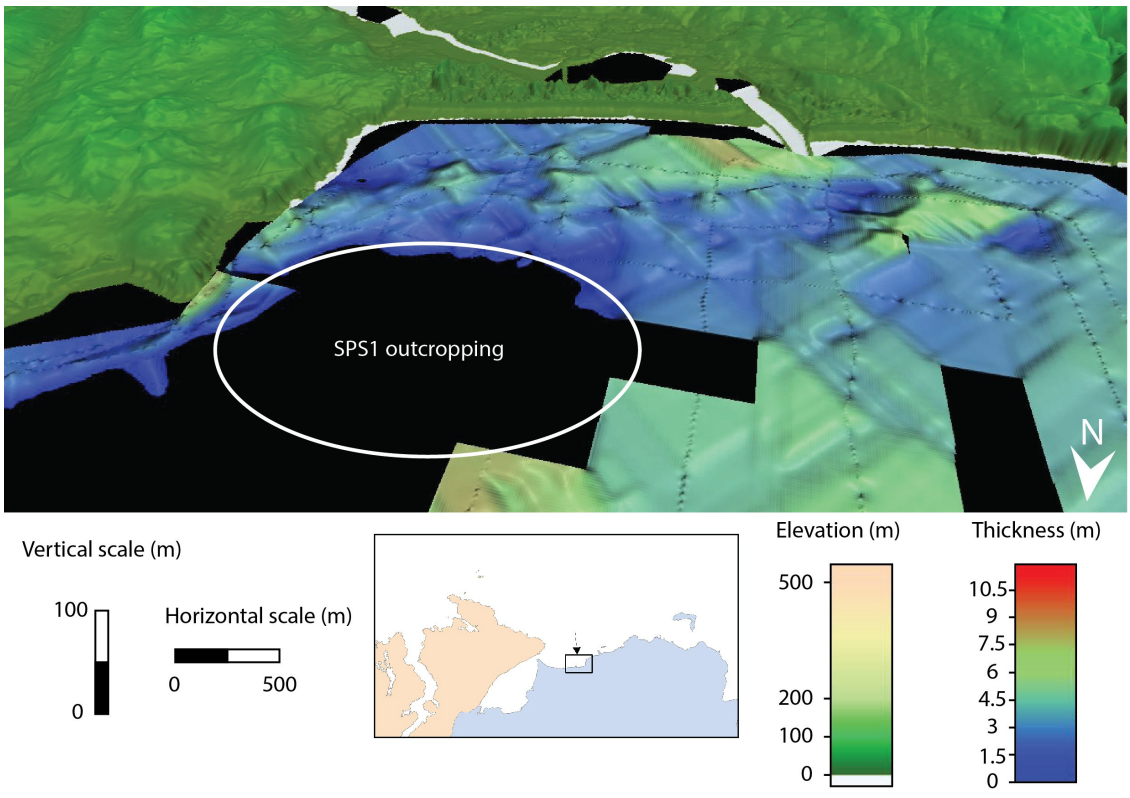

Figure 6.22: Oblique view of the interpolated thickness of unit SPS5.

6.1.5 Whitepark Bay

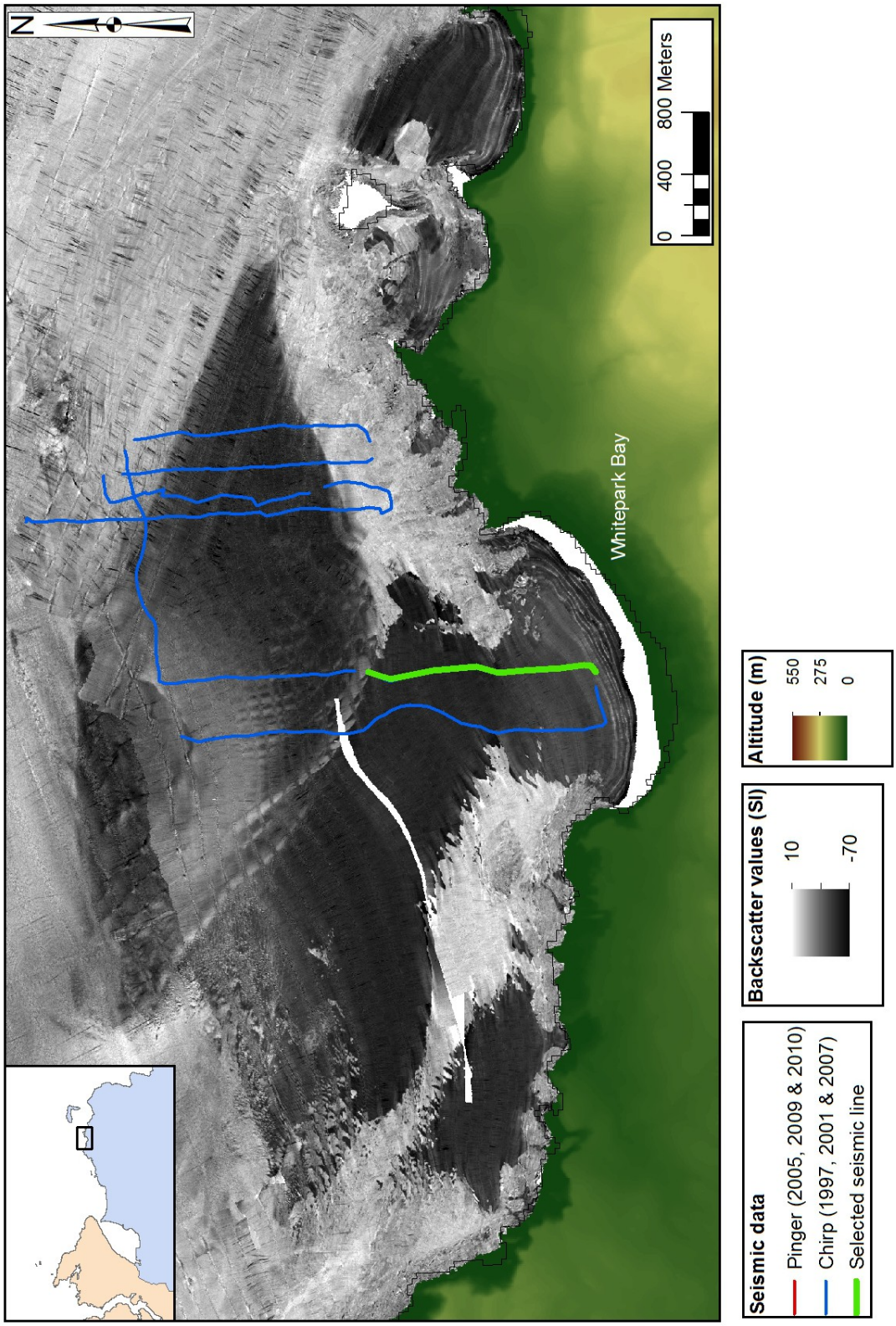

Figure 6.23: Location of the seismic line used for the presentation diagram (figure 6.24) in Whitepark Bay.

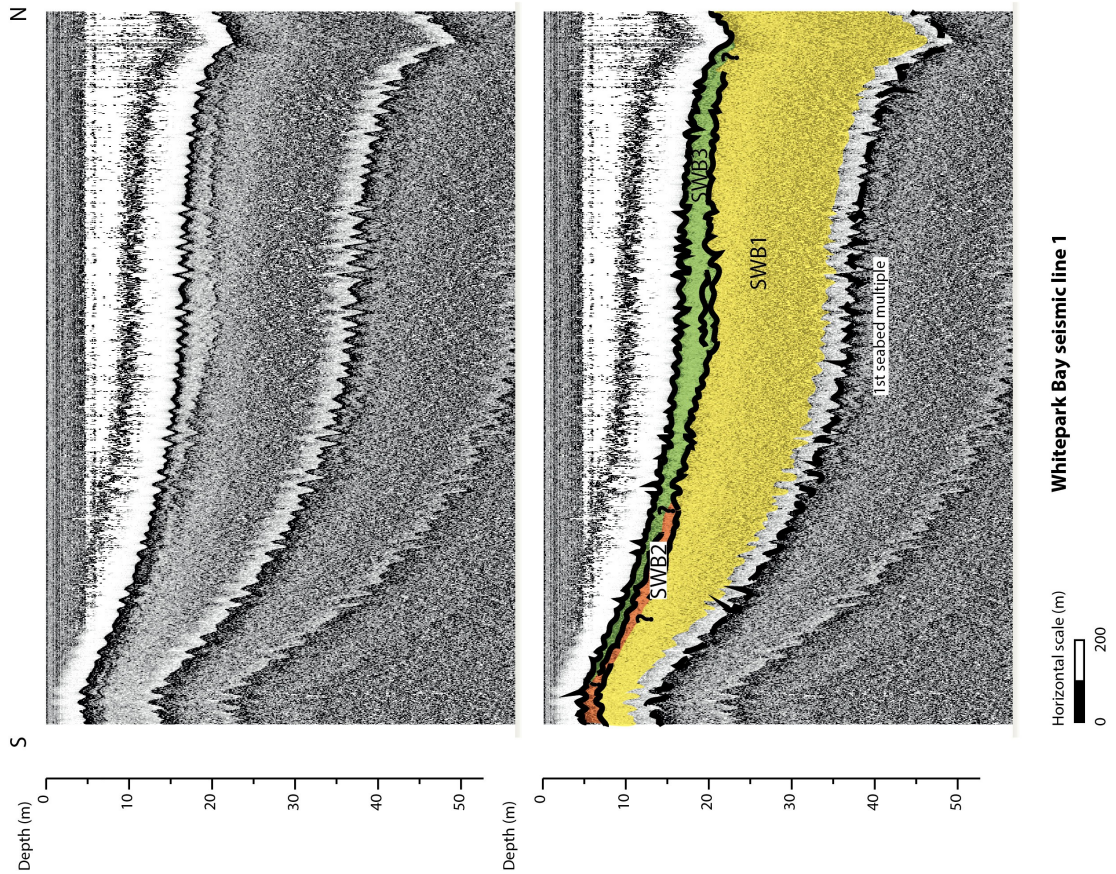

Figure 6.24: Seismic data line located in figure 6.23 and highlighted seismic units for Whitepark Bay described in table 6.5.

Unit	Top reflector	Acoustic signature	Thickness
SWB3	Continuous strong	Characterised by a strong continuous bottom reflector and acoustically transparent throughout with some chaotic point reflectors at the top. This units drapes over unit SWB1 as a slope front fill and contains some strong sub-parallel discontinuous reflectors similar to those seen in Runkerry Bay.	Up to 4m
SWB2	Discontinuous strong	Unit SWB2 appears in the higher ground as a slope front fill and was truncated by unit SWB3. The unit is transparent with some point reflectors and its bottom reflector appears only weakly.	Up to 3m
SWB1	Discontinuous weak to medium	Medium top reflector showing a continuous surface of high rugosity and outcropping in places. Concentration of chaotic relfectors toward the top but chaotic throughout.	unknown

Table 6.5: Description of seismic units highlighted in figure 6.24 for Whitepark Bay.

Unit SWB1 is limited by a discontinuous weak to medium top reflector (the acoustic basement here). The unit itself has a chaotic acoustic signature which becomes more transparent toward the top of the unit where distinct point reflectors appear. The top surface of the unit has a high rugosity and even outcrops in places. It slopes down seaward until a plateau lying at a distance of about 1km from the coast at a depth of about 19.5m for a length of about 1km (figure 6.25). It drops again then until a depth of 39m where it becomes undetectable due to a lack of seismic penetration.

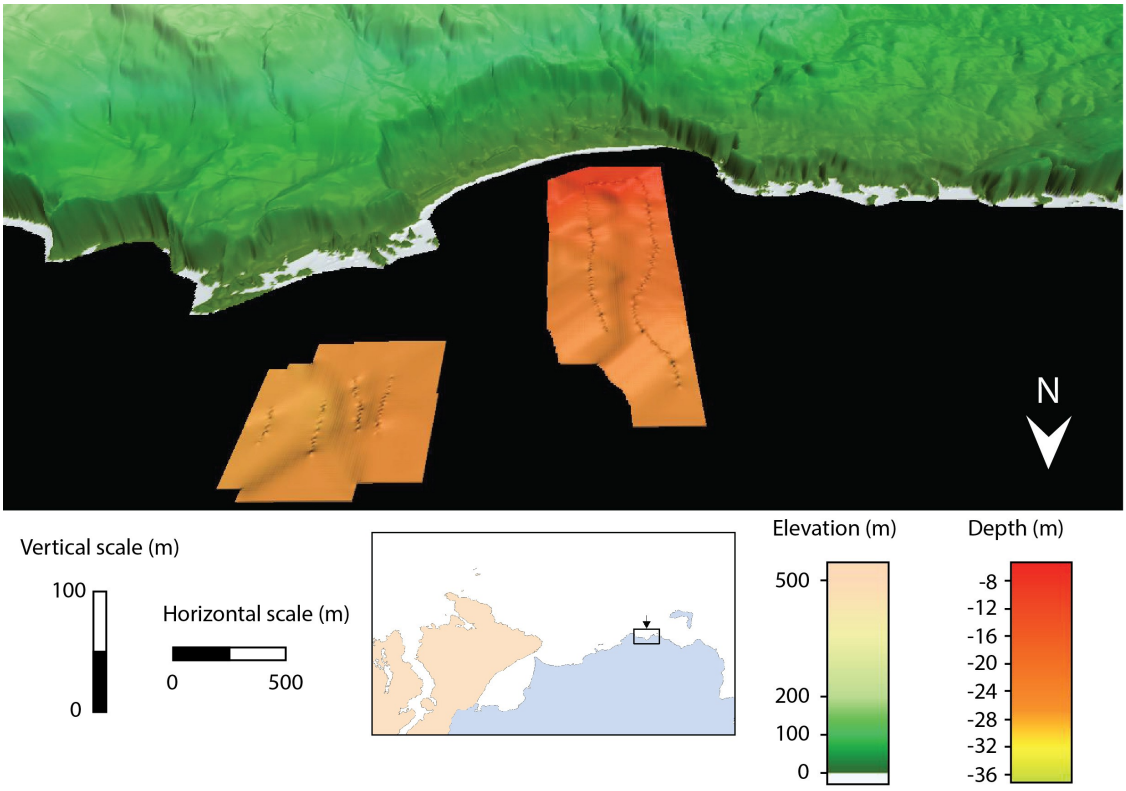

Figure 6.25: Oblique view of the interpolated surface of the top reflector of unit SWB1.

Unit SWB2 only appears in shallower water until a depth of 15m where it is clearly truncated by Unit SWB3 (figure 6.26). SWB2's acoustic signature is transparent with some point reflectors and its top reflector is discontinuous but with a strong intensity. It has a maximum thickness of about 3m (figure 6.27).

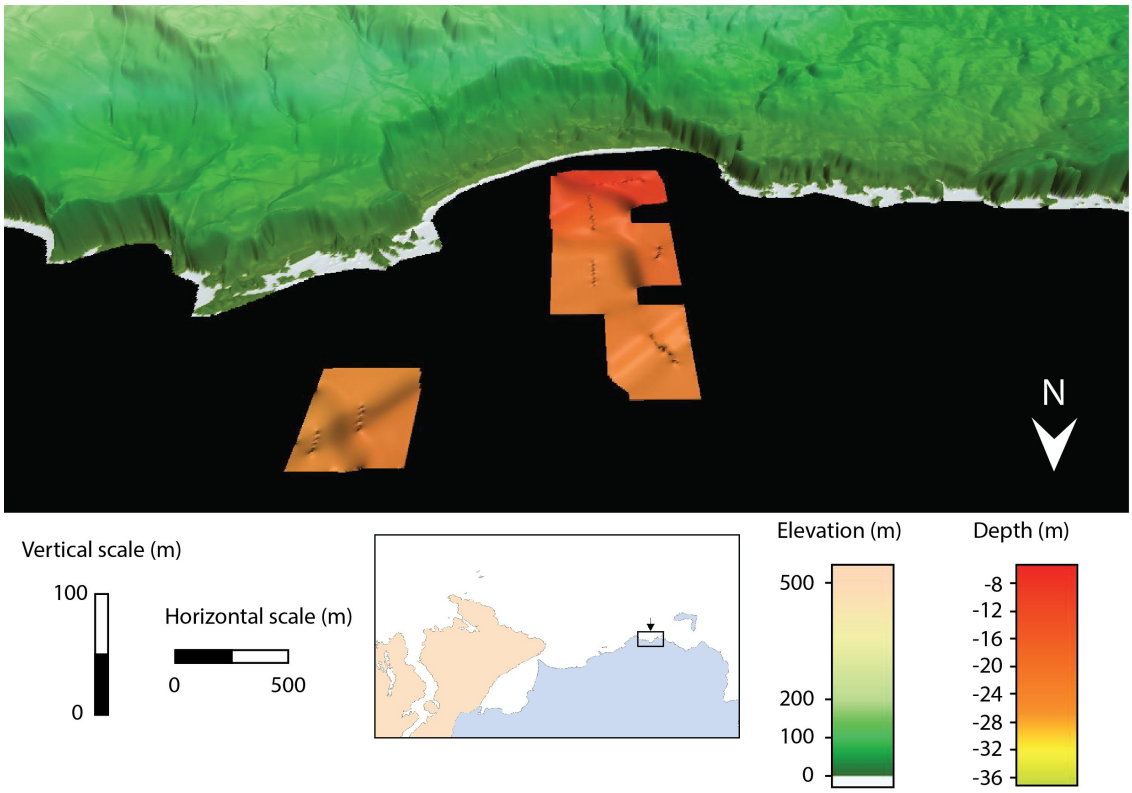

Figure 6.26: Oblique view of the interpolated surface of the top reflector of unit SWB2.

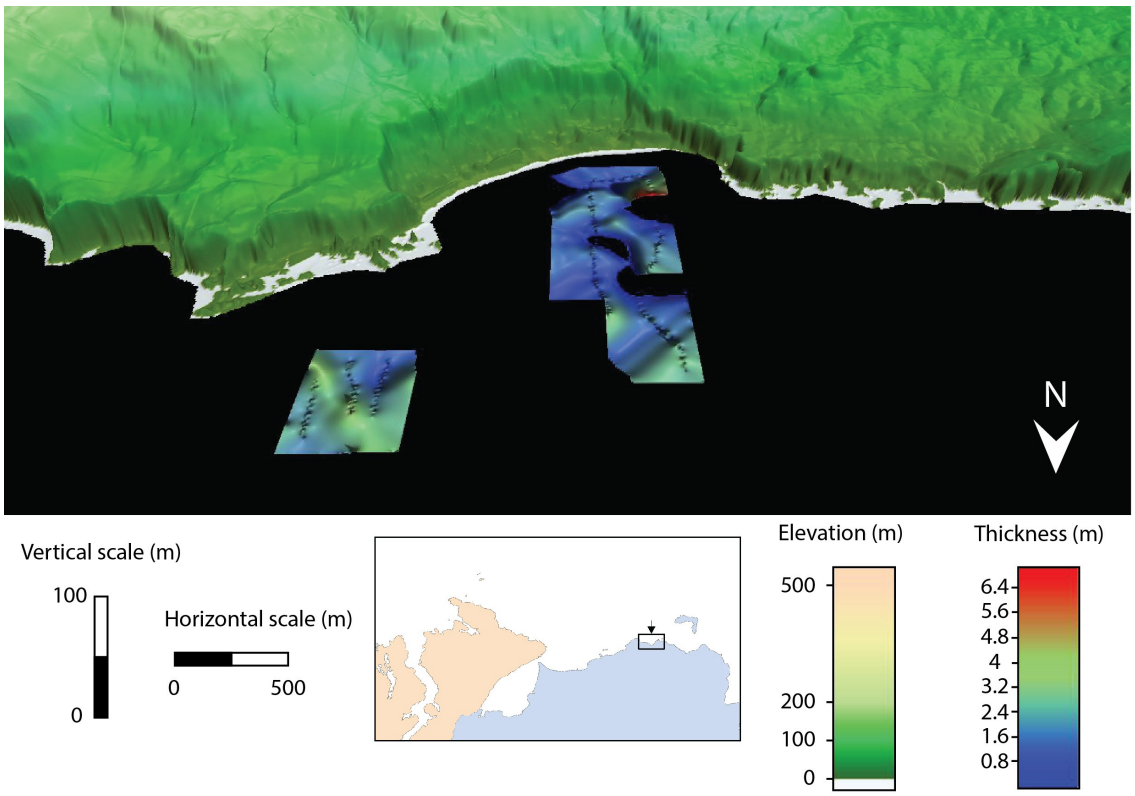

Figure 6.27: Oblique view of the interpolated thickness of unit SWB2.

Unit SWB3 is acoustically transparent but displays some point reflectors towards its top and some strong sub-parallel discontinuous reflectors similar to those seen in Runkerry Bay. SWB3 drapes over Unit SWB1 for most of the survey lines. Its top reflector at the seabed is continuous and strong in intensity and the unit's thickness is quite constant at about 4m until the sandbar that lies across the bay at about 1.6km from the coast. This unit appears as a slope front fill which is a strata filling the negative-relief in front of a bank (Mitchum et al., 1977) here formed by the top of unit SWB2.

6.1.6 Church Bay, Rathlin.

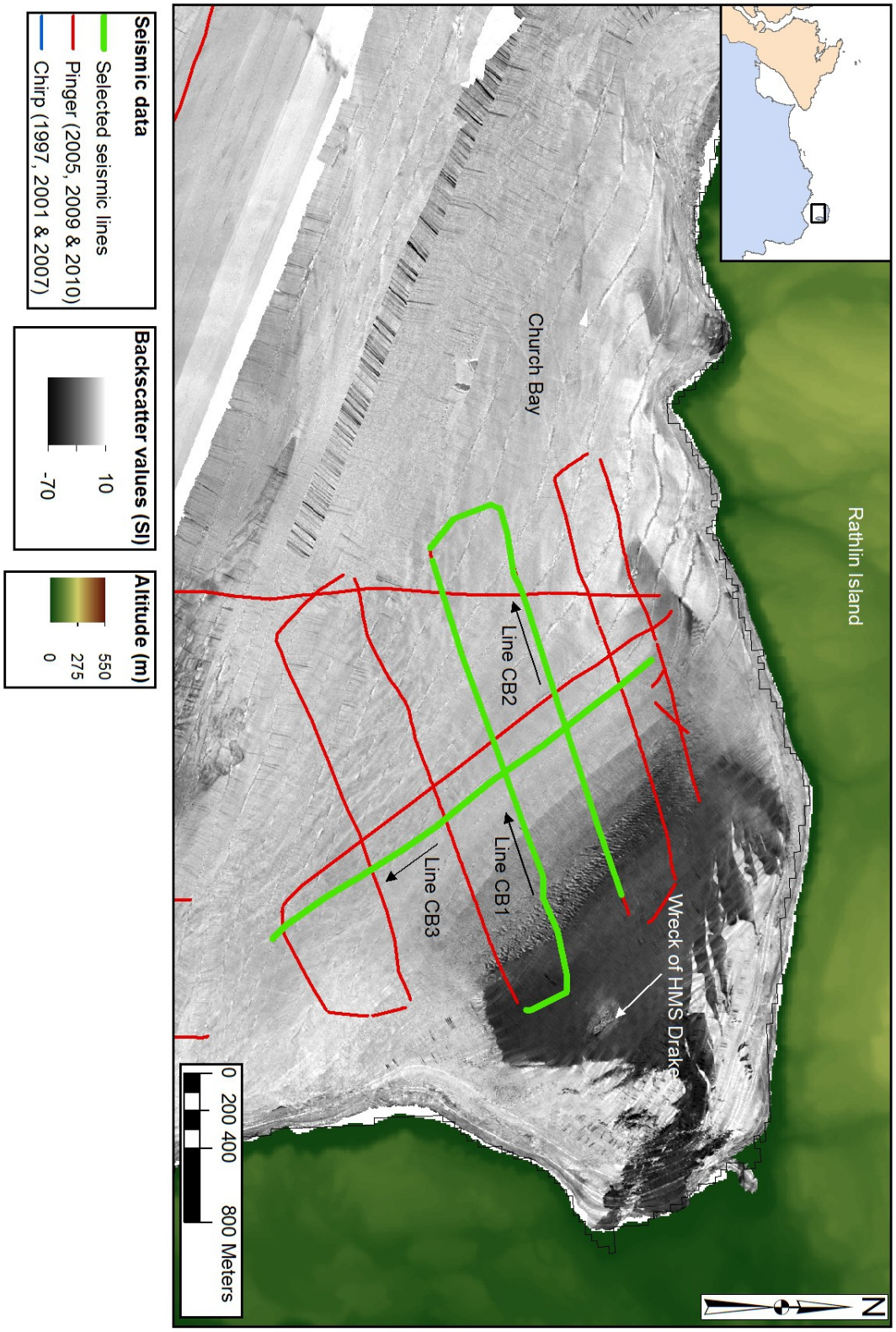

Figure 6.28: Location of the seismic lines used for the presentation diagrams (figures 6.29 to 6.31) in Church Bay.

Unit	Top reflector	Acoustic signature	Thickness
SCB6	Continuous medium to strong	Thin veneer at sea bed with transparent signature draping all underlying units.	0.5 to 1m
SCB5	Continuous strong	Characterised by a strong continuous and horizontal bottom reflector that appears to truncate internal reflectors of SCB4 at 14m depth but acoustically transparent throughout. The unit is deposited as a sheet over its bottom reflector and so is constrained only to shallower depth.	1 to 2m
SCB4	Strong and chaotic for 1 to 2m of thickness	High amplitude, discontinuous and parallel reflectors throughout. These are wavy and disrupted as though compacted from south west to north east but they disappear at deeper depth. Sharp contrast with other units both vertically and to a lesser extent laterally. SCB4 appears sigmoidal with internal reflector onlapping the unit below. Acoustic lack of penetration prevents to detect its bottom reflector except at deeper depth. Gas pockets appears at shallower depth (15m for top of gas anomaly).	Unknown but at least 27m and more than 35m in places. It thins at the bottomset
SCB3	Strong continuous when visible	Broadly transparent, some weak internal wavy parallel reflectors appear. This unit drapes the underlying one.	4 to 5m
SCB2	Broad, strong and chaotic	Top reflector showing a discontinuous surface of high rugosity and outcropping in places. The unit is chaotic but some point reflectors and some weak discontinuous sub-parallel internal reflectors appear in places. The unit appears to drape the acoustic basement	8 to 15m when visible
SCB1	Weak and discontinuous	This unit is also chaotic and shows very little contrast to SCB2. Its top reflector displays a surface of high rugosity.	unknown

Table 6.6: Description of seismic units highlighted in figures 6.29 to 6.31 for Church Bay.

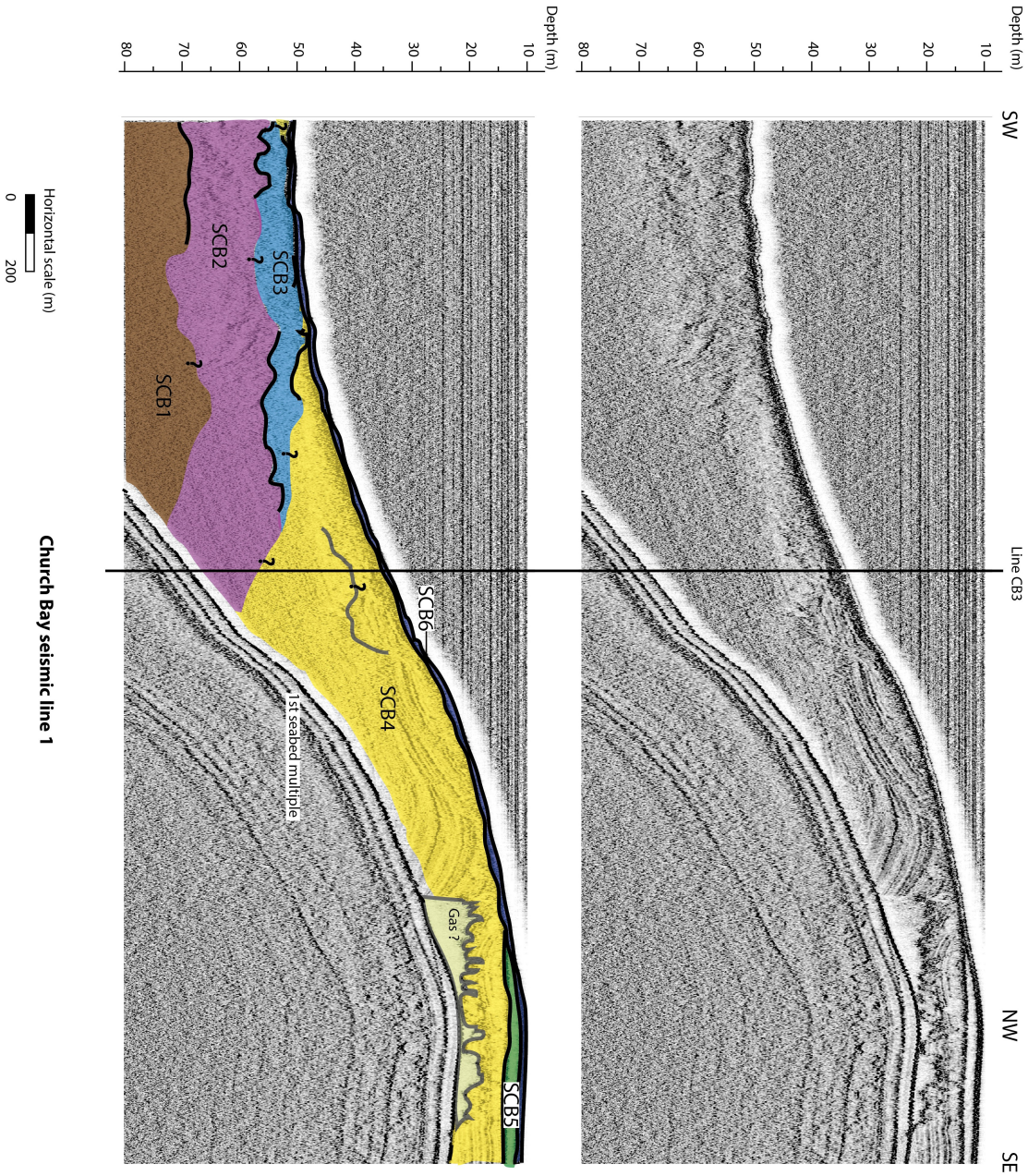

Figure 6.29: Seismic data and highlighted seismic units (described in table 6.6) for line CB1 (located on figure 6.28) at Church Bay. The intersection with line CB3 is displayed.

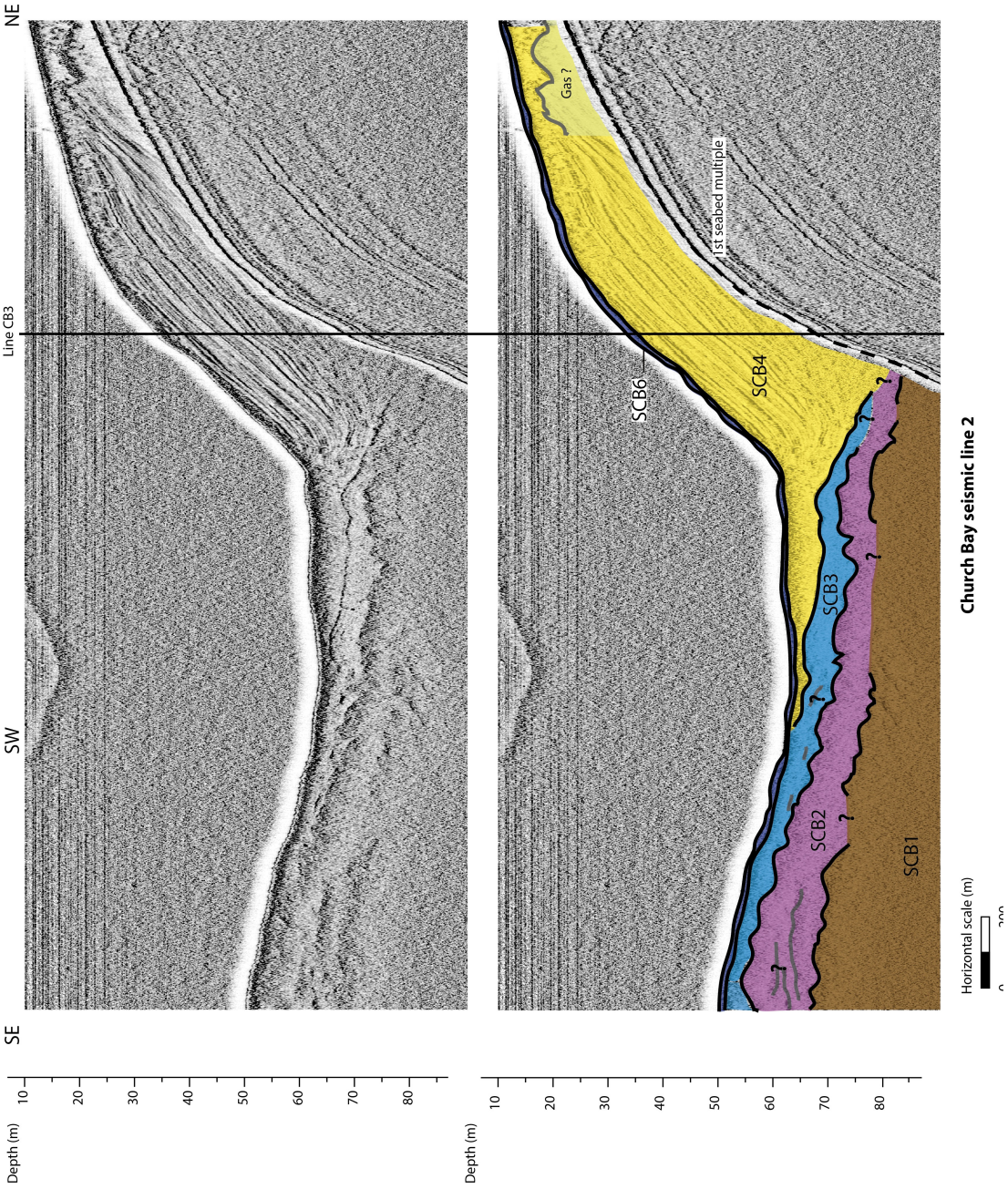

Figure 6.30: Seismic data and highlighted seismic units(described in table 6.6) for line CB2 (located in figure 6.28) at Church Bay. The intersection with line CB3 is displayed.

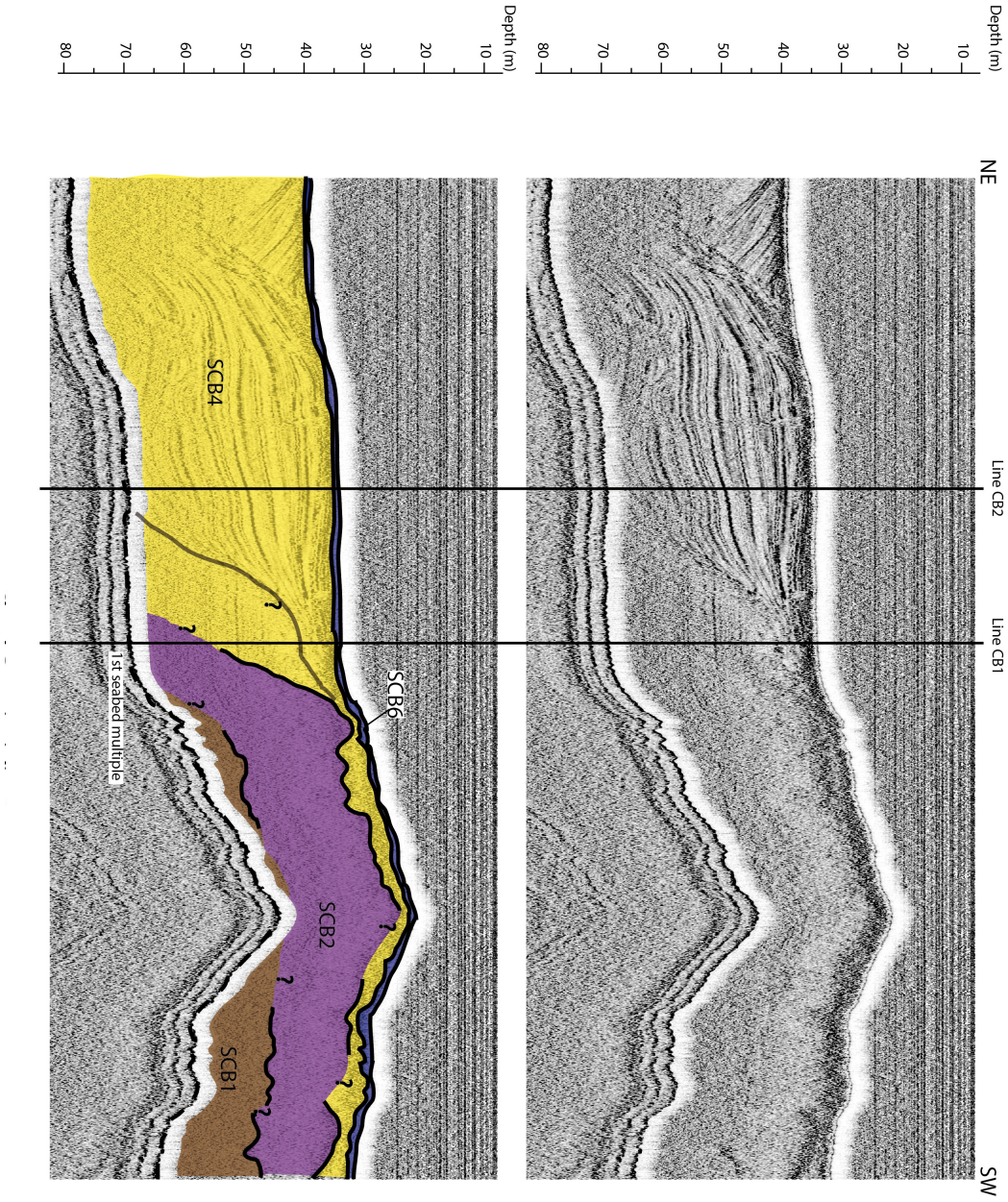

Figure 6.31: Seismic data and highlighted seismic units (described in table 6.6) for line CB3 (located in figure 6.28) at Church Bay. The intersections with lines CB1 and CB2 are displayed.

Unit SCB1 does not appear consistently throughout the survey as acoustic penetration decreases in shallower waters. Its top reflector, the acoustic basement here, is discontinuous and weak in intensity and its acoustic signature is chaotic. SCB1's top surface lies deeper westward and presents two depression that correlates with depressions visible on the bathymetry; the main one to the north west of the bay and another one to the south of the first one. A rise is visible at the centre of the survey, one which is slightly shifted north west of a rise visible on the bathymetry (figure 6.32).

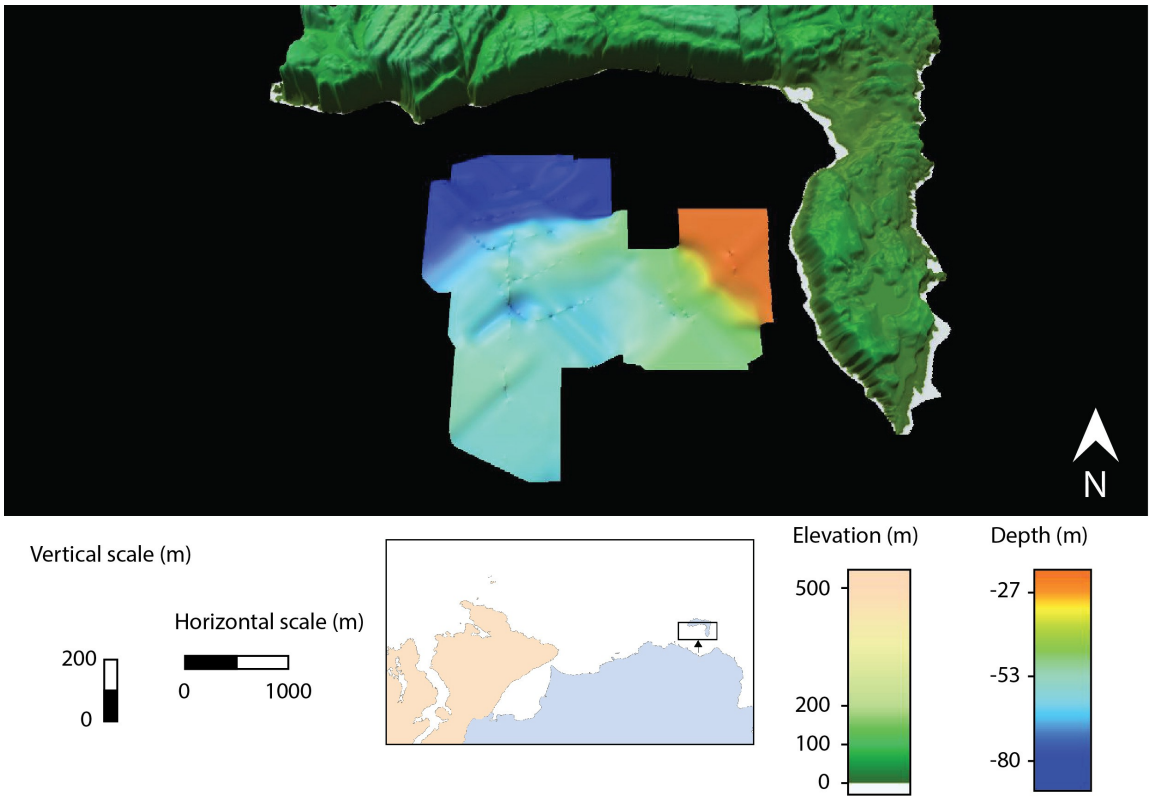

Figure 6.32: Oblique view of the interpolated surface of top reflector of unit SCB1.

The top reflector of unit SCB2 is broad and strong in intensity and appears to be made of a layer of point reflectors (chaotic). SCB2's acoustic signature is chaotic with some point reflectors and some weak discontinuous sub-parallel internal reflectors in places. It is virtually indistinct to unit SCB1 which it drapes. Unit SCB2 only appears in deeper waters of the main bathymetric depression of the bay and has a thickness of 8 to 15m when visible (figures 6.33 and 6.34).

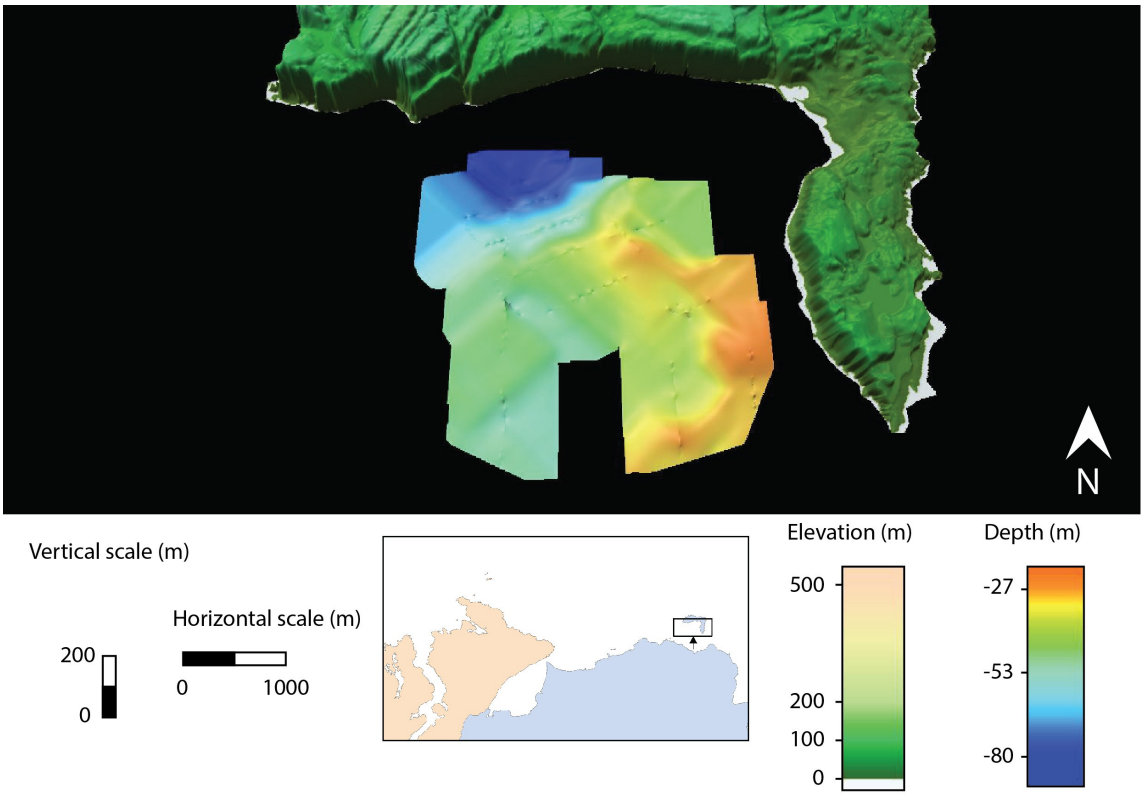

Figure 6.33: Oblique view of the interpolated surface of top reflector of unit SCB2.

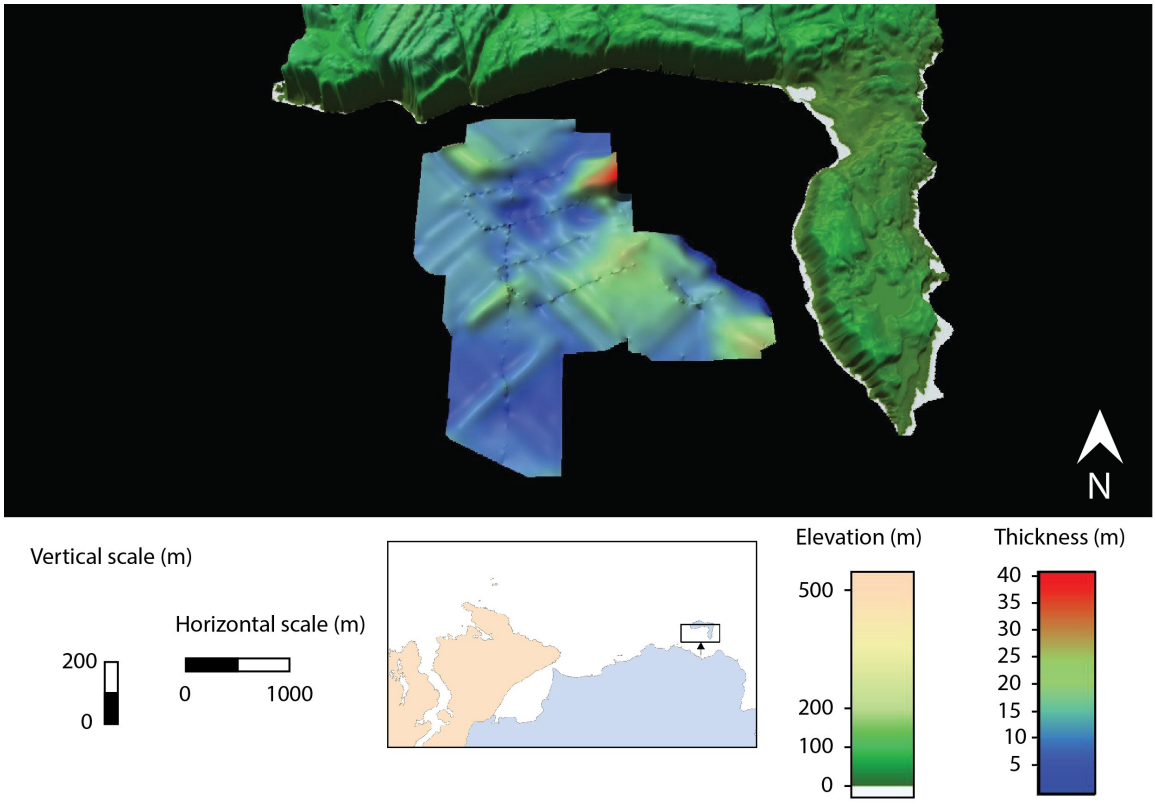

Figure 6.34: Oblique view of the interpolated thickness of unit SCB2.

Unit SCB3 is broadly transparent acoustically and displays some weak internal wavy parallel reflectors. Its top reflector is strong and continuous. Similarly to unit SCB2, it appears only in the deeper waters of the main depression and is draping the underlying unit (SCB2) with a thickness of 4 to 5m (figures 6.35).

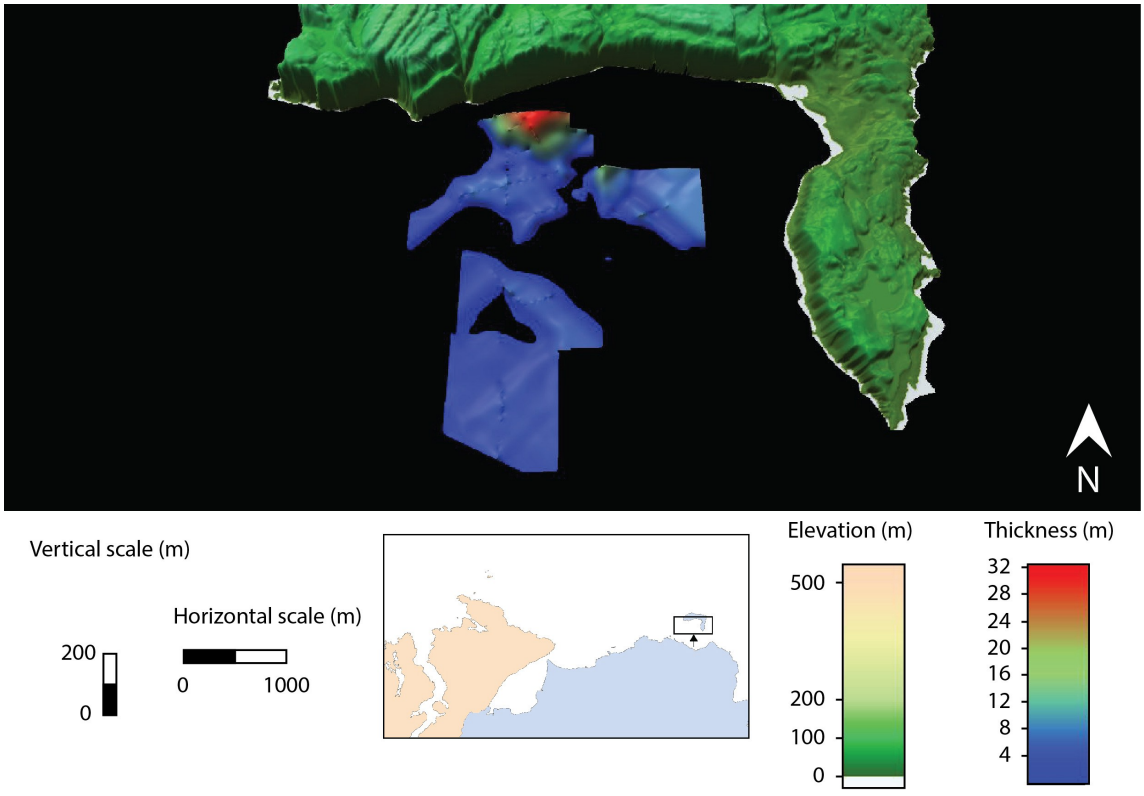

Figure 6.35: Oblique view of the interpolated thickness of unit SCB3.

Unit SCB4 is visible throughout the north of the bay both on the near and far shelf. It has a distinct acoustic signature of high amplitude, discontinuous parallel reflectors for the main part but becomes more transparent with point reflectors and no internal linear reflectors in the deeper waters. Unit SCB4's top reflector is strong and broad and appears formed of chaotic reflectors for a thickness of 1 to 2m. The unit's thickness is unknown for shallower waters due to the lack of penetration of the seismic signal and to apparent gas disturbance (at 15m depth for the top of the disturbance) but is at least 27 to 35m in places. As the unit thins out at the bottomset, it is 4 to 5m thick when its bottom reflector first appear (figure 6.30). From its wavy parallel internal reflectors, the unit appears as a slope front fill (as defined in Mitchum et al., 1977) but these reflectors disappear in the deepest water of the main bathymetric trough to the north west of the bay. The unit SCB4 appears

on the whole as sygmoidal progradation deposit as defined by Mitchum et al. (1977) as a prograding pattern form through progressive lateral development of gently sloping S-shaped depositional surfaces. Furthermore, this unit appears to have been truncated at a depth of 14m to create the base of the near shelf plateau which was covered by unit SCB5 later on.

SCB5 is a an acoustically transparent seismic unit with a continuous and strong top reflector. The unit is confined to the near shelf plateau to the east of the bay where it has been laid down sub-horizontally over an erosional surface at the top of unit SCB4 at 14m depth. It has a constant thickness of about 2m but thins out to the south west forming a bank on top of the unconformity (Mitchum et al., 1977).

Unit SCB6 is detected as a veneer over the whole bay and at all depths draping all underlying units with a thickness of 0.5 to 1m. Its acoustic signature is transparent and its top reflector at the seabed is continuous and medium to strong in intensity.

6.1.7 Ballycastle bay

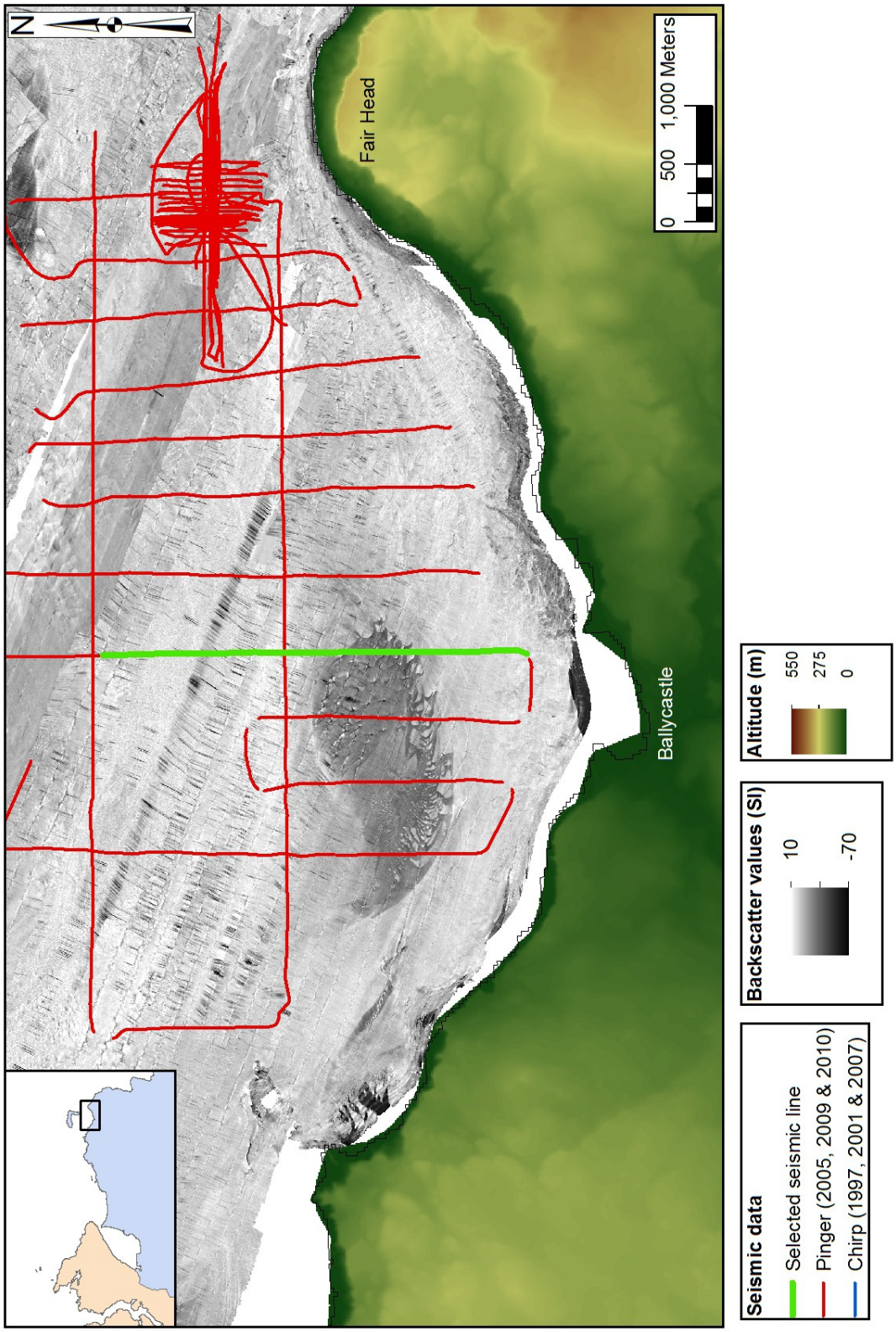

Figure 6.36: Location of the seismic line used in the presentation diagram (figure 6.37) in Ballycastle Bay.

Unit	Top reflector	Acoustic signature	Thickness
SBB6	Continuous medium to strong	Thin transparent veneer draping all underlying units for the majority but not the entirety of the bay.	1m
SBB5	Chaotic strong	Characterised by a strong continuous bottom reflector and acoustically transparent throughout with chaotic point reflectors at the top. This units drapes over unit SBB3 but is only present in patches. It appears to be coarsening upward and forms distinctive bedforms on the seafloor.	Up to 7m
SBB4	Continuous strong	It appears in the higher ground and drapes over the underlying units as a slope front fill. The unit is transparent throughout but displays chaotic reflection toward the top and has a more diffuse bottom reflector.	6 to 10m
SBB3	Chaotic strong	This unit fills unit SBB2's depressions in complex onlapping manner. This unit is transparent throughout and contains some diffuse non-parallel internal reflectors.	Up to 10m
SBB2	Chaotic, broad and strong	Strong top reflector showing a discontinuous surface of low rugosity but outcropping in places. This unit is chaotic throughout with some internal reflectors in places. Bottom reflector is invisible for most of the bay.	At least 5m
SBB1	Discontinuous, weak and undulating	Chaotic. Very little contrast with overlying unit.	unknown

Table 6.7: Description of seismic units highlighted in figure 6.37 for Ballycastle Bay.

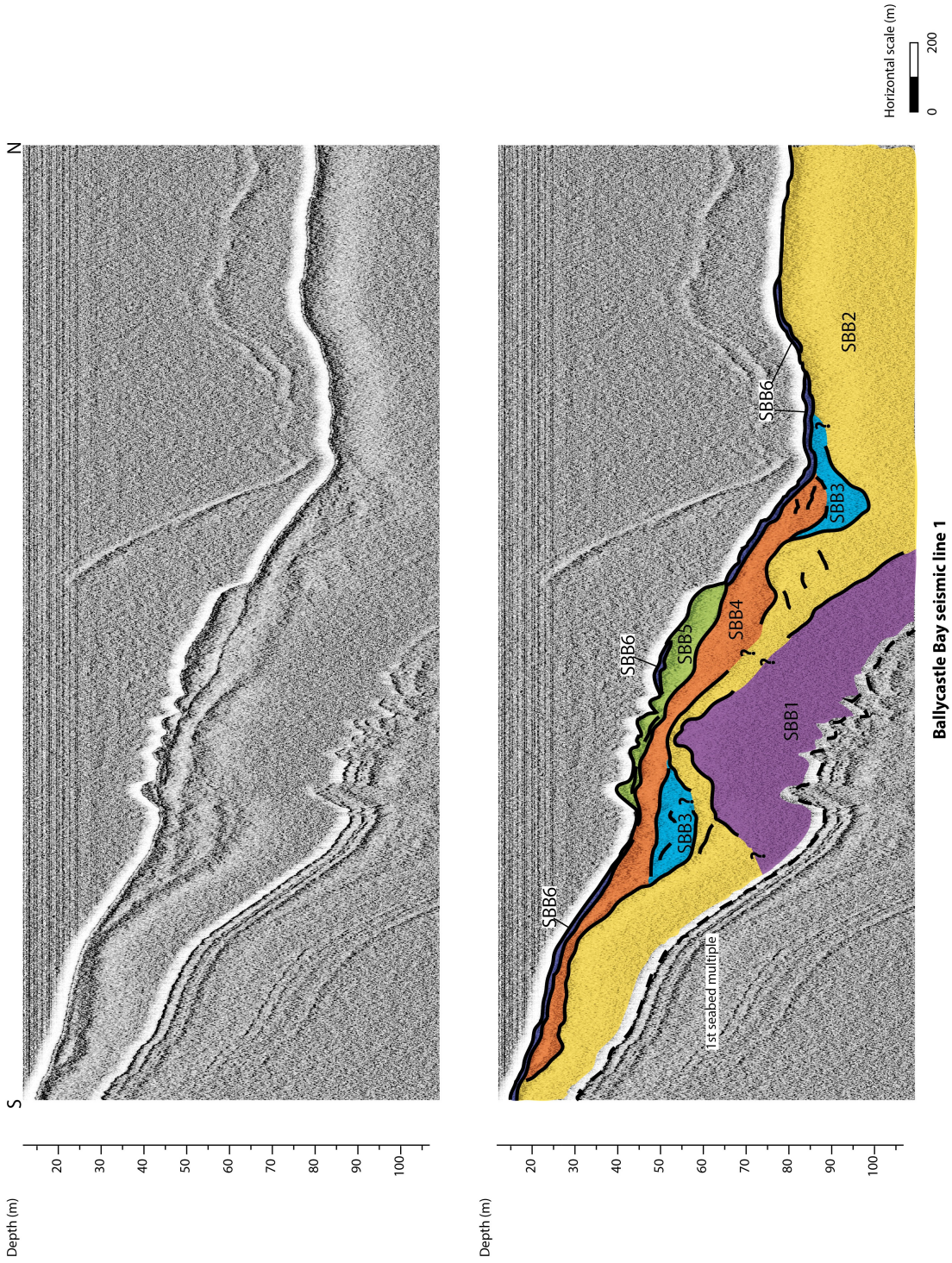

Figure 6.37: Seismic data line located in figure 6.36 and highlighted seismic units for Ballycastle Bay described in table 6.7

Unit SBB1 is chaotic acoustically and its top reflector, the acoustic basement here, is discontinuous, weak and undulating. This reflector's depth follows almost identically the seabed depth. It shows a plateau area at a depth of about 25m which extends 750m from the coast just off fair Head, as far as 1.9km halfway between Ballycastle town and Fair Head and 1.35km at Ballycastle town (figure 6.38). This plateau appears to continue along the coast to the west but only extends to 800m from the coast. This was already identified as a relict shore platform during earlier investigation of the bathymetric data (section 4.3.2.1 and figure 4.21). In the rest of the bay, this unit's top lies at about 90m depth in the main bathymetric depression of the bay directly north of Ballycastle town.

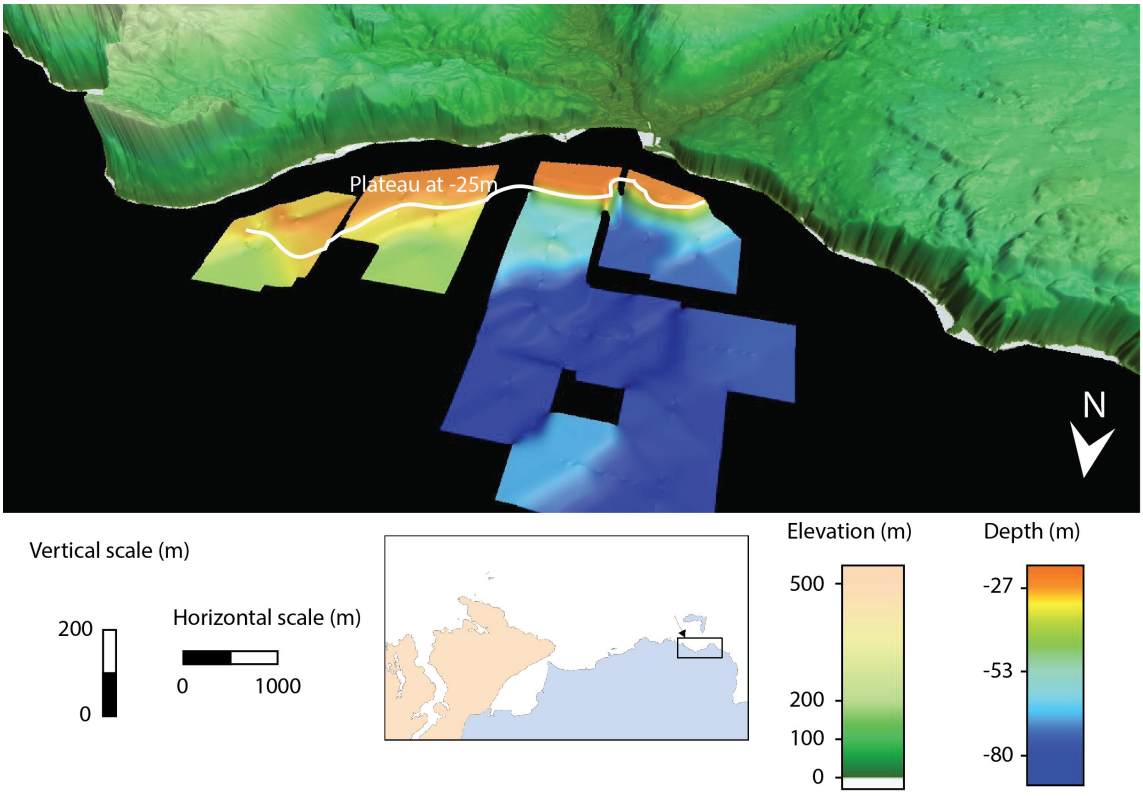

Figure 6.38: Oblique view of the interpolated surface of the top reflector of unit SBB1.

Unit SBB2 has a chaotic acoustic signature that gets more transparent towards its top with some internal reflectors in places. Its top reflector is discontinuous, strong in intensity, broad and appears to be composed of a layer of point reflectors. It forms a top surface with low rugosity but outcropping in places. SBB2 shows a similar surface morphology as the local bathymetry with a definite plateau at 20m depth embracing the coastline from Fair Head to the east to an area just 900m to the west of Ballycastle town

(figure 6.39). This plateau extends to a distance of about 1.5km from the coastline. Unit SBB2 drops down rapidly for the most part, apart from an area to the north east of the survey where the slope gradient is smoother, then to a maximum observed depth of 114.75m with a "ledge" at about 69m. Just south of the main depression appears an isolated area where unit SBB2's depth is higher than its surrounding at about 48m.

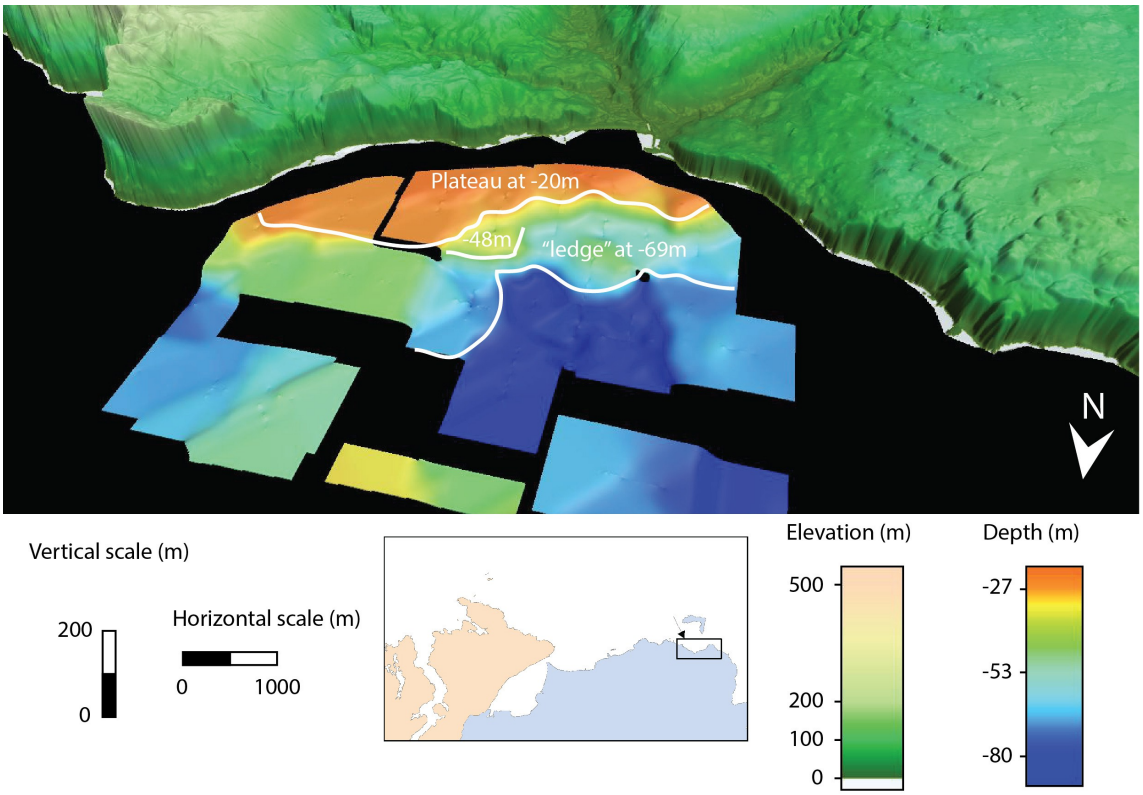

Figure 6.39: Oblique view of the interpolated surface of the top reflector of unit SBB2.

Unit SBB3 is mainly transparent acoustically with some diffuse non-parallel internal reflectors. Its top reflector is discontinuous, strong in intensity and appears composed of a layer of point reflectors. SBB3 does not appear throughout and slopes unevenly to the coast but follows the main changes in level of the seabed. It appears first at a depth of about 20.25m and slopes down to a maximum depth of 97.5m in the deepest basin straight north of Ballycastle town. It has an average thickness of about 4.5m but concentrates in depressions of units SBB2 and SBB1 with an average thickness of the order of 12m. These depressions appear on the plateau area of unit SBB2 (figure 6.39) but also at deeper depth and do not appear to form a particular pattern.

Unit SBB4 is acoustically transparent but displays chaotic reflections toward its top. Its top reflector is continuous and strong in intensity. SBB4 drapes the lower units SBB3, SBB2 and SBB1 sloping seaward from the plateau to the south at about 13.5m depth down to a depth of 96m in the bay (figure 6.40). It has a maximum thickness of 12m at the lower depth but only an average of 4.75m on the higher ground. It has the general morphology of a slope front fill (as defined in Mitchum et al., 1977).

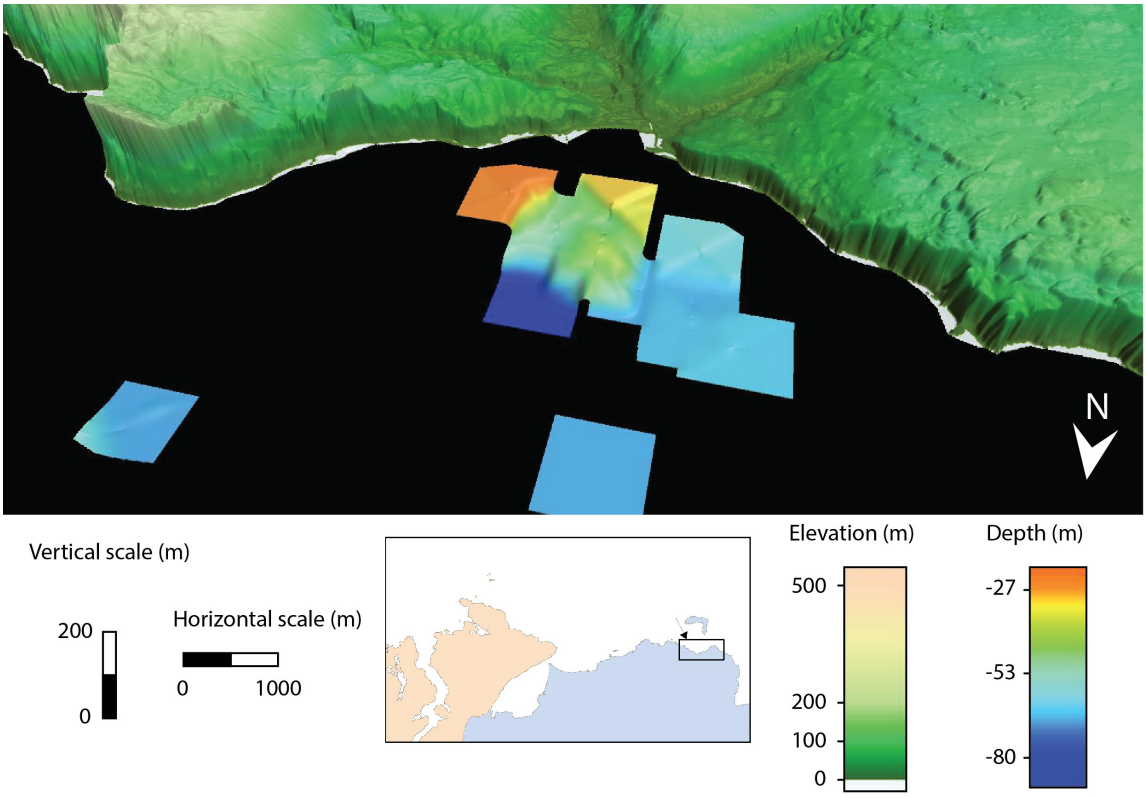

Figure 6.40: Oblique view of the interpolated depth of the top reflector of units SBB4.

Unit SBB5 has a transparent acoustic signature and its top reflector is strong in intensity but discontinuous and appears to be composed of a layer of point reflectors. The unit only appears as modern bedforms such as massive sand ripples where its bottom reflector shows a continuity with the seabed surrounding it that corresponds to the top of unit SBB4 (see figures 6.36 and 6.37). It has a maximum thickness of 7.5m.

Unit SBB6 is detected as an acoustically transparent veneer over most of the bay and at all depths with a thickness of 0.5 to 1m. Its top reflector at the seabed is continuous and medium to strong in intensity.

6.1.8 Lough Swilly

There has been limited work on Lough Swilly but of note are the seismic explorations of David Evans (Evans, 1973; Moore et al., 2011) where the bedrock appears to be covered by more than 100m of sediments in places and several channel cuts are visible interpreted as indicating several phases of deglaciations with different flow and/or RSL stillstands. A shoreline terrace is visible in the sediment column at around 20m depth west of Crummies Bay. The area around Lough Swilly also contains inter-tidal peat being eroded at White strand near Rathmullan showing remains of tree stumps having been flooded at the last transgression (Moore et al., 2011).

Unit	Top reflector	Acoustic signature	Thickness
SLS4	Continuous strong	Thin veneer over the whole survey acoustically transparent.	1m
SLS3	Broad chaotic strong	Unit SLS3 appears only in depressions of Unit SLS1 above unit SLS2. Its bottom reflector is continuous and rather diffuse with a number of chaotic reflectors. It contains a number of wavy parallel internal reflectors including some onlaps.	Up to 20m
SLS2	Discontinous and weak	Large and diffuse discontinuous top reflector draping unit SLS1. This unit appears to contain many chaotic point reflectors.	At least 28m
SLS1	Discontinuous medium to strong	Large and diffuse top reflector showing a discontinuous surface of high rugosity and outcropping in places and is chaotic throughout.	Unknown

Table 6.8: Description of seismic units highlighted in figure 6.42 for the Lough Swilly area.

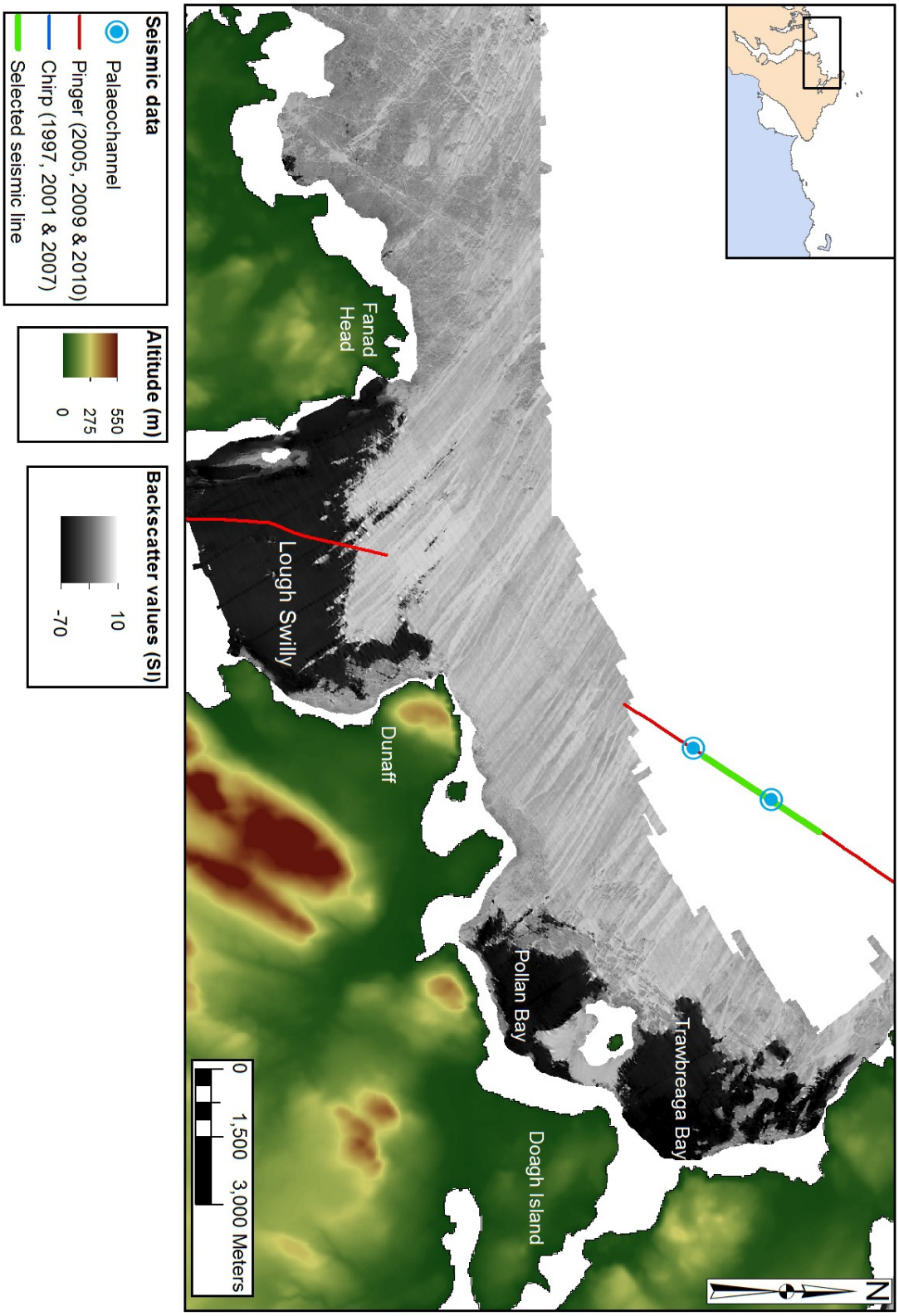

Figure 6.41: Location of seismic line used for the presentation diagram (figure 6.42) with the position of the identified potential palaeochannels highlighted in the Lough Swilly area.

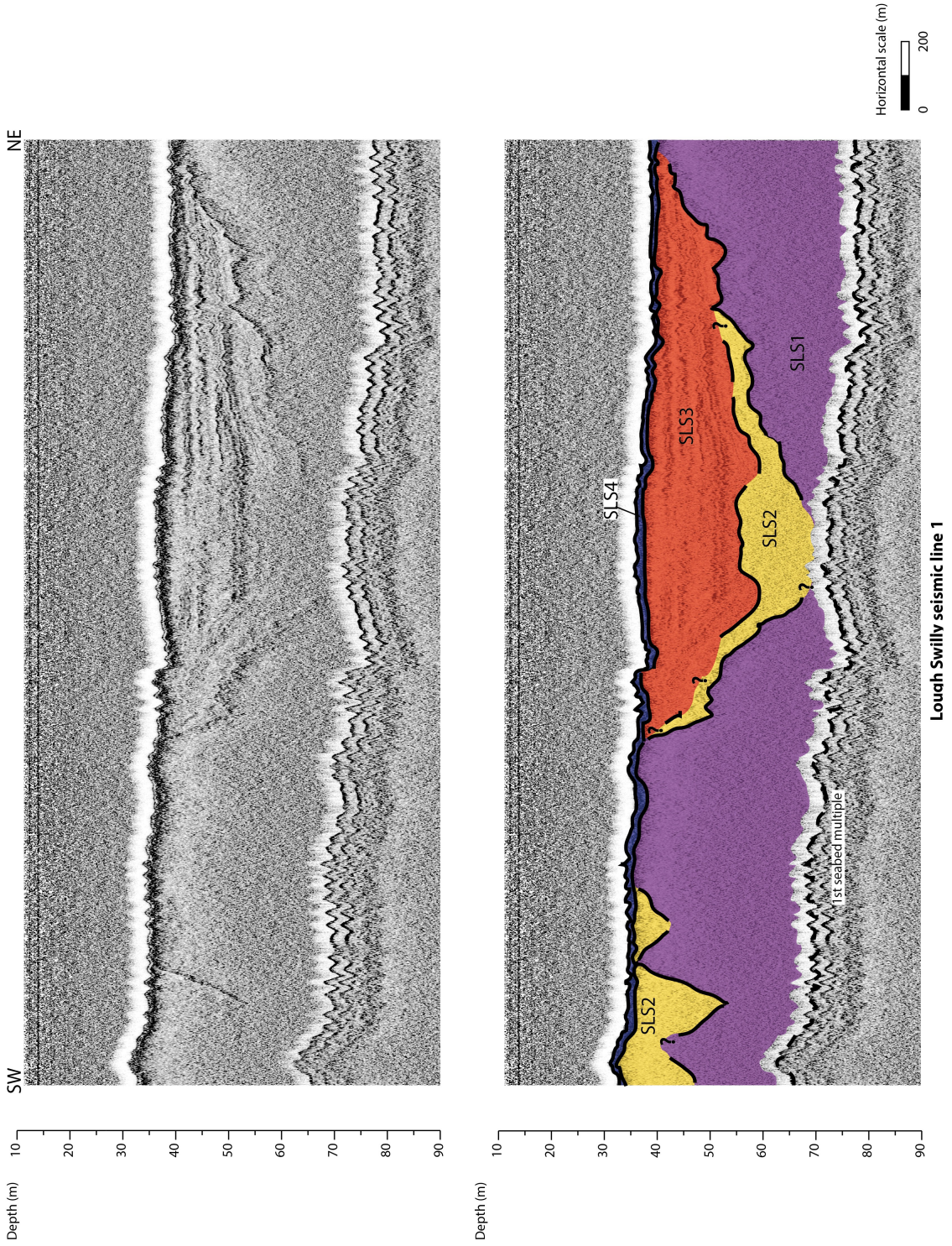

Figure 6.42: Seismic data line located in figure 6.41 and highlighted seismic units for the Lough Swilly area described in table 6.8.

Figure 6.42 presents a section of the seismic line located to the north east of the mouth of Lough Swilly to the west of the Inishowen peninsula. Another seismic line surveyed inside the lough itself is of little interest due to the very shallow waters encountered and the poor penetration of the seismic resulting. The units described here are nevertheless common to the 2 lines of the general area. Due to the only one line of seismic data for the area, no interpolation of the depth and thickness of the units described here are presented.

Unit SLS1 is chaotic acoustically and its top reflector is discontinuous and medium to strong in intensity. This top reflector outcrops on the sea floor in many places west of the Inishowen peninsula with maximum depth of 67.5m in particular depressions. When outcropping, it corresponds to areas of lower backscatter value (figure 6.41). One of these depressions is displayed in figure 6.42 and could be described as a palaeochannel based on this one section. This potential palaeochannel has a width at its mid point of about 1km and is fully filled with sediments with a total thickness of about 30m and a bottom depth of 67.5m. Another potential palaeochannel is found further south where its location is displayed on figure 6.41. It has a mid point width of about 1.2km and is fully covered by sediments with a minimum thickness of 25m. Its bottom depth is unknown but is below 60m.

Unit SLS2 is chaotic acoustically but appears more transparent towards its top with some point reflectors. Its top reflector is discontinuous and weak in intensity. SLS2 drapes over unit SLS1 and covers all its depressions including the one presented in figure 6.42 . It has an average thickness of about 10m but reaches more than 20m in these depressions.

Unit SLS3 contains a number of wavy parallel internal reflectors as well as some some onlaps. Its top reflector is continuous and strong in intensity and appears to composed of a layer of point reflectors. SLS3 only appears inside depressions of unit SLS1 where its thickness is up to 20m draping over unit SLS2.

Unit SLS4 is a thin (1m thickness) transparent veneer draping all underlying units. Its top reflector at the seabed is continuous and strong.

Inside the estuary, the penetration depth of the seismic is more limited and the top of unit SLS1, when visible only deep inside the estuary, has a depth ranging from 17 to 28m. Unit SLS3 has an average thickness of 7.5m followed then by unit SLS2 whose extent is unknown. No further potential palaeochannels were detected.

6.1.9 Lough Foyle

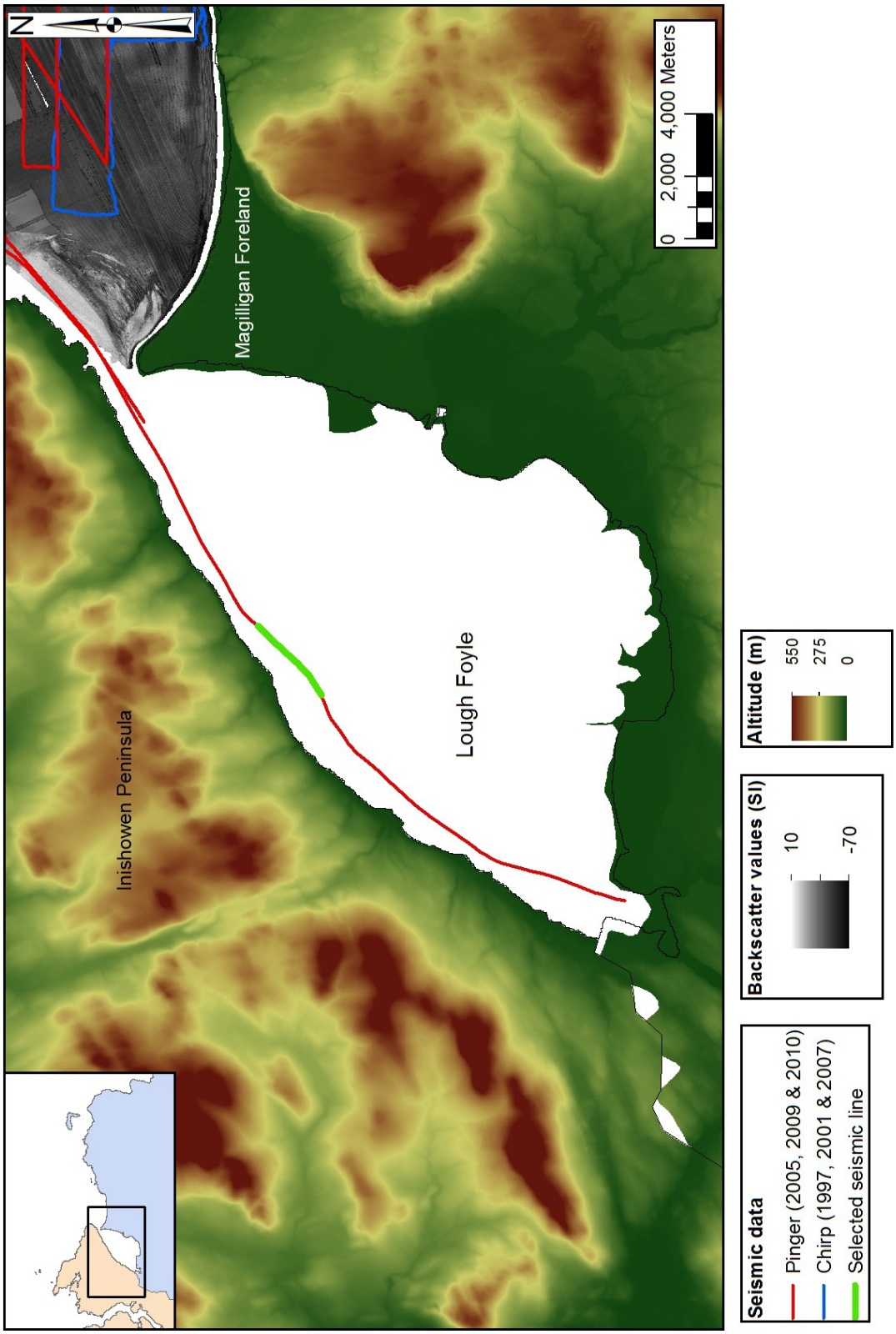

Figure 6.43: Location of seismic line used in the presentation diagram (figure 6.44) in Lough Foyle.

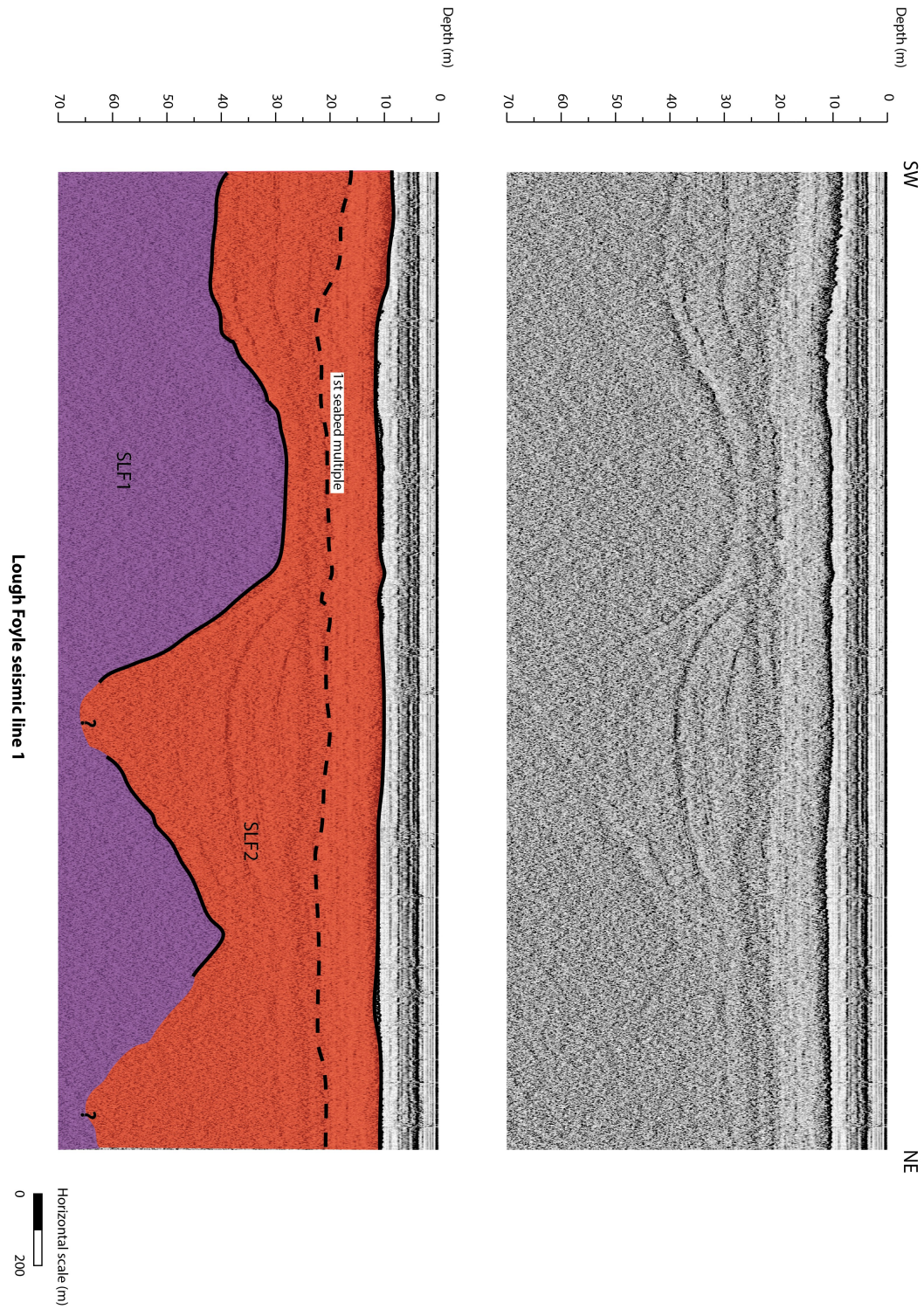

Figure 6.44: Seismic data line located in figure 6.43 and highlighted seismic units for the Lough Foyle area described in table 6.9.

Unit	Top reflector	Acoustic signature	Thickness
SLF2	Continuous strong	Unit SLF2 onlaps over unit SLF1. It contains a number of wavy parallel internal reflectors.	30m in average. Up to 60m in places.
SLF1	Discontinuous medium to weak	Large and diffuse top reflector showing a discontinuous surface of medium rugosity and outcropping in places. Chaotic throughout.	Unknown

Table 6.9: Description of seismic units highlighted in figure 6.44 for the Lough Foyle area.

Similarly to the previous area, only 1 line of seismic data was collected and most of it was at very shallow depth. Nevertheless, we can recognise the evolution of two seismic units along the line from inside the estuary towards the offshore.

Unit SLF1 appear at depth ranging from 24.75 to 81 m but does not appear further north of a location about 3km south of the Magilligan straight. It is chaotic acoustically and has a top reflector (the acoustic basement here) that is discontinuous and medium to weak in intensity. The surface created by this reflector has a low rugosity and presents some large depressions. Three of these are visible in figure 6.44 and could be described as palaeochannels. The potential palaeochannel furthest to the north east in figure 6.44 has a mid point width of about 500m and is filled by sediment with a minimum thickness of 20m. Its bottom depth is unknown but lies below 60m. The potential palaeochannel in the centre of figure 6.44 has a mid point width of about 700m and is filled by sediment with a total thickness of 35m. Its bottom depth is at 65m. The potential palaeochannel furthest to the south west in figure 6.44 has a mid point width of about 400m and is filled by sediment with a total thickness of 6m. Its bottom depth is at 42m. Further similar depressions are visible further to the south west of the displayed part of the seismic line (figure 6.70) and will be discussed in more detail in section 6.4.1.

Unit SLF2 has an average thickness of 30m and a maximum visible thickness of 60m in a depression of Unit SLF1 described above. It contains many wavy parallel internal reflector that are more visible at depth and drapes over unit SLF1 and SLF2's top reflector at the seabed is continuous and strong.

6.2 Analysis of the sediment cores

The results from the scanning and logging processes allowed the comparison of changes in measured density, Pwave velocity, electrical resistivity and magnetic susceptibility with observed changes in average grain size, inclusions and colours along the length of the cores. This prompted the recognition of several lithofacies in the cores retrieved from the 3 areas. The logs from the 14 cores are presented in appendix 6.1 and the different lithofacies are described in the sections below per area cored.

6.2.1 Church Bay

7 cores were collected in Church Bay, including three cores with close to 5m of sediments retrieved. Their locations is summarised in table 3.6 and plotted on figure 3.15.

6.2.1.1 Lithofacies recognised

5 lithofacies were recognised for the cores collected in Church Bay and their description is summarised in table 6.10 below. The simplified log of four cores (CBT1, CB5, CB1 and CB2) selected on their singularity are presented in figures 6.45 to 6.48.

Lithofacies name	Description	Top contact	Thickness (m)	Seismic unit correlation
Marine Sand (MS)	Grey brown fine to medium sand with rounded clasts and shell fragments	seabed	0.1	Top of SCB6
Top Sand (TS)	Fine to very fine very well sorted greyish brown sand. It contains 1 to 2 % shell fragments and some rounded clasts	seabed	5	SCB5
Coarse Sand (CS)	Bed of broken shells in coarse sand matrix with granules of Basalt.	conformable with MS or seabed	0.3 in average but up to 1m for 1 core	Top of SCB4 ? Or SCB6
Laminated Sands (LS)	Interbedded bluish grey very fine sand to silt with greyish brown fine to medium sand. It contains less than 1% of shell fragments and seldom rounded clasts only in 1 core	Unconformable with TS or conformable with CS	Unknown for most but 3m in 1 core	SCB4
Deep Coarse Sand (DCS)	Light brown well sorted medium to coarse sand with 5 % of coarse shells. Some large intact inarticulated bivalves are present	Conformable with LS	Unknown (at least 1.5m)	SCB3

Table 6.10: Description of the lithofacies recognised for Church Bay.

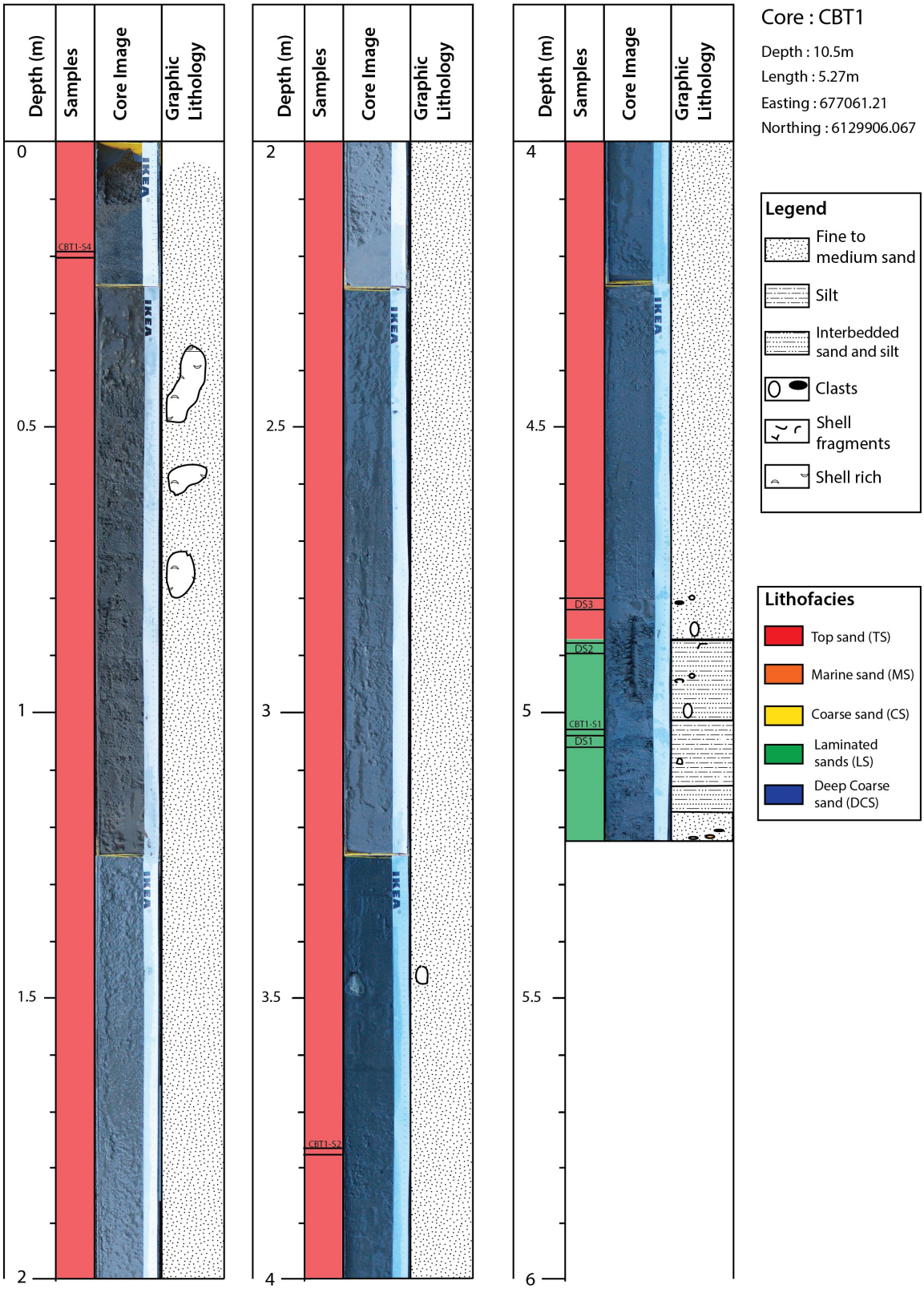

Figure 6.45: Simplified core log of core CBT1 (full log in appendix 6.1, core CBT1).

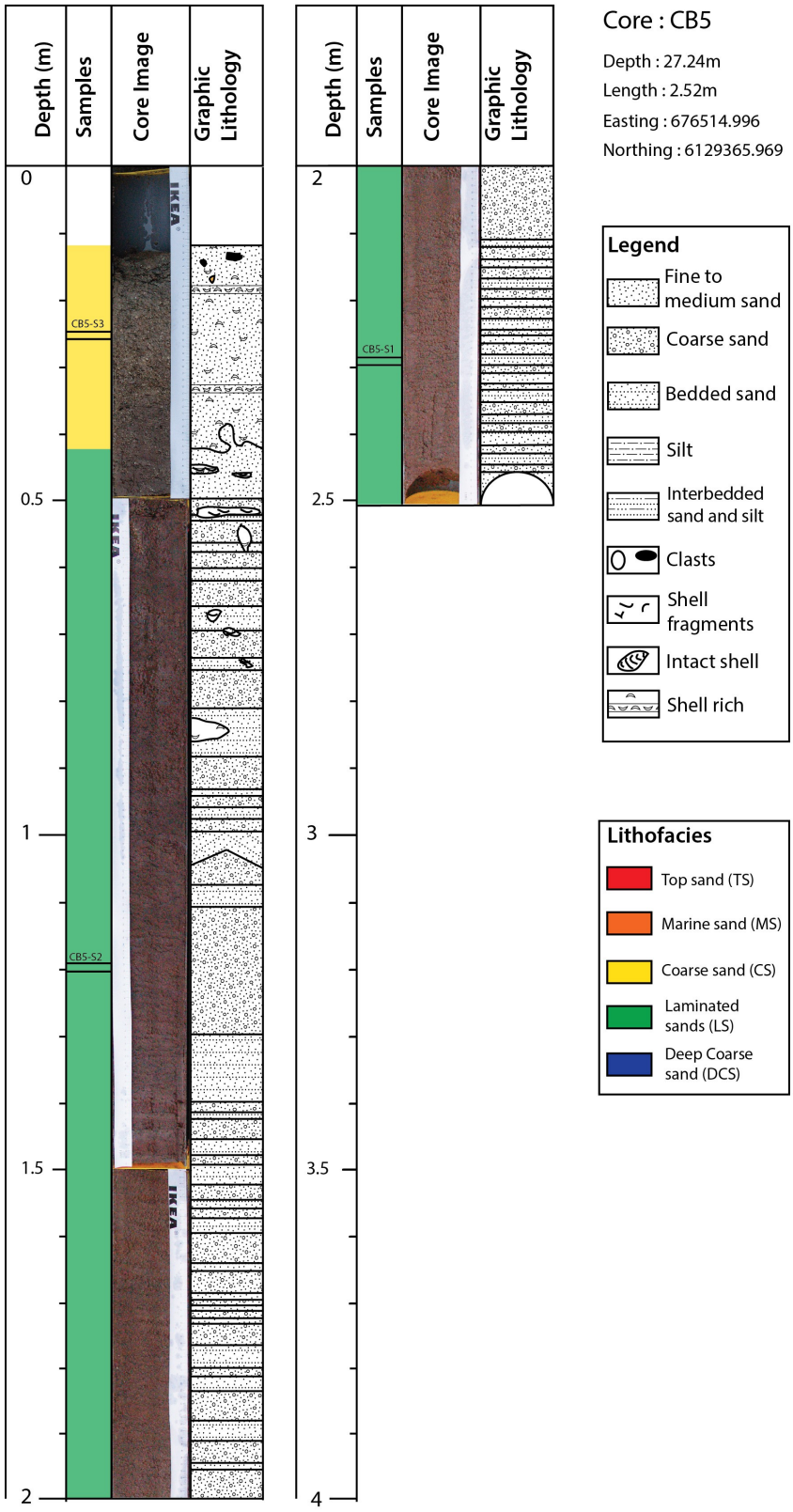

Figure 6.46: Simplified core log of core CB5 (full log in appendix 6.1, core CB5).

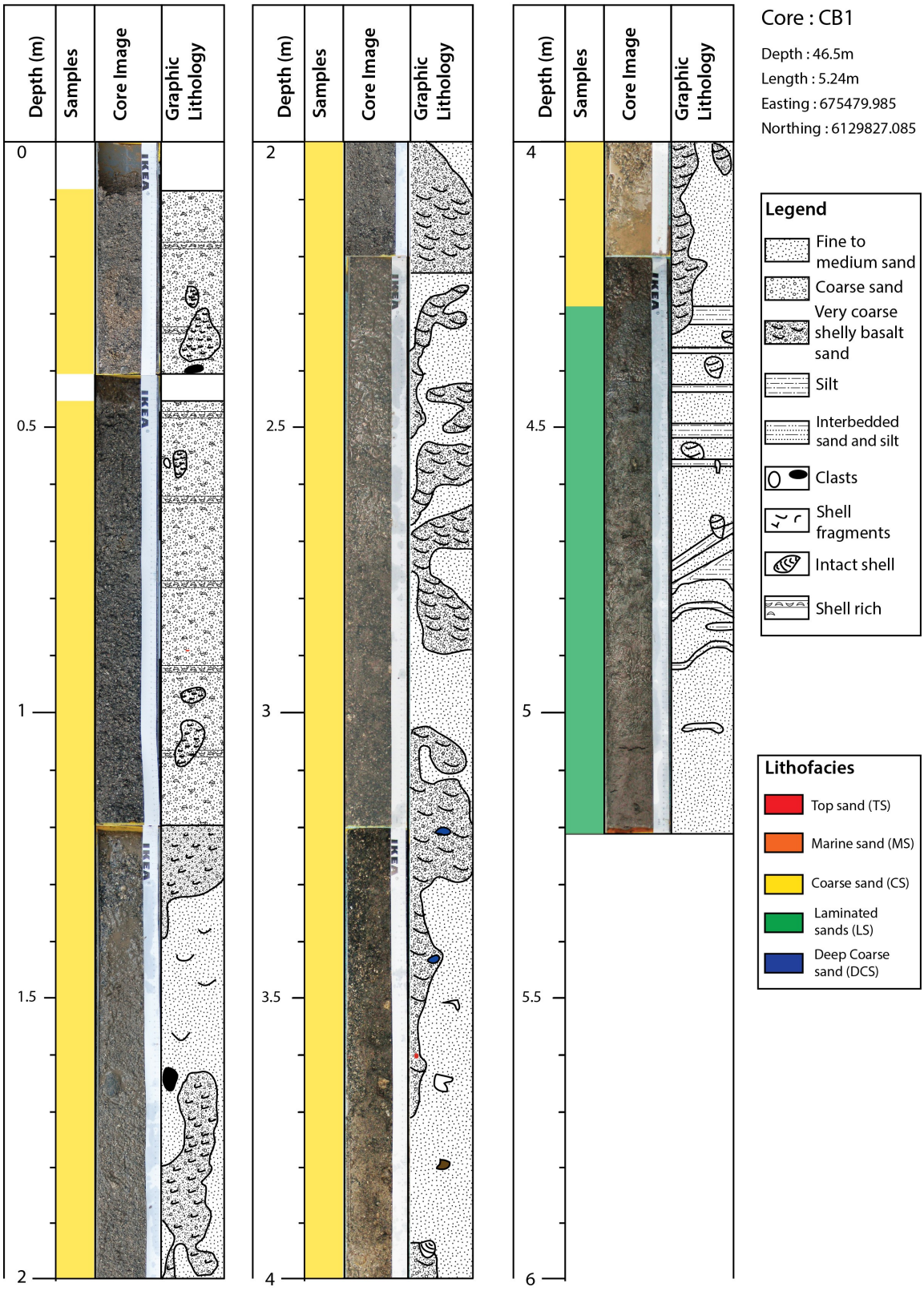

Figure 6.47: Simplified core log of core CB1 (full log in appendix 6.1, core CB1).

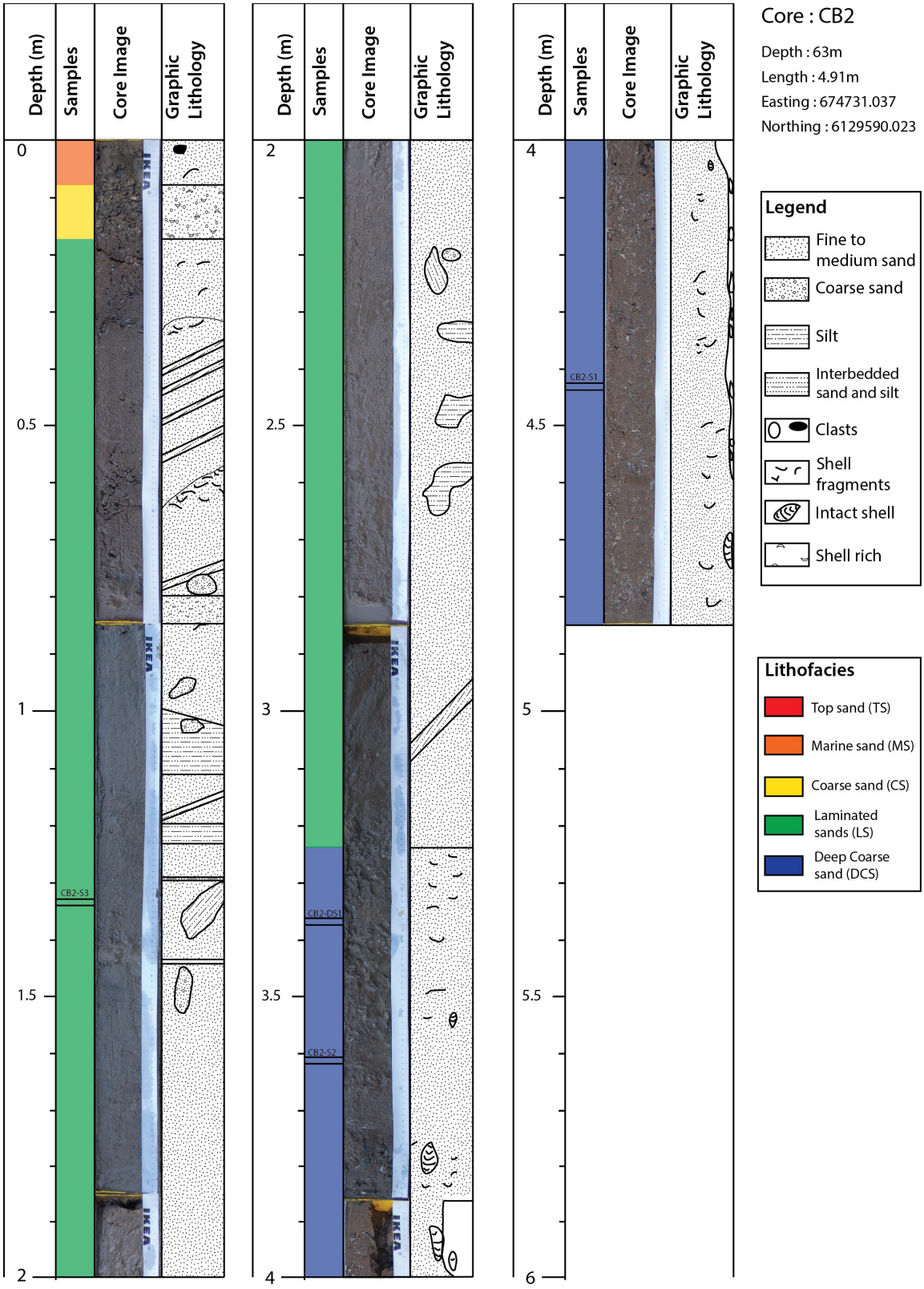

Figure 6.48: Simplified core log of core CB2 (full log in appendix 6.1, core CB2).

Marine Sand (MS):

This lithofacies was recognised as the topmost in 3 out of the 7 cores (figure 6.48). It is composed of grey brown fine to medium well sorted sand with some rounded clasts and shell fragments. It is only 10cm thick and lies conformably over the underlying Coarse Sand (CS) lithofacies. Its position and thickness made it very difficult to recognise any particular physical signature from the scanning process as most of its content was located in the top part of the core section where there are unavoidable alterations due to the plastic cap.

Top Sand (TS):

This lithofacies was only recovered in the shallowest core (CBT1, figure 6.45) on the inner shelf platform of Church Bay. There it is 5 m thick and is composed of fine to very fine very well sorted greyish brown sand with 1 to 2% shell fragments and only 1 rounded clasts was found in this core. It lies unconformably over the underlying Laminated Sand (LS) lithofacies. It is a massive lithofacies that is water saturated. It presents an average density of 2.02 g/cm^3, an average magnetic susceptibility of 140 (SI), an average Pwave velocity of 1560 m/s and an average resistivity of 0.85 Ohm.m.

Coarse Sand (CS):

This lithofacies was recognised in 6 of the 7 cores from Church Bay (figures 6.46 to 6.48). It forms the uppermost lithofacies or second uppermost lithofacies (under MS) where found and it lies conformably over the underlying LS lithofacies. It is composed of poorly sorted coarse shell fragments in a matrix of coarse sands with Basalt granules and has a thickness ranging from 0.1 to 1m with an average of 0.3m . Over the various cores, it presents an average density of 2.08 g/cm^3, an average magnetic susceptibility of 160 (SI), an average Pwave velocity of 1570 m/s and an average resistivity of 1.41 Ohm.m.

Laminated Sand (LS):

This lithofacies was found in every cores collected in Church Bay (figures 6.45 to 6.48). It lies unconformably below TS but conformably below MS and CS and above the Deep Coarse Sand (DCS) lithofacies. Its thickness is unknown as it was the lowest lithofacies hit for most cores except the deepest core (CB2) where it is 3m thick. It is composed of

interbedded bluish grey very fine sand to silt with greyish brown fine to medium sand both very well sorted. It contains less than 1% of shell fragments and very few rounded clasts only in 1 core. Some of the bedding was inclined at a 30° angle and/or was interrupted by patches of coarser poorly sorted sand with shell fragments. Over the various cores, it presents an average density of 2.07 g/cm^3, an average magnetic susceptibility of 84 (SI), an average Pwave velocity of 1608 m/s and an average resistivity of 1.16 Ohm.m.

Deep Coarse Sand (DCS):

This lithofacies was only hit in the deepest core (CB2, figure 6.48) of the area and was found to be the lowest lithofacies recovered there. It lies conformably below LS and was found over a length of 1.6m with its overall thickness there unknown. It is composed of light brown well sorted medium to coarse sand with about 5% of coarse shells including large intact inarticulated bivalves shells. It presents an average density of 2.14 g/cm^3, an average magnetic susceptibility of 175 (SI), an average Pwave velocity of 1670 m/s and an average resistivity of 1.28 Ohm.m.

6.2.1.2 Correlation between seismic units and lithofacies

Through the average P-Wave velocity for each of the lithofacies, a direct comparison of the seismic data and the retrieved core is presented for each of the cores in appendix 5.4.

The MS lithofacies cannot be correlated to any seismic units due to its low thickness that is below the vertical resolution of the seismic data for the area.

The TS lithofacies is easily correlated to the unit SCB5. This unit was only expected to be hit in the one core where TS was recognised (figure 6.49). However, the unit expected thickness and the recovered lithofacies's thickness do not match with the lithofacies being twice as thick as what was expected from the seismic. This could be due to a different Pwave velocity than the 1500 m/s used to convert travel time to depth but in this case, the lithofacies's average Pwave velocity was measured at 1560m/s. This difference does not account for the variation observed. It is possible that further deposition occurred at the location cored between the 2009 seismic survey and the 2012 coring survey but unlikely that it would show such a difference. Besides, the seismic data show the unit

SCB6 overlying SCB5 at the coring location but no change in lithofacies was observed on the retrieved core as TS was the first lithofacies hit. Some other unknown factor might be behind the distortion of the seismic data but it is also likely that the location cored differs from the location of the seismic survey due to inaccuracies for either or both of the surveys.

The CS lithofacies appears to correlate to the seismic unit SCB6 (figure 6.50) albeit with some thickness differences for cores CB1 (figures 6.47 and 6.51 where SCB6 is much thinner than CS), CBT1 (where CS is not recognised in the core), CB2 and CBT7 (where SCB6 is much thicker than CS). SCB6 is visible as the top seismic unit in most of the Church Bay area (section 6.1.6) and could therefore be highly mobile and account for these variations in thickness. However, the seismic signature of such a lithofacies made of coarse sand and shell fragments is expected to be much more chaotic and contain many reflection hyperbolae than unit SCB6 which appears mostly acoustically transparent on the data. In fact, the top of unit SCB4 displays those seismic characteristics and sits just below unit SCB6 and so could also be considered as a correlation for the CS lithofacies. This correlation is also problematic due to the lack of reflector marking the bottom of that spread of reflection hyperbolae whereas CS has a clear conformable contact with the underlying lithofacies LS. The correlation with SCB6 is then favoured.

The LS lithofacies is correlated to unit SCB4. It is omnipresent over the Church Bay area and its thickness and upper and lower contact present a good match to the seismic data for the 7 cores retrieved. Furthermore, the bedded nature of the lithofacies corresponds well with the observed wavy parallel internal reflectors of SCB4 (see core logs in appendix 6.1 and figures 6.45, 6.46, 6.47, 6.48 and 6.50). The correlation is not perfect however where in core CB1 the overlying CS is much thicker than unit SCB6 which lowers the depth of the upper boundary of LS over the expected upper boundary of SCB4, and where in core CBT1, a similar problem occurs with lithofacies TS as explained above. Nevertheless, overall the correlation is strong and satisfactory.

The DCS lithofacies is easily correlated to unit SCB3 (figure 6.50). This unit was only expected to be hit in the one core where DCS was recognised. It allows the study of the lower boundary of unit SCB4 correlated to lithofacies LS which appears as a conformable contact with lithofacies DCS (figure 6.48).

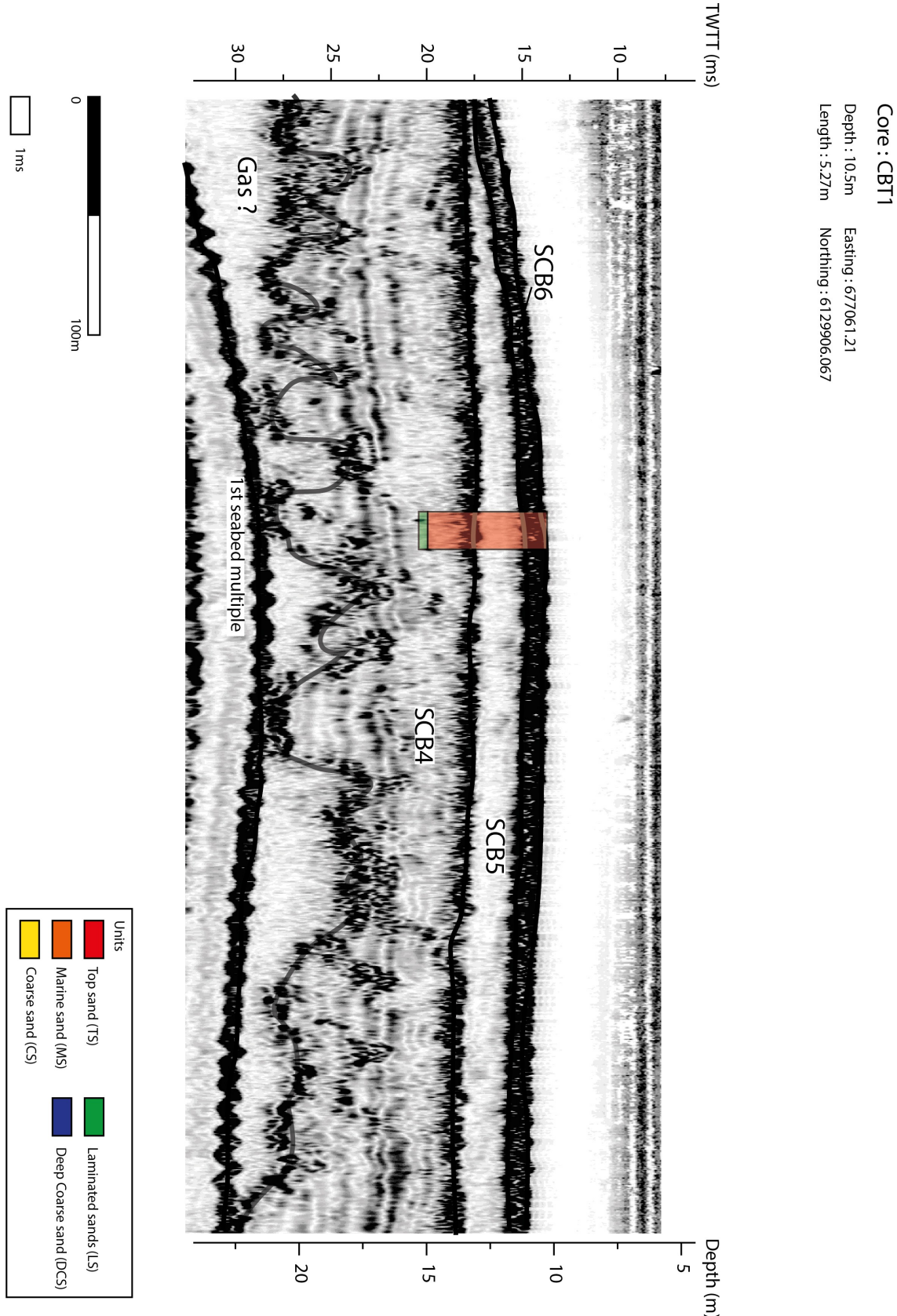

Figure 6.49: Simplified core log of CBT1 plotted over corresponding Pinger seismic data (zoomed in area of figure 6.29).

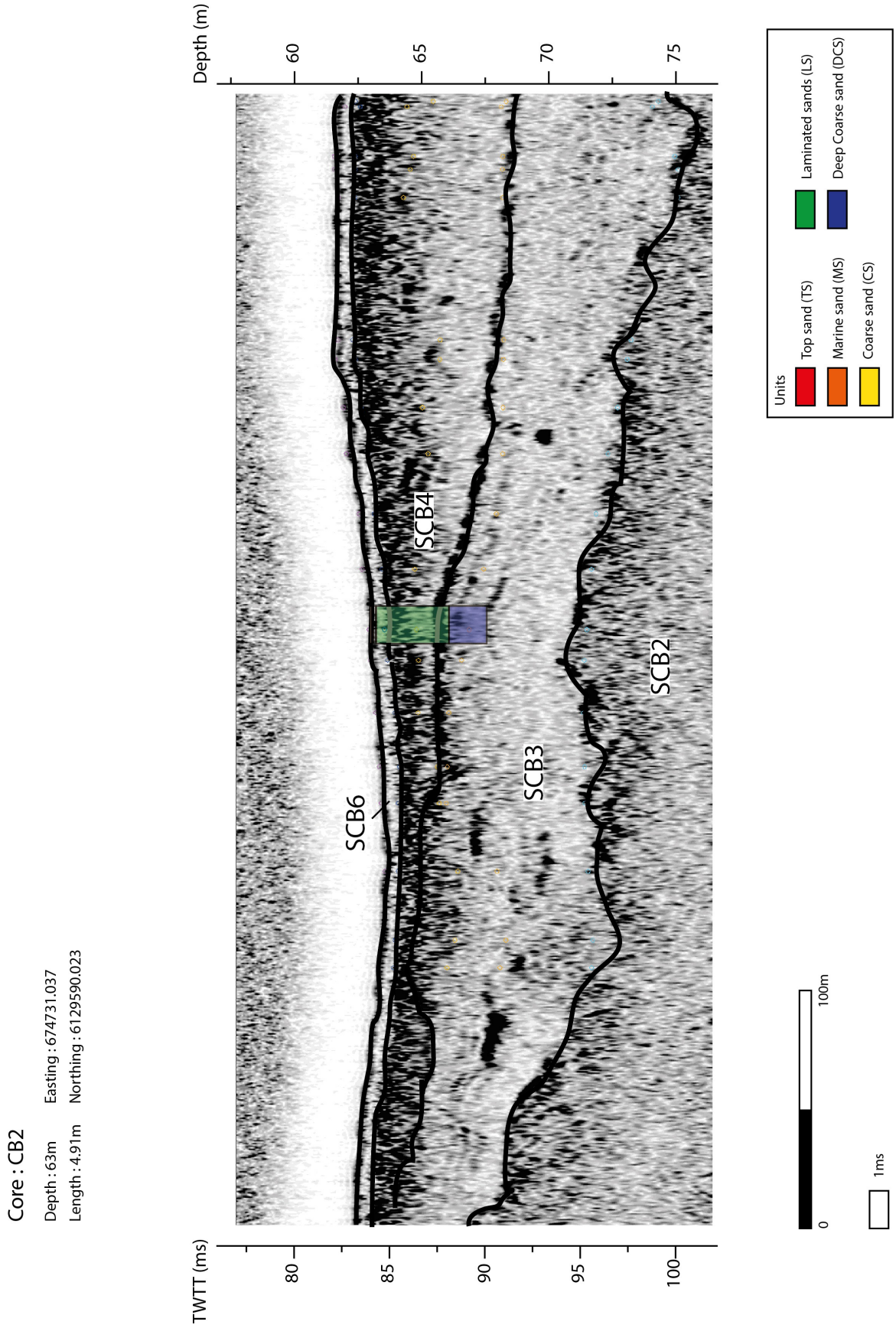

Figure 6.50: Simplified core log of CB2 plotted over corresponding Pinger seismic data (zoomed in area of figure 6.30).

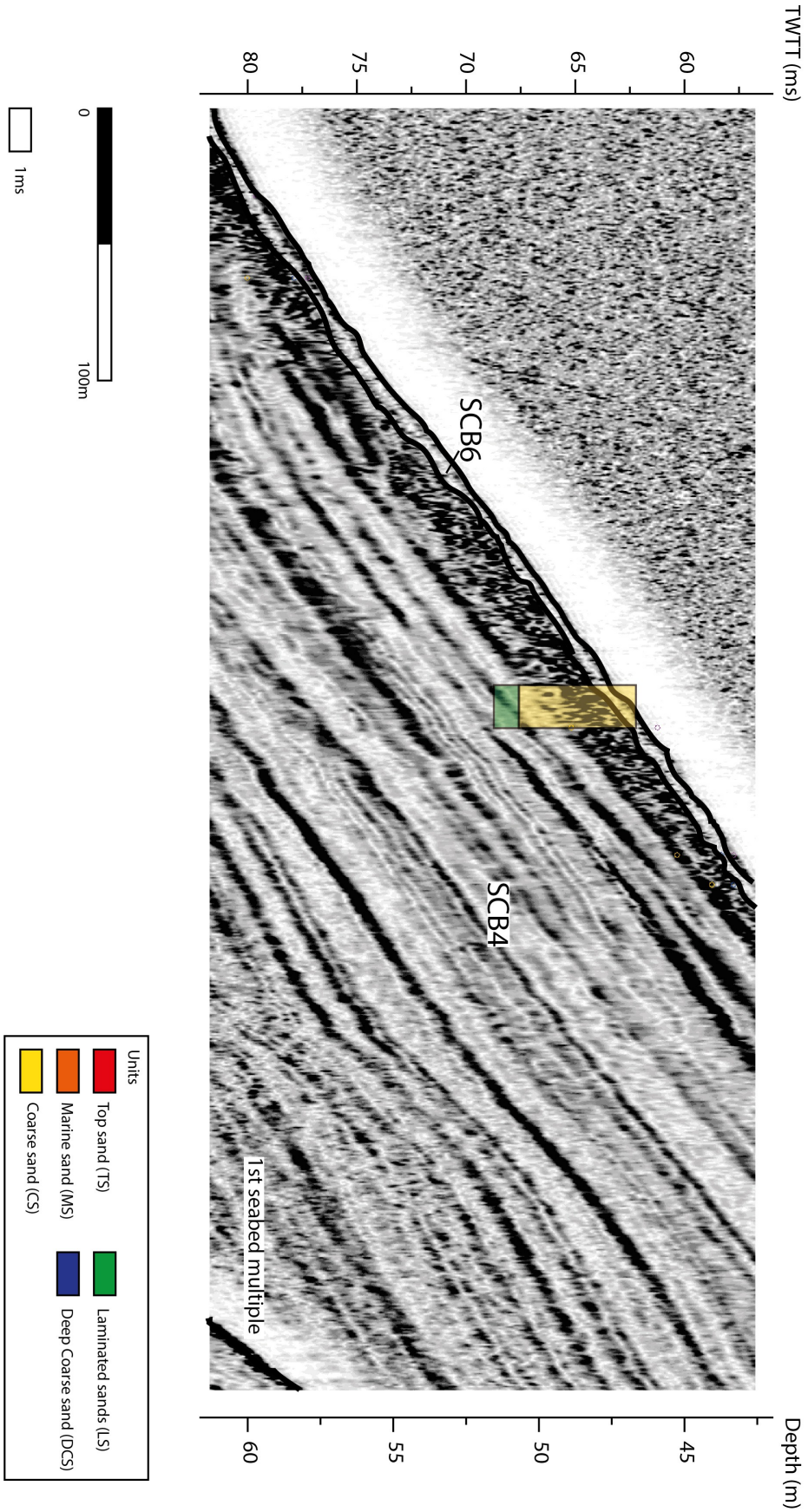

Figure 6.51: Simplified core log of CB1 plotted over corresponding Pinger seismic data (zoomed in area of figure 6.30).

6.2.1.3 Biostratigraphy based on foraminifera assemblages

The 10 samples processed were picked from in order to retrieve 200 to 300 individuals for identification and comparison of the assemblages:

- 3 samples were collected from core CB5, retrieved at 27m depth, each at about 1m distance from the other; 2 from the lithofacies LS and 1 from the surficial CS (figures 6.46 and 6.51 and appendix 6.1, CB5).
- 3 samples were collected from core CBT1, retrieved at 10m depth; 2 from the lithofacies TS (including 1 at 12cm from the seabed) and 1 from the lithofacies LS at the bottom of the core (figures 6.45 and 6.52 and appendix 6.1, CBT1).
- 4 samples were collected from core CB2, retrieved at 63m depth; 1 from the lithofacies MS at 3 cm from the seabed, 1 from the lithofacies LS and 2 from the lithofacies DCS (figures 6.48 and 6.53 and appendix 6.1, CB2).

The coarse sampling strategy was selected due to time constraints and with an effort to understand gross environmental change as a contrast in assemblages from one lithofacies to the next. In total, 4 samples were picked from the lithofacies LS, 2 from the lithofacies TS and DCS and 1 from the lithofacies CS and MS. Only a fraction of these samples were picked except for the 2 samples from lithofacies DCS where the totality of the sample was picked but less than 100 individuals were present (appendix 6.3). These 2 samples, CB2-S1 and CB2-S2, were then considered barren and their assemblage could not be compared to the other samples. The results of the identification for the 10 samples is presented for the 3 cores in figures 6.52 to 6.54.

As mentioned above, the lithofacies DCS contained so few individuals that it is considered to represent a barren assemblage.

The lithofacies LS presented an assemblage of mainly *Elphidium* species (in particular *E. excavatum*) and *Cassidulina obtusa*. Present are also some substrate-fixed species (in particular *Cibicides lobatulus*), some planktonic species (in particular *Neogloboquadrina incompta*), some *Quinqueloculina* species (in particular *Q. semilunum*) and some from other orders. Individuals picked from this lithofacies were relatively smaller than the ones from the other samples. This assemblage corresponds to temperate seas and modern assemblages found in the Celtic Sea or the English Channel (Murray, 2006).

The lithofacies TS, CS and MS presented very similar assemblages that appear to indicate similar conditions at the time of deposition. The typical assemblage is composed of mainly substrate fixed species (in particular *Cibicides lobatulus*). Present are also some *Elphidium* species (in particular *E. excavatum*) especially in lithofacies CS, some planktonic species (in particular *Neogloboquadrina incompta*) especially in lithofacies TS, some *Quinqueloculina* species (in particular *Q. semilunum*) and some from other orders. These 3 lithofacies are the uppermost found in the area and so the assemblage here reflect the modern temperate deposition conditions. The preponderance of substrate fixed species is due to the modern local high energy waves depositing a coarse sand and shell sheet for these species to find sanctuary (Murray, 2006).

The two main assemblages are distinct as being either *Elphidium*-rich, with a preponderance of *Elphidium excavatum*, or rich in substrate fixed species, in particular *Cibicides lobatulus*. Murray (2006) doesn't present a difference in the sea temperature of these assemblages deposits but gives a sedimentary origin for their difference:

- substrate fixed species are associated with coarser sand and shells as is the case for lithofacies CS and, to a certain extent, TS and MS
- *Elphidium* rich assemblages are associated with finer sand to mud deposits as is the case of the silty beds of LS.

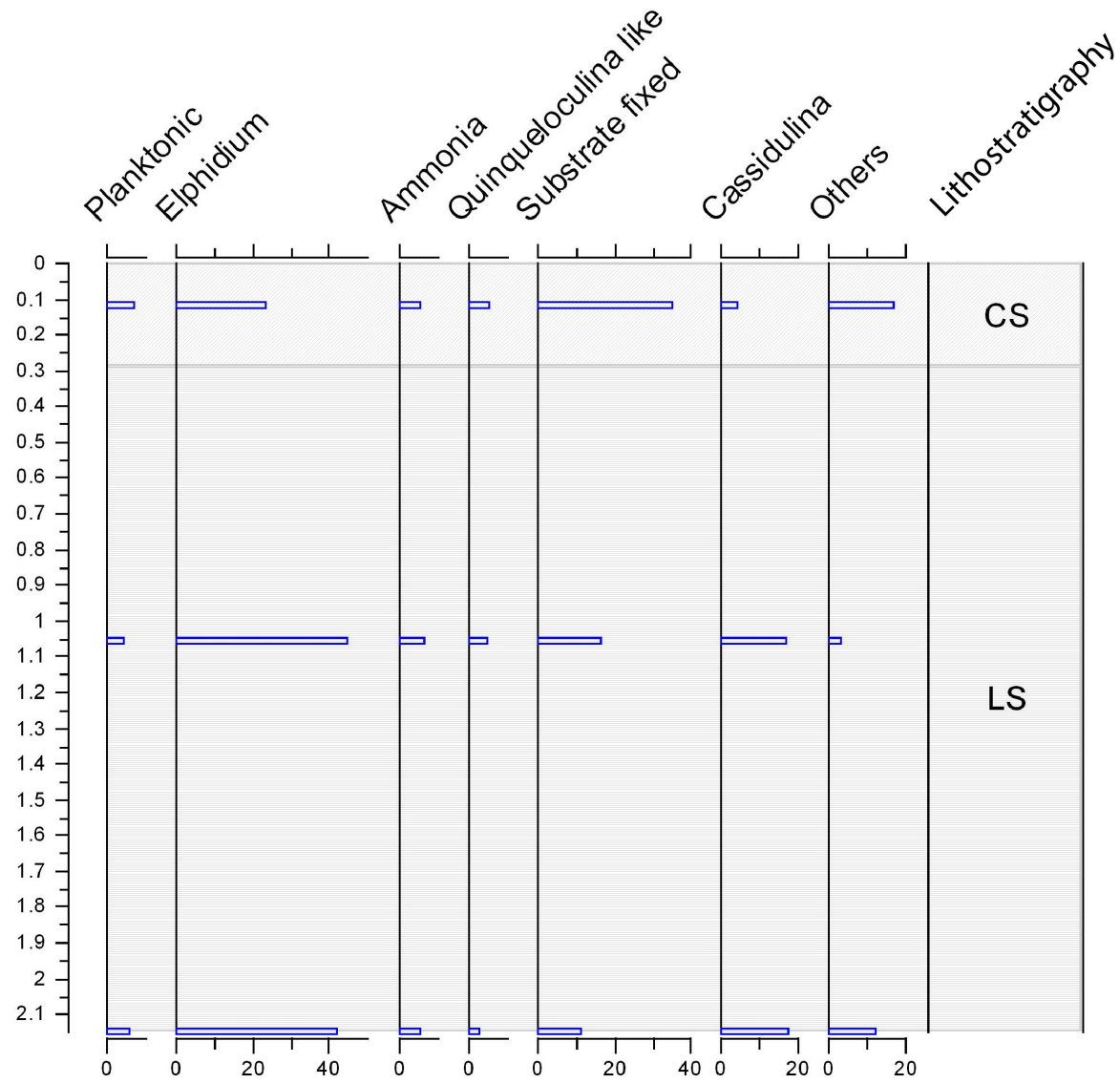

Figure 6.52: Relative proportion of main orders of foraminifera for core CB5 with associated sub-bottom lithostratigraphy.

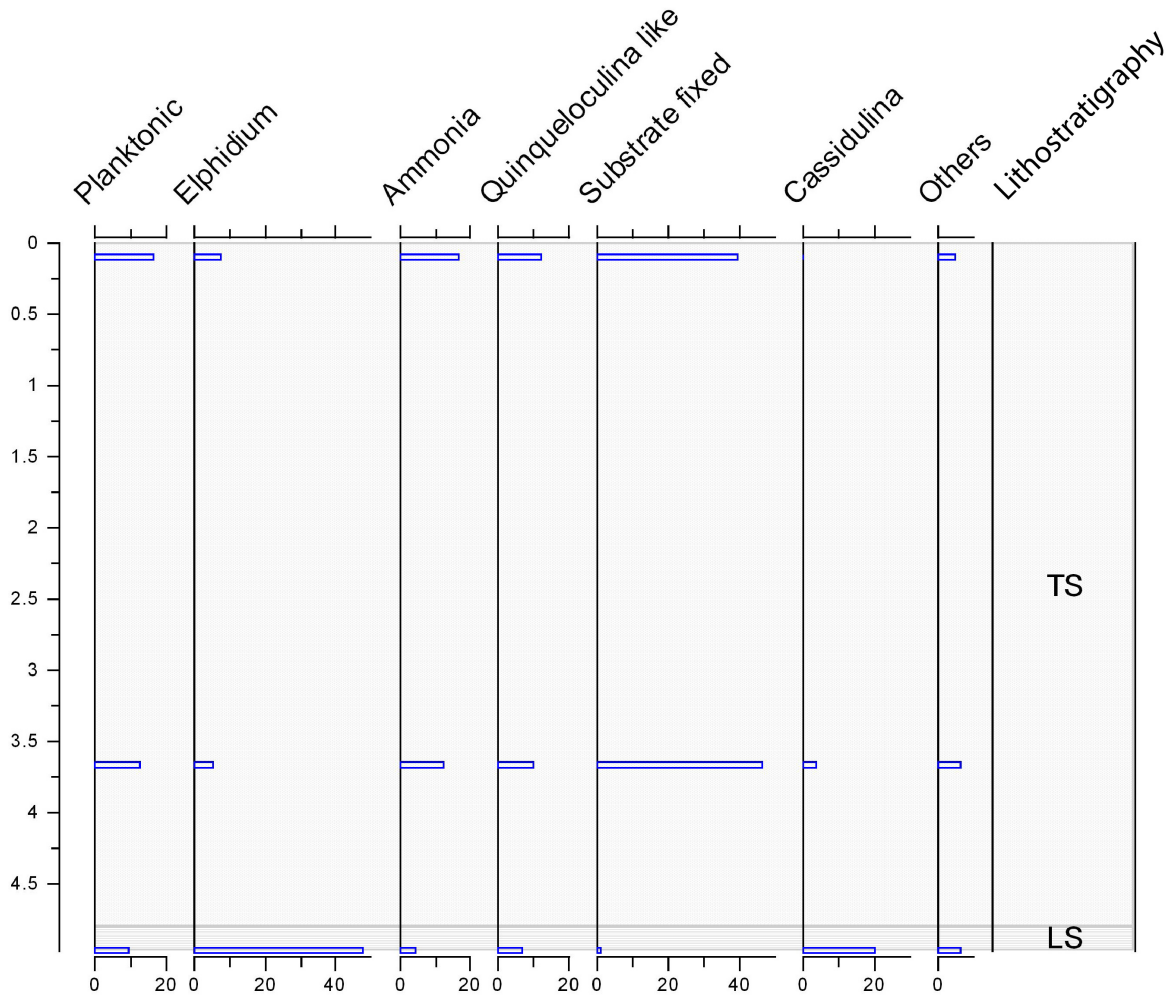

Figure 6.53: Relative proportion of main orders of foraminifera for core CBT1 with associated sub-bottom lithostratigraphy.

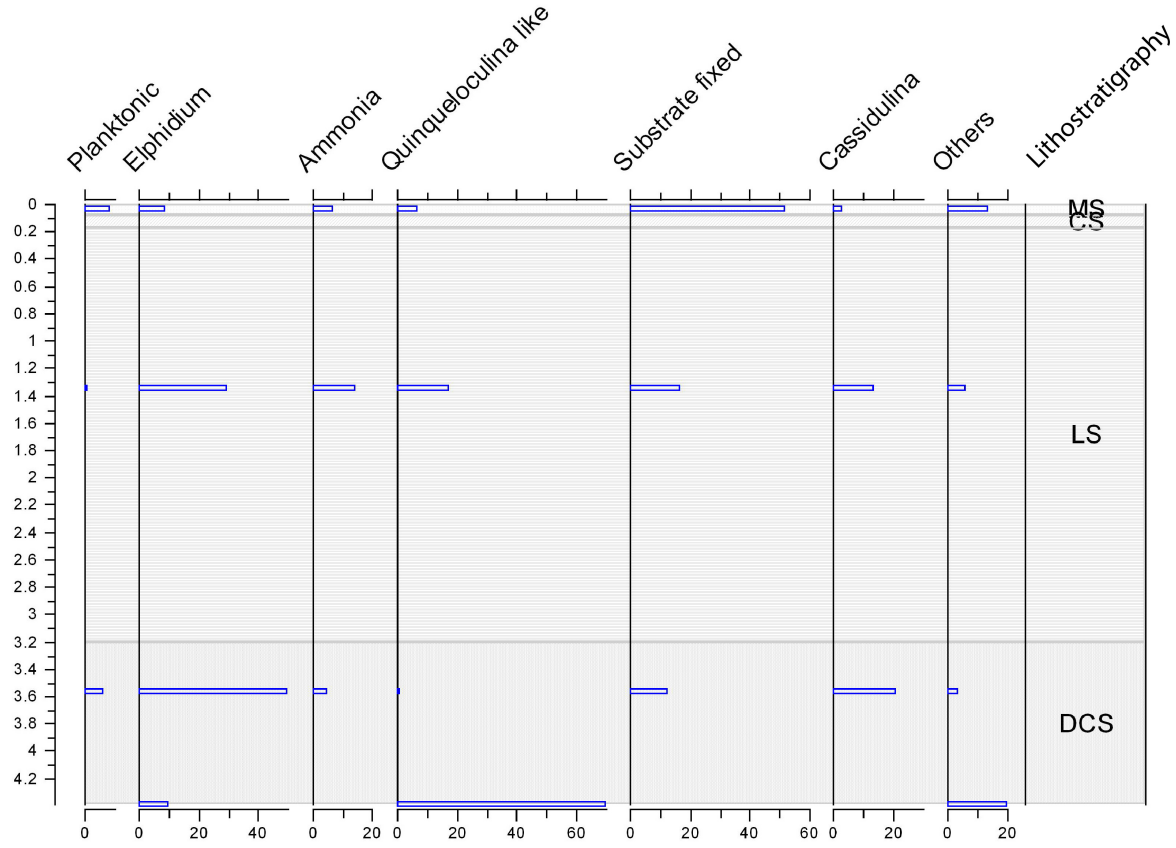

Figure 6.54: Relative proportion of main orders of foraminifera for core CB2 with associated sub-bottom lithostratigraphy.

6.2.1.4 Radiocarbon dating

The 4 samples sent for radiocarbon dating were collected from 2 different cores; 3 from CBT1 and 1 from CB2. The sample in CB2 was chosen for its potential in dating the deposition of lithofacies DCS and giving a maximum age constraint for the deposition of lithofacies LS. The samples in CBT1 targeted the erosional surface at the top of lithofacies LS in the hope of constraining its age by both a maximum and a minimum date. Figure 6.55 presents the location and calibrated results of these samples in the 2 cores and their relative place in the stratigraphy. The samples were composed of articulated and unarticulated bivalves whose size were over 250 μm. The raw radiocarbon and calibrated dates are presented in appendix 6.4.

The 1 sample collected from CB2 was taken from the lithofacies DCS in order to get a general idea of the age of its deposition but mainly to give time constraint to the first deposition of lithofacies LS. Similarly the 3 samples from CBT1 aimed at precisely dating the contact between the eroded top surface of lithofacies LS and the start of deposition of lithofacies TS.

The dates obtain define a general time frame for the deposition of lithofacies LS as it is more recent than 17150 (+/-300) years BP. And the unconformity between LS and TS appears to date to around 11000 years BP. However, the three dates obtained in core CBT1 do not sit as chronologically expected with the deepest sample displaying a younger date. This could be due to active reworking of the lower strata around the erosional contact and further dates below or above the contact are necessary to precisely constrain this erosional event.

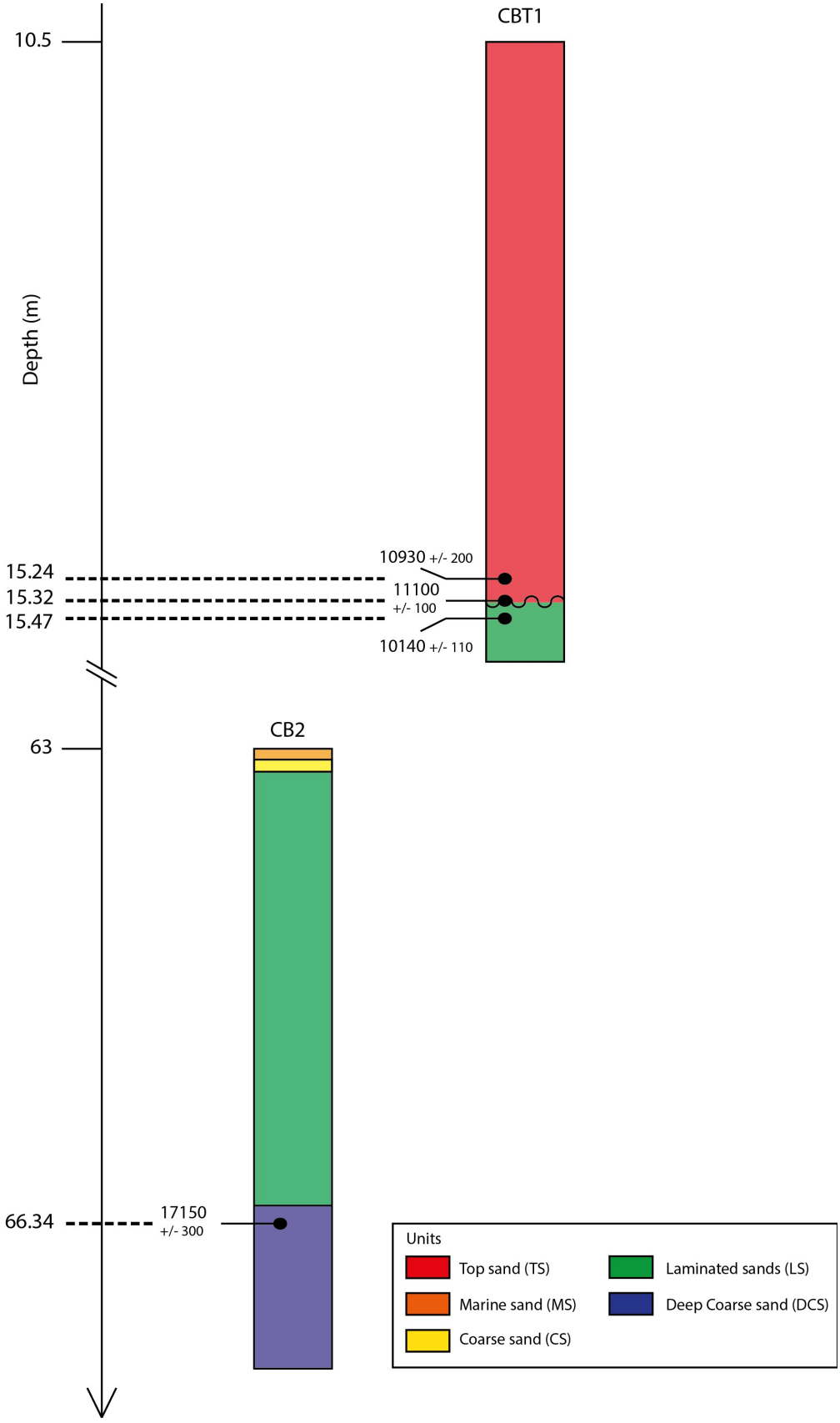

Figure 6.55: Depth of dated samples of bivalves for cores CBT1 and CB2 in Church Bay. The dates indicated are calibrated years BP.

6.2.2 Runkerry Bay

4 cores were collected in Runkerry Bay with an average of 2m of sediments retrieved. Their locations is summarised in table 3.6 and plotted on figure 3.16.

6.2.2.1 Lithofacies recognised

3 lithofacies were recognised for the cores collected in Runkerry Bay and their description is summarised in table 6.11 below. The simplified log of two cores (RK2 and RK4) selected on their singularity are presented in figures 6.56 to 6.57.

Lithofacies name	Description	Top contact	Thickness (m)	Seismic unit correlation
Marine Sand (MS)	Light grey very well sorted medium sand with hardly any shell fragments.	seabed	1 to 2	SRK5
Bedded sands and pebbles (BS)	Laminated beds of fine to medium sand alternating layers containing Chalk grains and Basalt grains. There are two layers of rounded granules and pebbles at the bottom of the unit.	unconformable with MS	0.45	Internal reflector of SRK5
Finer Sand (FS)	Grey very well sorted fine to medium sand	unconformable with MS but conformable with BS	Unknown (at least 1m)	Lower half of SRK5

Table 6.11: Description of lithofacies recognised for Runkerry Bay.

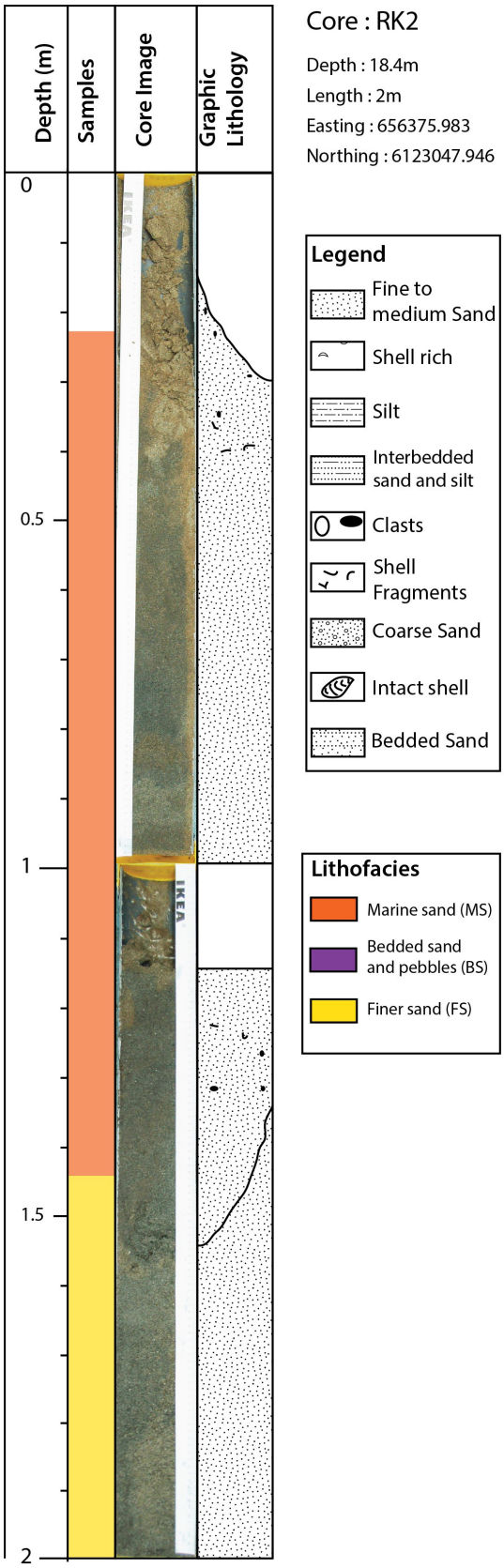

Figure 6.56: Simplified core log of core RK2 (full log in appendix 6.1, core RK2).

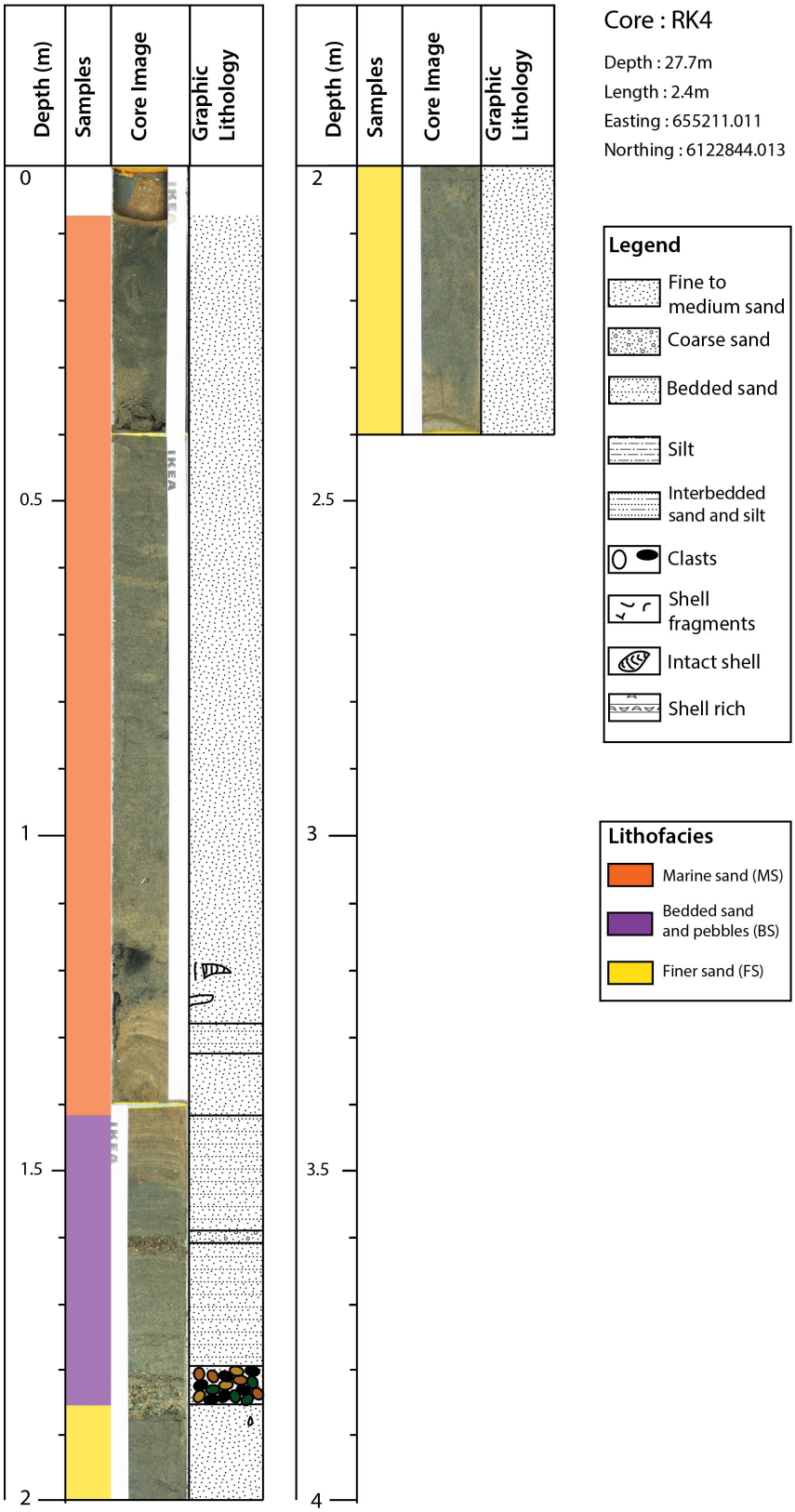

Figure 6.57: Simplified core log of core RK4 (full log in appendix 6.1, core RK4).

Marine Sand (MS):

This lithofacies was recognised as the topmost lithofacies in all the cores collected in Runkerry Bay (figures 6.56 and 6.57). It is composed of light grey medium very well sorted sand with hardly any shell fragments. It is 1 to 2m thick when fully sampled and lies unconformably over the underlying Bedded Sand and Pebbles (BS) and Finer Sand (FS) lithofacies. Over the various cores, it presents an average density of 1.8 g/cm^3, an average magnetic susceptibility of 85 (SI), an average Pwave velocity of 1509 m/s and an average resistivity of 0.93 Ohm.m.

Bedded Sands and pebbles (BS):

This lithofacies was only hit in 1 core (RK4, figure 6.57) where it was 0.45m thick. It is composed of laminated beds of fine to medium sands alternating layers containing a majority of Chalk grains and Basalt grains. A thin layer (3cm) of rounded granules lies in the middle of these beds and a thicker layer (7cm) of rounded pebbles lies at the bottom. This lithofacies is located at an unconformity between the overlying MS and underlying FS. It presents an average density of 1.95 g/cm^3, an average magnetic susceptibility of 43 (SI), an average Pwave velocity of 1600 m/s and an average resistivity of 0.91 Ohm.m.

Finer Sand (FS):

This lithofacies was found in 2 out of the 4 cores of Runkerry Bay where it lies as the lowermost lithofacies (figures 6.56 and 6.57). It sits unconformably below MS but conformably below BS. Its thickness is unknown but the lithofacies was found over 1m in length in 1 of the cores. It is composed of grey very well sorted fine to medium sand. Over the various cores, it presents an average density of 1.78 g/cm^3, an average magnetic susceptibility of 50 (SI), an average Pwave velocity of 1470 m/s and an average resistivity of 0.88 Ohm.m.

6.2.2.2 Correlation between seismic units and lithofacies

The MS lithofacies is correlated to the unit SRK5 (figure 6.58). MS was recognised as the uppermost lithofacies for the 4 cores retrieved for the area. The transparent acoustic signature of the unit corresponds well with the massive sand nature of the MS lithofacies.

The BS lithofacies was only recognised in core RK4 where it appears to correlate to an internal reflector of unit SRK5 (figure 6.58). This reflector appears wavy parallel to the seabed surface and has an acoustic signature made of hyperbolae which corresponds well to the the two layers of granules and pebbles found in the lithofacies. This internal reflector was only found in the seismic data around the area of the core target and at an average depth of -30m.

The FS lithofacies was recognised in 2 of the 4 cores of the area and only when a prominent internal reflector of unit SRK5 was crossed. It is hence correlated to the bottom part of unit SRK5 (figure 6.58) but is very similar in nature and physical parameter to the MS lithofacies. The internal reflector forming the upper boundary of the lithofacies is interpreted as an erosional contact between relatively modern marine sand sediments.

The seismic correlation shows that the core RK6 stops at another internal reflector which can be due to the gravelly layers described above for lithofacies BS preventing the vibrocorer to progress (figure 6.59). Similarly, in core RK5, the lower limit of the core appears to correspond to the upper limit of unit SRK4. The nature of this contact could also be more gravelly but we are unable to confirm.

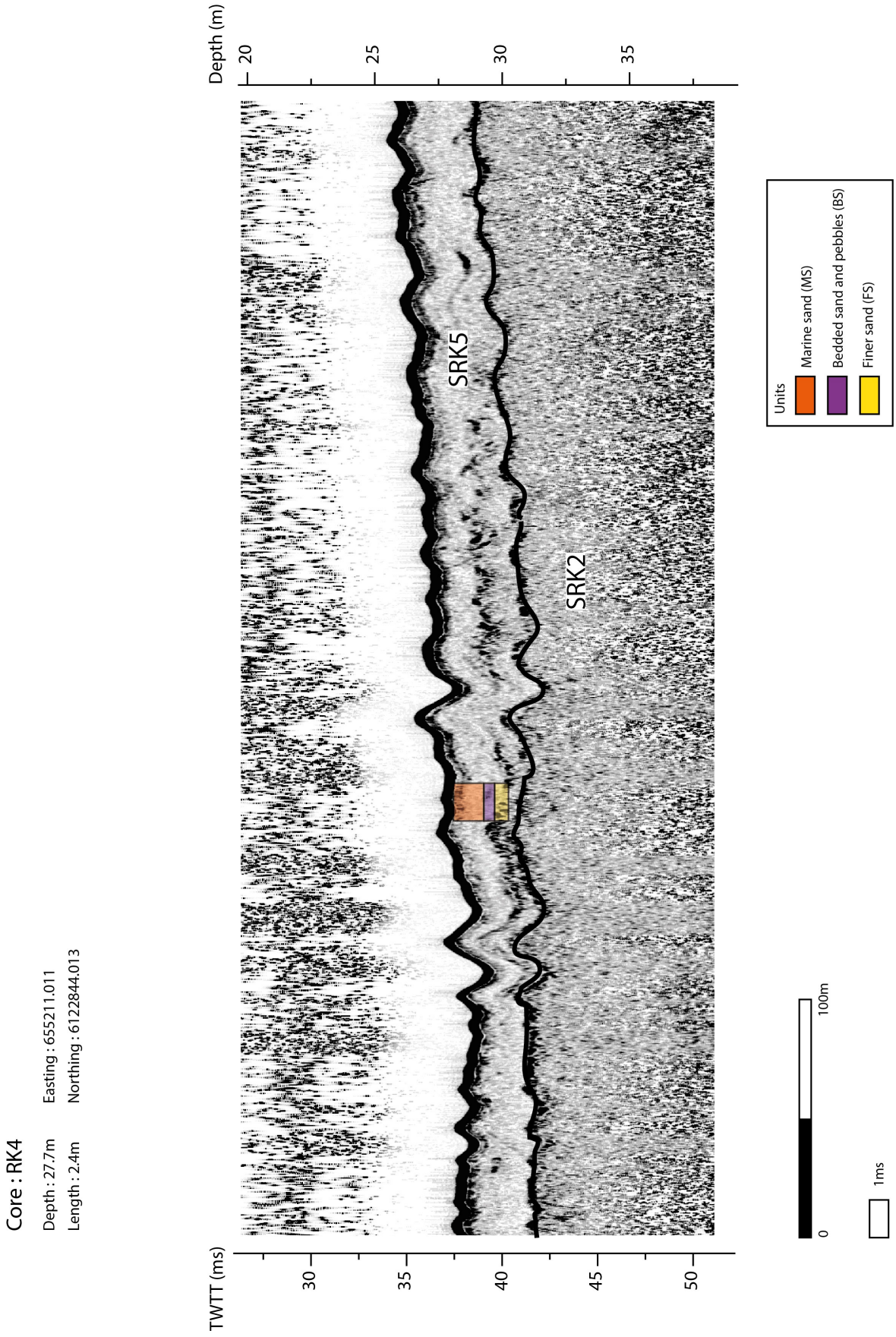

Figure 6.58: Simplified core log of RK4 plotted over corresponding Chirp seismic data.

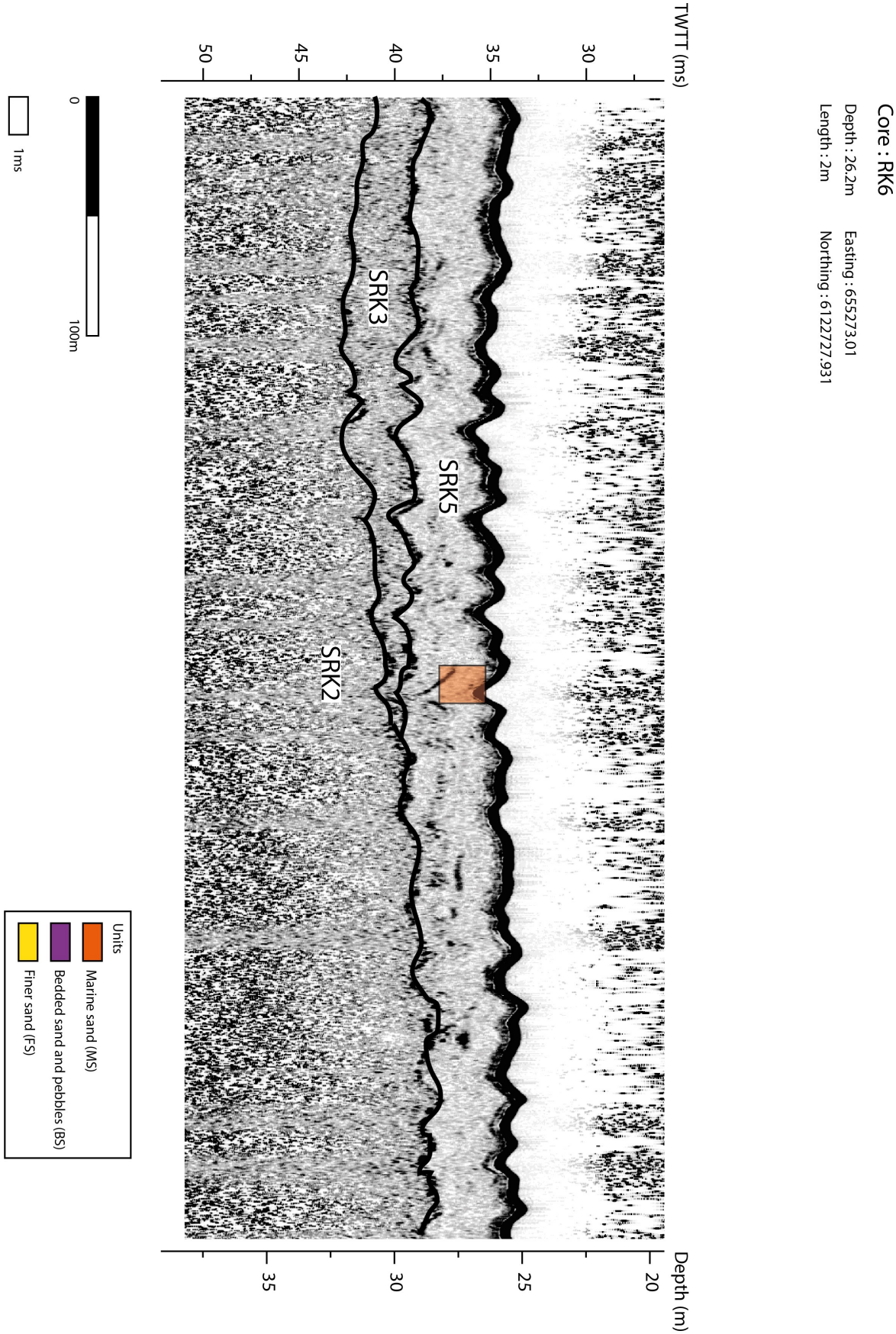

Figure 6.59: Simplified core log of RK6 plotted over corresponding Chirp seismic data (zoomed in area of figure 6.11).

6.2.2.3 Biostratigraphy

No micropalaeontological analysis were carried out for the lithofacies recognised in this area due to the limited recovery of the coring process. Only the top seismic unit was recovered and the depositional environment of the recognised lithofacies is assumed as modern.

6.2.3 The Bann estuary area

3 cores were collected in the Bann estuary area with an average of 1.5m of sediments retrieved. Their locations is summarised in table 3.6 and plotted on figure 3.17.

6.2.3.1 Lithofacies recognised

1 lithofacies was recognised for the cores collected in the Bann estuary area and its description is summarised in table 6.12 below. The simplified log of one core (PS3) selected on its singularity is presented in figure 6.60.

Lithofacies name	Description	Top contact	Thickness (m)	Seismic unit correlation
Marine Sand (MS)	Light brown medium sand with some isolated large shell fragments.	seabed	Unknown (at least 1.5m)	SPS5

Table 6.12: Description of the lithofacies recognised for the Bann estuary area.

Marine Sand (MS):

This unit was the only unit recovered in all the cores collected in the Bann estuary area (figure 6.60). It is composed of light brown medium sand with some isolated shell fragments. Its thickness is unknown but the unit was found over 1.5m in length in 1 core. Over the various cores, it presents an average density of 2 g/cm^3, an average magnetic susceptibility of 42 (SI), an average Pwave velocity of 1650 m/s and an average resistivity of 0.93 Ohm.m.

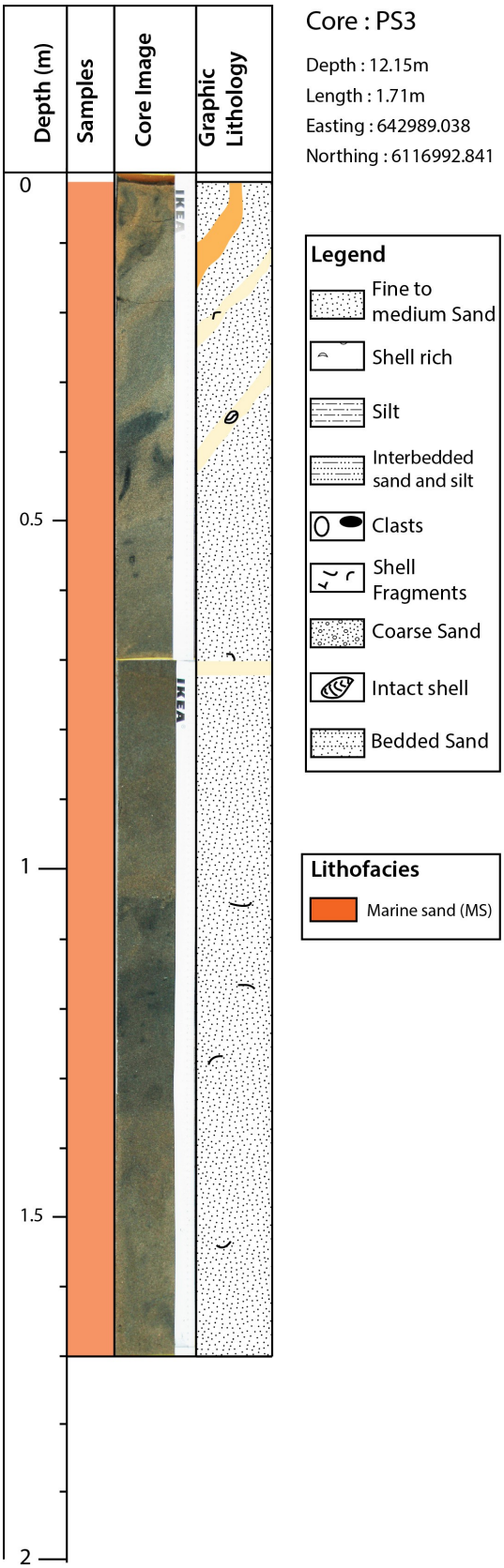

Figure 6.60: Simplified core log of core PS3 (full log in appendix 6.1, core PS3).

6.2.3.2 Correlation between seismic units and lithofacies

The MS lithofacies was recognised as the uppermost lithofacies for the 3 cores retrieved for the area and is correlated to the unit SPS5 (figure 6.61). MS. The transparent acoustic signature of the unit corresponds well with the massive sand nature of the MS lithofacies.

The seismic correlation shows that, at the location for cores PS3 and PS4, internal reflectors of unit SPS5 were crossed but no changes in the lithofacies were observed on the cores retrieved (figure 6.61). This could be due to the fact that in fact, the seismic data is slightly contracted and these reflectors formed a lower boundary that the corer could not penetrate.

6.2.3.3 Biostratigraphy

No micropalaeontological analysis were carried out for the lithofacies recognised in this area due to the limited recovery of the coring process. Only the top seismic unit was recovered and the depositional environment of the recognised lithofacies is assumed as modern.

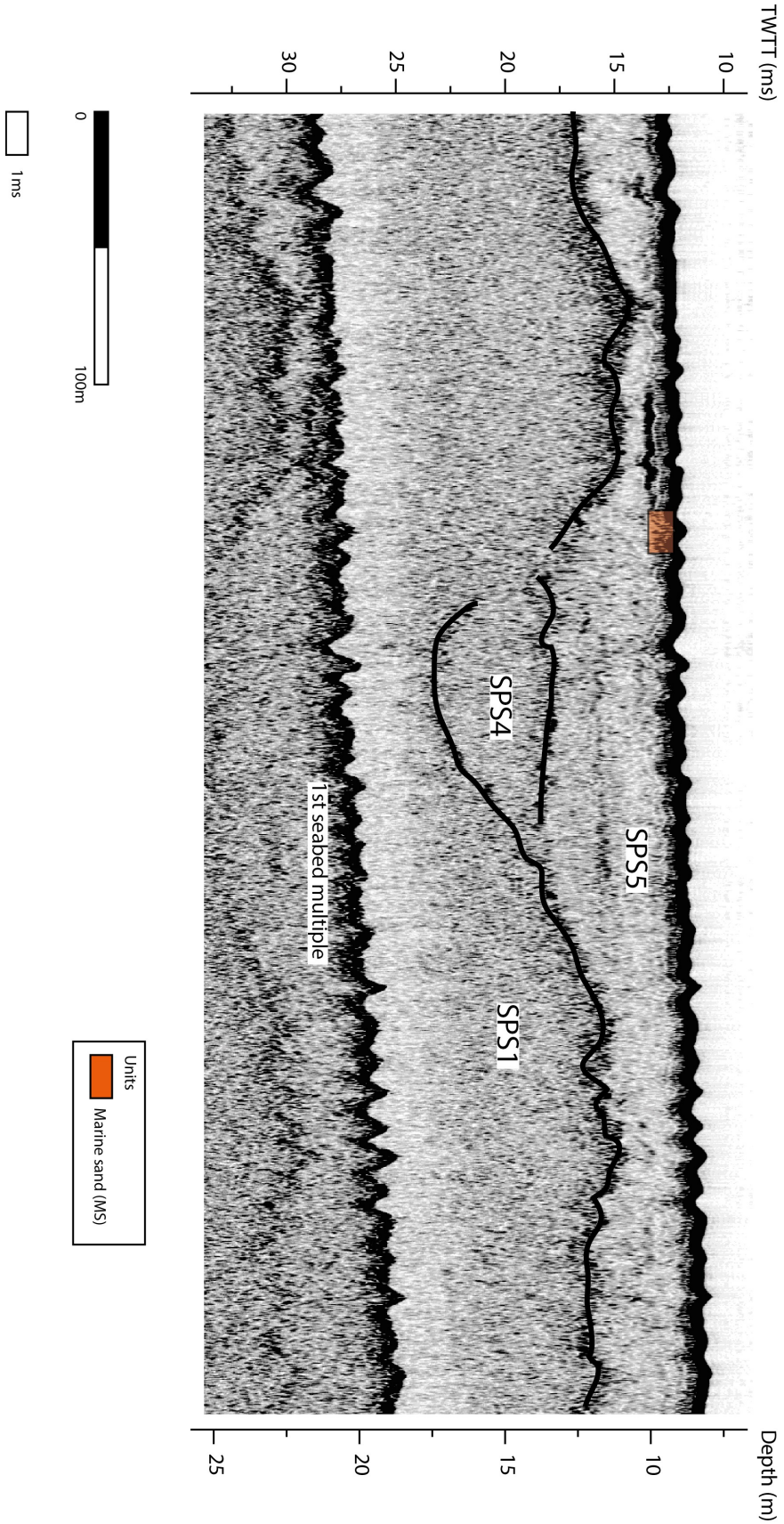

Figure 6.61: Simplified core log of PS4 plotted over corresponding Chirp seismic data (zoomed in area of figure 6.17).

6.2.4 Conclusions on bays targeted for coring

6.2.4.1 Depositional scenario for Church Bay

In the Church Bay area, 4 out of the 6 seismic units recognised were sampled in the coring process. This can help us give an insight into the recent depositional history for the bay. The outcropping nature of the upper boundary of SCB1 (see figures 6.31 and 6.32) would suggest that it represents the local bedrock potentially as it was left behind after the British Irish ice sheet retreated from this coastline. Due to its chaotic acoustic signature with point reflectors and draping morphology, unit SCB2 is interpreted as a unit of either glacial till or glacial diamict. Its relative thinness where the unit is visible (figure 6.34) could be the result of a limited period of deposition associated with ice movement.

Unit SCB3 was sampled and described as lithofacies DCS and appears to be a marine sand deposit with rapid deposition and/or reworking. This interpretation is based on its coarse sand and large intact bivalve shells components with hardly any microfaunal individuals. This reduced planktonic signal could be due to winnowing of the deposit although unlikely due to its depth (from 50 to 70m) which precludes any strong wave influence, even at the modelled lowstands for the area (section 2.4.3). Alternatively, it could be the result of slumping material from the main slope of the near shelf as it is only seen draping unit SCB2 at the bottom of this slope. Unit SCB3 was dated to 17150 years BP (+/- 300) which would make this deposit contemporary with the recently suggested date (Clark et al., 2012) for the readvance of Scottish ice responsible for the formation of the Armoy moraine (section 2.2.1). This readvance could then be the origin of this unit as the ice movement pushed sediments down the slope. Such a readvance would have isostatic effects on the local RSL, as the ice would locally depress the land but as yet, the thickness and length of time the Scottish ice was flowing or resting on this area are unknown. Nevertheless, such processes would have tectonic effects which could result in unconsolidated sediment instability and turbidity deposition.

Unit SCB4 was sampled and described as lithofacies LS. This unit is unique in the regional seismic datasets. Nowhere else are such extensive wavy parallel continuous internal reflectors been recorded (see figure 6.29 to 6.31). These correspond to beds of sands and silt containing a majority of smaller bivalves shells and smaller foraminifera

(relatively to those found in the other lithofacies of the area), potentially deposited seasonally with the finer sediments found in times of lower marine energy (figures 6.46 and 6.62 and appendix 6.1, core CB5). This would indicate conditions different to today where no particular seasonality is observed in Church Bay. Besides the finer nature of the sediments retrieved in LS suggests an environment with lower energy perhaps associated with falling RSL. But this could also be due to a change in sediment supply or a change in general climate conditions particularly when taking into account the sheltered nature of the bay. The SCB4 unit covers the underlying units as a slope front fill and appears on the whole as sygmoidal progradation deposit (section 6.1.6). Foraminifera assemblages collected from this unit indicates conditions similar to those found in the English Channel or the Celtic Sea at present and the dating evidence indicates a deposition constrained to after 17150 years BP (+/-300) and suggests marine deposition occurred until at least 11100 years BP (+/- 100). However a conflicting earlier date was found 15 cm below the later one which could indicate reworking of the sediment or that the deposition incorporated older foraminifera. Nevertheless, these two constraints place the deposition of lithofacies LS at the start of the Holocene just after the Younger Dryas (section 1.1.1) during the modelled period of lower than present RSL for the area (section 2.4.3 and figure 2.20). Additionally, RSL is here constrained as being above -66m elevation by 17150 years BP (+/- 300) and around -15m elevation by about 10000 years BP.

The topset of unit SCB4 is missing as the upper unit SCB5 truncates some of its internal reflectors (figure 6.29). This unconformity forms a platform at the depth of about 15m and it is suggested that wave action is responsible for the removal of the topset of unit SCB4. The TS lithofacies then covered this platform with about 5m of massive water saturated marine sand sediments with hardly any clasts or shells visible. The foraminifera biota of TS is composed mainly of substrate attached species which suggests temperate marine waters. The dating evidence points to a minimum age of 10930 years BP (+/- 200) for this deposit. The absence of bedding or any variation in the sediment column beside a coarsening downward, toward the unconformity (figure 6.45 and appendix 6.1, core CBT1) could be indicative of a rapid RSL rise allowing massive sand deposition above the unconformity with little wave reworking of the sediment.

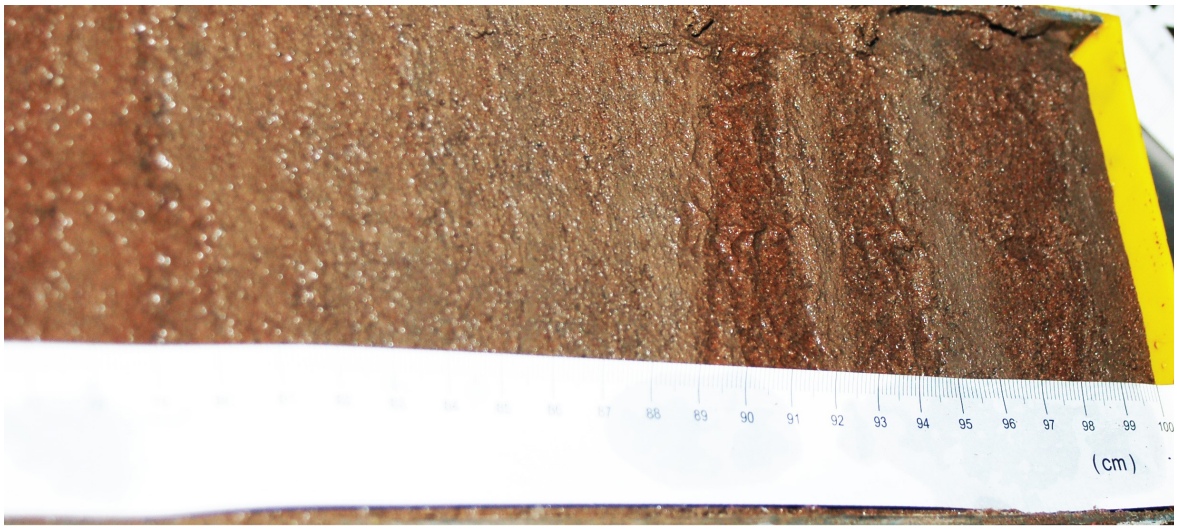

Figure 6.62: Oblique picture of section of core CB5 showing beds of sand (in lighter brown) and silt (in darker brown) of lithofacies LS corresponding to internal reflectors of unit SCB4.

Finally, the whole bay was covered with lithofacies CS and in places MS. CS appears to be a shell hash where finer sediments are winnowed away and probably deposited dynamically as MS.

Figure 6.63 presents the various lines of evidence and their correlation used to propose a depositional environment and associated RSL evolution for Church Bay with two potential RSL evolution curves; one with RSL falling steadily following the glacial retreat to the erosional surface level at 15m depth after deposition of lithofacies LS and another one with a more complex RSL evolution during deglaciation time before the deposition of lithofacies LS and but still falling to the erosional surface after the deposition of LS.

Church Bay, Rathlin, North Antrim

Epoch	Seismic unit	Lithofacies	Foraminifera assemblage	Depositional environment	RSL evolution
Holocene	SCB6	MS and CS: Bed of shells and coarse sand with granules overlaid in places by medium marine sands.	Mainly composed of substrate fixed and some of the *Elphidium* species.	Modern conditions of deposition of regional reworked sediment from high energy coast in sheltered bay environment.	m.s.l. ?
	SCB5	TS: Massive fine sand	Mainly composed of substrate fixed species and some of the *Quinqueloculina* species. Some planktonic species also present.	Temperate marine waters in fast rising RSL.	
	SCB4	LS: Interbedded silt and medium sand with some rounded clasts and shell fragments.	Mainly composed of *Elphidium* species and some *Cassidulina*. Most specimens are smaller than found in 2 overlying lithofacies.	Seasonal deposition of silt and sand in lower energy environment. Temperate marine waters in falling RSL.	-15m
LGM	SCB3	DCS: Coarse sand with large intact inarticulated bivalve shells.	Mostly barren; not enough specimens for assemblage recognition.	Slumping of winnowed material ?	?
	SCB2	Till ?	Unsampled	Glacial retreat	?

10930 +/- 200
11100 +/- 100
10140 +/- 110
17150 +/- 300

Figure 6.63: Seismic, lithological, microfaunal and dating evidence for Church Bay with proposed depositional scenario.

6.2.4.2 Depositional scenario for Runkerry Bay and the Skerries

This study only marginally enhances our understanding of the deposition story of this area as similar difficulties to those encountered by the previous coring survey (Kelley et al., 2006) of the area were experienced; in particular, a lack of deep penetration of the vibrocorer probably due to coarse sand and gravel. It confirms the findings from Kelley et al. (2006) as to the nature of the superficial seismic unit named here SRK5 as modern marine fine to medium sand and as to the nature of one of its internal reflector found to be 2 layers of granules and pebbles at depth of about 30m (figures 6.57 and 6.64 and appendix 6.1, core RK4). This deposit identified here as lithofacies BS could be the result of a storm event where material were displaced from a spread of gravel extending from the north end of Runkerry strand and visible on the backscatter data as an area not covered by modern marine sands. A similar event could be the origin of the unconformity at the top of lithofacies FS before the deposition of lithofacies BS. Additionally, it could be a gravel head indicative of a littoral deposit as suggested by Kelley et al. (2006). This lithofacies is not present over the whole basin as parts of the seabed show a lack of medium sand sediments on the backscatter data (values c. -15 SI compared to -70 SI of medium sand background); a "channel" following the gap between Ramore Head (Portrush) and the westernmost island of the Skerries, an area along the coast from the White Rocks to Portballintrae extending north of the White Rocks into a rocky outcrop zone and the area mentioned above from the north of Runkerry strand into the coast of the Giant's Causeway. Absence of deposition there is due to local tidal current conditions and the underlying substrate of bedrock.

Following the previous work of Quinn et al. (2009, 2010) and due to the fact that the two areas form the same basin, we can correlate the seismic unit described here for Runkerry Bay to those in the skerries area and the terrestrial section at Portballintrae described in McCabe et al. (1994) (Table 6.13).

The bottom unit SRK1 is directly correlated to the local bedrock due to the morphology of its top reflector outcropping in places of known bedrock outcrops. Unit SRK2 is here correlated as a combination of both units SM and D from the Skerries. No reflectors were detected inside unit SRK2 that could have separated it between a deposit of diamict or till and a deposit described as Shallow Marine as visible on the terrestrial

section at Portballintrae (McCabe et al., 1994) and as two distinct units in the Skerries (Quinn et al., 2009; 2010). Perhaps this is due to weak impedance contrast between the two deposits in the area or a removal of the Shallow Marine deposit at these depth linked with regressive wave action. This correlation would indicate this unit to represent the overlaying of the bedrock by first subglacial muddy diamict deposit followed by rythmical deposition of sand and mud in a shallow marine environment potentially associated with falling RSL (McCabe et al., 1994; Quinn et al., 2010).

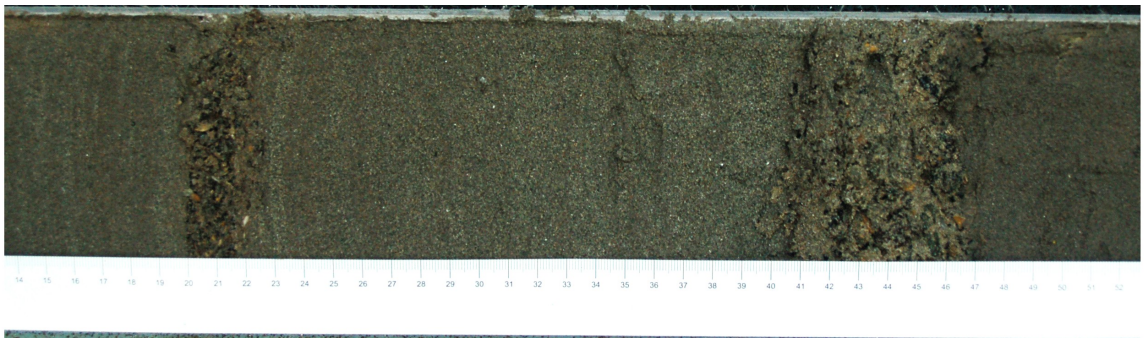

Figure 6.64: Oblique picture of section of core RK4 showing bedded sands between the two layers of granules (left) and pebbles(right) of lithofacies BS corresponding to internal reflector of unit SRK5.

Due to their acoustic signatures and locations in the stratigraphic column, the units SRK4 and SRK3 are correlated with the unit RS identified in the Skerries as regressive sand by Quinn et al. (2009; 2010). This identification, based on the erosional surface this unit sits over and its correlation with the top unit in the Portballintrae section (McCabe et al., 1994), strongly suggest these units' origin as reworked sand deposits during RSL fall (see section 6.1.3). Unit SRK4 presents the same morphology as unit RS but unit SRK3 is isolated in deeper waters. Nevertheless, the fact that both units, who share the same acoustic signature, sit unconformably below a unit of modern sand would indicate that they are in fact the same original unit of which the middle part was reworked by a later transgression. The top and bottom of unit RS presents unconformities with the units it is in contact with and a palaeochannel, interpreted as subaerial in origin (Cooper et al., 2002 and section 6.1.3), has been cut into its top surface to a depth of 14m . This suggests that some of the sand sheet was subaerially exposed. However, the high-energy internal reflector found inside the channel and interpreted as peat was also found as an internal reflector in the top unit of marine sand in the area. This internal refletor was crossed by this study's coring survey and found to be only an erosional contact between two marine sand

deposits. This puts the precise nature of the palaeochannel in doubt. Nevertheless the channel's geometry still suggest a subaerial origin which corresponds to the unit T of Quinn et al. (2009; 2010).

This unit was covered in some parts of the Skerries by a unit identified as Beach Sand (BS) detected down to about 12m depth (Quinn et al., 2009; 2010) but which was not recognised in this study's analysis of the seismic data in Runkerry Bay.

Skerries Area	Runkerry Bay	Lithology
Marine Sand (MS)	SRK5	Fine to medium sands with some internal layers of granules and pebbles (Kelley et al., 2006; this study)
Beach Sand (BS)	Not recognised	unsampled
Terrestrial deposit (T)	Not recognised	Unsampled but correlated with intertidal peat from Portrush west strand (Wilson et al., 2011).
Regressive Sand (RS)	SRK4	Unsampled but correlated with interbedded sands and sandy gravels (McCabe et al., 1994)
Regressive Sand (RS) ?	SRK3	Unsampled but interpreted here as a regressive sand deposit at deeper depth.
Shallow Marine (SM)	SRK2 ?	Unsampled but correlated with rythmically bedded sands and muds (McCabe et al., 1994)
Diamict (D)	SRK2 ?	Unsampled but correlated with stacked beds of muddy diamict (McCabe et al., 1994)
Bedrock (B)	SRK1	Varies along the coastline but understood here as mainly Cretaceous Chalk overlain by Palaeocene Basalt.

Table 6.13: Correlation between seismic units of the Skerries and Runkerry Bay with associated description.

6.2.4.3 Depositional scenario for the Bann estuary area

Previous work in the Bann estuary/Portstewart area focussed on the main subhorizontal reflector for the area where evidence for a palaeochannel has been cut into (Quinn et al., 2009; 2010). This reflector correlates with the top reflector of unit SPS1. Based on its acoustic signature, this unit is interpreted here as a glacial deposit whether identified as Till or Diamict perhaps overlain by a shallow marine deposit as in the Skerries/Runkerry Bay area. The presence of an inferred palaeochannel (see section 6.1.4), which was interpreted as former extension of the river Bann (Quinn et al., 2010; figures 6.65 to 6.67), suggests that this surface was subaerially exposed down the base of this channel at 18m depth. Indeed this surface slopes down seaward to a plateau at about 19m depth which could correspond to the level of the last deglaciation period lowstand for the area (section 2.4.3 and figure 2.21). Unit SPS4 is interpreted as a coarse sand deposit inside the channel potentially linked with rising RSL from its lowstand and filling the channel.

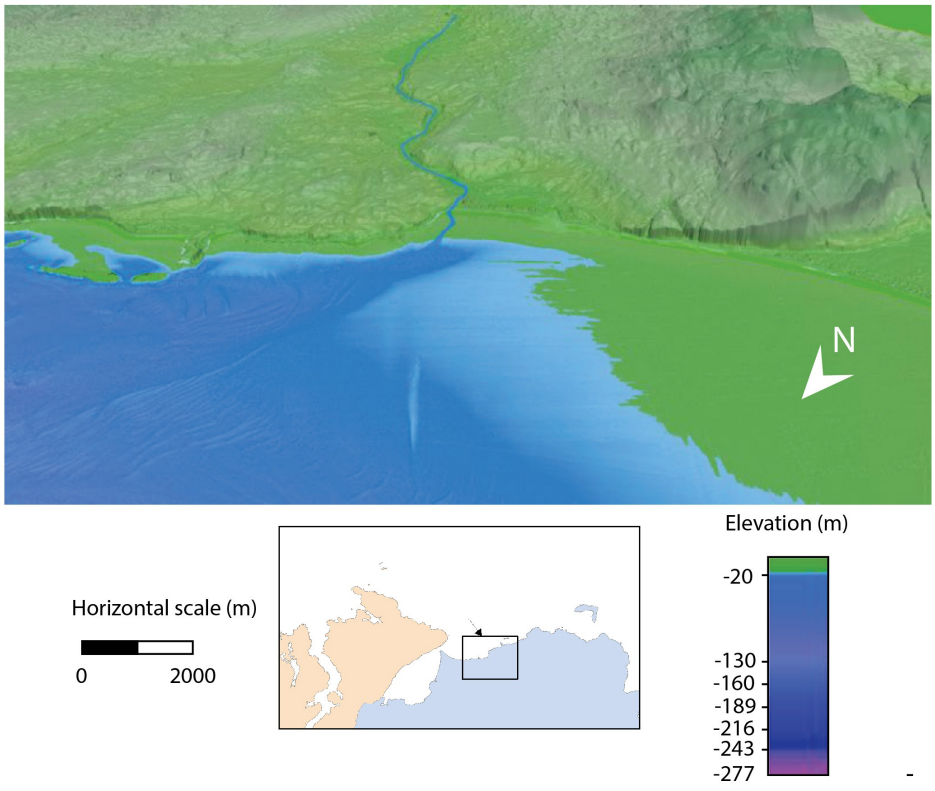

Figure 6.65: Palaeogeographic reconstruction for RSL at -14m for the Bann estuary using the 1m resolution bathymetry and position of palaeochannel identified on seismic data for the former course of the river Bann (from Quinn et al., 2010).

Similarly, units SPS2, SPS3 and SPS5 are interpreted as various marine sands deposited in rising RSL and in the more stable modern conditions In particular, Carter (1982) suggests that the original sand used in the formation of the beach ridges of the Magilligan foreland was originally coming from the near shelf until the foreland stabilised and started to erode away. The peninsula is now experiencing severe erosion both from wave action (Carter, 1982). This change in environmental condition may be responsible for the observed contrast between the two most superficial seismic units of the area. Similarly, the various units can be due to changes in sediment sources. Further sampling of these units with petrographical comparison to the sands of the Magilligan foreland could give further insights into the area's coastal environment. SPS5 appear to have come from the erosion and reworking of the dune barrier sand. Indeed, unit SPS5 corresponds to lithofacies MS composed of medium sand.

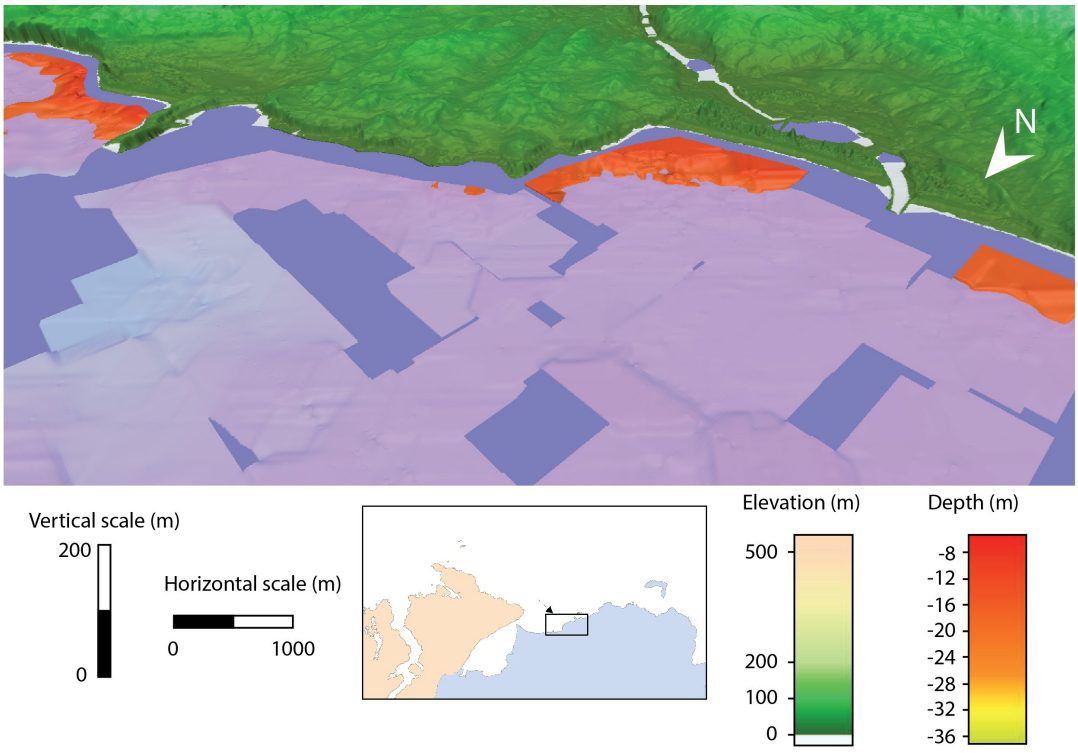

Figure 6.66: Palaeogeographic reconstruction using the 5m resolution DEM of the top reflector of unit SPS1 and a flat plane representing a former RSL at -14m. The representation depicts a more realistic position of the former coastline based on the seabed at the time rather than using the modern bathymetry (figure 6.65).

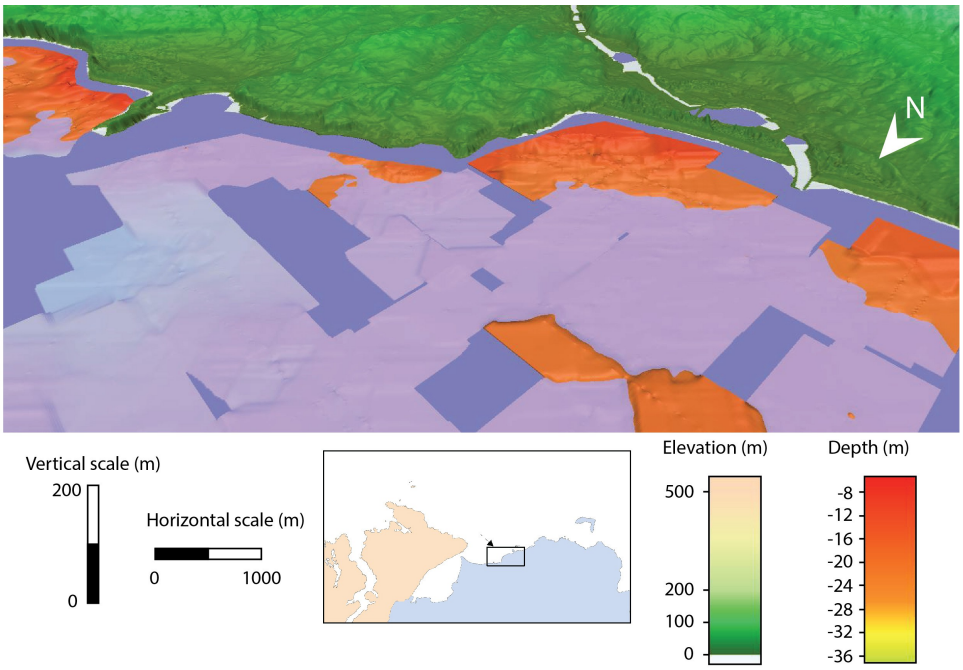

Figure 6.67: Palaeogeographic reconstruction using the 5m resolution DEM of the top reflector of unit SPS1 and a flat plane representing a former RSL at -18m, the level at which lies the bottom of the identified palaeochannel (section 6.1.4).

6.3 General correlation of seismic units and interpretation for the northern Irish coast

Figure 6.66 plots the various seismic units described for each bay above with their average thickness in their respective locations. This, with the added knowledge from the seismic units acoustic signature, location in the stratigraphic columns, identification and description from the coring survey and the comparison with the terrestrial section at Portballintrae (McCabe et al., 1994) allows a general correlation of these units and interpretation respective to the depositional environment and RSL conditions (Abbott & Carter, 2007; Cooper, 2007; Zecchin & Catuneanu, 2013; Catuneanu & Zecchin, 2013). This regional correlation is presented in table 6.14 and figure 6.69. The general age of the correlated depositional units presented is based on the dating evidence and the modelled RSL curves for the area (section 2.4.3) giving constraints for the deglaciation periods of regressions and transgressions.

The results presented above concerning the Skerries, Runkerry Bay and the Bann estuary area (sections 6.2.4.2 and 6.2.4.3) were easily correlated due to the similitudes in

seismic instrument used (Chirp) and the fact that some of the seismic lines were continuous from one bay to the next. Seismic unit BS interpreted as Beach Sand in the Skerries area (Quinn et al., 2009; 2010) was not presented in the overall correlation as it was not recognised in this study and no other evidence of such a deposit was found.

The three seismic units recognised in Whitepark Bay (SWB1-3) are correlated in stratigraphic order (see table 6.5) with a glacial till/diamict deposit, the regressive coarse sand deposit and the modern mobile medium sand of Portballintrae (McCabe et al., 1994). Noticeably, SWB2 lies unconformably over SWB1 down to a depth of 14m. Although isolated, the seismic signatures of these units using the Chirp data allows a relatively direct comparison with the 3 areas mentioned above.

Church Bay and Ballycastle Bay stand much more on their own in that respect due to the different seismic instrument used for their survey (Pinger, see section 3.4.1). They were correlated together as far as possible due to the fact that some seismic lines stretched between the two bays. Nevertheless, a tentative correlation with the units recognised in the other bays with seismic data measured with a Chirp instrument is given thanks to the coring survey in Church Bay allowing the recognition of similarities with the lithofacies in the terrestrial Portballintrae section (McCabe et al., 1994).

Most units appear to have similarities in at least one other bay, even unit SCB5 which was correlated with unit SPS4 in the Bann estuary based on their proposed conditions of deposition though they present different settings and acoustic signatures. These proposed conditions of rapid RSL rise are due to the setting of the two units over a sub-horizontally cut erosional surface for SCB5 (section 6.2.4.1) and inside a palaeochannel for SPS4 (section 6.2.4.3).

A correlation of SCB4 with the unit SM of the Skerries is presented namely because of a tentative correspondence made between the interbedded sands and muds recognised in the Portballintrae section (correlated with unit SM by Quinn et al., (2009)) and the interbedded sands and silt recognised in the lithofacies LS (correlated with unit SCB4 in section 6.2.4.1). This correlation is extended to the Jura formation of the Hebrides/Malin sea area presented in table 6.1 (section 6.1.1) based on the proposed date for its base at 16470 years BP corresponding to the minimum age of deposition of SCB4 and their corresponding acoustic signature. However, their lithology do not correspond with the Jura formation being composed of silty clay without the alternating sand and silt of lithofacies

LS but this could be due to its distal geographical location. Micropalaeontological data from this formation indicates fluctuating conditions of warm and cold temperature which could be responsible for the interbedded signal of LS (section 6.2.4.1).

Similarly, a morphological correspondence is made between the unit SBB4 and the units linked with regressive coarse sand in the other bays. These units are associated with erosional contacts either above and below and all cover the seaward slope of the bays down to a terminal depth (figures 6.6, 6.11, 6.17 and 6.37). Furthermore the rising abundance of point reflectors visible in the seismic data is interpreted as a coarsening upwards sequence linked with regressive or prograding facies (Cooper, 2007). In the case of SBB4, this depth is much lower (96m) than for the other bays (15m for Whitepark Bay, 19m for the Bann estuary, 20m in Runkerry Bay). This is the most problematic of the correlations made here and it is likely that another depositional cause is responsible for SBB4 rather than the interpreted sand sheets deposition during a period of RSL fall for the other bays. For example, it could the result of a similar type of slumping proposed for unit SCB3 in Church Bay (section 6.2.4.1).

The interpretation of unit SCB5 correlated with lithofacies TS as a transgressive sand is due to its massive nature with little or no variation in grain size (appendix 6.1, CBT1) and its location above an erosional surface at the top of a lithofacies with smaller grain sizes (LS). These are characteristics of transgressive facies (Cooper, 2007).

The modern marine sand component has been subdivided into two units on the basis of the separation between SBB5 and SBB6. SBB6 and SCB6 appear as a thin (0.5 to 1m thick) veneer covering the two bays almost entirely, including unit SBB5 in Ballycastle Bay. It is possible that is an artefact of the Pinger instrument as it is also visible in the seismic line in Lough Swilly. But being absent from other Pinger data from the Lough Foyle and the outer Bann estuary area, they are still interpreted as stratigraphic units correlated in Church Bay with the CS lithofacies. Unit SBB5 is interpreted as mobile marine sand due to its association with seabed landforms visible on the bathymetry (section 6.1.7 and figures 6.36 and 6.37) and so is correlated with the other superficial units of the other bays.

The stratigraphy from the Lough Foyle and Lough Swilly seismic line were not correlated directly with the other bays due to the lack of seismic coverage of these areas and their relative isolation.

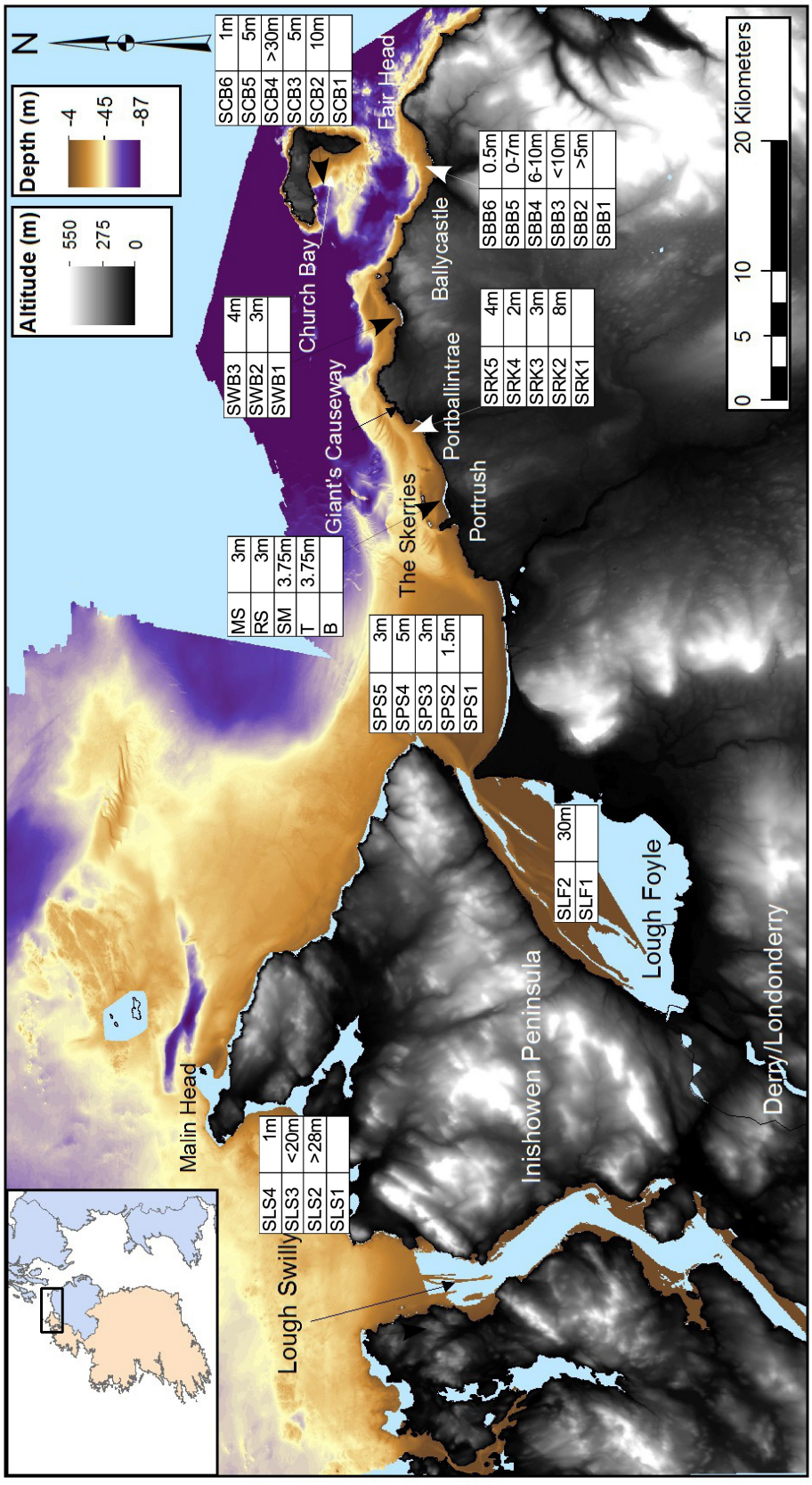

Figure 6.68: Seismic stratigraphy for the various bays of the study area.

Bann estuary	Skerries/ Runkerry	White park Bay	Ballycastle Bay	Church Bay	Thickness	Interpretation	RSL	Age
			SBB6	SCB6	0.5 to 1m	Modern marine coarse sand and shell bed covered in places by medium sand	Stable	Modern (from 5000 yrs BP to present)
SPS2, SPS3 & SPS5	MS/SRK5	SWB3	SBB5		3 to 7m	Highly mobile modern marine medium sand		
SPS4				SCB5	5m	Massive sand deposit	Rising	From base dated to 10930 +/-200 yrs BP to 5000 yrs BP
	RS/SRK3,SRK4	SWB2	SBB4?		3 to 5m (up to 10 for SBB4)	Coarse sand deposit	Falling (lowstand)	Around 12000 yrs BP
	SM/SRK2			SCB4	4 to 8m (more than 30 for SCB4)	Interbedded sand and silt or mud deposited in shallow marine conditions	Falling	From 16000 yrs BP to 12000 yrs BP. Top dated to 11100 +/- 100 yrs BP
			SBB3	SCB3	5 to 10m	Slumping deposit linked with glacial retreat ? Or readvance ?	Higher than present with rapid glacial uplift	Dated to 17150 +/- 300 yrs BP
SPS1	D/SRK2	SWB1	SBB2	SCB2	4 to 10m	Glacial till or diamict	Ice-covered	From LGM (20000 yrs BP) to 16000 yrs BP. Base dated to 17000 yrs BP
	SRK1		SBB1	SCB1		Bedrock		

Table 6.14: Correlation of the seismic units for the various bays of the study area with associated interpretation, age and RSL conditions.

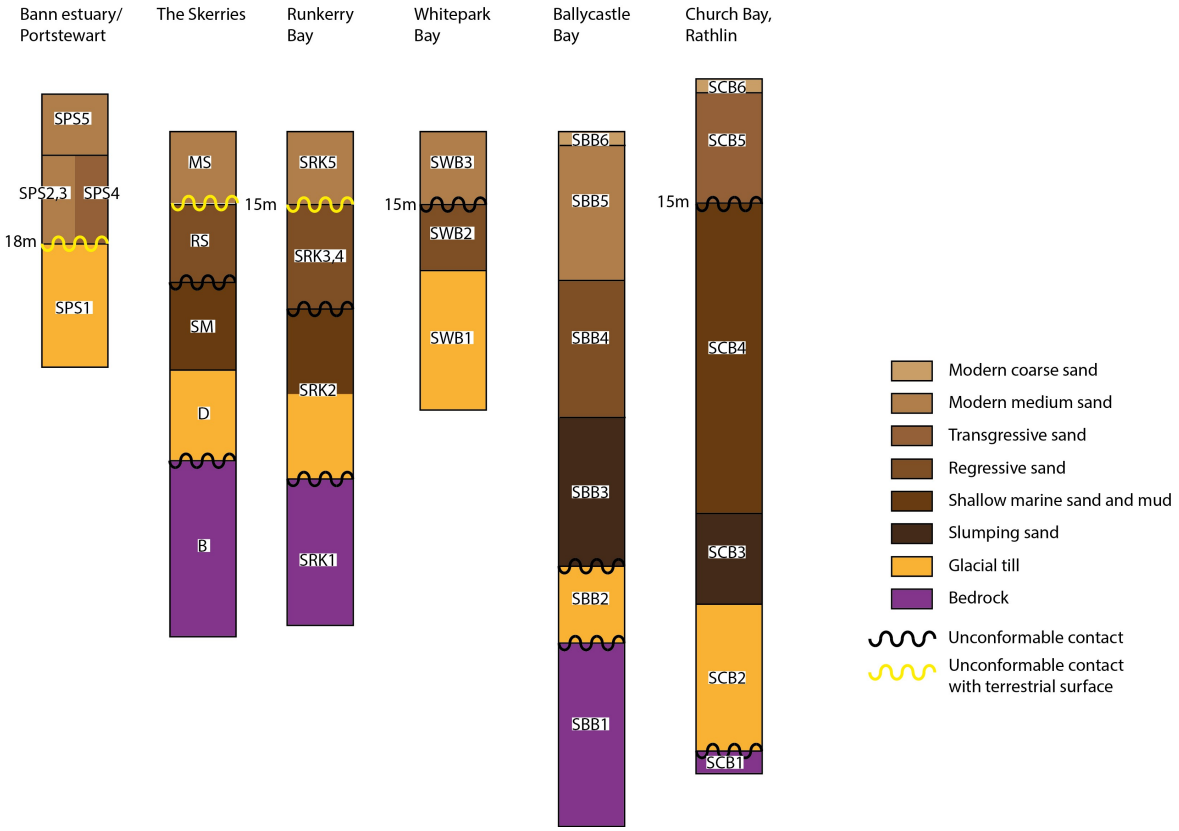

Figure 6.69: General stratigraphy from the correlated bays with tentative interpretation. The depth and thickness of the units are only indicative.

The notion of terrestrial surface associated with some of the unconformable contact in the stratigraphy (figure 6.69) is due to their association with inferred subaerially formed palaeochannel in the Bann estuary area (section 6.2.4.3) and the Skerries/Runkerry Bay area (section 6.2.4.2).

A recurrent unconformable contact appears above units correlated with regressive sands in the three areas of the Skerries, Runkerry Bay and Whitepark Bay. Similarly, an unconformity is associated with the local RSL lowstand (section 2.4.3) for Church Bay and the Bann estuary. In particular, some are associated with visible palaeochannels (potentially subaerially exposed terrestrial surface). The depth of these unconformities vary from one bay to the next from 15 to 18m depth. These depths are plotted from their respective bays in figure 6.70. The depth of 27m has been plotted on this figure for Ballycastle Bay, corresponding to a sub-horizontal erosional surface between SBB2 and SBB4. Although this is much lower than the other depths represented, it could correspond to a former RSL as well and deserves notice. Similarly, the depth of the deepest palaeochannels identified in the Lough Foyle and Lough Swilly area were also added.

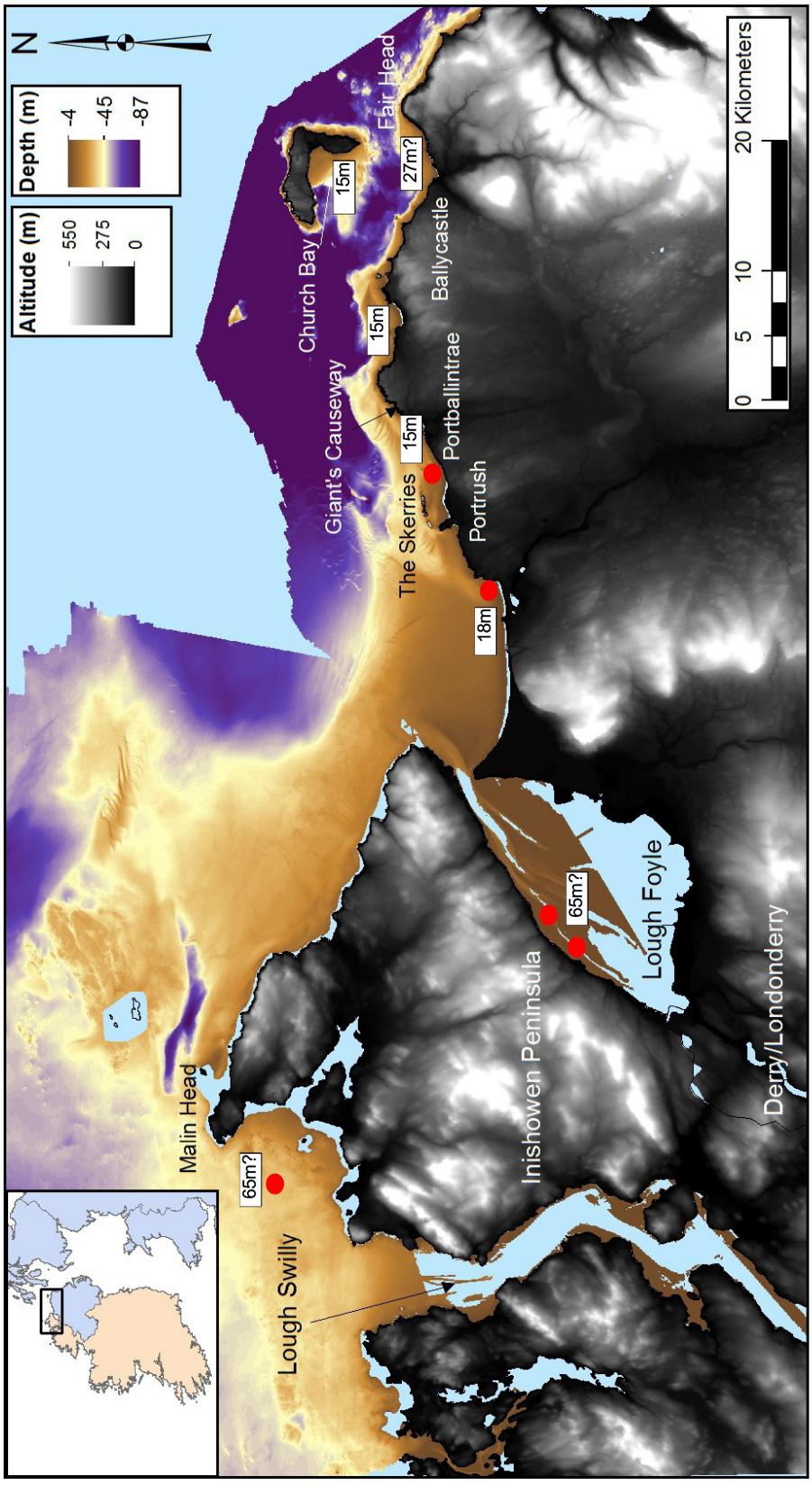

Figure 6.70: Lower depth of main unconformity identified between the various bays and location of palaeochannels (red dots).

6.4 Interpretation of the seismic stratigraphies of Lough Foyle and Lough Swilly

6.4.1 Lough Foyle

The scarce coverage of Lough Foyle prevents a clear interpretation of the seismic units. The two units recognised (section 6.1.9) are interpreted as a glacial till/diamict for the lowest in correlation with the units recognised in the studied bays to the east and a shallow marine deposit for SLF2 which appears to be subjected to ongoing deposition (table 6.15). The absence of deeper units is due to the lack of penetration of the seismic data at the shallow depth where the survey occurred. It is possible that the glacial till for Lough Foyle lies below than the recognised unit SLF1 but the depth of its top reflector correlate quite well with those where the units interpreted as glacial till for the other bays were found.

Seismic Units	Interpretation	RSL conditions	Age
SLF2	Tidally influenced deposit of interbedded sand and muds	Stable conditions	Modern
SLF1	Glacial till?	Higher than present	From 20,000 to 16,000 yrs BP

Table 6.15: Interpretation of the seismic units recognised in the Lough Foyle area.

Additionally, a number of potential palaeochannels were identified (figure 6.71), of which three are described in section 6.1.9. These are all formed on the surface of unit SLF1 and are filled entirely by SLF2 with a total thickness ranging from 3 to 30m. The bottom of these channels lie between 40 and 65m depth and their midpoint width range from 300 to 2000m. Figure 6.71 displays all the identified potential palaeochannels and their geographical relationships with river courses on land. When possible, a tentative palaeo-river course was drawn from the mouth of these rivers to the corresponding palaeochannel identified on the seismic data. Although, these links are based on very limited evidence, they could represent a former terrestrial surface at a time when the local RSL was much lower than present. And their location in the stratigraphy, similar to the one channel found in the Bann estuary area (section 6.1.4), tends to confirm the understanding of unit SLF1 as the expression of a glacial till. It is important to note that other river courses on land further north east of the area displayed in figure 6.71 do not have a corresponding potential palaeochannel.

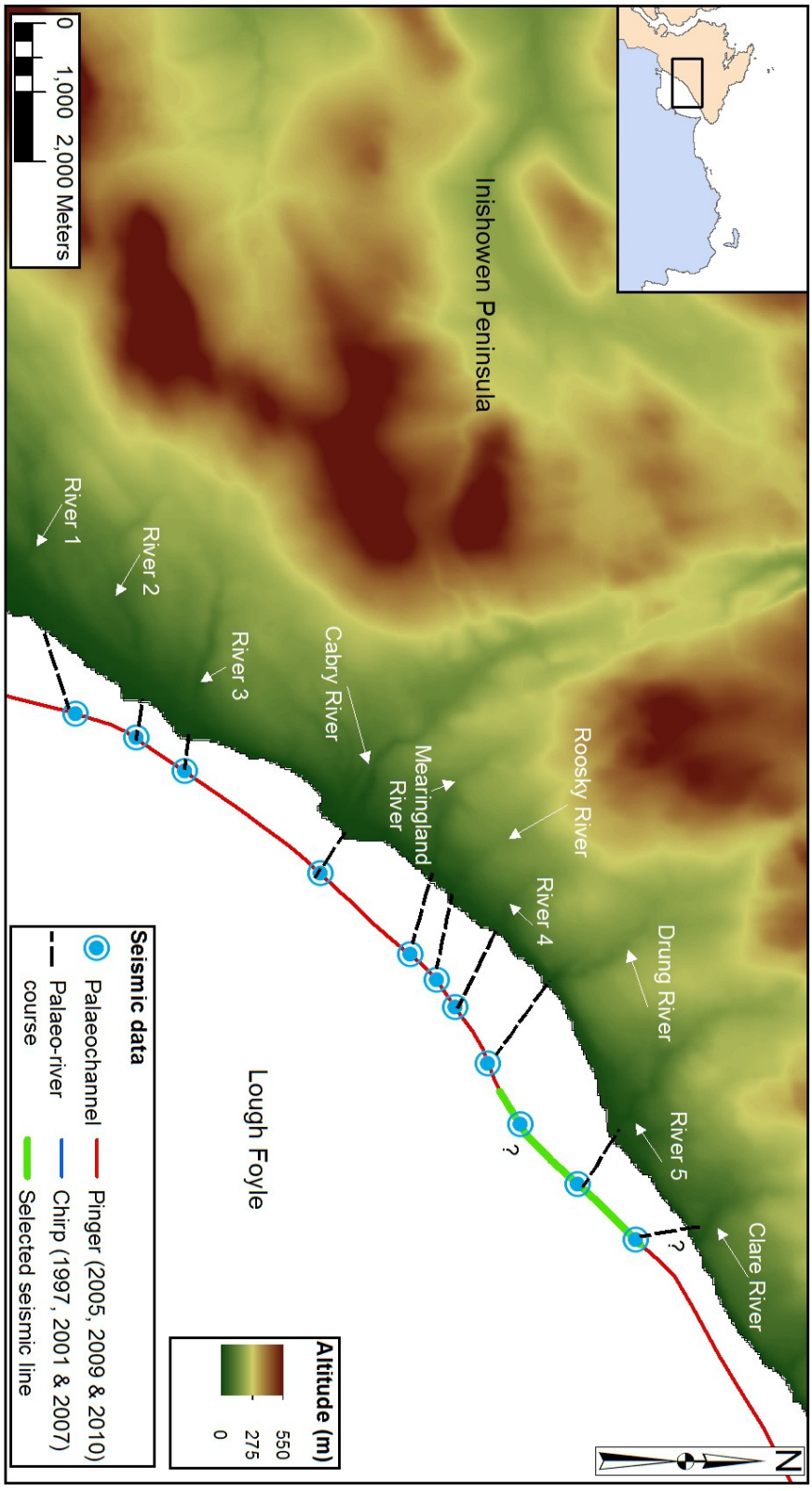

Figure 6.71: Map displaying the potential palaeochannels identified on the one seismic line at Lough Foyle. A tentative palaeoriver course was drawn for each geographically corresponding rivers on land (the rivers were given a number when they are not named in the Ordnance Survey maps).

6.4.2 Lough Swilly

The poor coverage of the Lough Swilly area prevented a more thorough study of its seismic stratigraphy (section 6.1.8) but some early interpretation can be made (table 6.16). Unit SLS1 is interpreted as bedrock due to the morphology of its surface outcropping in places of known bedrock outcrop on the seabed. The unit SLS2 draping SLS1 is interpreted as glacial till due to its acoustic signature usually associated with chaotic coarse sediment. This appears to correlate with similar interpreted units to the east of the study area. Unit SLS3's wavy parallel internal reflectors are interpreted as beds of contrasting nature such as sand and mud or silt. Such a deposit would require a depositional environment of lower energy than present and so could be linked with a RSL fall. It could also be the result of several storm events depositing coarse sand and gravel in layers between a more medium sand. Such a deposit could be the result of modern high energy conditions. Finally SLS4 is correlated to the other two units appearing as a shallow veneer of acoustically transparent in Ballycastle Bay and Church Bay and would then correspond to modern marine sand deposition.

Seismic Units	Interpretation	RSL conditions	Age
SLS4	Modern marine coarse sand and shell bed covered in places by medium sand	Stable conditions	Modern
SLS3	Tidally influenced deposit of interbedded sand and muds	Falling	From 16000 yrs BP to 12000 yrs BP
SLS2	Glacial till	Higher than present	From 20,000 to 16,000 yrs BP
SLS1	Bedrock		

Table 6.16: Interpretation of the seismic units recognised in the Lough Swilly area.

Two potential palaeochannels were identified in the Trawbreaga Bay area to the north of the mouth of Lough Swilly. These are recognised at the surface of unit SLS1 (figure 6.42), are described in section (6.1.8) and located on figure 6.41. They appear in the right alignment to be a continuation of the river courses formerly flowing through Trawbreaga Bay and Pollan Bay at a time when the local RSL was much lower than present (at least -65m).

6.5 General understanding of post deglaciation depositional environments for the study area

The general pattern of deposition recognisable throughout the correlated bays contains 7 different steps as presented in table 6.14 :

1. Glacial till/diamict

On land and on the close shelf, bedrock is eroded and subsequently covered by glacial till or diamict during the LGM. This deposit is not only visible across the island of Ireland but is also present in every area covered by seismic data for the study area as well as on the greater Malin-Hebrides sea area (the Hebrides/Minch Formation in section 6.1.1).

2. Coarse sediment slumping (turbidites) due to ice retreat and/or readvance

Post LGM, the ice sheet retreated and readvanced dynamically until the previously cited date of 16,000 yrs BP where the coast becomes ice free (Clark et al., 2012). This created some sediment instability that could potentially be behind the deposition of coarse sand (lithofacies DCS in Church Bay) for units SCB3 and SBB3.

3. Shallow marine deposit of interbedded sand and mud/silt

The isostatic rebound of the land mass associated with the melting of the ice sheets over Ireland, Britain and Scandinavia results in the local RSL falling. For coastal deposition, this means a lower wave energy and a deposition of finer sediments (like the lithofacies LS and the SM) in the more sheltered area of Church Bay and the Skerries and potentially as well for some parts of the west coast of Inishowen north of the mouth of Lough Swilly. Evidence from the offshore basins north of the study area indicate fluctuating conditions of warm and cold temperature. This deposition also occurred on what is land today as is visible in the Portballintrae section due to the fact that the RSL was still then above present by at least 10m (McCabe et al., 1994).

4. Wave erosion and regressive sand deposition

As RSL continued to fall, the top of the previously deposited till and shallow marine units came under tidal and wave influence and was eroded and regressive sand sheets were deposited. This occurred when the RSL is expected to have changed rapidly for the region due to the Meltwater pulse 1a at 13.500 yrs BP (Brooks et al., 2008; Bradley et al., 2011; Kuchar et al., 2012). This would have resulted in a very rapid RSL rise, expected from the Glacial Rebound Models to be of the order of about 8 to 10m, followed a continuation of the isostatic rebound for another 2,500 years until a final lowstand at 11,000 yrs BP. A regressive sand unit was not detected in each bays and this could be due to the very dynamic process described above that would resulted in rapid reworking of the sand deposit. Furthermore, in Ballycastle Bay, the depth range where unit SBB4 is detected suggest that the reworking of the regressive sand deposit have resulted in a slumping deposition as a slope front fill.

5. Evidence of subaerial exposure

With RSL lower than present, parts of the present coastal shelf were subaerially exposed as channels were cut on this surface. The main palaeochannel for the study area was cut probably by the river Bann on the exposed surface of unit SPS1 which was interpreted as the local expression of the glacial till. This palaeochannel has a base located at 18m depth and this is considered as the level of the lowstand here due to the absence of evidence of such palaeochannel further from the coast and at lower depth. The absence of regressive sand here could be due to its rapid reworking following deposition as RSL continued to fall. Further east, another palaeochannel is visible in the centre of the Skerries area cut on the upper surface of a regressive sand deposit (unit RS/SRK3) with its base at 14m depth. A number of potential palaeochannels were recognised further west in Lough Foyle and in Trawbreaga Bay with their bases found at much lower depth (-67m).

There is evidence of a terrestrial deposit at the west strand in Portrush, on the other side of Ramore Head from the Skerries, where intertidal peat has been found and its main growth was dated to between 7960-8,340 and 6,563-6,737 cal. yrs BP (Wilson et al., 2011). A recent find of intertidal peat was made at the site known as Eleven Ballyboes on the west coast of the Inishowen peninsula in Donegal where recent dives were able to recover a

sample dated at 8693–8985 cal. yrs BP (Westley, pers. Comm.). This gives a time constraint for the last transgression for the study area.

6. Transgressive sand deposition

Modelling suggests that the effect of local isostatic rebound was overcome by the global eustatic rise in the world ocean level from the time of the lowstand onwards (Brooks et al., 2008; Bradley et al., 2011; Kuchar et al., 2012). This transgression is associated with further erosion and reworking of the regressive sand deposit and with deposition of massive sand in more sheltered areas. This occurred mainly in Church Bay where the marine platform formed by the previous regression down to a depth of 15m was covered by a massive sand deposit 5m in thickness (Unit SCB5 correlated with lithofacies TS). Similarly, the above mentioned palaeochannel cut by the river Bann is filled by a deposit 5m in thickness (SPS4) whose acoustic signature would suggest is made of coarser sand.

7. Modern deposition of highly mobile medium sand and shell hash

GRMs are describing a general stabilisation of the RSL for the last 7,000 years as the global eustatic rise has slowed down and is now matched by the local isostatic rebound (Brooks et al., 2008; Bradley et al., 2011; Kuchar et al., 2012). This local rebound is still ongoing as RSL still falls by 2.4mm/year in Malin Head (Carter et al., 1989). Modern deposition of medium sand whose origin is the reworking of previously deposited regressive sands and glacial till. These deposits are 3 to 7m thick and are highly mobile on the surface due to the local high energy waves. They can form sand banks and linear bedforms visible on the bathymetry as in Ballycastle Bay (figures 6.36 and 6.37) and Whitepark Bay (figure 6.23).

In Church Bay, a thin deposit (0.5 to 1m thick) of coarser sand and broken shells (lithofacies CS) covers the underlying deposits. This appears to be present in Ballycastle Bay and to the west of the Inishowen peninsula as well. Local conditions there appear to winnow the finer sediment out of this deposit for deposition elsewhere.

6.6 Conclusion

This chapter presented the exploration of depositional RSL information by the integration and correlated interpretation of the local seismic data with a new coring survey. The seismic stratigraphy of 8 different bays were first described individually which allowed the recognition of areas with strategic importance for a coring survey. This was then undertaken in the areas of Church Bay, Runkerry Bay and the Bann estuary/Portsewart area where local depth and the thickness of the various units described were considered optimal for vibrocoring. Acoustic-lithological correlations were used to decipher the depositional scenarios of the cored areas which was then extrapolated to the whole northern irish coast.

This allowed the creation of a regional stratigraphy and the recognition of 7 main phases of sediment deposition for the study area spanning from the LGM to the present. The depositional scenario presented carries strong implications for the postglacial RSL change which will be investigated in chapter 7.

Chapter 7

Synthesis

In this chapter, the various lines of evidence from the study area will be compared and tested in light of their RSL meaning. This discussion will first present the evidence from the hard rock erosional features presented in chapter 4 with the added result of the erosional modelling presented in chapter 5. The RSL information contained in the findings of this study (chapters 4, 5 and 6) will then be presented and compared to modelled reconstruction of RSL change.

7.1 Hard rock evidence

7.1.1 Understanding of marine terrace formation

The wealth of information available in the JIBS datasets have allowed the recognition of a large corpus of submerged marine terraces formed in the local bedrock and potentially associated with past RSL. The bathymetric DEMs of 4m and 2m horizontal resolution for Northern Ireland and Donegal respectively were used to measure the main morphological parameters of more than 500 recognised features for the study area. One of the first line of investigation was based on the modelled differential isostatic rebound following the most recent deglaciation and visible in sea-level data across Ireland pointing to contemporaneous relict shorelines across the study area to be inclined toward the west (Brooks et al., 2008; Bradley et al., 2011; Kuchar et al., 2012 and section 2.4.3). No continuous shoreline was detected but the large range of features recognised provided a basis for a potential recognition of patterns linked with the RSL history of the study area.

Based on the average erosion rates for the types of lithologies of the study area, hard rock erosional features, which are the great majority of the recognised marine terraces (section 4.3.2), are unlikely to be the product of postglacial RSL (section 4.5). However, at least two of these features, the large near shelf in Church Bay and the area contained by the Skerries, Ramore Head and the east of Portrush town, were recognised as being carved in unconsolidated Quaternary sediments (based on seismic data presented in chapter 6 (section 6.1.2 and section 6.1.6)). These two features have then the best potential to extract postglacial RSL change information.

Backscatter data and some limited ground truthing dives have been able to show some of the recognised features to be either boulder fields not recognised at the resolution of the DEMs used or covered by modern sediment deposition. Nevertheless, a study on the lithological control on the morphology of the terraces was undertaken following the methods of the current literature (Sunamura, 1992; Dasgupta, 2010). In particular, the recent study by Thornton and Stephenson (2006) demonstrated the significant influence of rock resistance on the average depth of modern shore platforms at a cm to m scale. This is of importance when trying to relate erosional terraces to past RSL and so a range of correlations were sought between the various local factors on the morphology and median depth of the recognised features.

As no measurement of the range of rock resistance of the local lithologies was available, a first conclusion was drawn from the average width of the features recognised for each lithology where the narrowest platforms were found to be formed in the local Palaeocene Basalt. This was confirmed using the preponderance of type B platforms over type A that Sunamura (1992) had shown to be linked with rock resistance. The opposite is true for the modern shore platforms formed between Portrush and Portstewart (McKenna, 2002) which could be explained by more vigorous wave quarying today than when RSL was lower than present or that the structural control varies for the same lithology. These very lines of evidence are admittedly very loose and based on regional averages, assuming similar RSL and wave conditions for each of the localities. Nevertheless, this assumption was further tested in the modelling study presented in chapter 5 (see below).

Regardless of the rock resistance, structural and lithological control were found to be preponderant in the morphology of the terraces at the macro scale. The influence of exposure to the main wave action of the area, wind inducing waves from the north-west, was recognised but mainly for deeper features. Finally, terraces were found at a wide range of depth throughout the study area and for each of the three main type of lithologies. But the median depth of the platforms recognised was not found to correlate to any particular lithological or local and environmental factor. This does not dispute the findings of Thornton and Stephenson (2006) but only infers the mesoscale nature of the rock resistance influence on platform formation. Despite of the large number of features recognised, no major findings could be drawn on local differences in the RSL evolution for the study area beside the fact that they represent evidence for multiple submerged relict shorelines whose age is uncertain.

7.1.2 Dating the formation of these features

As mentioned previously, the rock resistance of the local lithologies is not available to date. However, published erosion rates for similar lithologies as those found in the study area indicate a much longer period of formation than the 20,000 years since the LGM. Furthermore, modelling of the profile erosion for characteristic profiles has confirmed the inherited nature of modern shore platform and the older origin of submerged terraces. Chapter 5 presented a first assessment of the recent GRMs for the study area. Using the

parameters of the simulated profiles corresponding best with the measured ones and presented in figure 5.6, we can extract the local lithologies rock resistance with Basalt (1150 Pa) profiles showing the hardest rock resistance to Sedimentary (1000 Pa) and then Metamorphic (850 Pa). This confirms the findings from the average width and preponderance of type B platforms displayed in the geomorphological study.

The extracted values of rock resistance are associated with erosional rates according to the various profiles morphological parameters (figure 7.1 and table 7.1). The parameters were obtained using the formulas described in section 3.3 for the erosional model. Although specific to particular angle of slope and environmental conditions, these were used to give a first assessment to the period needed for the formation of each of the recognised marine terraces. This was undertaken by dividing the average width of each of the features by the estimated erosion rates at Mid Tide corresponding to its lithology. Figure 7.2 represents the marine terraces recognised in the area of Ballycastle Bay and Church Bay according to the estimated period of time needed for their formation. Figure 7.3, on the other hand, presents these results for every recognised feature in the study area according to their median depth and the easting of their central point.

Associated Profiles	Coastal parameters used	computed erosion rates at MT	computed erosion rates at MHWN	Lithology associated
1 and 3	5º and 1000Pa	0.5mm/yr	0.69mm/yr	Chalk and Sedimentary
4	35º and 1150Pa	17.1mm/yr	23.3mm/yr	Basalt
5	5º and 240Pa	58.8mm/yr	80.2mm/yr	Unconsolidated sediment
6	5º and 850Pa	10.4mm/yr	14.1mm/yr	Metamorphic

Table 7.1: Computed erosion rates for the simulated profiles corresponding best to the measured ones.

Assuming the marine terraces recognised are formed by wave action in former RSL albeit with structural control, these figures point to a complex RSL evolution for the study area. Terraces estimated to require between 50,000 to 100,000 years for their formation are located at the same depth range as those estimated to require less than 5,000 years. The platforms identified in Ballycastle Bay appear to have formed over a much longer period of time than their counterparts around Rathlin Island. As these estimated rates were applied based on the lithology of the platforms, the main patterns observed are strongly linked with the local lithology. Furthermore, the simulated profiles parameters corresponded to particular environmental conditions of the characteristic measured profiles for the area. This means that the estimated period of time needed for the platform formation is here

comparable for the platforms and between the platforms of the stretches of coastline where the characteristic profiles were measured. We can then compare with slightly more confidence the areas of Ballycastle Bay East, Church Bay South, Portballintrae, Portrush and around Lough Swilly (corresponding to profiles 1 and 3 to 6, see figure 5.1). But even limited to these, no depth range is recognised with a preponderance of platforms forming over a particular period of time.

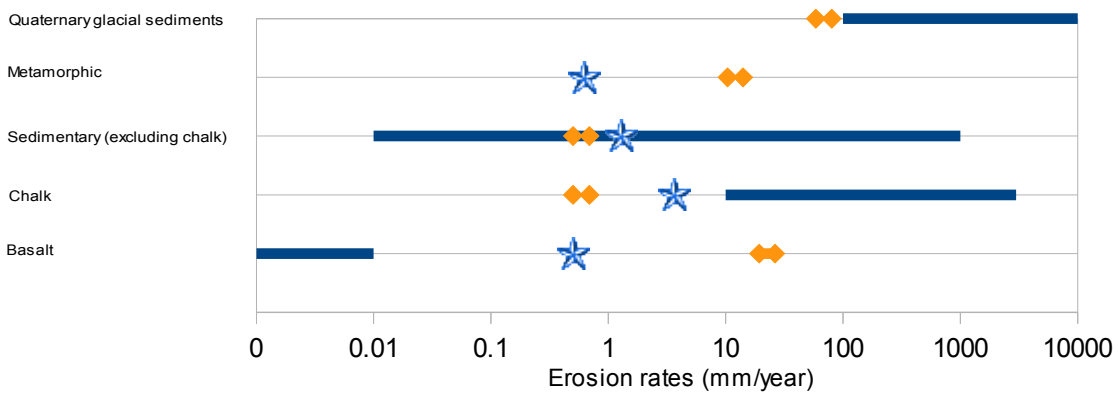

Figure 7.1: Computed erosion rates (yellow diamonds) plotted over the global average of measured erosion rates (stars) and the global range of recorded erosion rates from cliff retreats (lines) for various lithologies (Dasgupta, 2010).

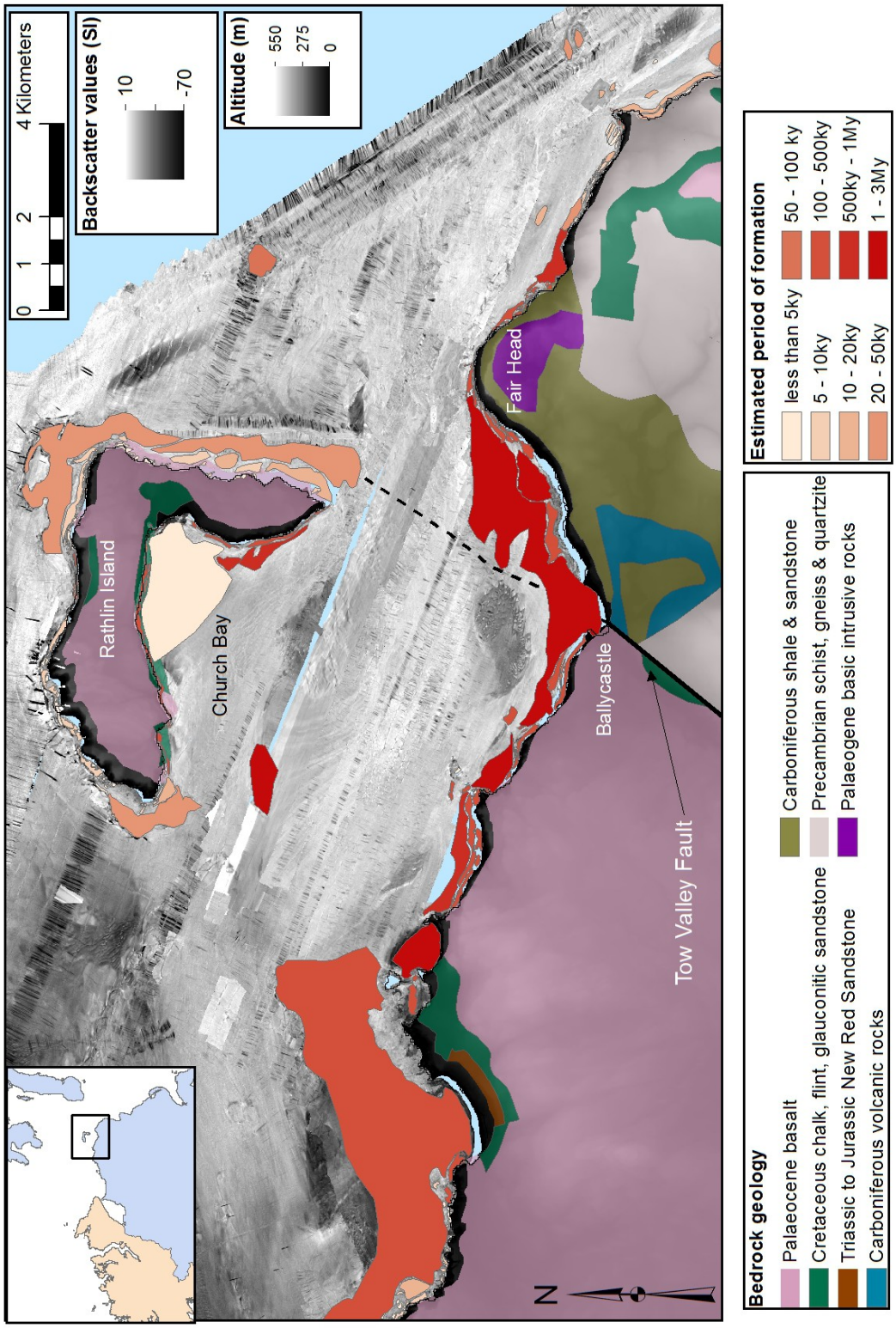

Figure 7.2: Estimated period of time needed for the formation of the recognised features for the Ballycastle Bay/Church Bay area.

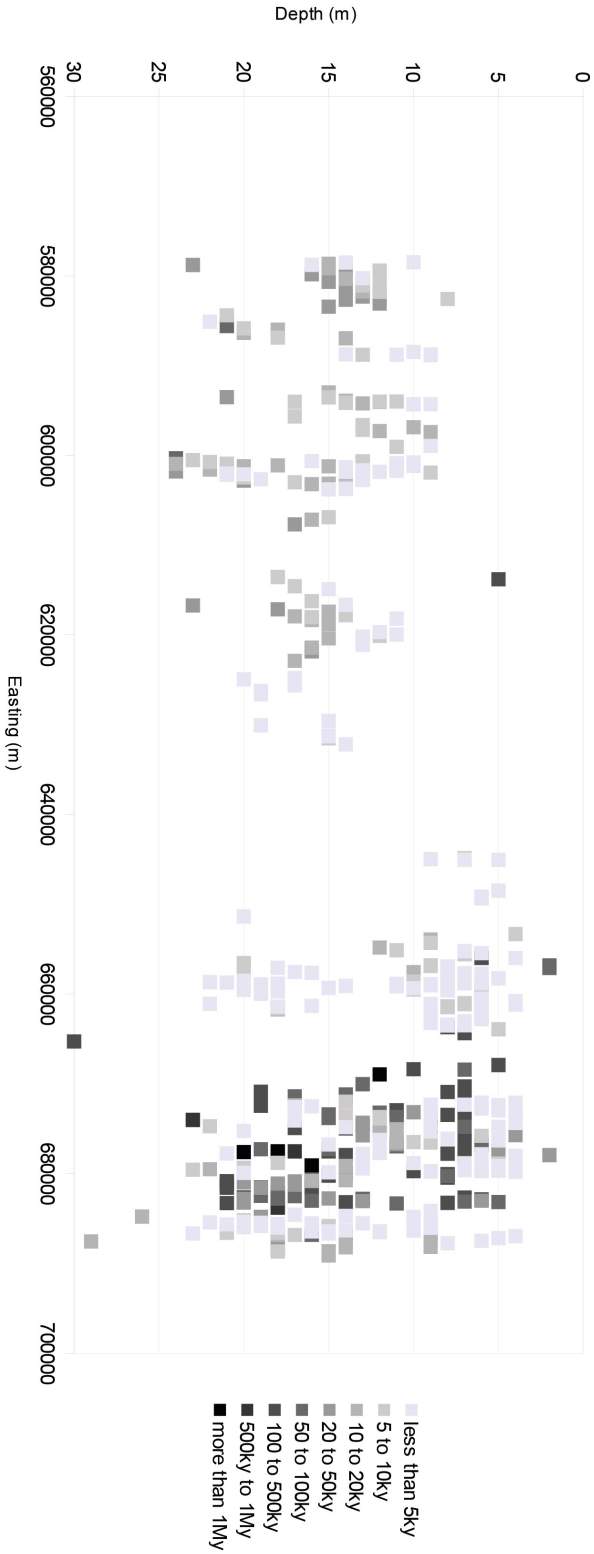

Figure 7.3: Location of each of the recognised features for the study area above 30m depth based on their central point's easting and their median depth. They are represented according to the estimated period of time needed for their formation.

The fact that narrow platforms requiring only a short amount of time (from 200 to 2000 years) to form are found at depth ranging from 5 to 25m indicates this range as the main range of evolution for the RSL of the study area. But features being present at every single depth of that range would translate into a steplike RSL evolution of less than 5,000 years stillstands over more than a 100,000 years period. None of the modelled RSL curves for the study area show more than 2,000 years of stable RSL necessary to form such features over the 20,000 years of the last deglaciation. This period of time appear to be roughly the same for each deglaciation period of the Quaternary (Coxon and McCarron, 2009 and figure 1.1). Some differences are clear though linked with variations in the ice distribution and ice load which would result in wide differences in the RSL change associated. The inferred age of the recognised terraces could be explained by a repeated RSL evolution over this depth range, potentially during the interglacial phases of the Quaternary with cyclical conditions of ice loading and melting. That would imply similar ice build up and distribution for the Quaternary. Further work in extending the range of the GRM, similar to the works of Raymo et al. (2011), could give interesting insights in the potential cyclical nature of Quaternary RSL change in the glacial margins.

The fact that many features in this range would require much longer than the modelled 5,000 years to form could be the result of frost weathering promoting rapid shore platform development as in the formation of strandflats (Bird, 2000) or stable RSL at these depths over large period of time during one or several glacial stages of the Quaternary. Alternatively the modelled erosion rate could be erroneous.

7.1.3 Particular platforms with a recent origin

Cliff-Platform Junction evidence from the modelling study indicate that models with more ice than previously thought correspond better to measured profiles (section 5.3.2). Although the measured CPJs could only be estimated from the topographical data of low horizontal resolution but high vertical one, their comparison with the CPJ from simulated profiles using the four more recently published GRM's points to the Hub-min model for the best fit (Kuchar et al., 2012). This is however not the case when comparing the whole simulated profiles with the measured one where the Bradley et al. (2011) model was preferred. Tables 7.2 and 7.3 present the depths and length of the periods of stable RSL for these two published GRMs and for the three selected areas. None of the models' curves show a particular period of stable RSL but each of the inflexion of the curves imply a longer period of time for the RSL at that depth range which was approximated here at 1,000 years.

Area	Depth	Period
North Antrim	4-6m	1000*2
Derry	7-8m	1000*2
Lough Swilly	11m	1000
Lough Swilly	16m	1000
Lough Swilly	24m	1000

Table 7.2: Depth and length of period of stable RSL as modelled by Bradley et al. (2011).

Area	Depth	Period
North Antrim	10m	1000
Derry	3m	1000
Derry	7m	1000
Derry	15m	1000
Lough Swilly	11m	1000
Lough Swilly	19-20m	1000

Table 7.3: Depth and length of period of stable RSL as modelled in Hub-min by Kuchar et al. (2012).

The recognised terraces that correspond to these criteria in terms of location, depth and estimated period needed for their formation are only few. They are very narrow with average width of 10 to 100m and are mainly made of basalt, which has a strong structural control over the morphology and depth of these features, beside the Giant's Causeway coast (figure 7.4) and around the north and east coast of Rathlin Island (figure 7.5). These two maps also show the two distinctly identified large terraces formed in unconsolidated sediments, south of the Skerries in figure 7.4 and at Church Bay in figure 7.5. Although these are found at depths below the modelled lowstands for their region (21m and 15m respectively), they were added to the map as their recent age is demonstrated by the seismic stratigraphies presented in chapter 6 and talked about in more detail in the next section. It is important to stress that these were selected based on the recently published modelled curves of which findings do not reconcile all available RSL data for Ireland (section 2.4.2). Further identified terraces of adequate width and lithology found at other depths and locations of the study area could have been formed entirely or partially during the last deglaciation period but are not displayed in figures 7.4 and 7.5.

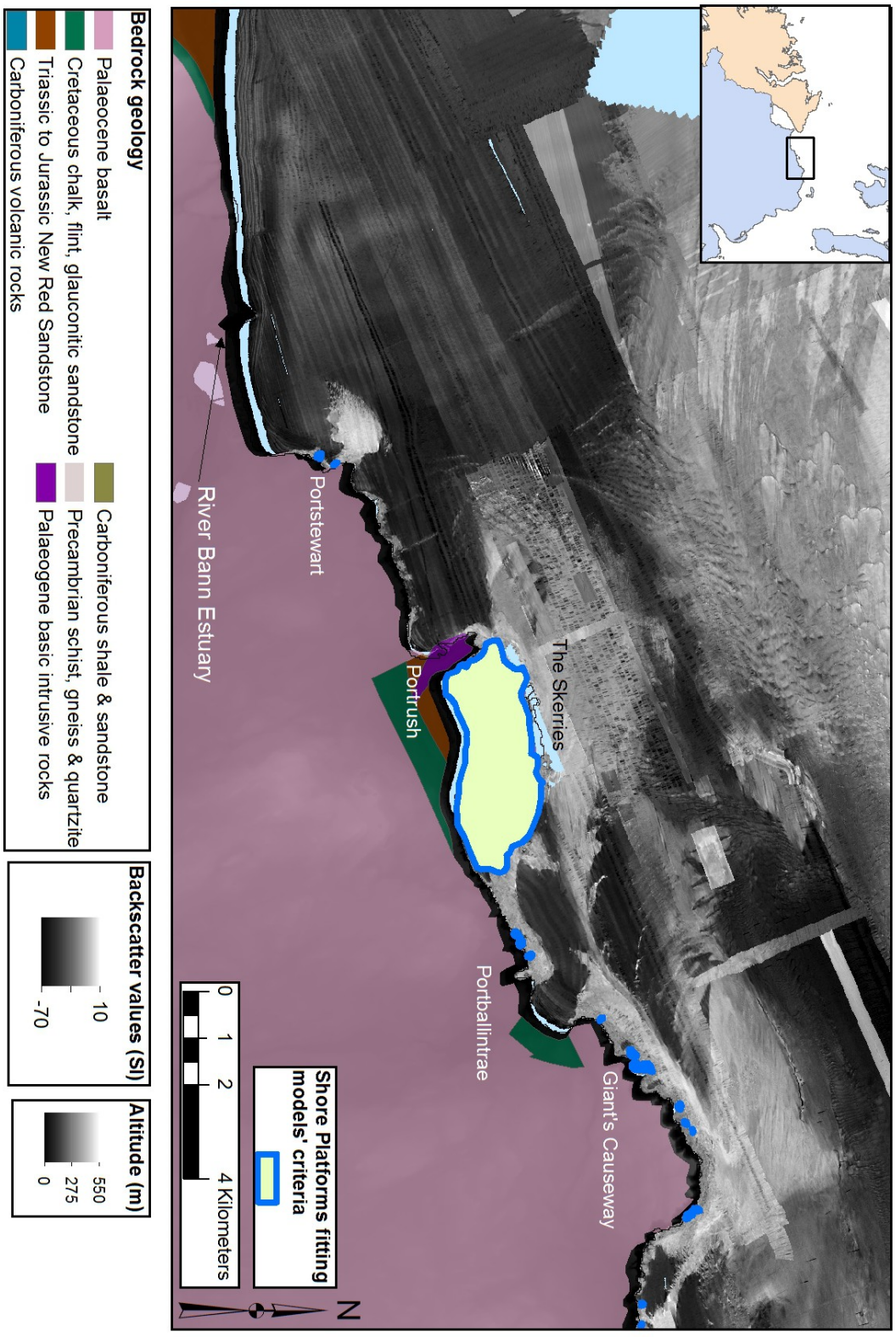

Figure 7.4: Shore platforms which fit the criteria from the modelled RSL for the last deglaciation period for the Causeway coast area.

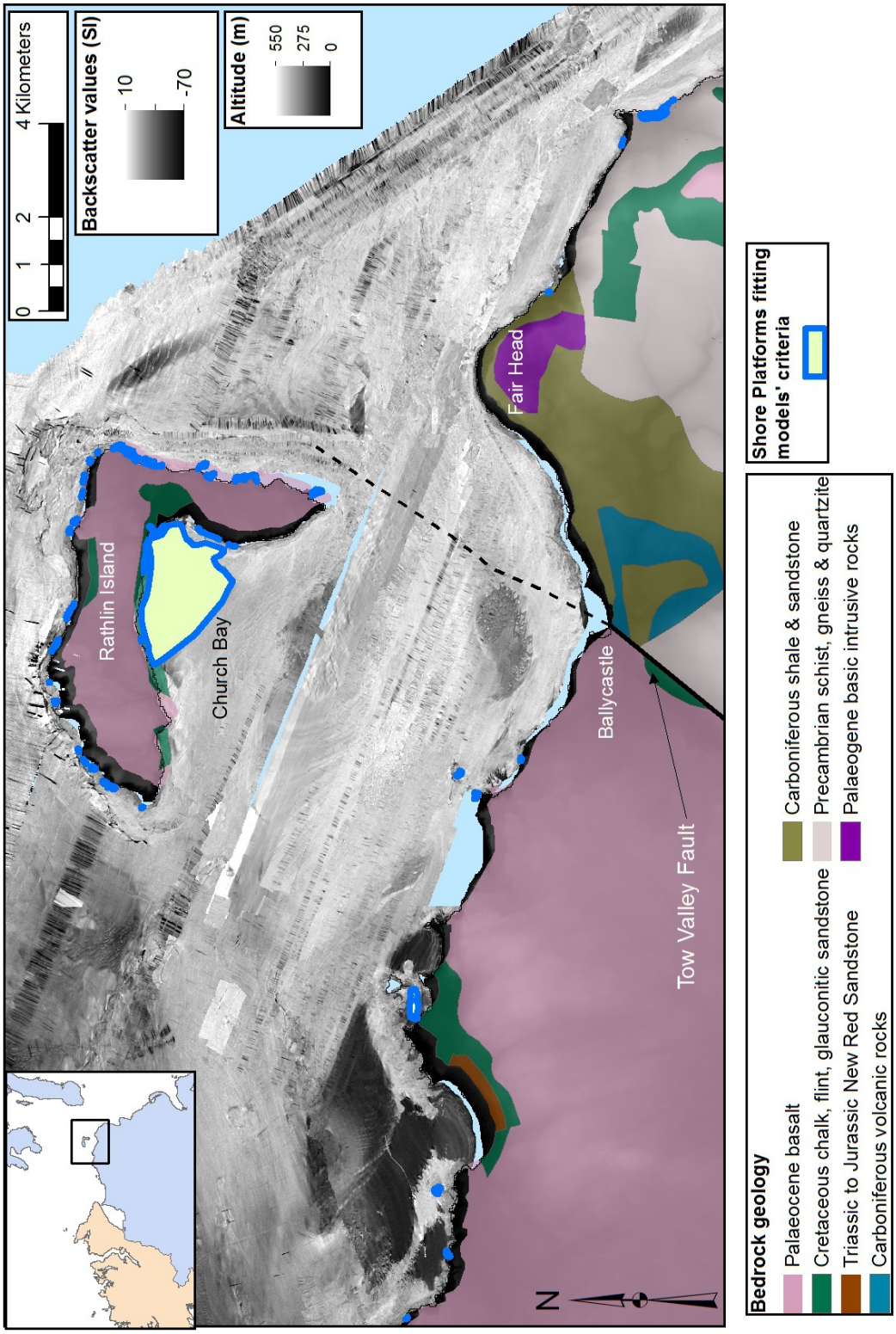

Figure 7.5: Shore platforms which fit the criteria from the modelled RSL for the last deglaciation period for the Ballycastle Bay/Church Bay area.

7.2 Additional information on RSL for the study area

7.2.1 Comparison of new RSL evidence to modelled curves

The seismic data presented and analysed in chapter 6 was used to build a general understanding of the recent depositional history for the eastern part of the study area where most datasets were from. Seismic units were identified from data from various instruments, taken from separate bays and interpreted using the limited coring survey in Church Bay and Runkerry Bay and the terrestrial section at Portballintrae. It is thus an extrapolation of the more definite stratigraphies of Church Bay and Runkerry Bay based on the acoustic signatures of the various seismic units recognised and their stratigraphic relationships to one another.

The assembled general stratigraphy of the area relates the major phases of RSL change (figure 6.69 and section 6.3). In particular, a major unconformity is identified with the latest lowstand of the local RSL and was dated based in Church Bay at approximately 11000 years BP at 15m depth (section 6.2.1.4) although there are some issues with the dates obtained. The recognition of an unconformity is based on the contrast of lithofacies and of foraminifera assemblages found on both side of this erosional contact. Although found in different stratigraphical context, the main unconformities of the other bays, interpreted as being linked with this lowstand and in places associated with potentially sub aerially exposed surfaces, were correlated with the same date (section 6.3). The depth associated with this lowstand in the stratigraphy vary (figures 6.69 and 6.70) between 15m from Church Bay to the Skerries to 18m for the Bann estuary area. This last value is based on the base level of a large palaeochannel potentially associated with the river Bann (section 6.1.4 and Quinn et al., 2010) and a plateau of the associated erosional surface further seaward.

The date obtained for the erosional contact in Church Bay adds a new sea-level indicator for the study area, in particular for the GRMs selected North Antrim area, significantly the first offshore for the northern coast of Ireland. This data point's indicative meaning toward a contemporaneous RSL could place it as a limiting date showing the lowest influence of wave action (lowest astronomical tide). When the new findings are added to the modelled RSL curves, it appears the more recent GRMs underestimate the

extent of the local isostatic rebound at this time (figure 7.6). The underestimation is of 2.5m for the Brooks et al. (2008) model, 5m for the Hub-min (Kuchar et al., 2012) model, 8.5m for the Bradley et al. (2011) model and more than 10m for the Hub-max (Kuchar et al., 2012) model for the lowstand. This would tend to select the Brooks et al. (2008) and the Hub-min (Kuchar et al., 2012) as best fitted to the local sea-level data albeit with a small underestimation of the local isostatic rebound although the Hub-min model overestimate by almost 10m the level of the highstand from the Meltwater pulse 1a (see section 2.4.3) as evidenced by the limiting date (type 1) at that time.

Similarly, if we add the level of the erosional surfaces associated with the lowstands for the areas of the Skerries/Runkerry Bay and the Bann estuary, we can see a similar discrepancy with some of the models for the Derry area (figure 7.7). These two levels are disctinct but could be assimilated together to constrain the lowstand for the area with the deeper depth of 18m (section 6.5).

If the lowstand levels found in the bays of the Derry area correspond to the same more recent lowstand of the modeled curve, we can recognise that the Brooks et al. (2008) model and the Hub-min (Kuchar et al., 2012) model underestimate the lower level of the base of the inferred palaeochannel of the Bann estuary by only 2m. On the other hand, the Hub-max (Kuchar et al., 2012) model shows a discrepancy of 7m and the Bradley et al. (2011) model a discrepancy of 9.5m. Again this suggests the Brooks et al. (2008) and Hub-min (Kuchar et al., 2012) as best fitted to the local sea-level data.

Cooper et al. (2002) and Kelley et al. (2006) concluded there was enough seismic evidence for a lowstand at 30m depth on the Giant's Causeway coast (section 6.1.2). Although this study would interpret this data differently based on its extension to the wider region (section 6.3), the presence of an erosional surface at 27m depth in Ballycastle Bay and potential palaeochannels in Lough Foyle and Trawbreaga Bay (figure 6.70) whose bottom lies at depth up to 65m would provide a much different assessment of the current generation of GRMs for the study area. Considerations of fault activation linked with the melting of the ice load or an alternate interpretation of these as meltwater channels could help reconcile these features with our understanding of the RSL evolution. Nevertheless, these features as well as those fitting more closely the GRM's curves require further research in order to relate them to past RSL.

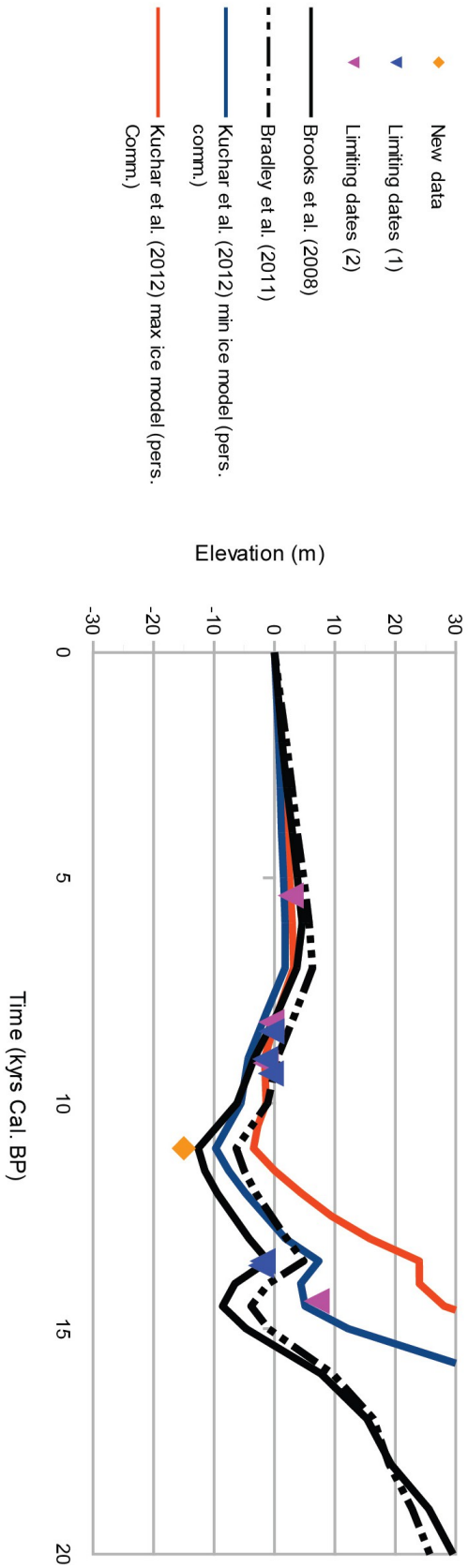

Figure 7.6: Sea-level data plotted over recently published modelled RSL curves for the North Antrim area.

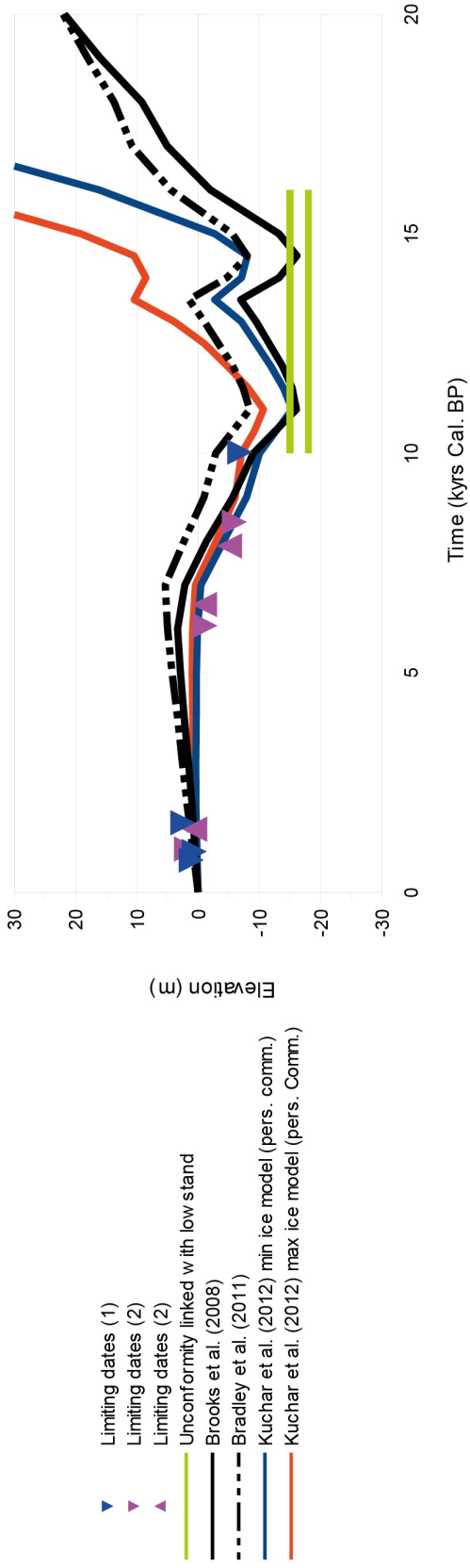

Figure 7.7: Sea-level data and erosional surface level plotted over recently published modeled RSL curves for the Derry area.

7.2.2 Any evidence of a differential glacial rebound ?

A difference of 3m is observed for levels associated in this study with a postglacial RSL lowstand in the area between Church Bay to the Bann estuary area (section 6.3 and figure 6.70). The fact that the level does not vary for over 25km and then drops suddenly by 3m in less than 10km is problematic but could be linked to other influences such as exposure to wind/wave and local tidal range or active faulting between Portstewart and the eastern side of Portrush. The depth of the levels associated with the lowstands, beside for Church Bay, were based only on seismic data. The assumption made there was a Pwave velocity consistent through the various media and fixed at 1500m/s. As we have seen in Church Bay, this assumption was incorrect and the depth there is based directly on coring evidence (section 6.2.1). Hence there can be variation of these levels of the order of 1m and this can further vary from one bay to the next.

Similarly the Cliff-platform junction evidence (section 5.2) from the modelled and measured coastal profile indicate a variation of about 1m between the areas of North Antrim and Derry and an additional 1m between the areas of Derry and Lough Swilly. This variation is small but visible and further precise measurement along the coastline would allow a clearer comparison from one area to the next.

One of the most consistent features of all GRMs for the study area is the fact that the deglaciation lowstand of the RSL were at lower depth in the west of the area, i.e. toward Lough Swilly, than to the east of the area, i.e. North Antrim. This difference is from 5 to 10m deeper between North Antrim and Derry and from 10 to 20m deeper between North Antrim and Lough Swilly. Unfortunately, the limited seismic data and modern sediment cover for the Lough Swilly area prevented any new insights on the level of the most recent lowstand. But a variation in level from the Derry to the North Antrim area is observed albeit of 3m rather than 5 to 10m which could be due to the type of evidences compared here.

Similarly, the modelled Holocene highstand has a different level from one of the modelled area to the next of the order of 1m which corresponds quite well with the Cliff-platform junction evidence.

Thus it is only with prudence that we say that the limited evidence points to some of the expected differential uplift for the study area.

7.3 General conclusions

This study aimed at using the available marine geophysical evidence for the northern coast of Ireland to investigate the potential for RSL information in the form of relict shorelines or stratigraphical contrast. As this stretch of coast has a very high energy environment linked with the rapid movement of marine sand along the shore leaving wide areas bare, the expectation could have been that the main information would be found more as an erosional signal than a depositional signal. The erosional information contained in the marine terraces is rich but hard to link with any RSL signal, in particular from the more recent RSL change (section 7.1). Modelling the development of the local rocky profiles allowed to test the influence of this recent change in particular in the level of the Cliff-Platform Junctions of these profiles (section 5.3.2). The much more precise information from the soft sediment stratigraphy is limited but allowed to uncover some definite evidence for the timing and depth of the most recent lowstand (section 7.2.1).

Most of the recently published GRMs show a generally good fit with the sea-level data of the study area, although showing some large discrepancies in other part of the Irish coast (section 2.4.2). But the lack of information relating to the timing and extent of the lowstand cast doubt on the general methodology of RSL change modelling (McCabe, 2008a). This study used the same type of data which was presented to question the reliability of the GRMs in the past (Cooper et al., 2002; Kelley et al., 2006; Quinn et al., 2008). A general agreement was found with the GRMs main consistent findings, i.e. the differential uplift observed in the Cliff-platform junction evidence (section 5.2) and in the depositional evidence linked with a RSL lowstand (section 7.2.2). Nevertheless, some newly identified potential palaeochannels in Lough Foyle and Trawbreaga Bay point to a much lower RSL lowstand with such a large discrepancy that it is unreconcilable with the range of recently published GRM's RSL curves (section 6.3).

The final concluding chapter will address the research questions presented in chapter 1 and offer some suggestions for further work.

Chapter 8

Conclusion

8.1 Evidence for RSL change in the offshore geophysical data

Most of the recently published GRMs show a generally good fit with the sea-level data of the study area, although showing some large discrepancies in other part of the Irish coast (chapter 2). The lack of information relating to the timing and extent of the lowstand has led to the development of some doubt toward the general methodology of RSL change modelling in the modern literature (McCabe, 2008a). This study aimed at assessing the current generation of GRM accuracy in their simulation of the rate and magnitude of RSL change for the northern coast of Ireland. This was addressed by examining the available marine geophysical evidence for the northern coast of Ireland for RSL information in the form of relict shorelines or stratigraphical contrast.

The study area has a very high energy environment linked with the rapid movement of marine sand along the shore leaving wide areas bare (chapters 2 and 4). The expectation for this study could have been that the main information would be found more as an erosional signal than a depositional signal. The erosional information contained in the marine terraces is rich but hard to link with any RSL signal, in particular from the more recent RSL change (chapter 4). Modelling the development of the local rocky profiles allowed to test the influence of this recent change in particular in the level of the Cliff-Platform Junctions of these profiles (chapter 5). The much more precise information from the soft sediment stratigraphy is limited but allowed to uncover some definite evidence for the timing and depth of the most recent lowstand (chapter 6).

The comparison of these results' implications with postglacial RSL point to a slight underestimation of the current GRMs' simulation of the magnitude of the last RSL lowstand. Furthermore, the westward differential glacial uplift consistently found in GRMs is somewhat visible in these new lines of evidence but not to the same extent as modelled. Nevertheless, newly identified potential palaeochannels to the west of the study area would point to a much deeper lowstand during postglacial RSL. When considering the more definite evidence, it appears the current generation of GRM is appropriate at simulating postglacial RSL change but some recommendations can be made for their future improvement.

8.2 General recommendations and further work

The CPJ results would indicate that the model Hub-min (Kuchar et al., 2012) is the best fitted to explain the recent development of the rocky shoreline of the study area (chapter 5). Although more precise measurement of this parameter is needed, this suggest that future GRM should be built with an ice model revisiting original trim line evidence (Ballantyne et al., 2007; 2008; Ballantyne, 2010) not as the highest mark of the ice sheet; hence in thickening the ice sheet more than the previously used ice model (Brooks et al., 2008). The evidence from the lowstand point to a slight (2 to 5m) underestimation of its depth for the Hub-min model. This could perhaps be remedied by a larger isostatic rebound which would fit the idea of a thicker local ice sheet.

An extension of this project's methodology, in particular the seismic exploration and associated ground truthing, to the rest of the Irish coast would help constrain recent RSL change further. Part of this is under way around the eastern and southern coast of Ireland under a NERC funded project led by the University of Ulster. We suggest to extend the study in the region of North Mayo in the west of Ireland where the largest discrepancies are observed between the sea-level data and the modelled curve (figure 2.17). Beside, a modelled stillstand of more than 3000 years at a depth of 40m would make for an obvious target of potential erosional signal.

This study highlighted the difficulties in relating hard rock erosional coastal features to a contemporary RSL which reflects the relative lack of interest of modern literature to their use in postglacial RSL study. Nevertheless, the modelling of their formation could bring great new insights in the RSL change and associated ice load and distribution of the Quaternary glaciations. Hence by using comprehensive and multi-technique studies, this thesis makes a valuable contribution to the study of palaeoclimatology in terms of ice sheet distribution and development, RSL change and coastal geomorphology for formerly glaciated margins.

References

Abbott, S. T., & Carter, R. M. (2007). Sequence Stratigraphy. In S. A. Elias (Ed.), *Encyclopedia of Quaternary Science* (pp. 2856–2869). Elsevier.

Alvarez-marrón, J., Hetzel, R., Niedermann, S., Menéndez, R., & Marquínez, J. (2008). Origin , structure and exposure history of a wave-cut platform more than 1 Ma in age at the coast of northern Spain: A multiple cosmogenic nuclide approach. *Geomorphology*, *93*, 316 – 334.

Anastasakis, G., & Piper, D. J. W. (2013). The changing architecture of sea-level lowstand deposits across the Mid-Pleistocene Transition: South Evoikos Gulf, Greece. *Quaternary Science Reviews*, *73*, 103–114.

Ballantyne, C. K. (2010). Extent and deglacial chronology of the last British-Irish Ice Sheet: implications of exposure dating using cosmogenic isotopes. *Journal of Quaternary Science*, *25*(4), 515–534.

Ballantyne, C. K., Stone, J. O., & McCarroll, D. (2008). Dimensions and chronology of the last ice sheet in Western Ireland. *Quaternary Science Reviews*, *27*(3-4), 185–200.

Ballantyne, C. K, McCarroll, D., & Stone, J. O. (2007). The Donegal ice dome, northwest Ireland; dimensions and chronology. *Journal of Quaternary Science*, *22*(8), 773–783.

Barnhardt, W. A., Belknap, D. F., & Kelley, J. T. (1997). Stratigraphic evolution of the inner continental shelf in response to late Quaternary relative sea-level change, northwestern Gulf of Maine. *Geological Society of America Bulletin*, *109*(5), 612–630.

Bassett, S. E., Milne, G. A., Bentley, M. J., & Huybrechts, P. (2007). Modelling Antarctic sea-level data to explore the possibility of a dominant Antarctic contribution to meltwater pulse IA. *Quaternary Science Reviews*, *26*(17-18), 2113–2127.

Beaman, R. J., Webster, J. M., & Wust, R. A. J. (2008). New evidence for drowned shelf edge reefs in the Great Barrier Reef , Australia. *Marine Geology*, *247*, 17 – 34.

Benetti, S., Dunlop, P., & Ó Cofaigh, C. (2010). Glacial and glacially-related features on the continental margin of northwest Ireland mapped from marine geophysical data. *Journal of Maps*, 14–29.

Benn, D. I., & Dawson, A. G. (1987). A Devensian glaciomarine sequence in western Islay, Inner Hebrides. *Scottish Journal of Geology*, *23*(2), 175–187.

Bennett, M. M., & Glasser, N. F. (2009). *Glacial geology: ice sheets and landforms*. Wiley.

Bird, E. (2000). *Coastal geomorphology: an introduction*. Wiley.

References

Blake, C. B. (2005). *Use of maerl as a biogenic archive*. Unpublished PhD thesis. Queen's University Belfast.

Blanco Chao, R., Costa Casais, M., Martínez Cortizas, A., Pérez Alberti, A., & Trenhaile, A. S. (2003). Evolution and inheritance of a rock coast: western Galicia, northwestern Spain. *Earth Surface Processes and Landforms*, *28*, 757–775.

Bowen, D. Q., & Gibbard, P. L. (2007). The Quaternary is here to stay. *Journal of Quaternary Science*, *22*(1), 3–8.

Bradley, S., Milne, G., Shennan, I., & Edwards, R. J. (2011). An improved glacial isostatic adjustment model for the British Isles. *Journal of Quaternary Science*, *26*(5), 541–552.

Brooke, B. P., Young, R. W., Bryant, E. A., Murray-Wallace, C. B., & Price, D. M. (1994). A Pleistocene origin for shore platforms along the northern Illawarra coast, New South Wales. *Australian Geographer*, *25*, 178–185.

Brooks, A., & Edwards, R. (2006). The development of a sea-level database for Ireland. *Irish Journal of Earth Sciences*, (24), 13–27.

Brooks, A. J., Bradley, S. L., Edwards, R. J., Milne, G. A., Horton, B., & Shennan, I. (2008). Postglacial relative sea-level observations from Ireland and their role in glacial rebound modelling. *Journal of Quaternary Science*, *23*(2), 175–192.

Brothers, L. L., Kelley, J. T., Belknap, D. F., Barnhardt, W. A., Andrews, B. D., & Maynard, M. L. (2011). More than a century of bathymetric observations and present-day shallow sediment characterization in Belfast Bay, Maine, USA: implications for pockmark field longevity. *Geo-Marine Letters*, *31*(4), 237–248.

British admiralty tide tables (2011) United Kingdom and Ireland, (np 201-11, vol. 1). UK Hydrographic Office, Taunton, Somerset.

Carolan, J. (2006). *Late Quaternary palaeoenvironmental change, Clew Bay, Co. Mayo, Ireland*. Unpublished PhD thesis. Queen's University Belfast.

Carter, D. J. T., & Draper, L. (1988). Has the north-east Atlantic become rougher ? *Nature*, *332*, 494.

Carter, R. W. G. (1972). *The coastal geomorphology of the Magilligan Foreland*. Unpublished D. Phil, thesis. New University of Ulster.

References

Carter, R. W. G. (1975). Recent changes in the coastal geomorphology of the Magilligan Foreland, Co. Londonderry. In *Proceedings of the Royal Irish Academy. Section B: Biological, Geological, and Chemical Science* (pp. 469–497).

Carter, R. W. G. (1982). Sea-level changes in Northern Ireland. *Proceedings of the Geologists' Association*, *93*(1), 7–23.

Carter, R. W. G. (1983). Raised coastal landforms as products of modern process variations, and their relevance in eustatic sea-level studies: examples from eastern Ireland. *Boreas*, *12*(3), 167–182.

Carter, R. W. G. (1991). *Shifting Sands: A study of the coast of Northern Ireland from Magilligan to Larne*. HMSO, Belfast.

Carter, R. W. G., Devoy, R. J. N., & Shaw, J. (1989). Late Holocene sea levels in Ireland. *Journal of Quaternary Science*, *4*(1), 7–24.

Carter, R. W. G., & Woodroffe, C. D. (1994). *Coastal evolution; late Quaternary shoreline morphodynamics*. Cambridge University Press.

Catuneanu, O., & Zecchin, M. (2013). High-resolution sequence stratigraphy of clastic shelves II: Controls on sequence development. *Marine and Petroleum Geology*, *39*, 26–38.

Clark, C. D., Hughes, A. L. C., Greenwood, S. L., Jordan, C., & Sejrup, H. P. (2012). Pattern and timing of retreat of the last British-Irish Ice Sheet. *Quaternary Science Reviews*, *44*, 112-146.

Coffey, G., & Praeger, R. L. (1904). The Antrim raised beach: a contribution to the Neolithic history of the north of Ireland. *Proceedings of the Royal Irish Academy. Section C: Archaeology, Celtic Studies, History, Linguistics, Literature*, *25*, 143–200.

Collina-girard, J. (2002). Underwater mapping of Late Quaternary submerged shorelines in the Western Mediterranean Sea and the Caribbean Sea. *Quaternary International*, *92*, 63–72.

Cooper, J. A. G. (2007). High Energy Coasts Sedimentary Indicators. In S. A. Elias (Ed.), *Encyclopedia of Quaternary Science* (pp. 2983–2993). Elsevier.

Cooper, J. A. G., Kelley, J. T., Belknap, D. F., Quinn, R., & McKenna, J. (2002). Inner shelf seismic stratigraphy off the north coast of Northern Ireland; new data on the depth of the Holocene lowstand. *Marine Geology*, *186*(3-4), 369–387.

References

Coxon, P., & McCarron, S. G. (2009). Cenozoic: Tertiary and Quaternary (until 11,700 years before 2000). In C. H. Holland & I. S. Sanders (Eds.), *The Geology of Ireland* (second edi., pp. 355–396). Edinburgh: Dunedin Academic Press.

Creighton, J. R. (1974). *A study of the Late Pleistocene geomorphology of North-Central Ulster, Northern Ireland*. Unpublished PhD thesis. Queen's University Belfast.

Cruslock, E. M., Naylor, L. A., Foote, Y. L., & Swantesson, J. O. H. (2010). Geomorphologic equifinality: A comparison between shore platforms in Höga Kusten and Fårö, Sweden and the Vale of Glamorgan, South Wales, UK. *Geomorphology*, *114*(1-2), 78–88.

Dasgupta, R. (2010). Whither shore platforms? *Progress in Physical Geography*, *35*(2), 183–209.

Darcy, R., & Flynn, W. (2008). Ptolemy's map of Ireland: a modern decoding. *Irish Geography*, *41*(1), 49–69.

Davidson-Arnott, R. (2010). *Introduction to Coastal Processes and Geomorphology*. Cambridge University Press, Cambridge.

Davies, H. C., Dobson, M. R., & Whittington, R. J. (1984). A revised seismic stratigraphy for Quaternary deposits on the inner continental shelf west of Scotland between 55° 30 "N and 57° 30"N. *Boreas*, *13*(1), 49–66.

Davies, T. A., Bell, T., & Cooper, A. K. (1997). *Glaciated Continental Margins: An Atlas of Acoustic Images*. (T. A. Davies, T. Bell, A. K. Cooper, H. Josenhans, L. Polyak, A. Solheim, … J. A. Stravers, Eds.). Springer Netherlands.

Devoy, R. J. (1983). Late Quaternary shorelines in Ireland: an assessment of their implications for isostatic land movement and relative sea-level changes. In D. E. Smith & A. G. Dawson (Eds.), *Shorelines and isostasy* (pp. 227–254). Dept Geog, Univ College, Cork, Ireland.: Academic Press, London.

Devoy, R. J. (1995). Deglaciation, Earth crustal behaviour and sea-level changes in the determination of insularity: a perspective from Ireland. *Geological Society, London, Special Publications*, *96*(1), 181–208.

Devoy, R. J. (2000). Implications of accelerated sea-level rise (ASLR) for Ireland. In *Proceedings of SURVAS Expert Workshop on European Vulnerability and Adaptation to Impacts of Accelerated Sea-Level Rise (ASLR), Hamburg, 19th* (pp. 52–66).

Dionne, J. C., & Brodeur, D. (1988). Frost weathering and ice action in shore platform development with particular reference to Québec, Canada. *Zeitschrift fur Geomorphologie, Supplement Band, d*, *71*, 117–130.

Dunlop, P., Shannon, R., Mccabe, M., Quinn, R., & Doyle, E. (2010). Marine geophysical evidence for ice sheet extension and recession on the Malin Shelf: New evidence for the western limits of the British Irish Ice Sheet. *Marine Geology*, *276*(1-4), 86–99.

Dziewonski, A. M., & Anderson, D. L. (1981). Preliminary reference Earth model. *Physics of the Earth and Planetary Interiors*, *25*, 297–356.

Eden, R. A., Ardus, D. A., Binns, P. E., McQuillin, R., & Wilson, J. B. (1971). *Geological investigations with a manned submersible off the west coast of Scotland 1969--1970. Report 71/16, Institute of Geological Sciences* (pp. 49). HMSO, London, UK.

Edwards, R. J. (2005). Sea levels: abrupt events and mechanisms of change. *Progress in Physical Geography*, *29*(4), 599–608.

Edwards, R. J. (2007a). Sea levels: Resolution and uncertainty. *Progress in Physical Geography*, *31*(6), 621–632.

Edwards, R. J. (2007b). Low Energy Coasts Sedimentary Indicators. In S. A. Elias (Ed.), *Encyclopedia of Quaternary Science* (pp. 2294-3005). Elsevier.

Edwards, R. J. (2008). Sea levels: Science and society. *Progress in Physical Geography*, *32*(5), 557–574.

Edwards, R. J. & Brooks, A. (2008). The island of Ireland: Drowning the myth of an Irish land-bridge? *Irish Naturalists' Journal Special Supplement*, 19–34.

Edwards, R. J., Brooks, A., Shennan, I., Milne, G., & Bradley, S. (2008). Reply: Postglacial relative sea-level observations from Ireland and their role in glacial rebound modelling. *Journal of Quaternary Science*, *23*(8), 821–825.

Emery, K. O., & Kuhn, G. G. (1982). Sea cliffs: their processes, profiles, and classification. *Geological Society of America Bulletin*, *93*(7), 644–654.

Evans, D. (1973). A Shallow Seismic Survey in Lough Swilly and Trawbreaga Bay , Co . Donegal. *Proceedings of the Royal Irish Academy*, *73*, 207–216.

Evans, D., Chesher, J. A., Deegan, C. E., & Fannin, N. G. T. (1982). *The offshore geology of Scotland in relation to the IGS shallow drilling programme 1970-1978. Report 81/12, Institute of Geological Sciences*. HMSO, London, UK.

References

Everard, C. E., Lawrence, R. H., Witherick, M. E., & Wright, L. W. (1964). Raised beaches and marine geomorphology. In K. F. G. Hosking & G. J. Shrimpton (Eds.), *Present views on some aspects of the Geology of Cornwall and Devon* (pp. 283–310). Royal Geological Society of Cornwall, Penzance.

Eyles, N., Boyce, J. I., Halfman, J. D., & Koseoglu, B. (2000). Seismic stratigraphy of Waterton Lake, a sediment-starved glaciated basin in the Rocky Mountains of Alberta, Canada and Montana, USA. *Sedimentary Geology*, *130*(3-4), 283–311.

Ferranti, L., Antonioli, F., Mauz, B., Amorosi, A., Dai, G., Mastronuzzi, G., Orru, P., Sanso, P. (2006). Markers of the last interglacial sea-level high stand along the coast of Italy: Tectonic implications. *Quaternary International*, *146*, 30–54.

Foote, Y., Plessis, E., Robinson, D., Hénaff, A. & Costa, S. (2006). Rates and patterns of downwearing of chalk shore platforms of the Channel: comparisons between France and England. *Zeitschrift für Geomorphologie, 144*, 93-115.

Fournier, A., & Allard, M. (1992). Periglacial shoreline erosion of a rocky coast: George River Estuary, northern Quebec. *Journal of coastal research*, *8*(4), 926–942.

Fyfe, J. A., Long, D., Evans, D., & Abraham, D. A. (1993). *United Kingdom Offshore Regional Report. The geology of the Malin-Hebrides sea area*. HMSO, London, UK.

Gill, E. D. (1973). Rate and mode of retrogradation on rocky coasts in Victoria, Australia, and their relationship to sea level changes. *Boreas*, *2*(3), 143–171.

Graham, D. K., Harland, R., Gregory, D. M., Long, D., & Morton, A. C. (1990). The biostratigraphy and chronostratigraphy of BGS Borehole 78/4, North Minch. *Scottish Journal of Geology*, *26*(2), 65–75.

Greenwood, S. L., & Clark, C. D. (2008). Subglacial bedforms of the Irish Ice Sheet. *Journal of Maps*, 332–357.

Haflidason, H., Sejrup, H. P., Kristensen, D. K., & Johnsen, S. (1995). Coupled response of the late glacial climatic shifts of northwest Europe reflected in Greenland ice cores: Evidence from the northern North Sea. *Geology*, *23*(12), 1059–1062.

Hancock, J. M. (1963). The Hardness of the Irish Chalk. *The Irish Naturalists' Journal*, *14*(8), pp. 157–164.

Hansom, J. D., & Kirk, R. M. (1989). Ice in the intertidal zone: examples from Antarctica. In E. Bird & D. Kelletat (Eds.), *Zonality of Coastal Geomorphology and Ecology. Essener Geographische Arbeiten* (Vol. 18, pp. 211–236).

Harkness, D. D. (1983). The extent of the natural 14C deficiency in the coastal environment of the United Kingdom. *Journal of the European Study Group on Physical, Chemical and Mathematical Techniques Applied to Archaeology*, *4*(9), 351–364.

Harris, M. S., Sautter, L. R., Johnson, K. L., Luciano, K. E., Sedberry, G. R., Wright, E. E., & Siuda, A. N. S. (2013). Continental shelf landscapes of the southeastern United States since the last interglacial. *Geomorphology, 203*, 6-24.

Holland, C. H., & Sanders, I. S. (2009). *The Geology of Ireland* (2nd edition., pp. 568). Edinburgh: Dunedin Academic Press.

Horton, B., Edwards, R. J., & Lloyd, J. (1999). UK intertidal foraminiferal distributions: implications for sea-level studies. *Marine Micropaleontology*, *36*(4), 205–223.

Huang, J. (2004). *Morphodynamics of a high energy beach system, Runkerry Strand, Northern Ireland*. Unpublished PhD thesis. University of Ulster.

Hubbard, A., Bradwell, T., Golledge, N., Hall, A., Patton, H., Sugden, D., Cooper, R., Stoker, M. (2009). Dynamic cycles , ice streams and their impact on the extent , chronology and deglaciation of the British – Irish ice sheet. *Quaternary Science Reviews*, *28*(7-8), 758–776.

Hughen, K. A. (2007). Chapter Five Radiocarbon Dating of Deep-Sea Sediments. *Developments in Marine Geology*, *1*, 185–210.

Hull, E., Nolan, J., Cruise, R. J., & McHenry, A. (1890). *Explanatory Memoir of Inishowen, County Donegal to accompany sheets 1, 2, 5, 6 and 11 (in part) of the maps of the Geological Survey of Ireland* (pp. 70). Dublin.

Jackson, D. I., Jackson, A. A., Evans, D., Wingfield, R., Barnes, R. P., & Arthur, M. J. (1995). *United Kingdom Offshore Regional Report. The geology of the Irish Sea*. HMSO, London, UK.

Jackson, D. W. T., Cooper, J. A. G., & del Rio, L. (2005). Geological control of beach morphodynamic state. *Marine Geology*, *216*(4), 297–314.

Juggins, S. (2007). *C2 Version 1.5 User Guide. Software for ecological and palaeoecological data analysis and visualisation. Newcastle University* (Vol. 73). Newcastle upon Tyne, UK.

References

Kelley, J T, Cooper, J. A. G., Jackson, D. W. T., Belknap, D. F., & Quinn, R. J. (2006). Sea-level change and inner shelf stratigraphy off Northern Ireland. *Marine Geology*, *232*(1-2), 1–15.

Kelley, J. T, Belknap, D. F., & Claesson, S. (2010). Drowned coastal deposits with associated archaeological remains from a sea-level " slowstand ": Northwestern Gulf of Maine , USA. *Society*, (8), 695–698.

Kilroe, J. R. (1888). Directions of ice-flow in the north of Ireland. *Quaterly Journal of the Geological Society of London*, *44*, 827–833.

King, E. L., Haflidason, H., Sejrup, H. P., Austin, W. E. N., Duffey, M., Helland, H., Klitgaard-Kristensen, D., & Scourse, J. D. (1998). End moraines on the northwest Irish continental shelf. In *Third ENAM II Workshop*. Edinburgh.

Knight, J., Coxon, P., McCabe, A. M., & McCarron, S. G. (2004). Pleistocene glaciations in Ireland. In J. Ehlers & P. L. Gibbard (Eds.), *Quaternary Glaciations Extent and Chronology Part I: Europe* (Vol. 2, Part 1, pp. 183–191). Elsevier.

Kuchar, J., Milne, G., Hubbard, A., Patton, H., Bradley, S., Shennan, I., & Edwards, R. (2012). Evaluation of a numerical model of the British-Irish ice sheet using relative sea-level data: implications for the interpretation of trimline observations. *Journal of Quaternary Science*, *27*(6), 597–605.

Lambeck, K. (1991). Glacial rebound and sea-level change in the British Isles. *Terra Nova*, *3*(4), 379–389.

Lambeck, K. (1993a). Glacial rebound of the British Isles; I, Preliminary model results. *Geophysical Journal International*, *115*(3), 941–959.

Lambeck, K. (1993b). Glacial rebound of the British Isles; II, A high-resolution, high-precision model. *Geophysical Journal International*, *115*(3), 960–990.

Lambeck, K. (1995). Late Devensian and Holocene shorelines of the British Isles and North Sea from models of glacio-hydro-isostatic rebound. *Journal of the Geological Society*, *152*(3), 437–448.

Lambeck, K. (1996). Glaciation and sea-level change for Ireland and the Irish Sea since Late Devensian/Midlandian time. *Journal of the Geological Society*, *153*(6), 853–872.

Lambeck, K., & Purcell, A. P. (2001). Sea-level change in the Irish Sea since the last glacial maximum; constraints from isostatic modelling. *Journal of Quaternary Science*, *16*(5), 497–506.

Lericolais, G., Auffret, J.-P., & Bourillet, J.-F. (2003). The Quaternary Channel River: seismic stratigraphy of its palaeo-valleys and deeps. *Journal of Quaternary Science*, *18*(3-4), 245–260.

Leroy, P., Cabioch, G., Monod, B., Lagabrielle, Y., Pelletier, B., & Flamand, B. (2008). Late Quaternary history of the Nouméa lagoon (New Caledonia, South West Pacific) as depicted by seismic stratigraphy and multibeam bathymetry A modern model of tropical rimmed shelf. *Palaeogeography, Palaeoclimatology, Palaeoecology*, *270*(1-2), 29–45.

Lisiecki, L. E., & Raymo, M. E. (2005). A Pliocene-Pleistocene stack of 57 globally distributed benthic δ 18 O records. *Paleoceanography*, *20*(1).

Long, A. J., Roberts, D. H., Simpson, M. J. R., Dawson, S., Milne, G. A., & Huybrechts, P. (2008). Late Weichselian relative sea-level changes and ice sheet history in southeast Greenland. *Earth and Planetary Science Letters*, *272*(1-2), 8–18.

McCabe, A. M. (2008a). Comment: Postglacial relative sea-level observations from Ireland and their role in glacial rebound modelling. *Journal of Quaternary Science*, *23*(8), 817–820.

McCabe, A. M. (2008b). *Glacial Geology and Geomorphology: The Landscapes of Ireland.* (pp. 274). Edinburgh: Dunedin Academic Press.

McCabe, A. M., & Clark, P. U. (2003). Deglacial chronology from County Donegal, Ireland: implications for deglaciation of the British-Irish ice sheet. *Journal of the Geological Society*, *160*(6), 847–855.

McCabe, A. M., & Dunlop, P. (2006). *The Last Glacial Termination in Northern Ireland*. *Geological Survey of Northern* (pp. 93). Belfast: Geological Survey of Northern Ireland.

McCabe, A. M., Haynes, J. R., & Macmillan, N. F. (1986). Late-Pleistocene tidewater glaciers and glaciomarine sequences from north County Mayo, Republic of Ireland. *Journal of Quaternary Science*, *1*(1), 73–84.

McCabe, A. M., Carter, R. W. G., & Haynes, J. R. (1994). A shallow marine emergent sequence from the northwestern sector of the last British ice sheet, Portballintrae, Northern Ireland. *Marine Geology*, *117*(1-4), 19–34.

References

McCabe, A.M., Cooper, J. A. G., & Kelley, J. T. (2007). Relative sea-level changes from NE Ireland during the last glacial termination. *Journal of the Geological Society*, *164*(5), 1059–1063.

McCann, N. (1988). An Assessment of the Subsurface Geology between Magilligan Point and Fair Head , Northern Ireland. *Irish Journal of Earth Sciences*, *9*(1), 71–78.

McDowell, J. L., Knight, J., & Quinn, R. (2005). High-resolution geophysical investigations seaward of the Bann Estuary, Northern Ireland coast. In D. M. Fitzgerald & J. Knight (Eds.), *High Resolution Morphodynamics and Sedimentary Evolution of Estuaries* (pp. 11–31). Springer.

McKenna, J. (1990). Quaternary shore platforms. In P. Wilson (Ed.), *Field guide No. 13: North Antrim and Londonderry.* (pp. 11–13). Irish Association for Quaternary Studies.

McKenna, J. (2002). Basalt cliffs and shore platforms between Portstewart (Co Derry) and Portballintrae (Co Antrim). In J. Knight (Ed.), *Field Guide to the Coastal Environments of Northern Ireland. International Coastal Symposium (ICS), University of Ulster, Coleraine, Northern Ireland* (pp. 157–164).

McKenna, J. (2008). Quaternary raised shorelines on the north coast of Ireland. In N. J. Whitehouse, H. M. Roe, S. McCarron, & J. Knight (Eds.), *North of Ireland: Field Guide.* (pp. 208–215). Quaternary Research Association, London.

McKenna, J., Carter, R. W. G., & Bartlett, D. (1992). Coast Erosion in Northeast Ireland:- Part II Cliffs and Shore Platforms. *Irish Geography*, *25*(2), 111–128.

Mitchum, R. M., Vail, P. R., & Sangree, J. B. (1977). Seismic Stratigraphy and Global Changes of Sea Level, Part 6: Stratigraphic Interpretation of Seismic Reflection Patterns in Depositional Sequences. *American Association of Petroleum Geologists*, 117–123.

Mitrovica, J. X., & Milne, G. A. (2003). On post-glacial sea level; I, General theory. *Geophysical Journal International*, *154*(2), 253–267.

Moore, R., Cooper, J. A. G., Dunlop, P., Jackson, D. W. T. (2011). Geology and Geomorphology. In J. A. G. Cooper (Ed.), *Lough Swilly: a living landscape* (pp. 17-34). Four Courts Press.

Movius, H. L. (1953). Graphic representation of postglacial changes of level in northeast Ireland. *American Journal of Science*, *251*(10), 697–740.

Muhs, D. R., Simmons, K. R., Schumann, R. R., Groves, L. T., Mitrovica, J. X., & Laurel, D. (2012). Sea-level history during the Last Interglacial complex on San Nicolas Island, California: implications for glacial isostatic adjustment processes, paleozoogeography and tectonics. *Quaternary Science Reviews*, *37*, 1–25.

Murray, J. W. (1979). *British nearshore foraminiferids: keys and notes for the identification of the species* (Vol. 16). Springer Netherlands.

Murray, J. W. (2006). *Ecology and applications of benthic foraminifera*. Cambridge University Press, Cambridge, UK.

Naylor, L. A., Stephenson, W. J., & Trenhaile, A. S. (2010). Rock coast geomorphology: Recent advances and future research directions. *Geomorphology*, *114*(1-2), 3–11.

Neill, S. P., Scourse, J. D., Bigg, G. R., & Uehara, K. (2009). Changes in wave climate over the northwest European shelf seas during the last 12,000 years. *Journal of Geophysical Research*, *114*(C06015).

Neill, S. P., Scourse, J. D., & Uehara, K. (2010). Evolution of bed shear stress distribution over the northwest European shelf seas during the last 12,000 years. *Ocean Dynamics*, *60*(5), 1139–1156.

Nicholls, R. J., Wong, P. P., Burkett, V., Codignotto, J., Hay, J., McLean, R., Ragoonaden, S., Woodroffe, C. D. (2007). Coastal systems and low-lying areas. In M. L. Parry, O. F. Canziani, J. P. Palutikof, P. Van der Linden, & C. E. Hanson (Eds.), *Climate Change 2007: Impacts, Adaptation and Vulnerability. Contribution of Working Group II to the Fourth Assessment Report of the Intergovernmental Panel on Climate Change.* Cambridge University Press, Cambridge.

Nolan, S. (2013). White Cliffs collapse: Tonnes of chalk crash from world famous landmark into the Channel near Dover. *Daily Mail*, [online] (Last updated 08:30 GMT, 25 March 2013). Available at: <http://www.dailymail.co.uk/news/article-2298504/White-Cliffs-collapse-Tonnes-chalk-crash-world-famous-landmark-Channel-near-Dover.html> [Accessed on 10 April 2013].

Ó Cofaigh, C., Dunlop, P., & Benetti, S. (2012). Marine Geophysical evidence for Late Pleistocene ice sheet extent and recession off northwest Ireland. *Quaternary Science Reviews*, *44*, 147–159.

Orford, J. D., Betts, N. L., Cooper, J. A. G., & Smith, B. J. (2010). *Future coastal scenarios for Northern Ireland* (pp. 178). Report for the National Trust (NI), Belfast.

References

Orme, A. R. (1966). Quaternary Changes of Sea-level in Ireland. *Transactions of the Institute of British Geographers*, *39*, 127–140.

Parry, M. L., Canziani, O. F., Palutikof, J. P., Van Der Linden, P., & Hanson, C. E. (2007). *Climate Change 2007: Impacts, Adaptation and Vulnerability. Contribution of Working Group II to the Fourth Assessment Report of the Intergovernmental Panel on Climate Change.*

Passaro, S., Ferranti, L., & Alteriis, G. De. (2010). The use of high-resolution elevation histograms for mapping submerged terraces: Tests from the Eastern Tyrrhenian Sea and the Eastern Atlantic Ocean. *Quaternary International*, 1–12.

Peacock, J. D. (1981). Scottish Late-glacial marine deposits and their environmental significance. In J. W. Neale & J. Flenley (Eds.), *The Quaternary in Britain* (pp. 222–236). Pergamon Press.

Pedoja, K., Husson, L., Regard, V., Cobbold, P. R., Ostanciaux, E., Johnson, M. E., Kershaw, S., Saillard, M., Martinod, J., Furgerot, L., Weill, P., Delcaillau, B. (2011). Relative sea-level fall since the last interglacial stage: Are coasts uplifting worldwide? *Earth-Science Reviews*, *108*(1-2), 1–15.

Peltier, W. R., Shennan, I., Drummond, R., & Horton, B. (2002). On the postglacial isostatic adjustments of the British Isles and the shallow viscoelastic structure of the Earth. *Geophysical Journal International*, *148*(3), 443–475.

Plets, R., Clements, A., Quinn, R., Strong, J., & Breen, J. (2012). Marine substratum map of the Causeway Coast , Northern Ireland. *Journal of Maps*, *8*(1), 1–13.

Portlock, J. E. (1843). *Report on the geology of the County of Londonderry and of parts of Tyrone and Fermanagh* (pp. 784). Dublin.

Praeger, R. L. (1895). The Raised Beaches of Inishowen. *The Irish Naturalists' Journal*, *4*(10), 278–285.

Praeger, R. L. (1896). Report upon the Raised Beaches of the North-East of Ireland , with Special Reference to Their Fauna. *Proceedings of the Royal Irish Academy*, *4*, 30–54.

Prior, D. B. (1965). Late glacial and post-glacial shorelines in north-east antrim. *Irish Geography*, *5*(2), 173–187.

Quinn, R, Forsythe, W., Benetti, S., Bell, T., McGrath, F., Plets, R. M. K., Robinson, R., Westley, K. (2008). *Archaeological applications of the Joint Irish Bathymetric Survey (JIBS) data* (pp. 95).

Quinn, R., Forsythe, W., Plets, R., Westley, K., Bell, T., Mcgrath, F., Robinson, R., Benetti, S. (2009). *Archaeological applications of the Joint Irish Bathymetric Survey [JIBS] data -Phase 2-* (pp. 110).

Quinn, R. Plets, R., Clements, A., Westley, K., Forsythe, W., Bell, T., Robinson, R., Benetti, S. (2010). *Archaeological applications of the Joint Irish Bathymetric Survey [JIBS] data - Phase 3* - (pp. 162).

Raymo, M. E., Mitrovica, J. X., Leary, M. J. O., Deconto, R. M., & Hearty, P. J. (2011). Departures from eustasy in Pliocene sea-level records. *Nature Geoscience*, *4*(5), 328–332.

Roberts, M. J., Scourse, J. D., Bennell, J. D., Huws, D. G., Jago, C. F., & Long, B. T. (2011). Late Devensian and Holocene relative sea-level change in North Wales , UK. *Journal of Quaternary Science*, *26*(2), 141–155.

Robinson, D. A., & Jerwood, L. C. (1987). Sub-aerial weathering of chalk shore platforms during harsh winters in southeast England. *Marine Geology*, *77*(1), 1–14.

Rohling, E. J., Fenton, M., Jorissen, F. J., Bertrand, P., Ganssen, G., & Caulet, J. P. (1998). Magnitudes of sea-level lowstands of the past 500,000 years. *Nature (London)*, *394*(6689), 162–165.

Rovere, A., Vacchi, M., Firpo, M., & Carobene, L. (2011). Underwater geomorphology of the rocky coastal tracts between Finale Ligure and Vado Ligure (western Liguria, NW Mediterranean Sea). *Quaternary International*, *232*(1-2), 187–200.

Scott, D. S., & Medioli, F. S. (1978). Verical zonations of marsh foraminifera as accurate indicators of former sea-levels. *Nature*, *272*, 528–531.

Sejrup, H. P. (1987). Molluscan and foraminiferal biostratigraphy of an Eemian-Early Weichselian section on Karmøy, southwestern Norway. *Boreas*, *16*(1), 27–42.

Sejrup, H. P., Hjelstuen, B. O., Torbjørn Dahlgren, K. I., Haflidason, H., Kuijpers, A., Nygård, A., Praeg, D., Stoker M. S., & Vorren, T. O. (2005). Pleistocene glacial history of the NW European continental margin. *Marine and Petroleum Geology*, *22*(9-10), 1111–1129.

Sella, G. F., Stein, S., Dixon, T. H., Craymer, M., James, T. S., Mazzotti, S., & Dokka, R. K. (2007). Observation of glacial isostatic adjustment in “stable” North America with GPS. *Geophysical Research Letters*, *34*(L02306).

References

Shennan, I., Horton, B., Innes, J., Gehrels, R., Lloyd, J., McArthur, J., & Rutherford, M. (2000a). Late Quaternary sea-level changes, crustal movements and coastal evolution in Northumberland, UK. *Journal of Quaternary Science*, *15*(3), 215–237.

Shennan, I., Lambeck, K., Flather, R., Horton, B. P., McArthur, J. J., Innes, J. B., Lloyd, J., Rutherford, M. M., Wingfield, R., Andrews, J. E. (2000b). Modelling western North Sea palaeogeographies and tidal changes during the Holocene. *Geological Society Special Publications*, *166*, 299–319.

Shennan, I., Peltier, W. R., Drummond, R., Horton, B., Clark, P. U., & Mix, A. C. (2002). Global to local scale parameters determining relative sea-level changes and the post-glacial isostatic adjustment of Great Britain. *Quaternary Science Reviews*, *21*(1-3), 397–408.

Shennan, I., Bradley, S., Milne, G., Brooks, A., Bassett, S., & Hamilton, S. (2006). Relative sea-level changes, glacial isostatic modelling and ice-sheet reconstructions from the British Isles since the last glacial maximum. *Journal of Quaternary Science*, *21*(6), 585–599.

Sissons, J. B. (1963). Scottish Raised Shoreline Heights with Particular Reference to the Forth Valley. *Geografiska Annaler*, *45*(2-3), 180–185.

Smart, C. C., & Hale, P. B. (1987). Exposure and inundation statistics from published tide tables. *Computers & Geosciences*, *13*(4), 357–368.

Smith, D. E., Davies, M. H., Brooks, C. L., Mighall, T. M., Dawson, S., Rea, B. R., Jordan, J. T., Holloway, L. K. (2010). Holocene relative sea levels and related prehistoric activity in the Forth lowland , Scotland , United Kingdom. *Quaternary Science Reviews*, *29*(17-18), 2382–2410.

Solomon, S., Qin, D., Manning, M., Marquis, M., Averyt, K., Tignor, M. M. B., Miller, H. L., Chen, Z. (2007). *Climate change 2007: The physical Science Basis. Contribution of Working Group I to the Fourth Assessment Report of the Intergovernmental Panel on Climate Change.* Cambridge University Press, Cambridge.

Stanford, J. D., Hemingway, R., Rohling, E. J., Challenor, P. G., Medina-Elizalde, M., & Lester, a. J. (2011). Sea-level probability for the last deglaciation: A statistical analysis of far-field records. *Global and Planetary Change*, *79*(3-4), 193–203.

Stephens, N. (1963). Late-glacial sea-levels in North-East Ireland. *Irish Geography*, *4*(5), 345–359.

Stephens, N. & Synge, F. M. (1965). Late-Pleistocene Shorelines and Drift Limits in North Donegal. *Proceedings of the Royal Irish Academy*, *64*, 131–153.

Stephens, N., Creighton, J. R., & Hannon, M. A. (1975). The late-Pleistocene period in north-eastern Ireland: an assessment 1975. *Irish Geography*, *8*(1), 1–23.

Stephenson, W. J., & Finlayson, B. L. (2009). Measuring erosion with the micro-erosion meter—Contributions to understanding landform evolution. *Earth-Science Reviews*, *95*(1), 53–62.

Stephenson, W. J., Kirk, R. M., Hemmingsen, S. A., & Hemmingsen, M. A. (2010). Decadal scale micro erosion rates on shore platforms. *Geomorphology*, *114*(1), 22–29.

Stephenson, W. J., & Naylor, L. A. (2011). Geological controls on boulder production in a rock coast setting: Insights from South Wales, UK. *Marine Geology*, *283*, 12–24.

Stoker, M. S., Pheasant, J. B., & Josenhans, H. (1997). Seismic methods and interpretation. In T. A. Davies, T. Bell, A. K. Cooper, H. Josenhans, L. Polyak, A. Solheim, M. S. Stoker & J. A. Stravers (Eds.), *Glaciated Continental Margins: An Atlas of Acoustic Images* (pp. 9–26). Springer Netherlands.

Stoker, M. S., Golledge, N. R., Phillips, E. R., Wilkinson, I. P., & Akhurst, M. C. (2009). Lateglacial-Holocene shoreface progradation offshore eastern Scotland: a response to climatic and coastal hydrographic change. *Boreas*, *38*(2), 292–314.

Stone, J., Lambeck, K., Fifield, L. K., Evans, J. M., & Cresswell, R. G. (1996). A Lateglacial age for the Main Rock Platform, western Scotland. *Geology*, *24*, 707–710.

St-Onge, G., Mulder, T., Francus, P., & Long, B. (2007). Chapter Two Continuous Physical Properties of Cored Marine Sediments. *Developments in Marine Geology*, *1*, 63–98.

Strasser, T. F., Runnels, C., Wegmann, K., Panagopoulou, E., Mccoy, F., Digregorio, C., Karkanas, P., Thompson, N. (2011). Dating Palaeolithic sites in southwestern Crete , Greece. *Journal of Quaternary Science*, *26*(5), 553–560.

Sunamura, T. (1992). *Geomorphology of Rocky Coasts (Coastal Morphology and Research Series)* (pp. 314). John Wiley & Sons.

Swantesson, J. O. H., Gómez-Pujol, L., Cruslock, E. M., Fornoós, J. J., & Balaguer, P. (2006). Processes and patterns of erosion and downwearing on micro-tidal rock coasts in Sweden and the western Mediterranean. *European Shore Platform Dynamics. Zeitschrift für Geomorphologie, Supplement Band*, *144*, 137–160.

References

Symes, R. G., Egan, F. W., McHenry, A. (1888). *Explanatory Memoir to accompany sheets 7 and 8 of the maps of the Geological Survey of Ireland* (pp. 66). Dublin.

Synge, F. M., & Stephens, N. (1966). Late- and Post-Glacial Shorelines, and Ice Limits in Argyll and North-East Ulster. *Transactions of the Institute of British Geographers*, (39), 101–125.

Thébaudeau, B., Trenhaile, A. S., & Edwards, R. J. (2013). Modelling the development of rocky shoreline profiles along the northern coast of Ireland. *Geomorphology,* http://dx.doi.org/10.1016/j.geomorph.2013.03.027

Thornton, L. E., & Stephenson, W. J. (2006). Rock Strength: A Control of Shore Platform Elevation. *Journal of Coastal Research*, *22*(1), 224–231.

Trenhaile, A. S. (1972). The shore platforms of the Vale of Glamorgan, Wales. *Transactions of the institute of British Geographers*, *56*, 127–144.

Trenhaile, A. S. (1978). The shore platforms of Gaspé, Québec. *Annals of the Association of American Geographers*, *68*, 95–114.

Trenhaile, A. S. (1987). *The Geomorphology of Rock Coasts*. Oxford University Press, Oxford.

Trenhaile, A. S. (1997). *Coastal Dynamics and Landforms*. Oxford University Press, Oxford.

Trenhaile, A. S. (1999). The width of Shore Platforms in Britain, Canada and Japan. *Journal of Coastal Research*, *15*(2), 355–364.

Trenhaile, A. S. (2000). Modeling the development of wave-cut shore platforms. *Marine Geology*, *166*, 163–178.

Trenhaile, A. S. (2001). Modeling the Quaternary evolution of shore platforms and erosional continental shelves. *Earth Surface Processes and Landforms*, *26*, 1103–1128.

Trenhaile, A. S. (2002). Rock coasts, with particular emphasis on shore platforms. *Geomorphology*, *48*(1-3), 7–22.

Trenhaile, A. S. (2008). Modeling the role of weathering in shore platform development. *Geomorphology*, *94*(1-2), 24–39.

Trenhaile, A. S. (2010). The effect of Holocene changes in relative sea level on the morphology of rocky coasts. *Geomorphology*, *114*(1-2), 30–41.

Trenhaile, A. S. (2012). Cliffs and rock shores. In J. D. Hansom & B. W. Flemming (Eds.), *Estuarine and Coastal Geology and Geomorphology: Treatise on Estuarine and Coastal Science* (Vol. 3, pp. 171–191).

Trenhaile, A. S. & Mercan, D. W. (1984). Frost weathering and the saturation of coastal rocks. *Earth Surface Processes and Landforms*, *9*(4), 321–331.

Trenhaile, A. S. & Bryne, M.-L. (1986). A theoretical investigation of the Holocene development of rock coasts, with particular reference to shore platforms. *Geografiska Annaler*, *68A*, 1–14.

Trenhaile, A. S. & Kanyaya, J. I. (2007). The role of wave erosion on sloping and horizontal shore platforms in macro- and mesotidal environments. *Journal of Coastal Research*, *23*, 298–309.

Trenhaile, A. S., Pérez Alberti, A., Martínez Cortizas, A., Costa Casais, M., & Blanco Chao, R. (1999). Rock coast inheritance: an example from Galicia, northwestern Spain. *Earth Surface Processes and Landforms*, *24*, 605–621.

Turner, A. J., Woodward, J., Dunning, S. A., Shine, A. J., Stokes, C. R., & Cofaigh, C. Ó. (2012). Geophysical surveys of the sediments of Loch Ness, Scotland: implications for the deglaciation of the Moray Firth Ice Stream, British-Irish Ice Sheet. *Journal of Quaternary Science*, *27*(2), 221–232.

Uehara, K., Scourse, J. D., Horsburgh, K. J., Lambeck, K., & Purcell, A. P. (2006). Tidal evolution of the northwest European shelf seas from the Last Glacial Maximum to the present. *Journal of Geophysical Research*, *111*(C09025).

Van Landeghem, K. J. J., Wheeler, A. J., & Mitchell, N. C. (2009). Seafloor evidence for palaeo-ice streaming and calving of the grounded Irish Sea Ice Stream: Implications for the interpretation of its final deglaciation phase. *Boreas*, *38*(1), 119–131.

Waelbroeck, C., Labeyrie, L., Michel, E., Duplessy, J. C., McManus, J. F., Lambeck, K., Balbon, E., Labracherie, M. (2002). Sea-level and deep water temperature changes derived from benthic foraminifera isotopic records. *Quaternary Science Reviews*, *21*(1-3), 295–305.

Walker, M., & Lowe, J. (2007). Quaternary science 2007 : a 50-year retrospective. *Journal of the Geological Society, London*, *164*, 1073–1092.

Wilson, P., Westley, K., Plets, R., & Dempster, M. (2011). Radiocarbon dates from the inter-tidal peat bed at Portrush , County Antrim. *Irish Geography*, *44*(2-3), 323–329.

References

Wingfield, R. (1990). The origin of major incisions within the Pleistocene deposits of the North Sea. *Marine Geology*, *91*(1), 31–52.

Woodman, P. C. (1985). *Excavations at Mount Sandel, 1973-77, County Londonderry*. HM Stationery Office.

Woodroffe, C. D. (2002). *Coasts: form, process and evolution*. Cambridge University Press Cambridge.

Wright, L. W. (1970). Variation in the level of the cliff/shore platform junction along the south coast of Great Britain. *Marine Geology*, *9*(5), 347–353.

Wright, W. B. (1937). *The Quaternary ice age* (Second edi.). London: Macmillan and Co., limited.

Young, R. W., & Bryant, E. A. (1993). Coastal rock platforms and ramps of Pleistocene and Tertiary age in southern New South Wales, Australia. *Zeitschrift für Geomorphologie*, *37*, 257–272.

Zecchin, M., Ceramicola, S., Gordini, E., Deponte, M., & Critelli, S. (2011). Cliff overstep model and variability in the geometry of transgressive erosional surfaces in high-gradient shelves: The case of the Ionian Calabrian margin. *Marine Geology*, *281*(1-4), 43–58.

Zecchin, M., & Catuneanu, O. (2013). High-resolution sequence stratigraphy of clastic shelves I: Units and bounding surfaces. *Marine and Petroleum Geology*, *39*, 1–25.